EFFECT OF MECHANICAL PRE-TREATMENT ON LEACHING OF BASE METALS FROM WASTE PRINTED CIRCUIT BOARDS

by

Willem Adolf Rossouw

Thesis presented in partial fulfilment
of the requirements for the Degree

of

MASTER OF ENGINEERING
(EXTRACTIVE METALLURGICAL ENGINEERING)

in the Faculty of Engineering
at Stellenbosch University

Supervisor
Christie Dorfling

December 2015

DECLARATION

By submitting this thesis electronically, I declare that the entirety of the work contained therein is my own, original work, that I am the sole author thereof (save to the extent explicitly otherwise stated), that reproduction and publication thereof by Stellenbosch University will not infringe any third party rights and that I have not previously in its entirety or in part submitted it for obtaining any qualification.

Date: 17 September 2015

ABSTRACT

The fast rate of technological development of electronic devices has led to a decrease in the service life of these devices. This is resulting in an increased rate of electronic waste generation. The recovery of metals from electronic waste prior to disposal is of environmental and economic interest.

Hydrometallurgical process routes consisting of multiple leaching stages have been proposed as an alternative to pyrometallurgical processes for the recovery of valuable metals from printed circuit board (PCB) waste. Pre-treatment of PCB waste prior to leaching involves disassembly, size reduction and physical separation. This is followed by an oxidative acid leach to recover base metals, where after cyanidation, aqua regia or thiourea leaching is applied for precious metal recovery. In order to minimise precious metal losses and to reduce the negative effect of base metals on the precious metal leach stage, a selective base metal leaching stage is critical.

The objectives of this project are to experimentally investigate the effects of the different mechanical pre-treatment steps on the acid leaching of base metals from waste printed circuit boards, and to subsequently propose a suitable leaching agent and operating conditions for selective leaching of the base metals. The physical separation steps included dense medium separation (DMS) and DMS followed by magnetic separation (MS). Different lixiviants (nitric acid and sulphuric acid) were compared, and the effects of variations in peroxide addition, temperature and solid to liquid ratio on leaching performance were also investigated. Suitable operating conditions for selective leaching of base metals can subsequently be proposed.

Increasing the temperature favoured nitric acid leaching: Cu leaching increased from 0% at 25°C to 84% at 85°C while co-extraction of Au was increased from 0% at 25°C to 12% at 85°C. Using sulphuric acid, the same increase in temperature decreased copper leaching from 37% to 0%. This decrease of copper leaching with increase in temperature using sulphuric acid was attributed to the rapid decomposition of hydrogen peroxide at 85°C. No significant co-extraction of Au was observed when using sulphuric acid as lixiviant.

Investigating the effect of peroxide addition indicated that continuous feeding of peroxide yielded 67% Cu recovery, while double the volume of peroxide added at time zero at 25°C yielded only 52% Cu recovery. Continuous feeding of peroxide resulted in less peroxide decomposition than when peroxide was batch fed at the beginning of the experiments. Further optimisation of the peroxide addition rate allowed a Cu recovery of 92% to be achieved with sulphuric acid at a peroxide feed rate of 1.2 mL/min and a temperature of 25°C after 8 hours; no noticeable gold dissolution was observed at these conditions.

Application of DMS using a mixture of tetrabromoethane (TBE) and acetone at an SG of 2.5 enriched metal content from 48 Wt% to 75 Wt%. Along with plastics, 70% of Au and 20% of Cu reported to the light fraction. The application of MS removed 67% of Fe and 61% of Ni. Although DMS successfully concentrated the feed and MS removed the majority of Fe and Ni, this did not show any significant benefit in leaching performance compared to untreated feed.

Investigation of H_2SO_4 concentration for un-concentrated feed showed that increasing the concentration from 1 M to 2.5 M H_2SO_4 decreased the time required for ~95% Cu extraction from 300 minutes to 240 minutes. Increasing the acid concentration further from 2.5 M to 4 M did not show significant benefit.

Results were used to suggest a suitable flow sheet for selective base metal removal from waste PCBs. The flow sheet consisted of a 1 M HNO_3 leach to remove Fe and Pb, followed by a 2.5 M H_2SO_4 leach to remove Cu, Ni and Zn. Au and Ag would remain in the residue. Experimental

validation of the flowsheet showed removal of 76% Fe and 98% Pb by the HNO_3 leach. The H_2SO_4 leach removed 97% Cu and 93% Zn. The solid residue contained 100% of the Au and 90% of the Ag; 66% of Al and 86% of Sn originally present in the feed also remained in the residue. The validation of the flowsheet confirmed the possibility for selective base metal removal from waste PCBs using a hydrometallurgical process route.

OPSOMMING

Die vinnige tempo van tegnologiese ontwikkeling van elektroniese toestelle lei tot 'n afname in die gebruiktydperk van hierdie toestelle. Hierdie lei tot 'n groeiende tempo van elektroniese-afval produksie. Metaalherwinning vanaf elektroniese-afval voordat dit weggegooi word, is van beide omgewings en ekonomiese belang.

Hidrometallurgiese prosesroetes wat uit veelvoudige logingstappe bestaan is voorgestel as 'n alternatief vir pirometallurgiese prosesse vir die herwinning van metale vanaf gedrukte stroombaan borde (GSB's). GSB's mag uitmekaar gehaal word, fyngemaal word en fisiese skeiding ontvang voordat dit geloog word. Hierdie word tipies gevolg deur 'n oksiderende suurloog om basismetale te verwyder, waarna sianied of thiourea loging aangewend word om edelmetale te herwin. 'n Selektiewe basismetaalloog is krities om edelmetaal verliese te minimeer en om die negatiewe uitwerking van basismetale op edelmetaalloging teen te werk.

Die doelwitte van die projek was die ondersoek van die effek van die verskillende meganiese skeiding stappe op die suurloging van basismetale vanaf GSB's. Gevolglik moes 'n gepaste loogmiddel en bedryfstoestande voorgestel word vir selektiewe verwydering van basismetale. Die meganiese skeiding stappe wat toegepas was, het swaarvloeistofskeiding (SVS) en magnetiese-skeiding (MS) ingesluit. Verskillende loogmiddels (salpetersuur en swaelsuur) was met mekaar vergelyk, die metode en hoeveelheid van waterstofperoksied byvoeging was ondersoek, asook die invloed van temperatuur en vastestof-tot-vloeistof-verhouding op logingsgedrag. Gepaste bedryfstoestande vir selektiewe basismetaalloging kan gevolglik voorgestel word.

Verhoging van temperatuur het salpetersuur-loging bevorder: geloogde Cu is verhoog vanaf 0% by 25°C tot 84% by 85°C terwyl die mate van Au-loging verhoog is van 0% by 25°C tot 12% by 85°C. Vir swaelsuur het dieselfde verhoging van temperatuur Cu-loging laat afneem vanaf 37% by 25°C tot 0% by 85°C. Die afname in die mate van Cu-loging behaal met 'n styging in temperatuur in die swaelsuur-stelsel kan toegeskryf word aan die snel- en volledige ontbinding van waterstofperoksied by 85°C. Geen merkbare hoeveelheid Au was verwyder met swaelsuur as loogmiddel nie.

Die ondersoek van peroksied byvoeging het gedui dat kontinue voering van peroksied 'n mate van 67% Cu-loging kon behaal, terwyl byvoeging van twee keer die hoeveelheid peroksied meteens by 25°C en tyd nul slegs 52% Cu-loging kon behaal. In vergelyking met enkellading byvoeging by tyd nul, beperk kontinue byvoeging van peroksied die onbinding daarvan deur toe te laat dat doeltreffende verkoelling kan geskied. Verdere optimering het gewys dat 'n mate van 92% Cu-loging behaal kon word met 'n peroksied voertempo van 1.2 mL 30% H_2O_2/min by 25°C na 8 ure. Geen merkbare hoeveelheid Au is geloog by hierdie toestande nie.

Toepassing van SVS met 'n mengsel van tetrabromo-etaan en asetoon met 'n digtheid van 2.5 g/cm^3 het die metaal inhoud van die voerstroom verryk vanaf 48 Wt% tot 75 Wt%. Saam met plastiek, het 70% van die Au en 20% van die Cu na die ligtefraksie gerapporteer. Die toepassing van magnetiese skeiding het 67% van die Fe en 61% van die Ni verwyder. Alhoewel SVS daarin geslaag het om die voer te konsentreer en MS die meerderheid van Fe en Ni verwyder het, het dit geen beduidende voordelige gevolge vir logingsgedrag gehad nie.

Ondersoek van die effek van H_2SO_4 konsentrasie op nie-gekonsentreerde voer het gewys dat verhoging van konsentrasie vanaf 1 M tot 2.5 M H_2SO_4 die tyd benodig om 95% Cu-loging te behaal verminder het vanaf 300 minute tot 240 minute. Verdere verhoging van swaelsuurkonsentrasie vanaf 2.5 M na 4 M het geen beduidende logingsvoordeel getoon nie.

Resultate is gebruik om 'n gepaste prosesroete voor te stel vir die selektiewe verwydering van basismetale vanaf GSB's. Die prosesroete het bestaan uit 'n 1 M HNO_3 loog om Fe en Pb te verwyder, gevolg deur 'n 2.5 M H_2SO_4 loog om Cu, Ni en Zn te verwyder. Au en Ag sou dan in die soliede residu agtergelaat word. Tydens eksperimentele bevestiging van die prosesroete is daar gedurende die salpetersuurloog 76% Fe and 98% Pb verwyder. Die swaelsuurloog het 97% Cu en 93% Zn verwyder. Die soliede residu het 100% van die Au bevat asook 90% van die Ag. 66% van die Al en 86% van die Sn aanvanklik in die monster teenwoordig het saam met die edelmetale in die residu agtergebly. Die suksesvolle eksperimentele uitvoering van die prosesroete het die moontlikheid van selektiewe basismetaalverwydering vanuit GSB's d.m.v. 'n hidrometallurgiese prosesroete bevestig.

ACKNOWLEDGEMENTS

I would like to express my gratitude to the following people and organisations:

- My supervisor, Dr Christie Dorfling, for his guidance and support.
- The administrative and technical staff at the Department of Process Engineering at Stellenbosch University.
- My family, in particular my parents, Danie and Marian Rossouw, and my uncle Gawie Rossouw, for their support.
- This work is based on research supported in part by the National Research Foundation of South Africa under grant number 87965 and by the Outotec Postgraduate Scholarship programme managed by the SAIMM Western Cape Branch. Any opinion, finding and conclusion or recommendation expressed in this material is that of the author and the NRF and other funding organisations do not accept any liability in this regard.

SYMBOLS

A	Absorbance
a_{ox}	Activity of the oxidising species
a_{red}	Activity of reducing species
d	Particle diameter
D_R	Diffusivity of reactant, R
F_c	Centrifugal force
F_g	Gravitational force
F_i	Electric image force
k_c	Reaction constant for chemically controlled reaction
k_d	Reaction constant for diffusion controlled reaction
ρ	Fluid density
ρ_p	Particle density
v_t	Terminal velocity
χ_m	Magnetic susceptibility
x	Fraction of metal reacted

ACRONYMS

[bmim]HSO_4	1-butyl-3-methyl-imidazolium hydrogen sulphate
BFR	Bromated flame retardants
DMS	Dense medium separation
EEE	Electric and electronic equipment
ICP-OES	Inductively coupled plasma optical emission spectrometer
MLCC	Multi-layer ceramic capacitor
MS	Magnetic separation
MSW	Municipal solid waste
PCB	Printed circuit board
PLS	Pregnant leach solution
R	Universal gas constant
STVB	Scrap television boards
SX	Solvent extraction
TBE	Tetrabromoethane
WEEE	Waste electric and electronic equipment
WPCB	Waste printed circuit board

LIST OF FIGURES

LIST OF TABLES

TABLE OF CONTENTS

1. INTRODUCTION

The rapid technological development of electronic devices has led to a decrease in the service life of these devices. Hence, an increased rate of electronic waste generation has been observed. The recovery of metals from electronic waste prior to disposal is of environmental and economic interest.

Printed circuit board waste typically contains 100-300 kg Cu and 100-400 g Au per ton of waste. This is notably more concentrated than their respective ores (typically Cu: 4-10 kg per ton ore; Au: 1-10 g per ton ore). Copper and gold recovery from electronic waste offers the largest financial incentive [1,2].

Both pyrometallurgical and hydrometallurgical process routes exist for metals recovery from electronic waste. Hydrometallurgical process routes are believed to offer distinct advantages over their pyrometallurgical counterpart, such as lower energy requirements and the ability to process lower feed grades [3].

Hydrometallurgical treatment of electronic waste generally involves the following steps: disassembly for removal of hazardous and reusable parts, size reduction, physical separation, successive leaching stages for metal dissolution and finally recovery of metals from leach solutions. The interaction between physical separation stages and leaching has not yet been investigated and this hampers the development of a well-integrated process.

This project aims to develop a better understanding of the interaction between physical separation stages and base metal leaching operations, and to subsequently propose a viable leaching process for selective base metal dissolution.

1.1. PROJECT MOTIVATION

No studies have compared the leaching of PCB waste directly after size reduction with leaching following one or more of the physical separation steps. [4]Hagenluken 2006 found mechanical pre-treatment steps to attribute to 20% losses of precious metals. Calculations done on results of Yamane et al. (2011) showed approximately 16% of gold being removed by magnetic separation and a further 37% of gold reporting to the non-conductive fraction during electrostatic separation[5]. Given the potential for large losses of valuable metals during physical separation, it is important to understand the role of these units in the integrated flow sheet. While the purpose of this proposed study is not to optimise or investigate particular physical separation units, it aims to evaluate the importance of these processing steps for the subsequent leaching operations.

Many studies have been performed on the mechanical pre-treatment of PCB waste, however further studies are required to pave the way for efficient application of a combination of mechanical and hydrometallurgical processing [6].

1.2. PROJECT OBJECTIVES

In order to develop a better understanding of the interaction between mechanical pre-treatment and leaching performance, the following objectives are to be achieved:

- Select a suitable lixiviant for base metal leaching based on both the selectivity- and extent of base metal dissolution.
- Determine the temperature for optimal leaching performance.
- Determine the effect of the percentage non-metals in the feed on leaching performance and explain fundamentally why these effects are observed.
- Determine the effect of the percentage ferrous metals in the feed on leaching performance and explain fundamentally why these effects are observed.
- Suggest a suitable flow sheet for base metals recovery from PCB waste based on interpretation of experimental results. The flow sheet should indicate the extent to which mechanical pre-treatment should be conducted on feed as well as suitable leaching conditions for selective- and complete base metal recovery.

Leaching performance in the context of this project refers to the extent of base metal dissolution and the selectivity of the leaching process for base metals.

1.3. PROJECT SCOPE

The project scope can be broadly divided into four parts, namely: disassembly, size reduction, mechanical separation and leaching.

PCB waste is firstly disassembled. Disassembly aims to remove hazardous and re-usable components from the PCBs. Disassembly can be conducted either manually, or by the immersion of whole PCBs in dilute nitric acid to dissolve solder to free components

Size reduction of PCB waste prior to leaching is crucial. Metal is typically embedded between layers of resin hence size reduction is applied in order to liberate metals and to promote exposure to the leaching solution. The boards are manually cut to size and then ground to liberate metals from the resin.

Mechanical separation is applied to reduce material volume and to increase the metals grade of the feed to the leaching stage. Typical physical separation processes applied to PCB waste are electrostatic separation, magnetic separation and density separation. Electrostatic and density separation are aimed at separating metals from non-metals based on differences in electro-conductivity and specific gravity, respectively. Magnetic separation aims to remove ferrous material such as iron and nickel. Mechanical separation will only be used for the purpose of feed preparation for the base metal leaching experiments; optimisation of different physical separation techniques is not included in the scope of this study.

Acids that have been investigated for copper leaching are nitric acid, sulphuric acid and hydrochloric acid. Spyrellis et al. (2009) reported adequate dissolution of copper to be achieved with all three above mentioned acids but named nitric acid to be more efficient [7]. Poor leaching of copper has been observed in the absence of an oxidising agent when using sulphuric acid or hydrochloric acid [8]. Nitric acid is a strong oxidising acid and has been used to effectively leach copper without the addition of a dedicated oxidising agent [9-13]. Various lixiviants will be evaluated at different operating conditions as part of this study. The treatment of the resulting leach solution is, however, not included in the scope.

1.4. THESIS OUTLINE

Section 2 provides an overview of electronic waste treatment. This is followed by a literature review on aspects related to metals recovery from printed circuit boards. This includes aspects such as disassembly, size reduction, mechanical separation and acid leaching. Section 3 includes a discussion of the equipment and methodology used for experiments. Experimental results are discussed in section 4 along with a suggested flow sheet for base metal removal. Conclusions and recommendations are discussed in section 5.

2. LITERATURE REVIEW

2.1. INTRODUCTION

Disposing electronic waste via landfilling is detrimental to environmental health due to its high content of heavy metals and bromated flame retardants (BFR). Conventional treatment of electronic waste involves an incineration process, either in an attempt at metal recovery (pyrometallurgical treatment) or as part of the combustion of municipal solid waste (MSW). Gasses produced from combustion contain brominated and mixed halogenated dibenzo-p-dioxins and dibenzofurans [14] which are known to be extremely toxic to human and environmental health [15].

Pyrometallurgical processes rely on precious metal content of electronic waste (e-waste) to be economical. However, precious metals use in electrical and electronic equipment has been steadily decreasing and is expected to continue doing so in the future. Precious metals content may be diluted by mixing of e-waste of different grades. The development of low cost treatment methods for recovery of metals from low grade e-waste is therefore increasing in importance. Hydrometallurgical processes are regarded as a low cost treatment alternative for low grade wastes [16].

Hydrometallurgical recovery of metals involves dissolution in acidic or alkaline medium. A two stage leaching process can be applied involving oxidative acid leaching of base metals followed by precious metal leaching using thiourea, thiosulfate or halide as leaching agent [17-19]. The advantages of hydrometallurgical processes compared to pyrometallurgical processes include lower energy requirements, no combustion of plastics containing flame retardants, lower capital expenditure, the ability to be run economically on a smaller scale as well as to process lower feed grades [11,16,18].

Waste PCBs generally contain approximately 40% metals, 30% ceramics and 30% plastics [1]. A major peculiarity of WEEE is presence of metals in their pure form, or in alloys [19].

Precious metals contribute significantly to the value of WEEE and their extraction is therefore of primary importance for the recycling operation to be economically viable [19]. However, the composition of PCB waste can vary considerably; hence, certain types of PCB waste do not contain appreciable amounts of precious metals. Table 1 shows the reported compositions of different types of electronic wastes. It can be seen from Table 1 that computer boards and cell phones generally have a higher metals content than television boards.

Base metals are known to negatively affect precious metals leaching. This is attributed to a high tendency to dissolve and consume reagent intended for precious metal leaching. Dissolved base metals then add to the impurities of the precious metal leach solution, making selective recovery of precious metals more difficult [17,20]. In order to minimise precious metal losses and to reduce negative effect of base metals on the precious metal leach stage, a selective base metal leaching stage is critical.

Hydrometallurgical recovery of metals from waste printed circuit boards (WPCBs) involves mechanical pre-treatment of wastes, leaching of metals with a suitable lixiviant, purification of pregnant leach solutions (PLS) and finally metals recovery [19].

TABLE 1: REPORTED COMPOSITIONS OF VARIOUS TYPES OF ELECTRONIC WASTE

Type of waste (Authors)	**Fe**	**Cu**	**Al**	**Pb**	**Sn**	**Ni**	**Au**	**Ag**	**Pd**
	Wt%						g/ton		
TV Boards(without components) [16]	0.04	9.2	0.75	0.003	0.72	0.01	3	86	3.7
TV Boards [21]	0.0043	10	10	1	1.4	0.3	20	280	10
TV Boards [22]	0.043	11.2	0.3	0.013	-	0.02	.14	48	-
PC Boards [23]	3.49	12.8	2.46	2.37	1.23	0.47	-	-	-
PC Boards [24]	-	21.9	-	0.297	0.38	0.003	31.8	53.7	271.8
PC Boards [21]	7	20	5	1.5	2.9	1	250	1000	110
PC Boards [25]	2.1	18.5	1.3	2.7	4.9	0.4	86	694	97
Mobile phones [21]	5	13	1	0.3	0.5	0.1	350	1380	210

Figure 1 shows the first stages of PCB waste treatment up until filtration of precious metal leach product. PCB waste is firstly disassembled to remove hazardous and reusable components. Disassembly is followed by size reduction and subsequent screening. Once the particles are of appropriate size, physical separation stages may be used to upgrade metals concentration by removing non-metals (by DMS, air classification, electrostatic separation, and eddy current separation). Ferromagnetic material may be removed by magnetic separation (MS).

Physical separation is followed by selective leaching of base metals. A filtration stage separates the base metal PLS from residue. The base metal PLS will undergo purification and metal recovery. Residue is subjected to cyanidation, thiourea or halide leaching for the dissolution of precious metals.

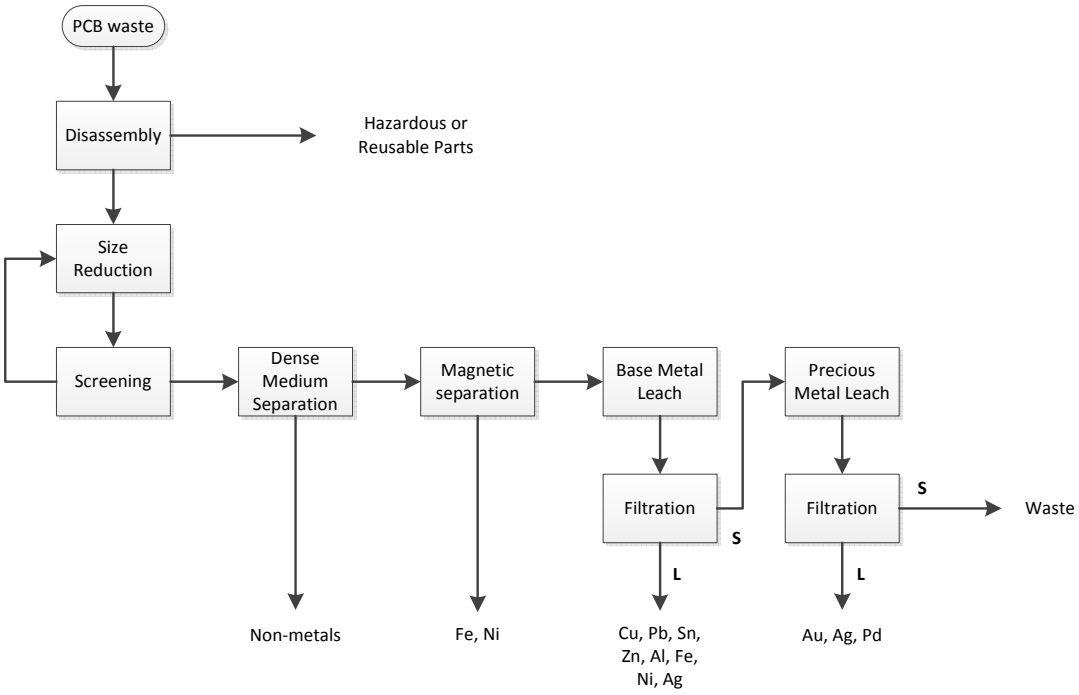

FIGURE 1: FIRST STAGES OF PCB WASTE TREATMENT

2.2. DISASSEMBLY OF WASTE PCBS

Before size reduction and subsequent processing, hazardous and reusable components need to be removed from the PCB waste. The disassembly of highly valuable components such as PCBs, engineering plastics and cables simplify subsequent recovery of material by producing more defined streams [26]. Dismantling allows for the pre-concentration of valuable metals [19] as well as extensive removal of impurity metals (such as Pb, Sb, Tl, and Fe) to low levels. This potentially benefits leaching by reducing acid consumption and may benefit downstream processes by the likely elimination of an expensive solution purification stage [22].

The majority of waste electric and electronic equipment (WEEE) were designed without any consideration of recycling issues. Product design at present and in the future will increasingly incorporate "Design for disassembly" principles [26]. This is aimed at simplifying end-of-life material recovery.

Disassembly of electronic equipment is conducted manually, automatically or by immersion to dissolve solder.

2.2.1. MANUAL DISASSEMBLY

Manual dismantling of WEEE is the most common form of dismantling [1,26,27]. Manual disassembly is costly [26] and may not be economically viable and projects are underway which attempt to automate or at least semi-automate the disassembly process [27]. Most observers see a continuing reliance on manual disassembly, at least in the short term [26].

Manual sorting involves the classification of WEEE into high- and low grade material; this is followed by the removal of capacitors and hazardous components such as batteries [26]. In practice, disassembly may either be partial or complete. Partial disassembly entails the removal of only a part or subassembly of components. Complete disassembly involves the separation of the product into all of its components.

In practice, selective disassembly is an integral part of the disassembly process as the reuse of components enjoys priority. The disassembly strategy may be either destructive or non-destructive [28]. Non-destructive disassembly includes recovery of reusable parts whereas destructive disassembly separates material types for recovery [28].

2.2.2. DISSASSEMBLY BY IMMERSION

Yang et al. (2011) removed welding-jointed electronic components from the PCB by treatment with dilute nitric acid [29]. Tin in the solder reacts with the nitric acid to form insoluble stannic acid, while the lead reacts with nitric acid to form soluble lead nitrate [29]. Tin and lead is therefore separated. The tin may be recovered from the stannic acid in subsequent processing steps. The lead ions in the leaching solution can be precipitated as $PbSO_4$ by adding sulphuric acid.

The objectives of dismantling with immersion are to dissolve (and recover) solder (consisting of Pb and Sn) to enable removal of the solder-attached components. The early recovery of solder in the recycling process eliminates the adverse influence posed by solder in the recycling of other metals, especially noble metals [30]. The leaching of copper at this stage is to be avoided. Copper is present in the middle layer of the boards and is therefore not significantly exposed to the nitric acid solution whilst there is still undissolved solder present [29]. The leaching of copper can be avoided by controlling the nitric acid concentration and immersed time [29]. This will necessitate the determination of optimum immersion time for the PCBs during which complete dissolution of lead is achieved without significant dissolution of copper. The boards contain mainly metal copper after this pre-treatment [29].

2.2.3. THERMAL DISASSEMBLY

Zhou and Qui (2010) recovered solder from whole WPCBs by immersion in hot diesel oil [30]. A rotating perforated drum was filled with PCB waste and immersed in oil at 240°C. The solder melted and the centrifugal force removed the molten solder from the WPCBs. Complete separation of solder was achieved at drum rotation of 1400 rpm for 6 min intermittently. Due the solder being immersed in oil during the recovery process, the chemical properties of the solder remained unchanged. The solder could therefore be reused directly or serve as a resource of lead and tin refining [30].

2.2.4. AUTOMATIC DISASSEMBLY

Disassembly of WEEE is almost exclusively a manual process at present and is therefore expensive. Automation of disassembly will greatly improve the profitability of the whole recycling process [26]. The greatest challenge facing automated disassembly is the heterogeneity of electronic waste. Manual removal of hazardous and reusable parts is followed by the identification of objects of interest by optical imaging equipment using identification algorithms. Local heat application and force is used to remove these items [27].

2.3. SIZE REDUCTION

In PCBs, metallic elements are mostly encapsulated by plastics or ceramics; a mechanical pre-treatment process is required to liberate the metals to facilitate an efficient extraction with acid or alkali [2,6]. Size reduction of WPCBs liberates metal from non-metal [31]. This is a key process, since comminution affects the efficiency of the subsequent mechanical separation [6,32,33]. A co-effect of size reduction is an increase in specific surface area of the material. A large specific surface area is ultimately beneficial for rapid and complete leaching of metals.

Size reduction generally improves separation efficiency as most separation equipment is designed for material showing homogeneity in physical characteristics. The cost of size reduction escalates as the particle size decreases [26].

Size reduction is generally carried out by impacting, shearing, milling, pulverisation or shredding. These operations are generally referred to simply as 'shredding'. The extent of size reduction (and resulting liberation) obtained from the equipment is a function of equipment design – mainly hammer speed. The power requirement of the equipment is related to feed composition, shredder geometry and particle size.

Due to PCBs being comprised of metals and reinforced resin, they have a high tenacity and hardness. This makes general crushing machines that depend on extrusion forces ineffective for inducing liberation of metals on PCBs [31].

The mixed characteristics of the waste mean that shearing forces are likely to result in the minimum energy expenditure to effect the desired size reduction. For this reason, hammer mills are common size reduction machines in resource recovery [31,34].

A two-step crushing procedure has been identified as an effective method of WPCB comminution [31]. This two-step crushing procedure involves crude crushing (using a jaw-, cone-, impact- or roll crusher) followed by pulverisation (using a globe mill, autogenous tumbling mill, or vibratom).

Table 2 from Das et al. (2009) shows the liberation of metals and gangue as a function of decreasing particle size [23]. PC waste was comminuted to below 500 µm and classified into size classes where after a microscopic liberation analysis was performed. It is noted from Table 2 that the percentage of metals also decreases as the particle size decreases.

TABLE 2: MICROSCOPIC LIBERATION DATA OF COMMINUTED PCB WASTE [23]

Size class (µm)	Liberated metal (%)	Interlocked (%)	Liberated gangue (%)
500-300	20.08	7.87	72.05
300-250	15.3	5.73	78.96
250-150	13.6	3.75	82.65
150-100	12.3	1.94	85.76
100-75	9.37	0	90.62
75-44	4.58	0	95.42
<44	-	-	-

Table 2 shows that decreasing particle size eliminates interlocked metal and gangue. Complete liberation of metals was seen to occur at particle size <100 µm. Due to the heterogeneity and the different sources of PCB waste, the particle size at which complete liberation is achieved may differ from that stated in Table 2. Consequently complete liberation of metals from non-metals in PCB waste has been detected at various particle sizes. Table 3 shows several different reported particle sizes said to have yielded either sufficient liberation for metals recovery. The difference in reported particle sizes is significant. Sufficient liberation has been reported for particle sizes ranging from 500 µm to 5000 µm.

TABLE 3: PARTICLE SIZES OF COMMINUTED PCB WASTE REPORTED TO YIELD COMPLETE LIBERATION OF METALS FROM NON-METALS

Author	Particle size at which liberation of metals from non-metals was achieved
Li, Lu et al. 2007	<0.6mm
Zhang, Forssberg 1997	<2mm
He, Li et al. 2006	<3mm
Eswaraiah, Kavitha et al. 2008	<1mm
Wu, Li et al. 2008	<0.6mm
Cui, Forssberg 2003	<5mm
Jiang, Jia et al. 2008	<0.6mm
Zhang, Forssberg 1998	<3mm
Wen, Zhao et al. 2005	<0.5mm
Veit, Diehl et al. 2005	<1mm

Several thermal treatments are available to aid the size reduction. In general, thermal treatments reduce the amount of energy required to perform size reduction and are performed as a pre-treatment to the size reduction process. Thermal treatments include the following:

Cryogenic embrittlement – Material is cooled to below the ductile-brittle transition temperature for metals as well as to below the glass transition temperature for polymers. The cooling is followed by size reduction. By inducing brittleness, material is fractured more readily. The embrittlement is induced using liquid nitrogen for the cooling [29].

Thermally assisted liberation (TAL) – Improved metal-plastic liberation can be achieved by heating the electronic scrap to 250°C followed by air quenching prior to size reduction and screening [34,35].

2.4. MECHANICAL SEPARATION

Mechanical separation is applied to electronic waste in order to reduce feed volume while simultaneously concentrating or enriching the valuable materials. In order to conduct physical separation, some physical property of the material needs to be selected to base the separation on, such as density, conductivity, magnetism, particle size, etc. [32]. The separation device exploits differences in the selected property in order to perform the desired separation. The heterogeneity of PCBs means that many physical separation processes exist which could potentially be used for feed volume reduction and concentration of valuable metals. Das et al. (2009) identified several properties of metals and non-metals contained within PC wastes which could potentially be used for separation [23]. These properties are summarised in Table 4.

TABLE 4: COMPARISON BETWEEN BENEFICIATION CRITERIA AND THE CONSTITUENTS [23]

PCB species	Specific gravity	Electrical conductivity	Hydrophobicity	Abundance in feed	Concentration criteria
Metals	High	Very high	Very low	High in coarse	Desliming, flotation, gravity, electrostatic
Non-metals	Low	Very low	High	High in fines	

Mechanical separation is of particular interest in metals recovery from waste PCBs for upgrading the concentration of valuable materials [1]. Hydrometallurgical extraction can be made simpler and more efficient by the attainment of higher grade metallic concentrates [6]. Unlike chemical processing, mechanical processing can be applied in such a way as to not bring forth secondary pollution such as harmful liquids or gasses [31,36]. Many previous studies have been done investigating the use of mechanical processing for metals recovery from electronic scrap [1,6,23,31,33,36-39].

2.4.1. CLASSIFICATION BY SIZE

The degree of liberation, particle size and particle shape are crucial parameters in mechanical separation. Size reduction equipment does not typically produce homogenously sized particles. Almost all mechanical recycling processes have an optimum size range where they are most effective [1]. Matching fragment size to the sorting process can significantly increase recovery efficiency [26].

Screening is therefore used to produce a stream of uniformly sized feed to a certain mechanical separation process [1]. Screening in metals recovery is applied by a rotating screen. Vibrating screens have also been used for screening, although the problem of wire blinding has been reported.

Zhao et al. (2004) investigated the effect of particle size on pneumatic separation and electrostatic separation [40]; both electrostatic- and pneumatic separation showed significant differences in copper recovery for the different size classes. It appeared that optimum particle size classes existed for pneumatic- and electrostatic separation. The work entailed the determination of optimum air velocities for each size class; this implies that using particles of non-uniform size would likely result in either poor separation or significant losses of metals to the tailings.

Different size classes of milled PCB waste have been shown to possess different distributions of metals [1,6,8,23,29,41-43]. The grade of metallic components in the particles has been shown to be higher with increasing particle size [6,23,43], while the degree of liberation has been shown to increase with decreasing particle size [23,40].

Das et al. (2009) suggested the removal of ultra-fine particles from the recovery process by classification due to its low metal content [23]. Figure 2 shows how metal concentration has been found to diminish for smaller particle size classes.

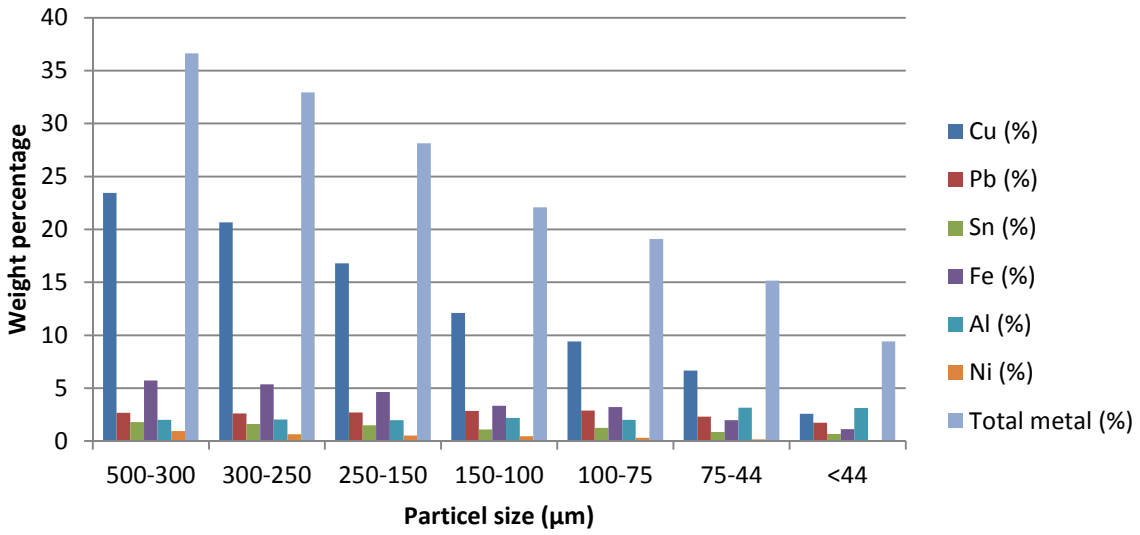

FIGURE 2: METAL DISTRIBUTION BETWEEN RESPECTIVE SIZE CLASSES OF COMMINUTED PCB WASTE [23]

The brittleness of non-metals (mostly resin, epoxy and ceramics) makes them easier to mill and therefore more prone to report to finer size fractions. The metals are inherently more ductile and therefore more difficult to mill compared to the brittle non-metals. Therefore the smaller size fractions are seen to be being made up of mostly non-metals and the larger size fractions containing the bulk of the metals (see Figure 2).

2.4.2. ELECTROSTATIC SEPARATION

The difference in electro-conductivity and density of metals and non-metals make for suitable conditions for the application of corona electrostatic separation [23]. Compared to air-current separation (which may release dusts) and fluidised bed separation (which may produce heavy metal rich waste water), corona electrostatic separation does not have any harmful environmental implication. Moreover, corona electrostatic separation is less energy intensive than both the former processes [31].

The corona electrostatic separation works by generating a high-voltage electrostatic field. The non-metal and metal particles entering the field are subjected to ion bombardment and electrostatic induction respectively. The conducting metal particles discharge rapidly to the earthed electrode and detach from the rotating roll.

The charged non-metal particles remains pinned to the rolling drum separator. This continues to happen so long as the electric image force (F_i) is greater than the sum of gravitational (F_g) and centrifugal (F_c) forces acting on the particle [31]:

$$F_i \geq F_g + F_c \qquad (2.1)$$

Separation is therefore achieved based on the difference in interaction of the electric field with conducting and non-conducting particles. Figure 3 shows the workings of a typical electrostatic separation machine: a roll-type corona electrostatic separator (RTS).

The RTS produces a middling fraction. The middling fraction forms due to faulty charging of particles. Fine particles of conductive and non-conductive nature may coalesce [40,44]. This coalescence phenomenon makes separation of fines by either electrostatic [44] or pneumatic

separation non-ideal [40]. The coalescence of fines mean that some trapped conducting material will wrongfully report to either middling or non-conducting fractions. This results in loss of valuable metals and will add to impurities in the non-conductive fraction. The middling fraction generally has a metal content of more than 50% and therefore requires further treatment [44].

Particle size influences separation performance [44]. Larger particles obtain small specific charges and therefore experience a small electrical pinning force. Their relatively larger mass results in a larger centrifugal force which may overcome the pinning force. This results in the coarse, non-conducting particle wrongfully reporting to the conducting fraction [39]. A particle size of between 0.6 mm and 1.2 mm has been noted as the most feasible for industrial application of corona electrostatic separation to separate metals from non-metals in PCB waste [18].

The pinning of large non-conductive particles to the drum can be enhanced by decreasing centrifugal force acting on the particle by decreasing the rotor speed. Pinning can also be increased by increasing the image force of the electrode system. The main parameters affecting separation are rotor speed, high voltage, particle size and interaction between high voltage and moisture or temperature [39].

Wu et al. (2008) re-applied electrostatic separation to the middling and non-conductive fractions of primary electrostatic separation. Significant improvement of metal recovery, a decrease in midling fraction by 45% and purification of the non-conductive fraction was achieved [44].

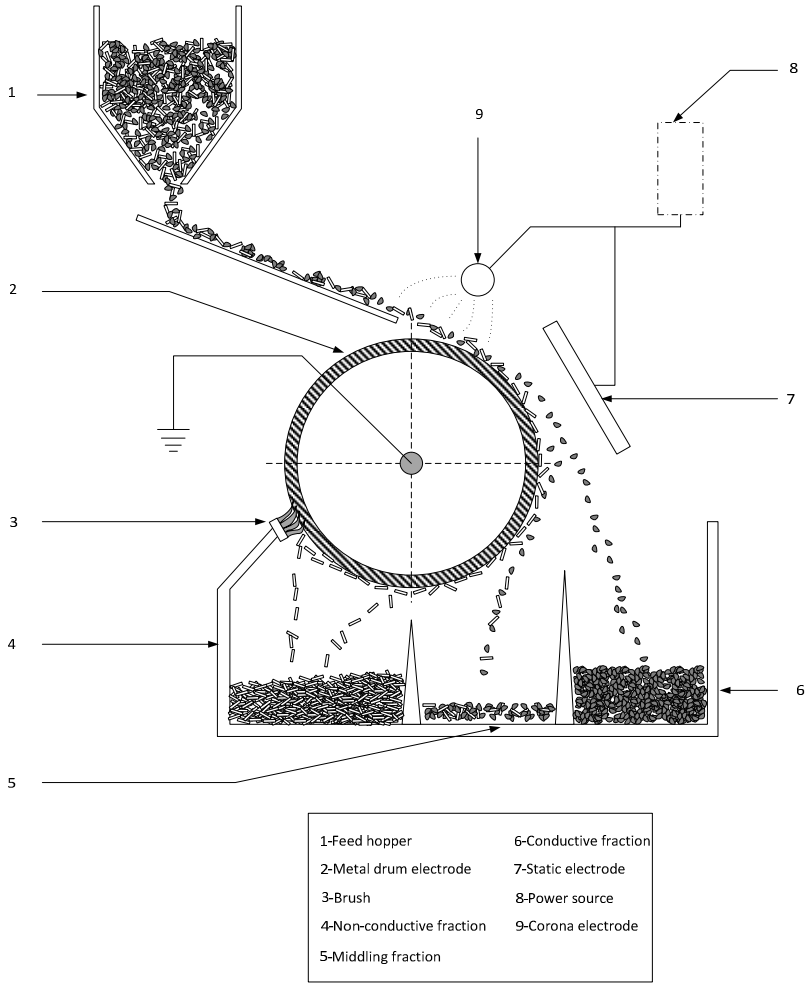

FIGURE 3: OPERATION OF A ROLL-TYPE CORONA ELECTROSTATIC SEPARATOR, REDRAWN [37]

2.4.3. MAGNETIC SEPARATION

Magnetic separation is used to separate ferromagnetic metals from non-ferromagnetic metals and non-magnetic material [32,45]. Rare earth alloy permanent magnets are capable of producing very high field strengths; this has led to advances in the design and operation of magnetic separators [1].

Material can be classified as diamagnetic, paramagnetic or ferromagnetic. The classification can be made based on the magnetic susceptibility of the material in question.

Diamagnetic materials include copper, gold, lead, silver, tin and zinc. These materials have a small negative susceptibility to an external magnetic field. Diamagnetic materials are slightly repelled by a magnetic field. They do not retain magnetic properties once the magnetic field is removed.

Paramagnetic materials include aluminium and magnesium. These materials slightly attracted by a magnetic field and have a weak positive magnetic susceptibility. Paramagnetic materials also do not retain magnetic properties once they are removed from a magnetic field.

Ferromagnetic materials include iron, nickel and cobalt. These materials have a large positive magnetic susceptibility. Ferromagnetic materials display a strong attraction to a magnetic field and are able to retain magnetic properties once removed from a magnetic field. Table 5 shows the magnetic susceptibility of several metals typically present in electric and electronic equipment.

TABLE 5: MAGNETIC SUSCEPTIBILITIES OF TYPICAL METALS FOUND IN ELECTRIC AND ELECTRONIC EQUIPMENT

Metal	Magnetic Susceptibility $\chi_m / 10^{-6}\ cm^3 mol^{-1}$
Aluminium	16.5
Copper	-5.46
Gold	-28
Iron	Ferro.
Lead	-23
Magnesium	13
Nickel	Ferro.
Silver	-19.5
Steel alloy	Ferro.
Tin	-37.4
Zinc	-9.15

Due to their high magnetic susceptibility, ferromagnetic materials such as iron, cobalt and nickel can be removed from comminuted electronic waste by magnetic separation [37]. Veit et al. (2005) showed that the amount of magnetic material contained within WPCBs may be small (see Table 6), but variable (see Table 1). The amount of iron remaining in the non-magnetic fraction was not reported.

Figure 4 shows the operation of a typical magnetic separation device.

TABLE 6: MASS FRACTION OF THE SAMPLE THAT REPORTED TO THE MAGNETIC FRACTION DURING MAGNETIC SEPARATION- CALCULATED FROM RESULTS OF VEIT ET AL. (2005) [37]

Sample size	% of sample that reported to the magnetic fraction (Printed circuit boards)	% of sample that reported to the magnetic fraction (Electronic components)
<0.25mm	0.82	1.23
0.25mm – 0.5mm	2.12	4.14
0.5mm – 1mm	3.16	4.22

It seems that magnetic separation is therefore not applied to significantly reduce feed volume, but rather to remove iron from the copper stream. The removal of iron prior to leaching would lead to a clean leach solution, therefore reducing downstream purification efforts. Magnetic separation has been shown to be inefficient for particle sizes larger than 5mm [42].

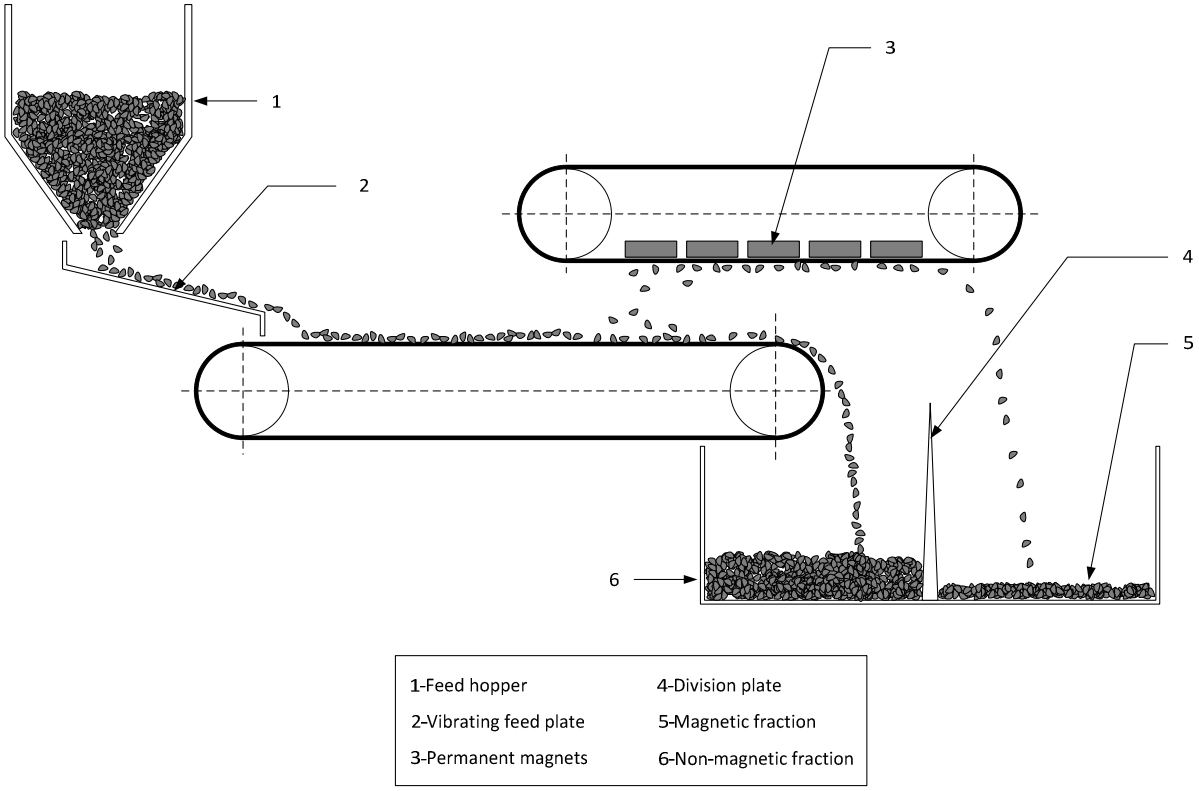

FIGURE 4: OPERATION OF A CONTINUOUS MAGNETIC SEPARATOR, REDRAWN [46]

A mixture of magnetic and non-magnetic material is fed via a vibrating feeder. The vibrating feeder ensures that the particles are spread out widely and evenly as they enter the magnetic separator. The material stream is exposed to a magnetic field. The magnetic materials (mainly iron and nickel) are attracted by the magnetic field and sticks to the overhead conveyor. The magnetic material then reports to a separate fraction thereby achieving magnetic based separation (please see Figure 4).

2.4.4. GRAVITY SEPARATION

Gravity separation is conducted based on a difference in density between particles. In the case of PCBs, the particles with high metal content will be denser than those particles consisting mainly of ceramics or plastics. Gravity separation therefore separates a light fraction from a heavy fraction.

Table 7 shows the densities of typical metals contained within electric and electronic equipment (EEE). Table 8 shows the densities of typical plastics encountered in EEE. It is seen from Table 7 and Table 8 that the densities of metals are generally significantly higher than that of the plastics. This confirms density based separation as a feasible basis for upgrading metal grade of PCB waste.

TABLE 7: DENSITIES OF TYPICAL METALS USED IN ELECTRIC AND ELECTRONIC EQUIPMENT [1]

Metal	**Specific gravity**
Gold	19.32
Lead	11.34
Silver	10.49
Copper	8.93
Nickel	8.90
Cu-Zn alloy (Ms 58)	8.40
Brass (Fe-free)	8.40
Steel alloy	7.70
Tin	7.29
Zinc	6.92
Aluminium	2.70
Magnesium	1.74

TABLE 8: DENSITIES OF TYPICAL PLASTICS USED IN ELECTRIC AND ELECTRONIC EQUIPMENT [1]

Plastics	**Specific gravity**
Polyesters (PET & PBT)	1.35
Polyvinyl chloride (PVC)	1.27
Polycarbonates (PC)	1.22
Nylon and Polyamide (PA)	1.14
Acrylonitrile butadienestyrine (ABS)	1.04
Polystyrene (PS)	1.04
Elastomer (SBR, neoprene, silicone, etc.)	1.04
Polyethylene (PE)	0.94
Polypropylene (PP)	0.90

Several types of gravity separation have been used for enriching metals grade of PCB waste. These include air classification [6,10,39,40], dense medium separation [23,33,34,41] and cyclone separation [32,47].

2.5.4.1. AIR CLASSIFICATION

Air classification separates particles based on differences in their terminal velocities. Newton's law may be used for the estimation of the particle settling velocity in turbulent flow [36], i.e. when the Reynolds number is above 4×10^3:

$$v_t = 1.74\left[\frac{(\rho_p - \rho)gd}{\rho}\right]^{0.5} \quad (2.2)$$

Equation 2.2 above shows the dependence of terminal settling velocity on both the particle density (ρ_p) and particle diameter (d). This implies that if separation is to be conducted based purely on a difference in densities, particle size should be held constant. Therefore air separation is conducted on closely sized feed [6,39,40]. This feed is separated into closely sized fractions beforehand and separation is conducted separately at appropriate respective air velocities. An air velocity should be selected that is higher than terminal velocity of the light fraction (non-metals) and lower than the terminal velocity of the heavy fraction (metals).

Air classification is typically conducted in a zig-zag classifier or an air table. Results from previous work performed by Yoo et al. (2009) imply that air classification is not an especially effective method of increasing metallic grade of PCB waste [6]. Significant increase in the metallic grade occurred only with particle size smaller than 0.6mm; however, metal losses of 40% were sustained during this enrichment [6]. Results from Zhao et al. (2004) showed for particle size 0.25 mm to 1 mm that any significant enrichment of copper grade via pneumatic separation occurred at the expense of good recovery [40]; for this size fraction copper losses of between 29% and 37% were reported with copper grade increase of only between 15% and 25%.

For the separation of coarse and irregular particles, electrostatic separation is more suitable than pneumatic separation [40].

2.5.4.2. DENSE MEDIUM SEPARATION

Dense medium separation, also known as sink-float separation, involves the creation of a fluid with a specific density which is intermediate to that of the metals and non-metals. This dense medium would encourage materials with a given specific gravity to either float or sink, thus establishing a density based separation [34].

In the case of electronic scrap, a dense fluid will be created that has a density higher than that of the non-metal fraction (these include plastics, epoxy resin and ceramics) and lower than that of the metals. Castro and Martins (2009) separated non-metals from metals using water [48], but more typically, a heavy organic liquid is used as the dense medium [36]. Zhang et al. (1997) and Veit et al. (2002) used tetra bromoethane (SG=2.97) as the dense medium and diluted it with acetone to a specific gravity of 2.5 in order to separate metals from plastics [33,41]. The addition of acetone also serves to lower the viscosity of the medium. Das et al. (2009) used pure bromoform with a specific gravity of 2.81 and reported that all plastics floated and metal bearing particles sank [23]. Poor settling kinetics for small size particles were observed [23]. With an appropriately chosen dense medium, effective separation of metals from non-metals can be achieved [33,41].

2.5. ACID LEACHING OF PRINTED CIRCUIT BOARDS

Leaching is the process of using a solvent to extract a soluble constituent from a solid [49]. Metals in WEEE are present in their native form or in alloy. This is of practical significance for the development of a suitable leaching process. An oxidative leaching process is generally required for the effective recovery of base and precious metals [19].

2.5.1. LIXIVIANTS

Numerous different leaching agents exist and they can be divided into the following categories: acids, bases and aqueous salt solutions. Acids are the most common leaching agents. The choice of a suitable lixiviant depends on the following factors [49]:

- Solubility: It is desired to have rapid and large solubility of the material in the leaching agent.
- Cost: The leaching agent should preferably be cheap so that losses of the leaching agent do not result in jeopardising the economics of the process. Special materials of construction of process equipment required to handle the leaching agent may incur additional costs. The ability of a leaching agent to be regenerated may determine its rate of consumption and hence influence process costs.
- Selectivity: The ideal leaching agent will only extract the desired component.
- Environmental impact: It is desired to not negatively influence the environment through the use of the lixiviant. The environmental impact of both the lixiviant and the resulting products should be considered during selection.

Various mineral acids and oxidants have been extensively investigated for the acid leaching of metals from e-waste: HCl, H_2SO_4, HNO_3/H_2O_2, NaClO, $HClO_4$ [19]. Some of the leaching parameters tested in previous work are shown in Table 9.

Bioleaching of electronic waste has received some recent attention. Bioleaching processes are suitable for small scale application and treatment of low grade materials, but require long residence times for metal extraction and suffer from metal toxicity. Bioleaching may be considered as a first stage leaching process for sulphate media soluble metals; precious metals as well as lead will remain un-leached and will require further treatment [19]. Shen et al. (2013) reportedly used a cyanide producing bacteria, Chromobacterium violaceum, to leach Au from silica and pyrite containing ore[50].

TABLE 9: LEACHING PARAMETERS TESTED IN PREVIOUS STUDIES

Type of Scrap	Particle sizes	Temp.	Leaching Time	Leaching Reagents	Metals	Extent of leach	Ref.
Solder	<7mm at 10g/L	90°C	30-50min	HNO_3, HCl	Pb, Sn	99.9% Pb 99.9% Sn	51
WPCB	<0.208mm 50g per 500mL leaching solution	60°C	10, 20, 30, 60, 120min	2.18N H_2SO_4, 3N HCl, 2.18N H_2SO_4 + 3N HCl, 3N HCl + 1N HNO_3	Cu, Sn	93% Cu 98% Sn	48
WPCB	<0.075mm, 0.075-0.1mm, 0.1-0.25mm, 0.25-0.5mm, >0.5mm 250mL leaching solution S/L=1/25	40-70°C	120min	bmimHSO_4, H_2O_2 30wt%	Cu	99% Cu	43
Pure Pb & Solder	500mL S/L=1/100	90°C	10-120min	0.1–0.5M HNO_3	Pb	99.9% Pb	52
WPCB	2.5mm^2, S/L=100/300 g/cm^3	23°C & 80°C	15, 30, 60, 120, 240, 360min	1-6M HNO_3	Pb, Sn, Cu	99% Cu 70% Sn 99% Pb	24
MLCC	500-300µm, 300-180µm, 180-90µm, <90µm 500mL leaching solution S/L=5g/L	90°C	90 min	1M HNO_3, 0.5M H_2SO_4, 1M HCl	Ni	97% Ni	8
WPCB	8-4mm, 4-2mm, 2-1mm, 1-0.5mm, <0.5mm S/L=1/10 g/mL	~23°C	3 h-disassembly by immersion, 120-180 min	2M HNO_3 immersion, H_2SO_4, H_2O_2 (30wt%)	Cu	96% Cu	29
WPCB	<3mm Base metal leach: S/L=1/10 w/v Precious metal leach: S/L=2/100 w/v	30°C, 40°C, 50°C	3h	1M & 1.5M & 2M H_2SO_4, 10, 15, & 20 mL H_2O_2 (30wt%) [ml/100ml] Thiourea (for Au & Ag)	Cu, Fe, Zn, Sn, Au	76% Cu 77% Fe 26% Sn 99% Zn 69% Au	17
STVB	<250µm S/L=2-10%w/v	30-70°C	120 min	0.2-1M, 2M, 3M & 5M HNO_3	Cu, Ag	99.9% Cu 68% Ag	22
STVB	<100µm S/L=2g/150mL	32-68°C	4h	0.45-1.6M H_2SO_4, 0.2-0.8M H_2O_2	Cu	98.8% Cu	4
WPCB	<2mm S/L=25-150g/L	50-80°C	>5h	1.2-2M H_2SO_4, H_2O_2, O_2	Cu	100% Cu	53
Mobile phones	<0.3mm S/L= ¼ w/v	80°C	4.5 h	1.2M, 1.5M, 2M H_2SO_4, 0.015M Fe^{3+}, 80 L/kg/h O_2, H_2O_2 (continuously added)	Cu, Ag	99% Cu 32% Ag	20

2.5.1.1. LIXIVIANT TYPES

Several different lixiviants have been used for the leaching base metals from electronic waste. The most prominent lixiviants are discussed.

NITRIC ACID

Nitric acid is relatively expensive compared to sulphuric acid and hydrochloric acid [22,49]. Recent bulk price of nitric acid was 500 USD/ton while sulphuric acid was 200 USD/ton[54] (Alibaba 2015). This corresponded to nitric acid being approximately 3 times more expensive than sulphuric acid per mol.

Nitric acid is usually handled in stainless steel equipment. The salts from nitric acid decompose readily at low temperatures to form nitric oxides (NO and NO_2) which can be captured and absorbed into water to yield HNO_3 [22,49]. This means the acid can be recovered from waste solutions [24,49]. The simplicity of regeneration and re-use of HNO_3 makes it an attractive leaching agent.

Consumption of nitric acid can be decreased by the addition of sulphuric acid. This converts the nitrates to sulphates according to the following reaction:

$$M(NO_3)_2 + H_2SO_4 \rightarrow 2HNO_3 + MSO_4 \quad (2.3)$$

Nitric acid has strong oxidising properties and has the ability to corrode most base metals [24]. Nitric acid is a strong acid and therefore dissociates completely according to reaction equation 2.4:

$$HNO_3 \rightarrow NO_3^- + H^+ \quad (2.4)$$

The nitrate ions may then act as oxidising agent by accepting electrons according to the following half-reactions:

$$NO_{3\,(aq)}^- + 4H_{(aq)}^+ + 3e^- \rightarrow NO_{(g)} + 2H_2O_{(l)} \qquad E^o = 0.96\,V \quad (2.5)$$

$$NO_{3\,(aq)}^- + 2H_{(aq)}^+ + e^- \rightarrow NO_{2(g)} + 2H_2O_{(l)} \qquad E^o = 0.80\,V \quad (2.6)$$

Due to its higher relative reduction potential, the reduction of nitrate ions (see eq. 2.5 and 2.6) can electrochemically sustain the oxidation of most base metals (Cu, Pb, Sn, Ni, Co, Fe and Zn), while not oxidising precious metals (Au, Pt and Pd). The reduction potentials of some prominent metals present in waste PCBs are displayed in Table 10.

TABLE 10: STANDARD REDUCITON POTENTIALS AT 25°C

Reduction half-reaction	Standard reduction potential at 25°C
$Au^{3+}_{(aq)} + 3e^- \rightarrow Au_{(s)}$	$E^o = +1.5\,V$
$Pt^{2+}_{(aq)} + 2e^- \rightarrow Pt_{(s)}$	$E^o = +1.1\,V$
$Pd^{2+}_{(aq)} + 2e^- \rightarrow Pd_{(s)}$	$E^o = +0.95\,V$
$Ag^+ + e^- \rightarrow Ag_{(s)}$	$E^o = +0.80\,V$
$Cu^{2+}_{(aq)} + 2e^- \rightarrow Cu_{(s)}$	$E^o = +0.34\,V$
$Pb^{2+}_{(aq)} + 2e^- \rightarrow Pb_{(s)}$	$E^o = -0.13\,V$
$Sn^{2+}_{(aq)} + 2e^- \rightarrow Sn_{(s)}$	$E^o = -0.14\,V$
$Ni^{2+}_{(aq)} + 2e^- \rightarrow Ni_{(s)}$	$E^o = -0.25\,V$
$Co^{2+}_{(aq)} + 2e^- \rightarrow Co_{(s)}$	$E^o = -0.28\,V$
$Fe^{2+}_{(aq)} + 2e^- \rightarrow Fe_{(s)}$	$E^o = -0.44\,V$
$Zn^{+2}_{(aq)} + 2e^- \rightarrow Zn_{(s)}$	$E^o = -0.76\,V$

The tendency of lead to readily dissolve in nitric acid is confirmed by thermodynamic simulation. Figure 5 shows that lead dissolution is favourable at low pH values with or without the presence of an oxidising agent. The surface in Figure 5 represents undissolved lead. Decreasing the pH or increasing the concentration of an oxidising agent is seen to favour lead dissolution.

Jha et al. (2011) reported lead dissolution to be a strong function of nitric acid concentration [51]. Increasing nitric acid concentration yielded more complete leaching of lead [52]. A redrawn Figure 6 shows how nitric acid concentration affected the rate and extent of lead dissolution [51].

Figure 7 shows the effect of nitric acid concentration and temperature on Cu leaching as reported by Mecucci and Scott 2002. At 23°C and 1 M HNO_3, Cu extraction was minimal, reaching only 8% after 360 minutes. Copper extraction was seen to be increased with increasing temperature and increasing acid concentration. At 6 M HNO_3, however, temperature was seen to have little effect. The reason for this was not reported.

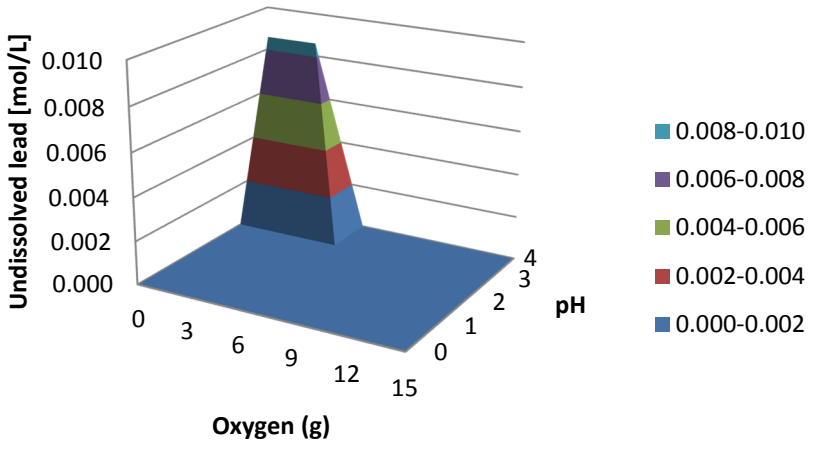

FIGURE 5: THERMODYNAMIC SIMULATION USING OLI SOFTWARE OF LEAD BEHAVIOUR AT 90°C WITH NITRIC ACID AND OXYGEN.

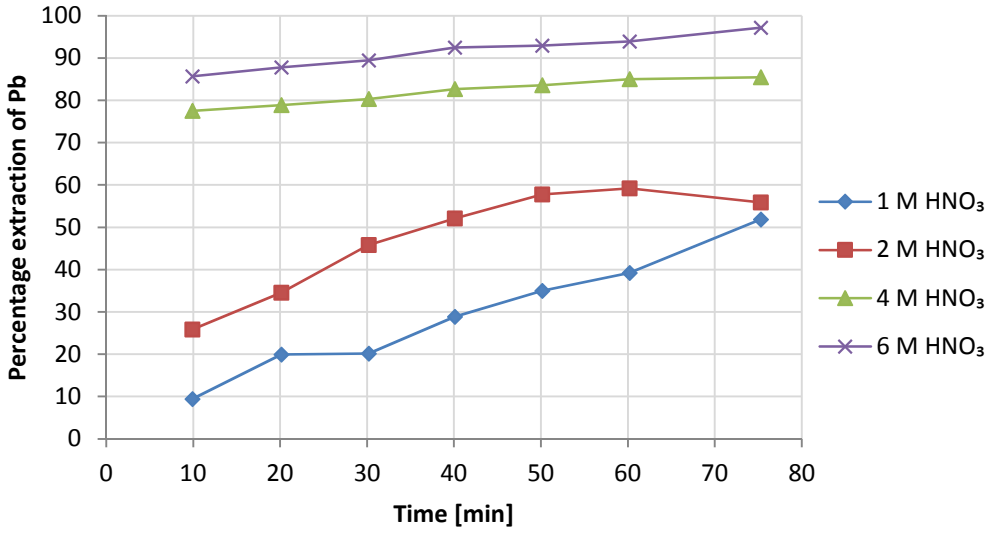

FIGURE 6: REDRAWN FIGURE OF LEACHING OF LEAD FROM SOLDER AT VARIOUS NITRIC ACID CONCENTRATIONS (WITH PULP DENSITY: 100 GRAMS/LITRE AND TEMPERATURE 90°C) [51]

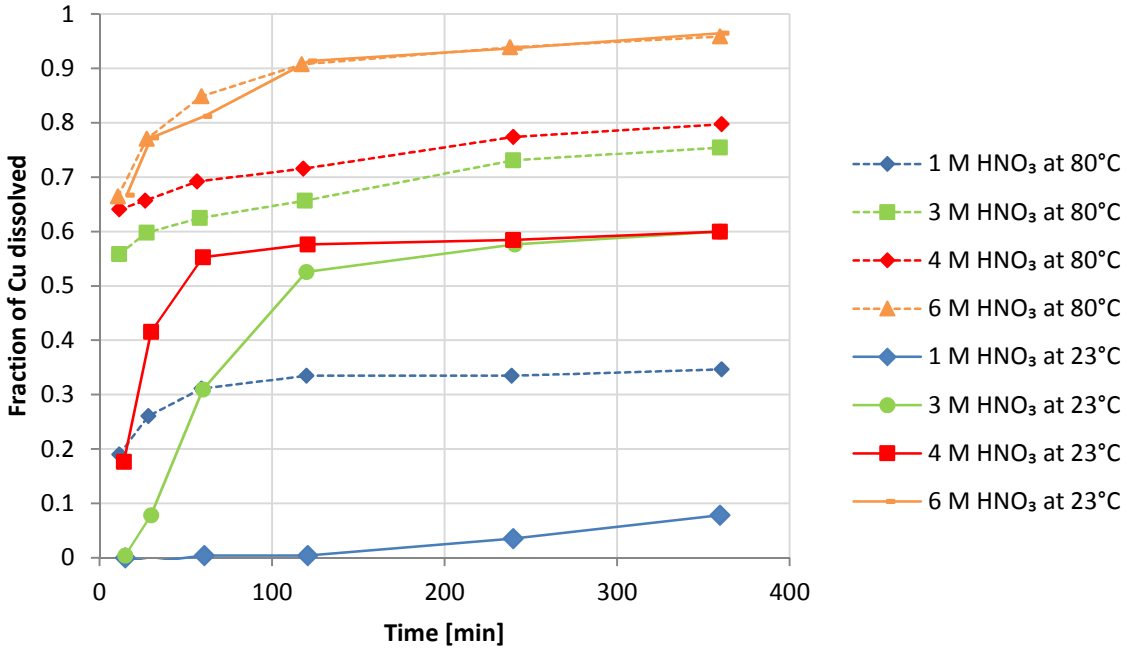

FIGURE 7: COPPER DISSOLUTION AT DIFFERENT CONCENTRATIONS OF NITRIC ACID AND DIFFERENT TEMPERATURES, SOLID TO LIQUID RATIO OF 1/3, RESULTS REDRAWN [24]

Bas et al. (2014) also reported Cu extraction to be a strong function of nitric acid concentration. The extraction of copper after 120 minutes was increased from 47.3% to 99.7% by increasing the nitric acid concentration from 1M to 5M at an S/L ratio of 0.6/10 at 70°C [22]. The same increase in nitric acid concentration also increased silver recovery from 14.4% to 68.2%. Nitric acid concentrations of $\geq 3M$ showed 99% recovery of copper after 120 minutes. The limited extraction of silver was attributed to its relatively high reduction potential (+0.8V) compared to that of Cu (+0.34V) (please see Table 10). The reduction potential of silver is similar to that of the nitrate ions (see eq. 2.5. and 2.6.). This may limit the nitrate ions' ability to oxidise silver. Higher

nitric acid concentrations or maintenance of a higher redox potential would be required for complete silver extraction [22].

Kim et al. (2007) attempted nickel leaching from multi layered ceramic capacitors (MLCCs) using HCl, HNO_3 and H_2SO_4 respectively [8]. The experiments were conducted without the addition of an oxidising agent. Nitric acid was clearly shown to be a more effective leaching agent for nickel recovery. Despite extensive use, hydrochloric and sulphuric acid are ineffective on their own and require the presence of a suitable oxidising agent [22].

Yang et al. (2011) treated whole waste PCB boards with dilute nitric acid (2 mol/L) to remove solder in order to disassemble mainboards. The treatment was done at 23°C for 3 hours and resulted in the formation of insoluble stannic acid and soluble lead nitrite [29].

Nitric acid has been found to be an especially suited leaching agent for lead [52]. High copper and lead extraction (>95%) was achieved by Mecucci and Scott (2002) using nitric acid [24]. The extractions were said to proceed according to the following equations:

$$3Cu^0 + 8HNO_3 \rightarrow 3Cu(NO_3)_2 + 4H_2O + 2NO \quad (2.7)$$

$$3Pb^0 + 8HNO_3 \rightarrow 3Pb(NO_3)_2 + 4H_2O + 2NO \quad (2.8)$$

$$Pb + 2HNO_3 \rightarrow Pb(NO_3)_2 + H_2 \quad (2.9)$$

The treatment of Sn with nitric acid may result in the formation of hydrous stannic oxide known as metastannic acid as shown in equation 2.10 [24,29]. Increasing nitric acid concentration to above 4 M leads to the formation of a passivating tin oxide film. This passivating film reduces the rate of tin dissolution and leads to the formation of metastannic acid [24]. The effect that this may have on lead dissolution was not reported. The precipitate can be removed by filtration or dissolved in hydrochloric acid [24,52]:

$$Sn + 4HNO_3 \rightarrow H_2SnO_{3(s)} + H_2O + 4NO_2 \quad (2.10)$$

Jha et al. (2011) also reported poor tin dissolution due to so called formation of salt [51]. Zinc and nickel react with nitric acid according to the following equations:

$$3Zn + 8HNO_3 \rightarrow 3Zn(NO_3)_2 + 4H_2O + 2NO \quad (2.11)$$

$$Ni + 4HNO_3 \rightarrow Ni(NO_3)_2 + 2H_2O + 2NO_2 \quad (2.12)$$

Kumari et al. (2010) reported the optimum leaching conditions for lead from solder using nitric acid to be 0.2 M at 90°C for 120 minutes at a S/L ratio of 1/100 [52]. The leaching reaction was found to be chemical reaction controlled. Mecucci and Scott (2002), however, found that the rate of lead dissolution increased with nitric acid concentration up to 6 M which was the maximum concentration tested. Results also showed lead dissolution occurring more rapidly at 80°C than at 23°C [24].

No studies were found where nitric acid was used in combination with a dedicated oxidising agent for the leaching of electronic waste treatment.

HYDROCHLORIC ACID

Hydrochloric acid is usually handled in rubber-lined equipment [49]. An oxidative environment is required for significant copper leaching since HCl is a non-oxidising acid and therefore no significant reaction is expected between Cu and HCl [55]. This is confirmed thermodynamically by positive reaction Gibbs energies [55]:

$$Cu + 2HCl_{(aq)} \rightarrow CuCl_2 + H_{2(g)} \qquad \Delta G^o_{80} = 92.58\frac{kJ}{mol} \qquad (2.13)$$

If oxygen is available to participate in the reaction, Cu is leached:

$$4Cu + 4HCl_{(aq)} + O_{2(aq)} \rightarrow 4CuCl_{(aq)} + 2H_2O \qquad \Delta G^o_{80} = -63.5\frac{kJ}{mol} \qquad (2.14)$$

Unlike Cu, Sn is leached with- and without the aid of an oxidising agent:

$$Sn + 2HCl_{(aq)} \rightarrow SnCl_2 + H_{2(g)} \qquad \Delta G^o_{80} = -56.1\frac{kJ}{mol} \qquad (2.15)$$

$$2Sn + 4HCl_{(aq)} + O_{2(aq)} \rightarrow 2SnCl_2 + 2H_2O \qquad \Delta G^o_{80} = -294.4\frac{kJ}{mol} \qquad (2.16)$$

Table 11 shows that the formation of most chloride salts of base metals are thermodynamically favourable.

TABLE 11: STANDARD REACTION GIBBS ENERGIES FOR THE FORMATION OF CHLORIDE SALTS

$2Ag_{(s)} + 2HCl \rightarrow 2\,AgCl_{(s)} + H_{2(g)}$	$\Delta G^o_r =$	-29	kJ/mol
$2Al_{(s)} + 6HCl \rightarrow 2AlCl_{3(s)} + 3H_{2(g)}$	$\Delta G^o_r =$	-685.8	kJ/mol
$Co_{(s)} + 2HCl \rightarrow CoCl_{2(s)} + H_{2(g)}$	$\Delta G^o_r =$	-79.2	kJ/mol
$Cu_{(s)} + 2HCl \rightarrow CuCl_{2(s)} + H_{2(g)}$	$\Delta G^o_r =$	14.9	kJ/mol
$Fe_{(s)} + 2HCl \rightarrow FeCl_{2(s)} + H_{2(g)}$	$\Delta G^o_r =$	-111.7	kJ/mol
$Ni_{(s)} + 2HCl \rightarrow NiCl_{2(s)} + H_{2(g)}$	$\Delta G^o_r =$	-68.4	kJ/mol
$Pb_{(s)} + 2HCl \rightarrow PbCl_{2(s)} + H_{2(g)}$	$\Delta G^o_r =$	-123.5	kJ/mol
$Zn_{(s)} + 2HCl \rightarrow ZnCl_{2(s)} + H_{2(g)}$	$\Delta G^o_r =$	-178.8	kJ/mol

Castro and Martins (2009) leached waste PCB boards without an oxidising agent from obsolete computers using 3 M hydrochloric acid [48]. Copper leaching was incomplete while tin leaching reached 89%. This is consistent with thermodynamic prediction. Kim et al. (2007) leached nickel without an oxidising agent and 1 M HCl achieved less than 40% nickel recovery after 90 minutes.

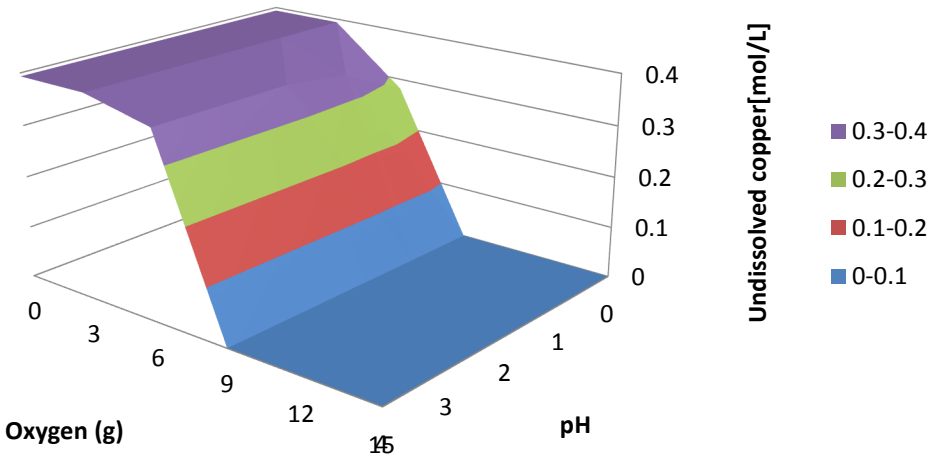

FIGURE 8: THERMODYNAMIC SIMULATION USING OLI SOFTWARE OF COPPER LEACHING AT 90°C WITH HYDROCHLORIC ACID AND OXYGEN. THE FIGURE SHOWS THE EFFECTS OF Ph AND OXYGEN PRESENCE ON THE DISSOLUTION OF COPPER.

The thermodynamic simulation shown in Figure 8 shows the inability of metallic copper to be leached with hydrochloric acid in the absence of oxygen even at pH 0. The surface in Figure 8 represents the concentration of undissolved copper. Copper is seen to dissolve as the presence of oxygen in the system is increased. The pH of the system does not seem to influence copper dissolution in the simulated range.

Castro and Martins (2009) leached tin and copper at 60°C with 3 M hydrochloric acid. The extent of tin dissolution reached 90% while copper dissolution reached only 33% [48]. The poor leaching of copper may be attributed to the absence of an oxidising agent.

Havlik et al. (2010) reported increased copper dissolution through application of thermal pre-treatment [55]. The increased dissolution was attributed to the formation of copper oxides. Copper oxides are well leached in hydrochloric acid as opposed to metallic copper:

$$CuO + 2HCl_{(aq)} \rightarrow CuCl_2 + H_2O \;\; \Delta G^o_{80} = \; -33.7 \frac{kJ}{mol} \qquad (2.17)$$

Spyrellis et al. (2009) performed a thermal pre-treatment at 500°C for 1h, to remove non-metals prior to leaching[7]. The pre-treatment was said to make for more effective dissolution; however, only 65% copper recovery was achieved using HCl. Leaching with nitric acid and sulphuric acid after thermal pre-treatment yielded 97.5% and 76.5% recovery, respectively. No mention was made of using an oxidising agent.

SULPHURIC ACID

Leaching of waste PCBs using sulphuric acid is generally performed with the aid of hydrogen peroxide as an oxidising agent. Oxygen produced from decomposed hydrogen peroxide (eq. 2.18) reacts with metallic copper forming cupric oxide (eq. 2.19); this reacts further with sulphuric acid to produce copper sulphate (eq. 2.20). Therefore hydrogen peroxide and sulphuric acid both together act as reactants in the leaching of copper[29] (please see Figure 9). The mentioned reactions were summed to produce the overall reaction shown in eq. 2.21:

$$H_2O_2 \rightarrow H_2O + \frac{1}{2} O_2 \quad (2.18)$$

$$Cu + \frac{1}{2} O_2 \rightarrow CuO + H_2O \quad (2.19)$$

$$CuO + H_2SO_4 \rightarrow CuSO_4 + H_2O \quad (2.20)$$

$$Cu + H_2O_2 + H_2SO_4 \rightarrow CuSO_4 + 2H_2O \quad (2.21)$$

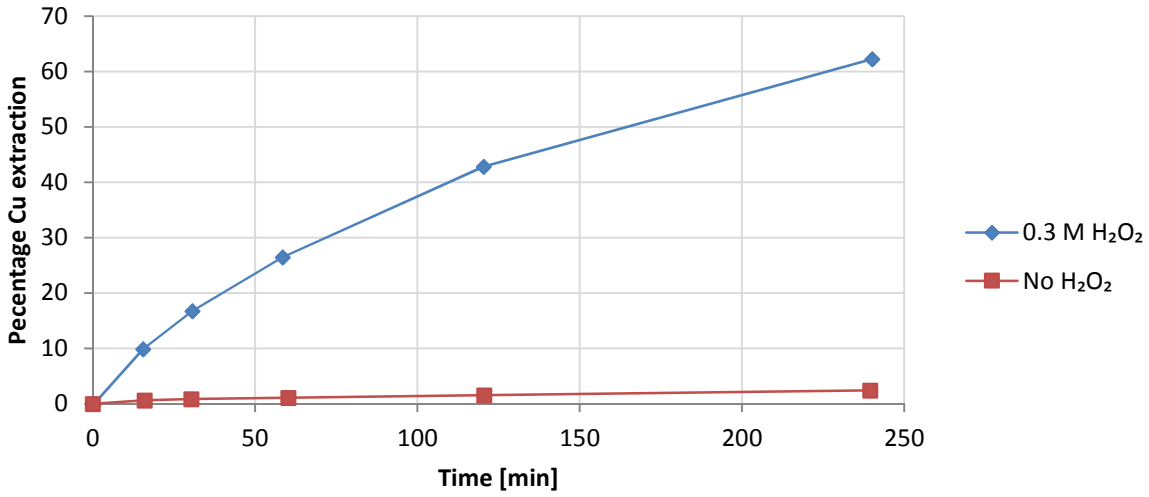

FIGURE 9: ENHANCEMENT OF COPPER EXTRACTION FROM SCRAP TV BOARDS IN THE PRESENCE AND ABSENCE OF H_2O_2 (0.3M) WITH 0.53 M SULPHURIC ACID AT 20°C REDRAWN [16]

Sulphuric acid leaching of waste PCBs has shown poor recovery of copper in the absence of an oxidising agent [19,48]. Results from Deveci et al. (2010) showed limited copper extraction of approximately 2% in the absence of an oxidising agent [16]. The lack of copper leaching in the absence of an oxidant was confirmed by a thermodynamic simulation conducted using OLI software.

The thermodynamic simulation was also used to predict the behaviour of lead during sulphuric acid leaching. The simulation showed complete conversion of all lead to lead sulphate in a sulphuric acid system irrespective of pH in the tested range of pH 0 to pH 4 or oxygen addition of 0 to 15 grams (20% excess oxygen).

The inability of sulphuric acid to leach lead is well known. In fact, lead-lined equipment is usually used when handling sulphuric acid. This is due the passivation-layer of protective lead sulphate that forms on the surface [49]. Lead sulphate formation was seen with and without an oxidising agent.

$$Pb^{2+}_{(aq)} + SO^{2-}_{4(aq)} \rightarrow PbSO_{4(s)} \quad (2.22)$$

The presence of appreciable amounts of iron leads to the formation of ferrous sulphate. Disposal of ferrous sulphate is achieved either by precipitation or crystallisation and decomposition [49].

Yang et al. (2011) leached copper using sulphuric acid and hydrogen peroxide. It was reported that increasing sulphuric acid concentration above 15 wt% (approximately 1.7 M) had no significant effect on copper dissolution. Increasing leaching temperature was reported to not significantly affect copper leaching due to the higher degradation rate of hydrogen peroxide and lower oxygen solubility at higher temperatures. The overall reaction of copper dissolution was reported to occur according to the following equation [29]:

$$Cu + H_2O_2 + H_2SO_4 \rightarrow CuSO_4 + 2H_2O \quad (2.23)$$

Copper recovery may be restricted by the solubility of $CuSO_4$ in sulphuric acid [29]. Figure 10 shows the solubility of copper sulphate and copper nitrate as a function of temperature. The solubility of copper sulphate is seen to be much lower than that of copper nitrate. This may necessitate the use of a lower relative solid to liquid ratio for a sulphuric acid leaching system.

Devici et al (2010) achieved >95% recovery of copper at 0.45M and 1.6M H_2SO_4 with 0.8M H_2O_2, 68°C at 2g per 150mL solution. Temperature and hydrogen peroxide were identified as the most influential factors. Quinet et al. (2005) leached 96.5% of copper using 2 M H_2SO_4 and hydrogen peroxide, however 30.6% co-extraction of silver was reported [20].

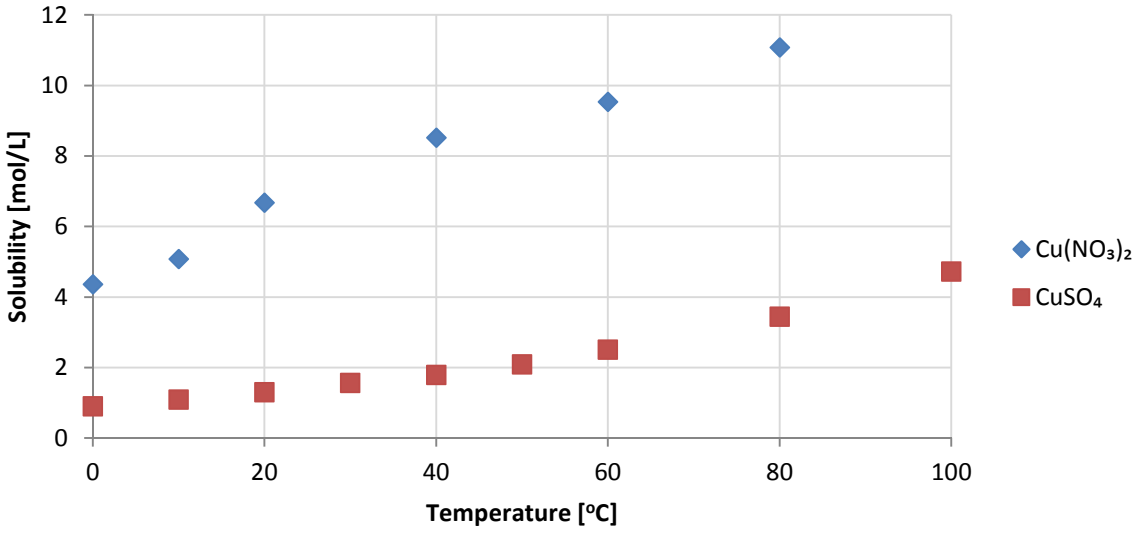

FIGURE 10: SOLUBILITY OF COPPER SULPHATE AND COPPER NITRATE IN WATER AS A FUNCTION OF TEMPERATURE, DRAWN FROM DATA TABLES [56]

Birloaga et al. (2014) compared different frequencies of hydrogen peroxide addition to the sulphate leaching system. The addition of all hydrogen peroxide at t=0 was compared to adding fractions at different set frequencies [57]. It was found that the most complete leaching of Cu, Zn, Fe and Al occurred when all the peroxide was added at the start of the experiment, i.e. at t=0 [57]. This observation was attributed to a higher oxidation potential achieved by adding peroxide at once.

COMBINATIONS OF LIXIVIANTS

Different leaching agents may be combined in order to improve dissolution of a desired material. Castro and Martins (2009) used a diluted mixture of nitric acid and hydrochloric acid and reported improved tin and copper recovery when compared to using only hydrochloric acid or sulphuric acid [48]. Figure 11, redrawn from Castro and Martins (2009), shows the rapid and complete extent of copper and tin dissolution with time using a mixture of nitric and hydrochloric acid.

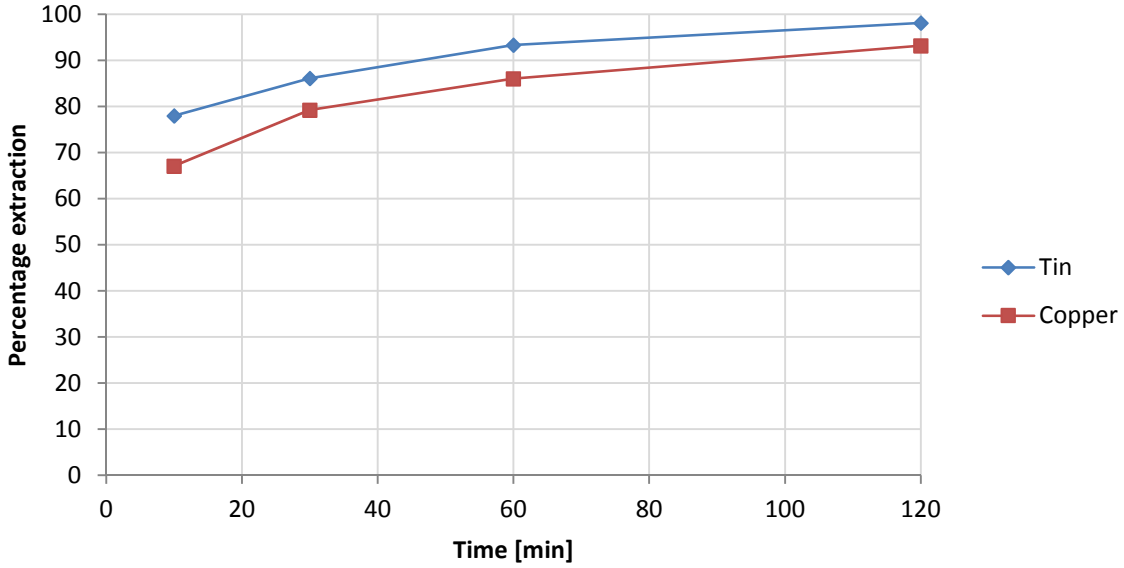

FIGURE 11: LEACHING USING A COMBINATION OF 3 MOL PER LITRE HYDROCHLORIC ACID AND 1 MOL PER LITRE NITRIC ACID, REDRAWN [48]

Aqua regia is also known as royal water due to its ability to dissolve gold (the most noble metal) [49]. Aqua regia is a mixture of one part concentrated nitric acid and three parts concentrated hydrochloric acid [24,49]. The main use of aqua regia is gold dissolution from alloys in refining processes. The dissolution action of aqua regia is due to the formation of nitrosyl chloride and chlorine according to the following mechanism [49]:

$$HNO_3 + 3HCl \rightarrow Cl_2 + NOCl + 2H_2O \quad (2.24)$$

$$Cl^- \rightarrow \frac{1}{2}Cl_2 + e^- \quad (2.25)$$

$$4H^+ + NO_3^- + 3e^- \rightarrow NO + 2H_2O \quad (2.26)$$

$$NO + \frac{1}{2}Cl_2 \rightarrow NOCl \quad (2.27)$$

Strong reducing and oxidising properties of aqua regia allows complete dissolution of base metals and precious metals [22,24]. Aqua regia is handled in glass containers.

2.5.1.2. THERMODYNAMIC SIMULATION OF LEACHING WITH DIFFERENT LIXIVIANTS

A simulation was conducted using OLI systems software in order to investigate thermodynamically favourable conditions for metal dissolution with different lixiviants:

- Nitric acid
- Hydrochloric acid
- Sulphuric acid

The simulated conditions were at 90°C and 1 atm. The specified feeds used are stated in Table 12. The feed material was chosen in such a way as to represent a situation where high concentrations of base metals and precious metals were present at metal to liquid ratio of 0.08. The reason for this was to investigate the selectivity of the leaching. The simulation determined the thermodynamically stable products that would result in the situation.

TABLE 12: FEED COMPOSITION TO THE THERMODYNAMIC SIMULATION

Feed to system	Mass (g)	Mol
Water	1000	55.55
Copper	25	0.39
Lead	5	0.024
Tin	5	0.042
Gold	5	0.025
Silver	5	0.046
Iron	5	0.089
Nickel	5	0.085
Zinc	5	0.076

The results from the simulation confirmed several reports from literature. The program database did not include metastannic acid, which would have been of particular interest to investigate. The results from the simulation are summarised graphically in Appendix B. The species which are not plotted in Appendix B were completely dissolved at the conditions examined according to the simulation.

2.5.1.3. REACTION CHEMISTRY

Acidic leaching may be non-oxidising, oxidising or reducing. When an acid's reaction involves only its hydrogen ion, then the reaction is considered non-oxidising. An oxidative acid has both hydrogen and its anion participating in the reaction. Nitric acid is an example as H^+ and NO_3^- often both participate in the reaction [49].

Table 13 shows that copper, gold and silver are reluctant to acidic leaching in the absence of an oxidising agent. A redrawn Figure 9 from Deveci et al. (2010) confirm the thermodynamic observation in Table 13 with regard to copper [16]. Figure 9 shows the inability of sulphuric acid to leach copper without an oxidising agent present.

This prompts consideration of a 2-stage leaching system, whereby the majority of low value metals (such as Al, Fe and Ni) may be leached under non-oxidative conditions, leaving behind Cu and precious metals. Cu is then leached in a second stage under oxidative conditions to yield a much purer Cu leach solution.

TABLE 13: THERMODYNAMIC DATA FOR OXIDATIVE AND NON-OXIDATIVE LEACHING OF METALS

Leaching in absence of oxidants		Oxidative leaching	
Reaction equation	ΔG_r^o	Reaction equation	ΔG_r^o
$Ag^0 + H^+ \rightarrow Ag^+ + \frac{1}{2}H_{2(g)}$	$77.1\frac{kJ}{mol}$	$Ag^0 + \frac{1}{4}O_2 + H^+ \rightarrow Ag^+ + \frac{1}{2}H_2O$	$-41.45\frac{kJ}{mol}$
$Al^0 + 3H^+ \rightarrow Al^{3+} + \frac{3}{2}H_{2(g)}$	$-485\frac{kJ}{mol}$	$Al^0 + \frac{3}{4}O_2 + 3H^+ \rightarrow Al^{3+} + \frac{3}{2}H_2O$	$-840.65\frac{kJ}{mol}$
$Au^0 + 3H^+ \rightarrow Au^{3+} + \frac{3}{2}H_{2(g)}$	$439.97\frac{kJ}{mol}$	$Au^0 + \frac{3}{4}O_2 + 3H^+ \rightarrow Au^{3+} + \frac{3}{2}H_2O$	$84.32\frac{kJ}{mol}$
$Cu^0 + 2H^+ \rightarrow Cu^{2+} + H_{2(g)}$	$65.5\frac{kJ}{mol}$	$Cu^0 + \frac{1}{2}O_2 + 2H^+ \rightarrow Cu^{2+} + H_2O$	$-171.6\frac{kJ}{mol}$
$Fe^0 + 2H^+ \rightarrow Fe^{2+} + H_{2(g)}$	$-78.9\frac{kJ}{mol}$	$Fe^0 + \frac{1}{2}O_2 + 2H^+ \rightarrow Fe^{2+} + H_2O$	$-316\frac{kJ}{mol}$
$Ni^0 + 2H^+ \rightarrow Ni^{2+} + H_{2(g)}$	$-45.6\frac{kJ}{mol}$	$Ni^0 + \frac{1}{2}O_2 + 2H^+ \rightarrow Ni^{2+} + H_2O$	$-282.7\frac{kJ}{mol}$
$Pb^0 + 2H^+ \rightarrow Pb^{2+} + H_{2(g)}$	$-24.4\frac{kJ}{mol}$	$Pb^0 + \frac{1}{2}O_2 + 2H^+ \rightarrow Pb^{2+} + H_2O$	$-261.5\frac{kJ}{mol}$
$Sn^0 + 2H^+ \rightarrow Sn^{2+} + H_{2(g)}$	$-27.2\frac{kJ}{mol}$	$Sn^0 + \frac{1}{2}O_2 + 2H^+ \rightarrow Sn^{2+} + H_2O$	$-264.3\frac{kJ}{mol}$
$Zn^0 + 2H^+ \rightarrow Zn^{2+} + H_{2(g)}$	$-147.1\frac{kJ}{mol}$	$Zn^0 + \frac{1}{2}O_2 + 2H^+ \rightarrow Zn^{2+} + H_2O$	$-384.2\frac{kJ}{mol}$

2.5.2. REACTION KINETICS

Mass transfer effects may significantly influence the kinetics in a leaching reaction. Three phases may be involved in the leaching process. They are the solid phase, leaching solution and gaseous phase (usually oxygen). Figure 12 shows the path of reactant and product during a typical leaching reaction involving these three phases.

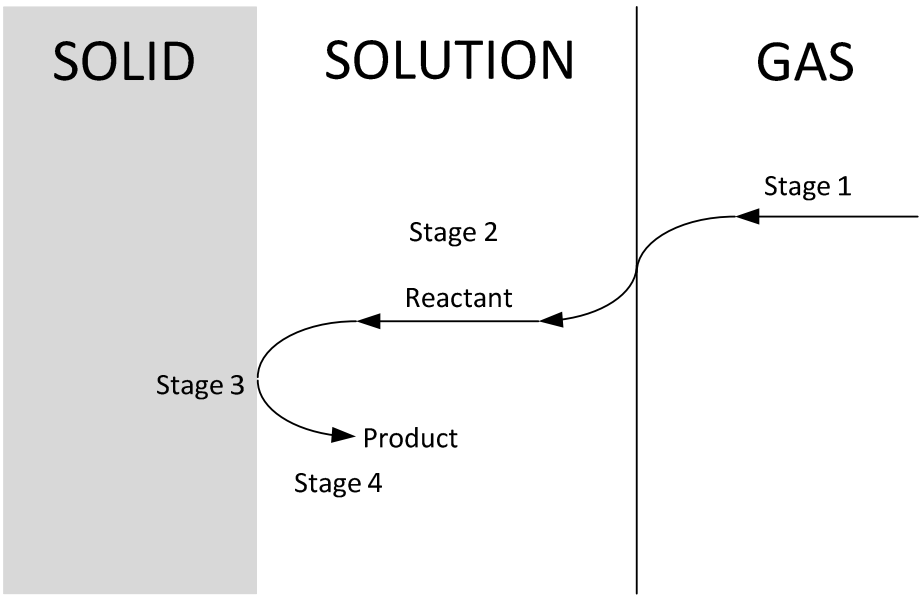

FIGURE 12: DIFFERENT STAGES IN A TYPICAL LEACHING PROCESS, REDRAWN [58]

In Figure 12, four stages in the leaching process is identified:

Stage 1: Gaseous reactant travels to the gas-solution interface and dissolves into the solution.

Stage 2: Reactant is transported through the solution phase to the solid-solution interface.

Stage 3: Chemical- or electrochemical reaction occurs at the solid-solution interface. This may include adsorption and desorption. If the reaction is electrochemical, ions and electrons travel across an electrical double layer.

Stage 4: Products are transported away from the interface to enter the solution bulk.

Any of the above mentioned stages may be the slowest, and therefore the rate determining stage. Usually the rate determining step is either stage 2 or stage 4, i.e. the diffusion stages. If this were to be the case then the reaction is said to be diffusion-controlled.

STAGE 1: DISSOLUTION OF GASEOUS REACTANT

If the oxidising agent is in the gaseous form, it must first be dissolved into the liquid phase. The dissolution reaction and its equilibrium constant are shown in eq. 2.25 and 2.26 below:

$$O_{2(g)} \leftrightarrow O_{2(sol^n)} \tag{2.28}$$

$$K_{sol} = \frac{[O_2]}{P_{O_2}} \tag{2.29}$$

The solubility of oxygen decreases with increasing temperature and the presence of other solutes. Oxygen used by the reaction must be sufficiently replaced in order for the reaction to continue. The rate of oxygen transfer into solution can be increased by vigorous agitation to increase interfacial area, as well as with a high oxygen partial pressure.

STAGE 2: DIFFUSION OF REACTANT THROUGH LIQUID SOLUTION

Figure 13 shows the typical concentration profile of reactant as a function of the distance from the solids-liquid interface.

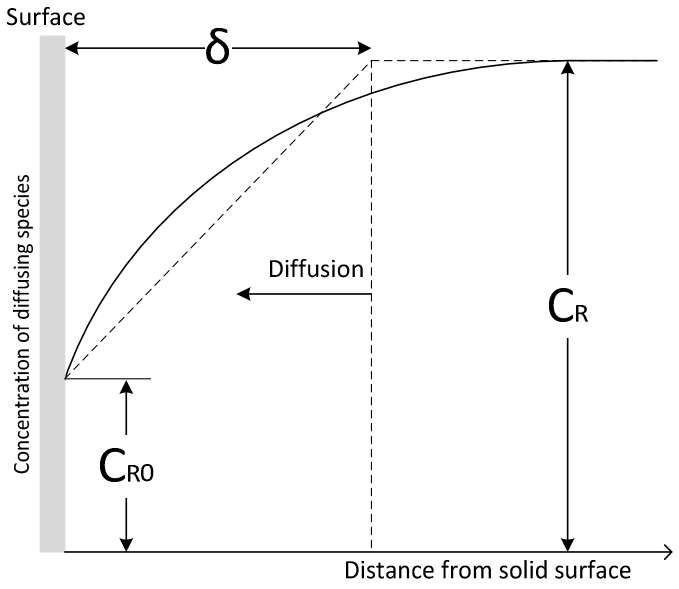

FIGURE 13: DIFFUSION OF REACTANT TO THE SOLID-SOLUTION INTERFACE

The reaction at the solid-solution interface causes the concentration of reactant to decrease as the interface is approached. The assumption of a linear concentration gradient allows application of Fick's first law of diffusion. The approximation is known as the Nernst Model. If a reaction is diffusion limited, Fick's first law reduces to the following:

$$\left(\frac{dn}{dt}\right)_R = \frac{D_R A c_R}{\delta} \tag{2.30}$$

Where $\left(\frac{dn}{dt}\right)_R$ is rate of reaction, D_R is the diffusion coefficient for the reactant through the boundary layer with thickness δ, A is the area and c_R is the concentration of reagent in the bulk fluid. A film diffusion controlled reaction will have the following kinetic equation [59]:

$$1 - (1 - x)^{\frac{2}{3}} = k_d t \tag{2.31}$$

Where t represents time, x represents the fraction of metal reacted and k_d represents the reaction constant for a diffusion controlled reaction. The reaction rate in a diffusion controlled reaction can therefore be increased be the following methods:

- Decreasing the particle size results in an increased specific surface area which favours faster diffusion.

Vigorous agitation may decrease the boundary layer thickness by as much as a factor of fifty, resulting in a rate increase by a factor of fifty (if the reaction is diffusion limited) [58].

- The diffusion coefficient follows an Arrhenius type relationship with regards to temperature:

$$D_R = D_{RO} \exp\left(-\frac{E^{**}}{RT}\right) \tag{2.32}$$

The diffusion coefficient is a weak function of temperature with a low diffusion activation energy ($\sim 20 kJ/mol$).

STAGE 3: THE CHEMICAL REACTION

Generally, reactions can be classified as either chemical or electrochemical. The dissolution process is favoured by anisotropy of the solid. Anisotropic sites favour water take-up, resulting in hydroxylation. (anisotropy: not uniform in all orientations)

When the rate of the chemical reaction is much slower than diffusion, then the chemical reaction rate determines the observed rate. Chemically controlled reactions can be identified based on their independence from agitation speed, since diffusion rate is not influential. Strong dependence of the reaction rate on temperature is also an indication of chemically controlled reaction. This is due to the exponential relationship of reaction rate with regards to temperature [49]. Figure 7 and Figure 14 show examples of reaction kinetics being a strong function of temperature. A surface reaction controlled reaction will have the following kinetic equation [60]:

$$1 - (1 - x)^{\frac{1}{3}} = k_c t \tag{2.33}$$

Where t represents time, x represents the fraction of metal reacted and k_c represents the reaction constant for a chemically controlled reaction. The Arrhenius expression is an empirical relationship which suggests an increase in reaction rate will occur with an increase in temperature.

$$k = Ae^{-\frac{E_a}{RT}} \tag{2.34}$$

The limitations for the Arrhenius expression are that the pre-exponential factor, A , and the activation energy, E_a , are both assumed to be independent of temperature. Many reactions exist which contradicts this assumption. However, the Arrhenius expression provides adequate description of the temperature dependence of reaction rate constants for a wide variety of reactions [61]. Modern theories of reaction rates predict that the reaction rate constant will adhere to the following equation [61]:

$$k = aT^m e^{-\frac{E'}{RT}} \tag{2.35}$$

The reaction rate, k , is still seen to be a strong function of temperature. The magnitude of k increases with increasing temperature (if $m \geq 0$).

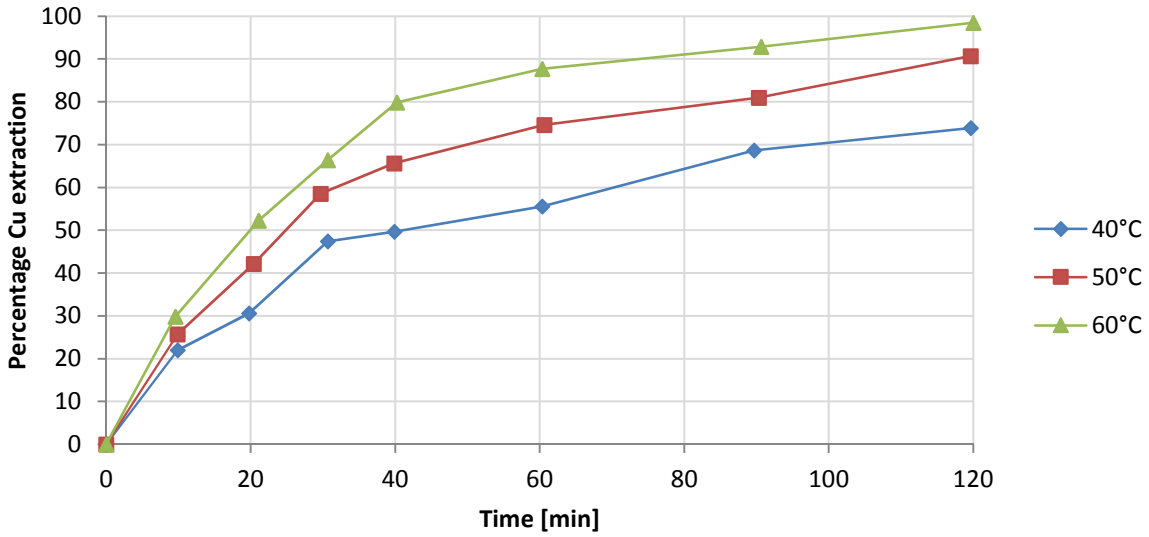

FIGURE 14: THE EFFECT OF TEMPERATURE ON LEACHING OF COPPER WITH [BMIM]HSO_4 USING 5 GRAMS WPCB POWDER, 75ML 10%(V/V) IONIC LIQUID AND 25ML HYDROGEN PEROXIDE, REDRAWN [43]

STAGE 4: REACTION AND DIFFUSION OF PRODUCTS AWAY FROM SOLID-LIQUID INTERFACE

Figure 15 shows the typical concentration profile of reaction product as a function of the distance from the solids-liquid interface.

Reaction products need to be transported away from the solid-solution interface to the bulk solution. This may also involve diffusion. Fick's law is applied in a similar way as in stage 2:

$$\left(\frac{dn}{dt}\right)_P = \frac{D_P A(c_{P0} - c_P)}{\delta} \tag{2.36}$$

The subscript, P , refers to reaction product. The product concentration c_{P0} depends on predecessor stages. The term $(c_{P0} - c_P)$ can be maximised by using fresh solution that does not contain product, i.e. $c_P = 0$. Agitation increases diffusion, although product diffusion is not often the rate limiting step [58].

If diffusion through a product layer controls the reaction rate, the reaction will have the following kinetics equation [60]:

$$1 - \frac{2}{3}x - (1-x)^{\frac{2}{3}} = k_d t \qquad (2.37)$$

In this equation k_d represents the reaction constant for a diffusion controlled reaction. The reaction constant can be calculated from known values of x and t. Fitting a kinetics equation to leaching results can be used as an indication of the rate limiting step.

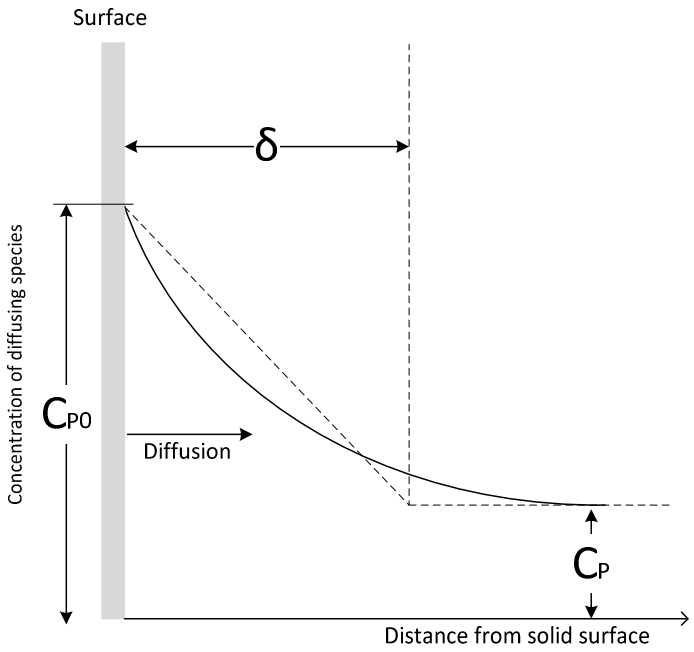

FIGURE 15: DIFUSION OF PRODUCT AWAY FROM THE SOLID-SOLUTION INTERFACE

In some leaching instances, an insoluble layer may form on the solid surface. An insoluble layer of stannic oxide is expected to form on the surface of solder when leaching with nitric acid at concentrations greater than 4 M [24]. Diffusion through the insoluble layer then usually becomes the rate limiting step. The insoluble layer thickens as the core shrinks. The rate of dissolution then decreases proportionally to the thickness of the insoluble layer.

2.5.3. EFFECT OF PARTICLE SIZE DISTRIBUTION

Few studies have been carried out investigating the effect of particle size on leaching of copper [29,43]. Huang et al. (2014), Yang et al. (2011) and Havlik et al. (2010) found increased leaching rate of copper with decreasing particle size. The increase in leaching rate with decreasing particle size was attributed to the increase in surface area per mass of particles [17,55].

Reducing particle size to below a critical level could impose attrition by increasing the extent of particle-particle collisions. This may hinder the permeation of leaching agent through the fine waste PCB powder and decrease leaching efficiency [43]. Huang et al. (2014) reported reduced copper leaching in the finer particle size fractions (<0.075 mm & 0.075-0.1 mm) due to this reason. Particle size plays a crucial role in the recovery of metals as most recycling processes have an effective size range [43].

Kim et al. (2007) reported leaching behaviour to be nearly independent of particle size for sizes below the 180-300µm size class [8].

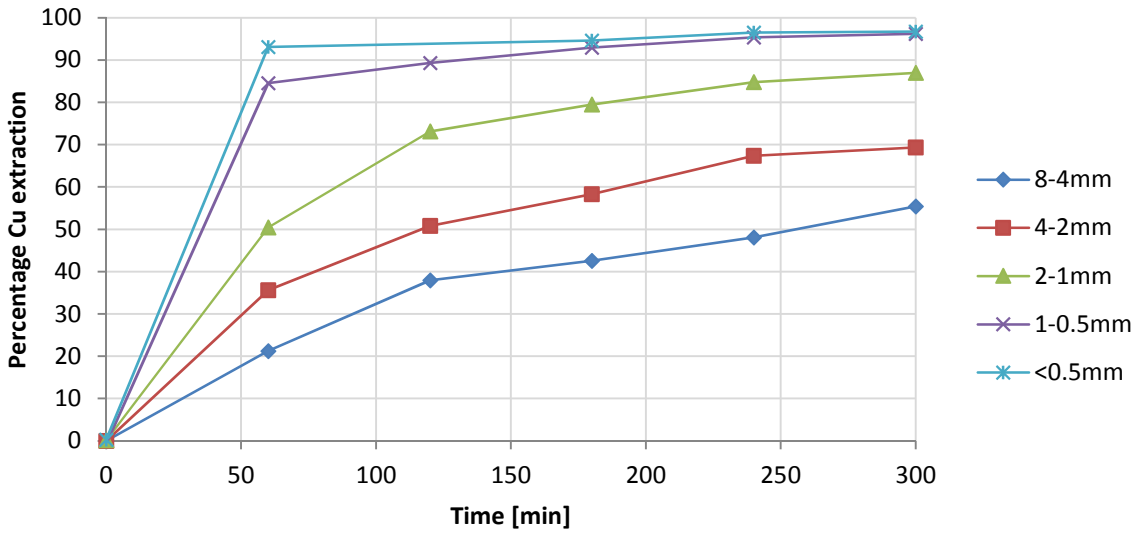

FIGURE 16: THE EFFECT OF PARTICLE SIZE ON COPPER RECOVERY IN 100ML 15% SULPHURIC ACID USING 10 GRAMS WPCB POWDER AND 10ML 30WT% H_2O_2 AT 23°C, REDRAWN [29]

Figure 16 shows results from Yang et al. (2011) depicting how particle size influenced leaching efficiency. As copper is present in the middle layer of PCBs, the small particle sizes expose more of the copper to the leaching solution which poses less mass transfer resistance leading to a faster reaction [29]. Yang et al. (2011) reported efficient leaching with particle size <1mm; decreasing the particle size to <0.5mm significantly increased energy consumption and had no effect on copper recovery [29].

2.5.4. EFFECT OF SOLID TO LIQUID RATIO

The extent of leaching of metals has been found to increase significantly with decrease in solid to liquid ratio [9,10,22,43,62]. A decrease in solid to liquid ratio implies a greater relative availability of leaching reagent for the reaction. Huang et al. (2014) reported significant increase in extent of Cu recovery in a diffusion controlled system by decreasing the S/L ratio from 1:2 to 1:25. This larger relative liquid volume lead to efficiency in mass transfer which accelerated copper leaching making the leaching reaction occur sufficiently [43].

Bas et al. (2014) reported high S/L ratio having an adverse effect on copper recovery due to increased reagent consumption. A decrease in Cu recovery from 82.4% to 43.2% was observed by increasing the S/L ratio from 2% w/v to 10%w/v in 1 M HNO_3 at 50°C [22]. However, results also seem to indicate that increasing the acid concentration proportionally to the S/L ratio could mitigate the decreased extent of Cu leaching observed.

Gharabaghi et al. (2012) and Yang et al. (2011) also reported increasing leaching efficiency with decreasing S/L ratio [29,62]. However, Gharabaghi et al. (2012) stated that decreasing the S/L ratio too much complicated subsequent filtration [62].

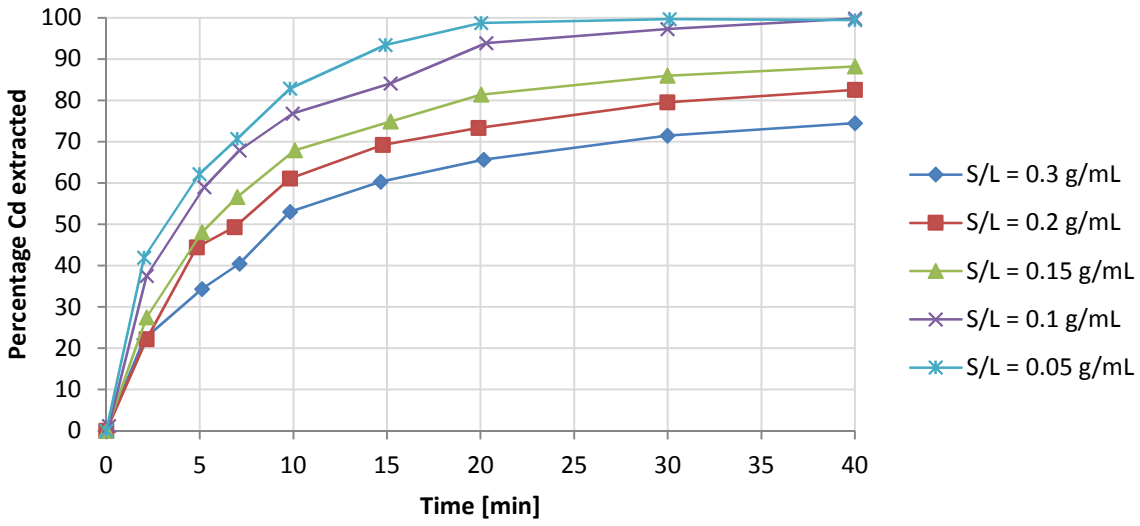

FIGURE 17: THE EFFECT THAT SOLID TO LIQUID RATIO HAD ON THE RECOVERY OF CADMIUM FROM HAZARDOUS WASTE USING SULPHURIC ACID (8% V/V, 25°C, PARTICLE SIZE <250μm) REDRAWN [62]

A high solid to liquid ratio implies a smaller relative volume of leaching solution. Therefore, if the leaching is conducted without temperature control, this smaller volume increases the reaction temperature which in turn may increase copper recovery [29].

Figure 17 shows results from Gharabaghi et al. (2012) where the effect of S/L ratio was investigated. It is seen that lower S/L ratios yield faster and more complete dissolution. However, it should be noted that lower S/L ratios imply that less waste is being treated at a time for a given reactor volume. It may therefore not make sense from an economical perspective to operate at a low S/L ratio.

2.5.5. EFFECT OF OXIDISING AGENT

Oxidative leaching may be regarded as an electrochemical cell in which the anodic process is sustained by a suitable cathodic process. This implies that the cathodic process will consist of the reduction of an oxidised species with potential more positive (usually more than 0.2V) than the anodic process [58]. The Nernst equation below shows that The potential of the cell will decrease unless the activity ratio, $\left(\frac{a_{ox}}{a_{red}}\right)$, is maintained:

$$E = E^o + \frac{RT}{zF} Ln\left(\frac{a_{ox}}{a_{red}}\right) \quad (2.38)$$

An oxidising agent is therefore required in order to reoxidise the reduced species as it forms. The electrode potential is pH dependant when hydrogen ions are involved:

$$O_2 + 4H^+ + 4e^- \rightarrow 2H_2O \quad (2.39)$$

$$E = E^o + \frac{RT}{zF}\ln\left(a_{O_2} \times {a_{H^+}}^4\right) \quad (2.40)$$

$$pH = -log(a_{H^+}) \quad (2.41)$$

$$E = E^o + \frac{RT}{4F}\ln\left(a_{O_2}\right) - \frac{RT}{F}pH \quad (2.42)$$

Equation 2.40 shows that the cell potential in the leaching reaction will decrease as the pH of the leaching solution is increased. An increase in oxygen activity will increase the electrochemical potential.

Oxygen, hydrogen peroxide and ferric iron are potential oxidants for leaching [20,49]. Quinet et al. (2005) reported the expected reactions and their ΔG_{80}^{o} for when these oxidising agents are used with sulphuric acid for copper dissolution to be the following:

$$Cu + Fe_2(SO_4)_3 \rightarrow CuSO_{4(aq)} + 2FeSO_{4(aq)} \qquad \Delta G_{80}^{o} = -95kJ \qquad (2.43)$$

$$Cu + H_2O_2 + H_2SO_4 \rightarrow CuSO_{4(aq)} + 2H_2O \qquad \Delta G_{80}^{o} = -329kJ \qquad (2.44)$$

$$Cu + \frac{1}{2}O_{2(g)} + H_2SO_{4(aq)} \rightarrow CuSO_4 + H_2O \qquad \Delta G_{80}^{o} = -209kJ \qquad (2.45)$$

2.5.5.1. AIR AND OXYGEN AS OXIDISING AGENTS

The benefit of using air as a source of oxygen for oxidising is that it is free. The low solubility of oxygen from air in water has been shown to slow leaching kinetics [63]. Figure 18 on the next page shows the solubility of oxygen in water as a function of temperature. It is seen that high oxygen solubility is favoured at lower temperatures. The solubility of oxygen is also seen to be dependent on the source of oxygen. If air (~22% O_2 , 78% N_2) is used to supply oxygen, the solubility of oxygen is seen to be 8.5 mg/L at 25°C. However, if pure oxygen is used instead of air, the solubility of oxygen at 25°C is 39 mg/L.

The benefit of using pure oxygen instead of air would be a relatively greater availability of dissolved oxygen to oxidise leaching reactions. The use of an oxidising agent in the gaseous form (such as air or pure oxygen) introduces a third phase to the reaction system. Oxygen is therefore required to diffuse/dissolve into the liquid phase before it can act as an oxidising agent. The dissolution of oxygen has in some cases been shown to be a rate limiting step in copper leaching from WPCBs [63]. This may however depend on reactor design and configuration.

The solubility of oxygen in diluted sulphuric acid is slightly decreased (2%) compared to pure water [29,64]. This places further limitation on the use of oxygen/air as an oxidising agent.

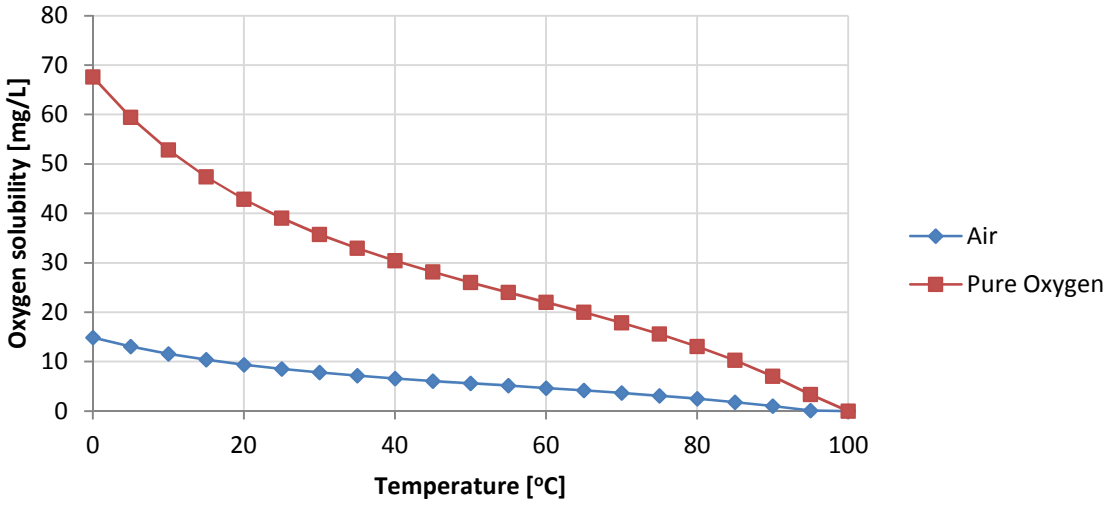

FIGURE 18: SOLUBILITY OF OXYGEN IN WATER AS A FUNCTION OF TEMPERATURE USING AIR AND PURE OXYGEN AS A SOURCE

2.5.5.2. HYDROGEN PEROXIDE AS OXIDISING AGENT

Hydrogen peroxide is a commonly used oxidising agent for enhancing metal extraction [24,65].

Hydrogen peroxide is more expensive than air and oxygen, and it cannot be regenerated [29]. The experimental conditions are easier to control using hydrogen peroxide and it is a more effective oxidant than air [29]. Quinet et al. (2005) showed that ferric ions and oxygen did not provide sufficient oxidation and a significant quantity of hydrogen peroxide was required to achieve high copper extraction [20]. Kamberovic et al. (2011) also opted for using hydrogen peroxide in addition to oxygen [66].

Yang et al. (2011) reported copper recovery to be a function of hydrogen peroxide addition as it actively participates in the reaction together with sulphuric acid [29]. Hydrogen peroxide addition has been shown to have a positive effect on the dissolution of Cu, Fe and Zn and a negative effect on Sn extraction [17]. The reason for the decreased extent of Sn extraction was not stated, however, Sn^{2+} has been known to gradually oxidise to $SnO_{2(s)}$ in sulphuric acid in the presence of oxygen [67]. The increased presence of hydrogen peroxide may therefore have accelerate the conversion of Sn^{2+} to SnO_2 leading to a decreased extent of Sn extraction.

Deveci et al. (2010) reported higher H_2O_2 consumption rates at high temperature 68°C compared to 32°C. The high H_2O_2 consumption was attributed to the increased rate of decomposition with increasing temperature as well as increased decomposition with copper ion production [16].

Birloaga et al. (2013) reported a negative effect for stirring rate due to hydrogen peroxide degradation at high agitation speed. The degradation of hydrogen peroxide produces the evolution of oxygen which absorbed onto particle surface, hindering particle-peroxide contact [17]. It was suggested that oxidative leaching be performed at low stirring rates in order to prevent hydrogen peroxide degradation.

Hydrogen peroxide is known to degrade at high temperatures to form water and oxygen. The decomposition of H_2O_2 in an H_2SO_4 system has been shown to be first order with respect to H_2O_2 concentration [68,69]. However, higher temperatures have been reported to accelerate peroxide decomposition [17,68,70] and to subsequently lead to decreased leaching performance [17,68,69]. Antonijevic 1997 reported reduced leaching performance in 2 M H_2SO_4 due to rapid

peroxide decomposition at temperatures > 40°C. Yazici and Deveci (2010) reported decomposition of 800 mg/L peroxide to increase from 11% at 30°C to 80% at 50°C after 180 minutes. The rate of peroxide decomposition was reported to increase 3.3-fold by increasing temperature from 30°C to 40°C [70]. Birloaga et al. 2014 reportedly avoided peroxide decomposition at lower temperatures of 22°C and 30°C. It was reported that no significant difference in leaching extent was observed between 22°C and 30°C. A greater extent of Cu and Fe extraction was achieved by adding peroxide in one or two batches rather than in small increments due to the achievement of higher oxidation potentials.

2.6. MATERIAL CHARACTERISATION

To determine PCB composition and the extent of metal dissolution, the PCB feed must be characterised. Aqua regia was used for this purpose in numerous previous studies [16,24,29]. Aqua regia is used either to digest feed samples or to digest residue remaining after leaching. A material balance can then be made by summing the amount of metal the in leaching solution with that left in residue.

Several variations of aqua regia digestion have been used. Deveci et al. (2010) determined metal content of scrap television boards (STVBs) by hot digestion in aqua regia. Yang et al. (2011) used aqua regia and perchloric acid to fully leach metals from their sample [29]. As an additional form of analysis, Birloaga et al. (2013) digested samples in a mixture of HF and aqua regia with the aid of microwave treatment for 1h, hereafter AAS analysis was performed.

Other methods of characterisation included that of Huang et al. (2014) who digested samples of waste PCBs using a microwave aided HNO_3-H_2O_2-HF system [43]. The aqueous sample was then analysed using ICP-OES. Birloaga et al. (2013) used X-ray fluorescence spectrometry to determine the chemical composition of samples [17]. Jeong et al. (2011) characterised leaching residue by a scanning electron microscope fitted with an energy dispersive X-ray spectrometer (or SEM-EDS) [10].

2.7. DETERMINING HYDROGEN PEROXIDE CONCENTRATION

Hydrogen peroxide concentration can be determined by several possible methods: titration, colorimetry, decomposition and by spectrophotometry.

Possible reagents for titration include potassium permanganate, ceric sulphate, sodium arsenite, titanium trichloride and potassium iodide-sodium thiosulphate.

The colorimetric method is only applicable for detection of a few ppm of peroxide [71].

2.7.1. DECOMPOSITION METHOD

The decomposition method is simple and reliable. It is based on the decomposition reaction of hydrogen peroxide with a suitable catalyst, followed by measuring the amount of oxygen produced.

$$2H_2O_2 \xrightarrow{catalyst} 2H_2O + O_2 \qquad (2.46)$$

The reliability of the decomposition method stems from the absence of any known side reactions. Although this method is inconvenient to apply in practice, it is an absolute method of analysis [71].

2.7.2. SPECTROPHOTOMETRIC METHOD

This method involves the formation of a complex between hydrogen peroxide and titanium (IV) ion. The titanium ion is introduced as a salt: potassium titanium (IV) oxalate $K_2TiO(C_2O_4)_2 \bullet 2H_2O$. The titanium-peroxide complex is orange-yellow in colour and maximum absorbance occurs at a wavelength of 400 nm [72].

The intensity of absorbance is dependent on concentrations of sulphuric acid and potassium titanium (IV) oxalate. The absorption of components other than TiO_2^{2+} can be allowed for by the subtraction of the absorbance of solutions which were prepared in the same way but leaving out hydrogen peroxide.

Once all hydrogen peroxide has complexed with titanium (IV), excess titanium (IV) potassium oxalate has little influence on absorbance up to a concentration of 0.1 M titanium (IV) potassium oxalate [72]. At constant titanium (IV) potassium oxalate and sulphuric acid concentration, the absorbance has a linear relationship with hydrogen peroxide concentration.

The absorbance of a solution is the sum of the absorbance of all species in solution [73].

$$A = \varepsilon_X b[X] + \varepsilon_Y b[X] + \varepsilon_Z b[Z] + \ldots \quad (2.47)$$

3. EXPERIMENTAL

3.1. EXPERIMENTAL DESIGN

Experimental work consisted of three phases. The first phase was aimed at the selection of a suitable lixiviant and leaching temperature. The second phase of experiments investigated the effects of mechanical pre-treatment, solid to liquid ratio and lixiviant concentration with the lixiviant and temperature selected based on the results from phase 1. Finally, possible optimal leaching conditions identified from phase 2 was investigated in phase 3 in order to suggest the most suitable operating conditions.

To recall, leaching performance in the context of this project refers to the extent of base metal dissolution and the selectivity of the leach for base metals.

Mechanical pre-treatment resulted in the generation of 3 different types of feed material. Received waste motherboards were partially disassembled manually. The disassembly was followed by size reduction and screening. The comminuted material then received one of three extents of mechanical separation:

i. In the first category, no mechanical separation was applied. This served as a control feed and was labelled No Sep. in Figure 19. The reason for not applying physical separation to this group was to be able to quantify the effects physical separation had on leaching efficiency.
ii. Dense medium separation (DMS) was applied. Dense medium separation was aimed at separating the liberated metals from non-metals. Feed material receiving only DMS was labelled DMS in Figure 19.
iii. DMS and magnetic separation (MS) were applied. Magnetic separation was aimed at removing ferromagnetic material, i.e. iron, nickel and cobalt. Feed material receiving both DMS and MS was labelled DMS+MS in Figure 19.

The use of these three different feeds enabled quantification of the beneficial effects of physical separation as a pre-treatment step by comparing the respective leaching efficiencies achieved with the different feeds.

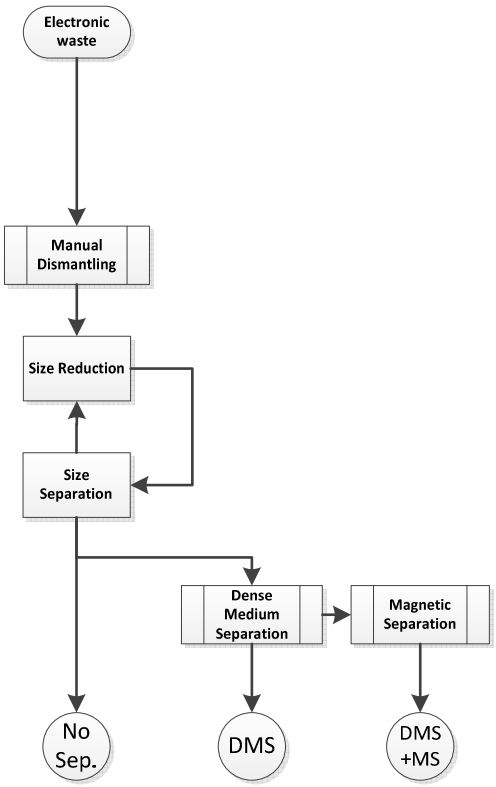

FIGURE 19: STRATEGY FOR FEED PREPARATION AND PHYSICAL SEPARATION APPLICATION

A representative sample of each feed category was analysed in order to determine the effects that the respective mechanical treatments had on metals content.

3.1.1. PHASE 1: SCREENING PHASE

The first phase entailed experimental work to determine the most suitable lixiviant for selective recovery of base metals. This involved a full mixed level factorial design investigating nitric acid and sulphuric acid at three different temperatures with and without the addition of hydrogen peroxide. The experimental design for phase 1 is shown in Table 14. In order to limit the number of experiments, only these three parameters were varied for phase 1. The remainder of the variables remained fixed at values stated in Table 15; the reasons for selecting the values are also stated.

TABLE 14: EXPERIMENTAL DESIGN FOR LIXIVIANT SELECTION AND TEMPERATURE SELECTION

Variable	**Levels**	**Set Points**		
Lixiviant type	2	1 M HNO_3 (-1)	1 M H_2SO_4 (1)	
H_2O_2	2	No H_2O_2 (-1)	200% excess (1)	
Temperature	3	25°C (-1)	55°C (0)	85°C (1)

The amount of hydrogen peroxide required to completely leach base metals (Al, Cu, Fe, Ni, Pb, Sn and Zn) was calculated from stoichiometry and waste PCB compositions found in literature. At the high level of peroxide (see Table 14) three times the required amount was added (i.e. 200% excess) due to expected degradation of hydrogen peroxide as a result of agitation and high temperature.

TABLE 15: FIXED PARAMETERS AND THEIR SET POINTS FOR PHASE 1

Parameter	Fixed set point	Reason for parameter set point
Lixiviant concentration	1 M	Based on expected metal content of the waste PCB samples, 1 M would be sufficient for complete base metal extraction according to stoichiometry. Although sulphuric acid is diprotic, it is only a strong acid with regards to the donation of its first proton. Therefore both nitric acid and sulphuric acid are tested at the same concentration.
Leaching time	5h	Based on the literature survey (see Table 9) this was deemed sufficient leaching time in order to draw meaningful conclusions with regards to leaching performance.
Feed and Particle Size	No Sep. at <2mm	No Sep. feed was chosen as it is the simplest to prepare (i.e. manual disassembly followed by comminution) The small particle size was chosen to ensure adequate liberation of metals and non-metals and to provide a large surface area for promoting efficient leaching.
Agitation speed	500 rpm	This agitation speed was the minimum agitation speed required to suspend particles.
Solid to liquid ratio	1:10 w/v	This S/L ratio has frequently been used in previous studies and was seen to yield satisfactory results (please see Table 9).

Processed results from phase 1 of experiments was used to select the most suitable lixiviant and leaching temperature based on factors defining optimal leaching performance in the context of this project:

i. Factor 1 is the extent of base metals dissolution. It is desired to leach base metals (especially copper) as completely as possible.
ii. The second factor is the selectivity of leaching with regards to base metals. It is desired to leave precious metals (Au, Ag) in the solid residue.

The lixiviant and temperature that showed the most potential with regards to these two factors was subsequently selected for further investigation in phase 2 and 3.

3.1.2. PHASE 2: OPTIMISATION

Results from phase 1 enabled selection of a suitable lixiviant and leaching temperature, which was kept constant during phase 2 and 3.

Phase 2 investigated the effects of mechanical pre-treatment, lixiviant concentration and solid to liquid ratio. Performing dense medium separation upgraded the metals content of the feed sample. This means that a given mass of feed sample which has received DMS will require a relatively larger amount of reagent for complete dissolution of base metals to be achieved. Experiments were therefore performed in three separate mixed level factorial designs.

TABLE 16: PART 1 OF PHASE 2 EXPERIMENTS

Variable	Levels	Set Points
Feed type	1	No Sep.
Solid to liquid ratio	1	0.1 kg/L
Lixiviant concentration	2	1M & 2.5M

Table 16 shows part 1 of phase 2 experiments. The feed sample used in part 1 was No Sep. feed meaning that it did not receive any mechanical pre-treatment. Part 1 therefore only tested the effect of acid concentration on leaching No Sep. feed.

TABLE 17: PART 2 OF PHASE 2 EXPERIMENTS

Variable	Levels	Set Points	
Feed type	2	DMS (-1)	DMS+MS(1)
Solid to liquid ratio	1	0.1 kg/L (0)	
Lixiviant concentration	2	2.5M(-1)	4M(1)

Table 17 shows part 2 of phase 2 experiments. The feed samples in part 2 received either DMS or both DMS and MS. The solid to liquid ratio was kept the same as that in part 1. More concentrated acid was used in part 2 than in part 1 in order to accommodate the higher expected metal grade of the feed.

TABLE 18: PART 3 OF PHASE 2 EXPERIMENTS

Variable	Levels	Set Points	
Feed Type	2	DMS(-1)	DMS+MS(1)
Solid to liquid ratio	1	0.06 kg/L*	
Lixiviant concentration	2	1M(-1)	2.5M(1)

*Same metal to liquid ratio as No Sep. feed in part 1 of phase 2

Table 18 shows part 3 of phase 2 experiments. The feed samples in part 3 were the same as that in part 2, i.e. they received either DMS or both DMS and MS. A solid to liquid ratio of 0.06 kg/L was used. This solid to liquid ratio was chosen to correspond to the same metal to liquid ratio as that of No Sep. feed in part 1. The same lixiviant concentrations as that in part 1 was therefore also used (see Table 16).

Parameters that remained fixed during phase 2 are listed in Table 19. The same particle size, leaching time and agitation speed was used as in phase 1.

Phase 2 would allow a conclusion to be made with regards to the benefit, or lack of benefit, of performing mechanical pre-treatment on comminuted feed. Results would give an indication of the most suitable conditions for optimal leaching performance.

TABLE 19: FIXED PARAMETERS AND THEIR SET POINTS FOR PHASE 2

Parameter	Fixed set point	Reason for parameter set point
Lixiviant	Determined in phase 1	Phase 1 would deliver a suggestion for an appropriate lixiviant
Temperature	Determined in phase 1	Phase 1 would deliver a suggestion for an appropriate temperature.
Leaching time	8h	Results from phase 1 suggested that leaching time in phase 2 should be extended.
Particle Size	<2mm	The small particle size was chosen to ensure adequate liberation of metals and non-metals and to provide a large surface area for promoting efficient leaching.
Agitation speed	500 rpm	This agitation speed was the minimum agitation speed required to suspend particles.

3.1.3. PHASE 3: PROCESS VALIDATION

Insights gained from results of phase 1 and 2 was used to suggest a suitable flowsheet for selective and complete leaching of base metals. This flowsheet was then validated experimentally. The extents of metals removal were reported and a conclusion made with regards to the inclusion or exclusion of mechanical pre-treatment in the flowsheet.

3.2. METHODOLOGY

3.2.1. EQUIPMENT

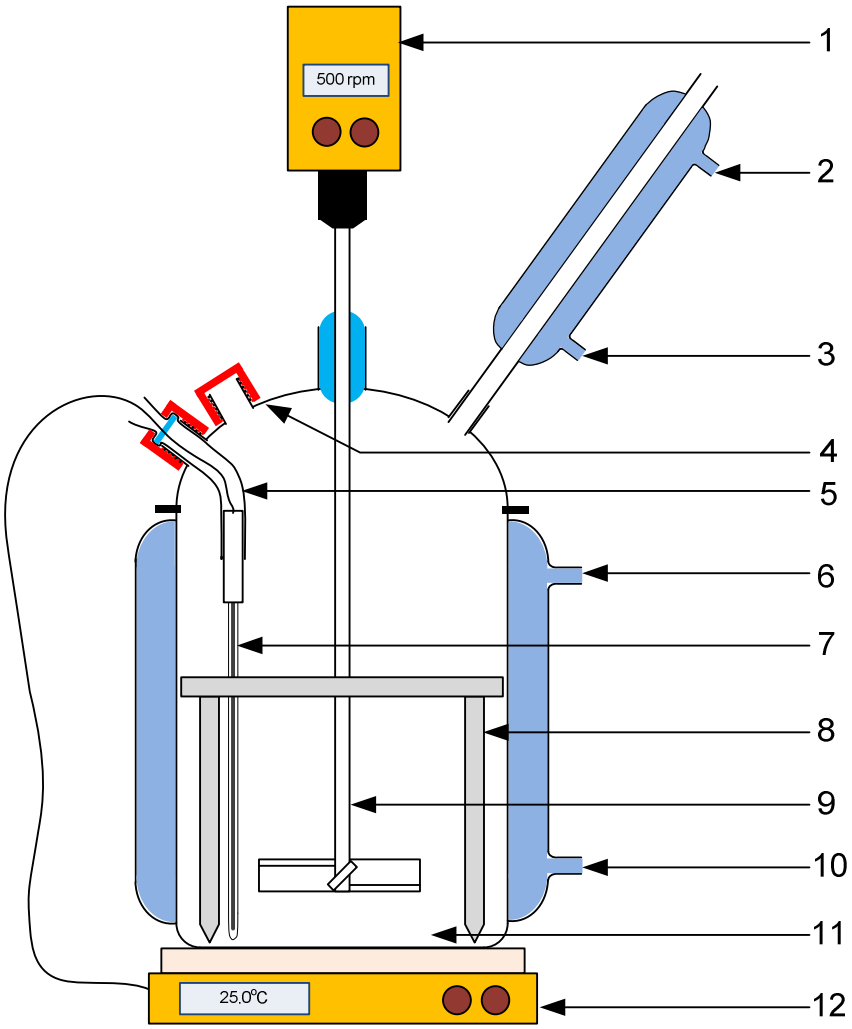

1	Overhead agitator motor	7	Glass coated thermometer
2	Condenser water, out	8	Teflon baffles
3	Condenser water, in	9	Teflon 4-blade impeller
4	Sampling port	10	Cooling jacket water, in
5	Sleeve for thermometer	11	Glass reaction vessel 1.7 L
6	Cooling jacket water, out	12	Hotplate with feedback control

FIGURE 20: DRAWING OF LEACHING EQUIPMENT USED FOR EXPERIMENTS

Figure 20 shows the equipment used for leaching experiments. The setup consisted of a 1.7 L glass reaction vessel with a diameter of 105 mm and a working volume of approximately 1 L. The vessel was fitted with a cooling jacket through which tap water (~16°C) was circulated for cooling when necessary.

Agitation was achieved through an overhead stirrer fitted with a four bladed Teflon impeller. The impeller diameter was 56 mm with blades angled at 45°. The impeller was positioned 20 to 30 mm from the bottom of the vessel. Mixing was assisted and vortex formation limited by 4 Teflon baffles.

A glass coated thermometer was fitted through a sleeve which was sealed tightly to prevent vapour losses through an opening (see Figure 20 item 5 and 7). The thermometer provided feedback to the hotplate for temperature control. The lid was fitted with a condenser to prevent vapour losses and preserve reaction volume. The lid was also fitted with a sampling port which remained sealed in between sampling. Batch wise feeding of peroxide was done through the sampling port using a funnel, where after the sampling port was closed. Continuous feeding of peroxide was done using a peristaltic pump with the feeding line entering the reactor through the condenser. pH and ORP were measured using an Eutech pH6+ portable meter.

A Retsch SM 100 mill was used for crushing the feed. Once screened, the crushed feed was split using a rotary splitter as shown in Figure 21. Solids residue remaining after leaching was filtered using 12.5 cm diameter qualitative filter paper and a vacuum pump.

FIGURE 21: ROTARY SPLITTER USED TO DISTRIBUTE FEED METARIAL EVENLY ACROSS SAMPLES

3.2.2. MATERIALS PREPARATION

3.2.2.1. DISASSEMBLY

Partial manual disassembly of waste PCBs involved the removal of components from the boards which were likely to damage the mill. This included large stainless steel components which are not of high value.

3.2.2.2. SIZE REDUCTION

The disassembled waste PCBs were first cut into small pieces of 3 cm x 3 cm using a band saw. The pieces were then shredded in a cutting mill (Retsch SM100). The first pass through the mill was made using the largest available passing size sieve: 20 mm. The crushed product was then classified using a 2 mm aperture size sieve. Oversized particles were returned to the mill using a progressively smaller passing size each time. After every pass through the cutting mill, the material was classified to remove particles smaller than 2mm.

The size reduction strategy is shown in Figure 22.

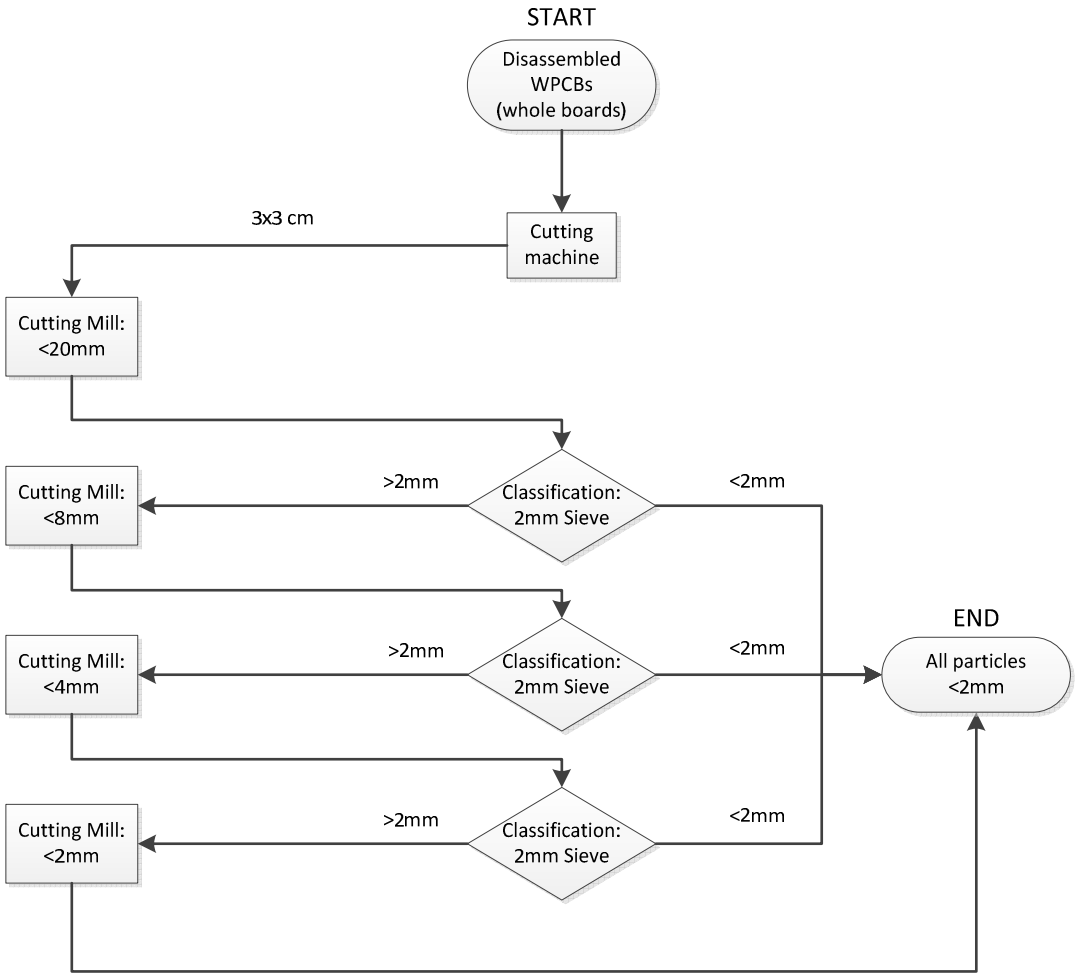

FIGURE 22: SIZE REDUCTION STRATEGY

The classification of particles in-between milling sessions will be done in order to avoid the formation of ultra-fines, which is likely to slow down subsequent dense medium separation and filtration.

3.2.2.3. PHYSICAL SEPARATION

As previously stated, the feeds were to receive either no physical separation, DMS or DMS and MS. No physical separation implies using the comminuted waste PCBs (<2 mm) as is after size reduction and screening, i.e. without attempting further enrichment prior to leaching. The intended application methods of DMS and MS will now be described.

REPRESENTATIVE SAMPLING

The comminuted material was first sampled on a rotating disk sampler (please see Figure 21) prior to physical separation. This ensured that the material was divided in a representative fashion into two different batches. The first batch did not receive physical separation treatment while the second batch did undergo physical separation.

DENSE MEDIUM SEPARATION

The separation of metals from plastics was conducted by dense medium separation. The heavy liquid used to perform the DMS was tetrabromoethane (TBE). TBE has a density of 2.97 g/cm^3 and was diluted with acetone to a density of 2.5 g/cm^3. The density of the mixture was determined using a measuring cylinder and a scale. The ratio of acetone to TBE used was 0.27:1 [33]. The acetone dilution also served to lower the viscosity of the heavy liquid, speeding up settling and separation during subsequent filtration.

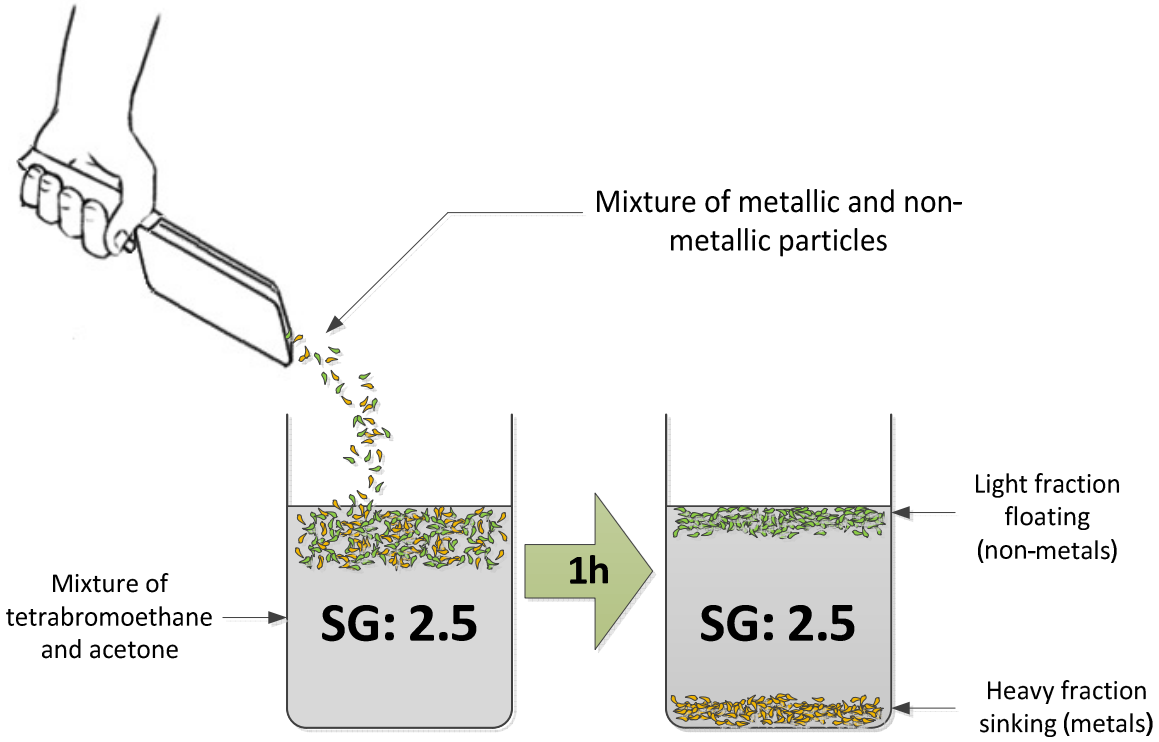

FIGURE 23: DENSE MEDIUM SEPARATION OF COMMINUTED WASTE PCBS FOR THE SEPARATION OF METALS FROM NON-METALS USING TETRABROMOETHANE AND ACETONE

Figure 23 shows a schematic representation of the separation method and application. An effective solid to liquid ratio for batch-wise DMS of comminuted waste PCBs was not found explicitly stated in literature. Therefore comminuted waste PCBs was thrown into 2L of heavy liquid in small increments whilst separation was visually monitored. Particle separation was almost instantaneous. The particles were allowed an hour to separate where-after the light fraction was scooped off using a sieve and the heavy fraction filtered out. The heavy fraction and the light fraction were then rinsed with acetone to remove any remnant TBE where-after they were dried.

MAGNETIC SEPARATION

Part of the heavy fraction recovered from DMS underwent magnetic separation (MS). The heavy fraction produced by DMS was split into two halves using a rotary splitter (see Figure 21). One half of the heavy fraction was subjected to MS. The MS was applied using a $10 \times 15 \times 2\ cm$ barium-iron permanent magnet supplied by Allmag Industries. The magnets were placed on a thin plastic sheet. The plastic sheet served as a means to avoid direct contact between the magnets and the magnetic particles.

Sampled heavy fraction material from DMS was spread out in thin layer on a table (please see Figure 24). With the magnet placed against the plastic sheet, magnetic material was pulled up by moving the plastic sheet and magnet at a height of 2-5 mm over the particles. Once magnetic material was loaded onto the base of the plastic board (as shown), the magnetic material was deposited into a separate container by pulling the plastic sheet down, away from the magnet. This freed ferromagnetic particles from the magnetic field, allowing them to fall into a separate container.

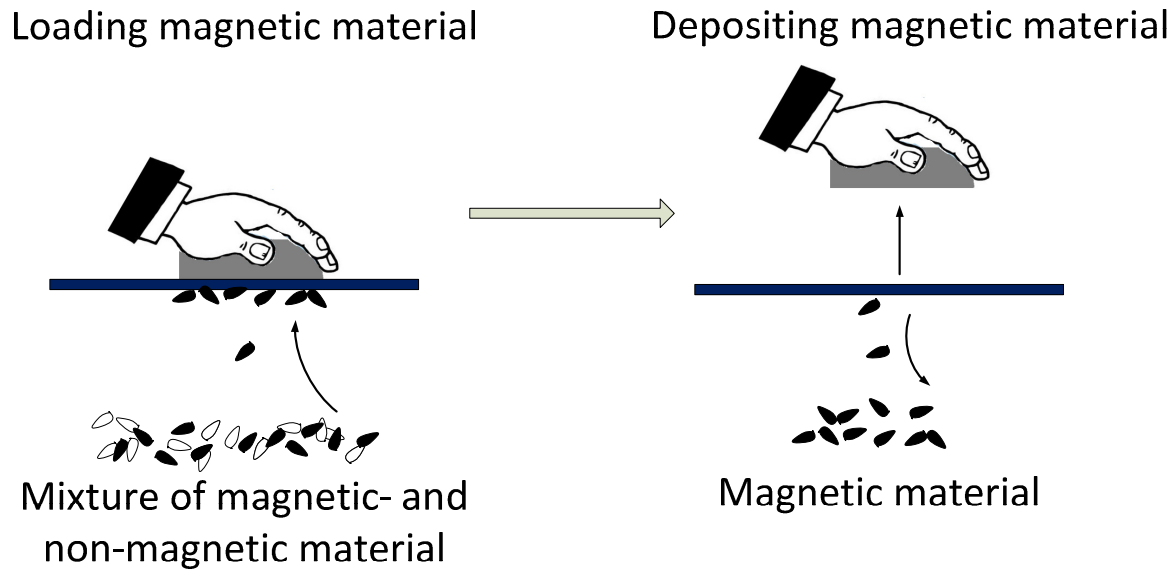

FIGURE 24: MANUAL APPLICATION OF MAGNETIC SEPARATION USING BARIUM-IRON MAGNETS AND A THIN PLASTIC BOARD TO AVOID DIRECT MATERIAL CONTACT

This loading and depositing of magnetic material was continued until no more material was pulled up by the magnet, i.e. until the majority of magnetic material had been removed.

3.2.2.4. LEACHING REAGENTS

Sulphuric acid and nitric acid were received at 98 Wt% and 55 Wt% respectively from Kimix chemicals. The desired concentration of acid was prepared by dilution of concentrated acid in distilled water. The required amount of concentrated acid was calculated based on the desired volume and molarity of the diluted acid and the concentration of the concentrated acid. These calculations are shown in Table A 1 and Table A 2 in appendix A. The concentrations that were used during phase 1 and 2 were the following:

- 1 M: According to the PCB compositions found in literature, 1 M of acid would be sufficient for complete base metal dissolution at the intended S/L ratio.
- 2.5 M: This concentration corresponded to 150% excess acid, allowing the effect of acid concentration to be observed.

- 4 M: High level for feed with enriched metal grade and allowed the effect of acid concentration to be observed.

Once a specific acid had been selected, the diluted acid was prepared at each of the concentrations stated. Samples of the prepared acid will then be titrated using dilute sodium hydroxide and an indicator in order to confirm the molarity of the acid.

The hydrogen peroxide was used as received from Kimix chemicals at 30 Wt%.

3.2.2.5. MATERIAL CHARACTERISATION

Representative samples were taken for analysis after each separation step in order to determine the extent and selectivity of the physical separation process. Following every leaching test, the residue remaining was digested in aqua regia. Aqua regia digestion allowed for a mass balance to be performed for every leaching run and allowed variation in feed composition to be quantified.

3.2.3. EXPERIMENTAL PROCEDURE AND ANALYSIS

The experimental setup for leaching is shown in Figure 20. A volume of 500mL diluted acid of the concentration stipulated by the experimental design was poured into the reaction vessel. The diluted acid was then brought to the desired leaching temperature. Next, the crushed sample was poured into the vessel. Hydrogen peroxide addition was then started at t=0.

Samples of 3 mL were taken at 15, 30, 60, 120, 180, 240 and 300 minutes. The ORP and pH of the samples were also measured. All samples were filtered directly after sampling. Solid residue remaining after leaching was digested in aqua regia for 24 hours at 55°C. Aqueous samples were diluted in dilute (2%) HNO_3 and analysed using ICP-OES.

3.2.4. INTERPRETATION OF ANALYTICAL RESULTS

Overall leaching performance was judged based on extent of base metal dissolution, selectivity of leaching with regards to base metals, and reagent consumption. Although reagent consumption was not initially considered during optimisation, it will provide valuable information regarding the economics of the process. Repeat runs were performed at 25°C and initial S/L ratio of 1/10 using 1 M H_2SO_4 for each of the three feed types.

DETERMINING THE EXTENT OF METALS EXTRACTION

Firstly, the extent of metal extraction was expressed as the percentage of metal extracted into the leaching solution from the original specimen:

$$\%Metal\ leached = \frac{metal\ extracted\ into\ leach\ solution}{total\ metal\ in\ WPCB} \times 100\% \qquad (3.1)$$

Two methods were considered for determining the total amount of metals present in the system:

- Representative samples from all 3 feed types could be acquired by means of the rotary sampling device. The feed samples could then be digested in aqua regia and aqueous samples would be filtered, diluted and analysed. Complete dissolution of all metals would be assumed in aqua regia and the aqueous analysis would be assumed representative of the total metal content of the three respective feeds.
- Solid residue remaining after the experiment is digested in aqua regia and aqueous samples are analysed using ICP-OES. The aqua regia is assumed dissolve all remaining

metals. The analytical results from the leaching test and that of the aqua regia digestion is used to back-calculate the metals composition prior to leaching.

The second option was chosen because it allowed the determination of the composition of each feed sample used. With both the mass of metal leached and the mass of metal remaining the residue known, the extent of leaching could be calculated more accurately. With variation in feed composition expected, this method allowed variation in feed composition to be quantified and confidence intervals to be calculated for the expected mass of respective metals in feed samples.

DETERMINING LEACHING SELECTIVITY

It was desired to selectively leach base metals. The selectivity could be quantified by the following expression:

$$Selectivity = \frac{Mass\ of\ base\ metals\ dissolved}{Mass\ of\ precious\ metals\ dissolved} \tag{3.2}$$

Due to several experimental runs not extracting detectable amounts of Au or Ag, the selectivity could often not be calculated.

The base metals analysed for were: Al, Cu, Fe, Ni, Pb, Sn and Zn.

The precious metals analysed for were: Au and Ag.

DETERMINING REAGENT CONSUMPTION

The measurement of pH during the course of an experiment was initially used as an indication of acid consumption. Acid concentration could not be accurately be determined by a neutralisation titration due to expected side reactions such as iron precipitation. Due to some of the runs being performed at pH values of <0, the available pH meter could not measure the pH. The pH was subsequently estimated by calculating the stoichiometric amount of H^+ that was consumed according to eq. 3.3 based on the observed extent of metal dissolution; the metals, M, considered for the calculation include Ag, Al, Au, Cu, Fe, Ni, Pb, Sn and Zn. The amount of consumed H^+ was deducted from that present in the diluted acid at time zero in order to calculate the pH.

$$M_{(s)} + 2H^+ + \frac{1}{2}O_2 \rightarrow M^{2+}_{(aq)} + H_2O_{(l)} \tag{3.3}$$

Attempts were made to determine the amount of free hydrogen peroxide in the system using a spectrophotometric method. A 1 mL sample was mixed with titanium oxalate in an acidic system. The titanium oxalate selectively forms a complex with hydrogen peroxide. The concentration of hydrogen peroxide was then determined by absorbance of UV at a wavelength of 400 nm. Although this analysis proved accurate when analysing stock samples, the samples taken from experiments needed to be analysed immediately due to peroxide decomposition continuing even after sampling. This decomposition was due to catalysis by Cu and Fe ions. Due to limited availability of the UV spectrophotometer and time intensive dilution requirements leaving experiments unattended, this analysis was later abandoned.

4. RESULTS AND DISCUSSION

4.1. PHASE 1: SCREENING

Recall that phase 1 of the experiments was aimed at identifying a suitable lixiviant, selecting a suitable leaching temperature and deciding on the inclusion or exclusion of hydrogen peroxide. The extents of metal leached in all experiments at several time intervals are shown in Appendix C.

4.1.1. THE EFFECT OF LIXIVIANT

Figure 25 shows that no significant amount of copper was leached with sulphuric acid in a non-oxidative environment. This lack of copper leaching was expected due to a positive ΔG_r^o for copper leaching (see Table 13). Castro and Martins (2009) also reported a lack of copper leaching using sulphuric acid in a non-oxidative environment [48].

Figure 25 shows nitric acid dissolving 76% of copper in the first 60 minutes. Due to nitric acid's oxidative nature, the addition of a dedicated oxidising agent was not required.

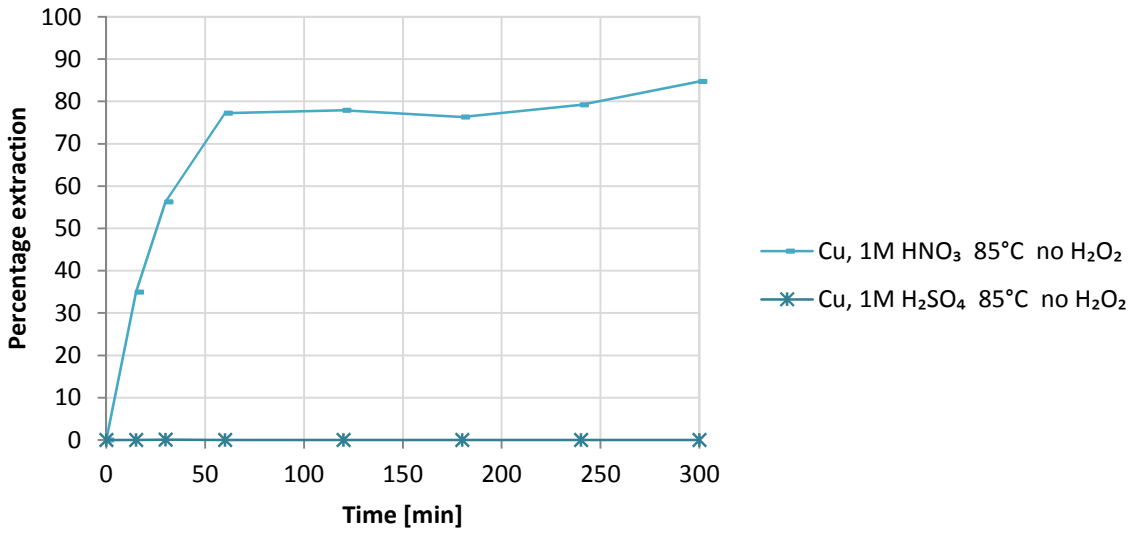

FIGURE 25: COMPARING THE USE OF 1M HNO_3 AND 1M H_2SO_4 FOR LEACHING COPPER AT 85^{0}C IN THE ABSENCE OF HYDROGEN PEROXIDE, S/L RATIO=1:10 W/V

The change in pH during the experiments depicted in Figure 25 is shown in Figure 26. The rapid rise in pH observed for nitric acid in Figure 26 suggests that complete leaching of Cu may have been limited by availability of leaching agent. This implies that a more concentrated solution of nitric acid may provide a greater extent of leaching. Although Cu leaching appeared to stop after 60 minutes, the leaching of Al and Zn still continued, causing the rise in pH observed between 60 minutes and 120 minutes in Figure 26.

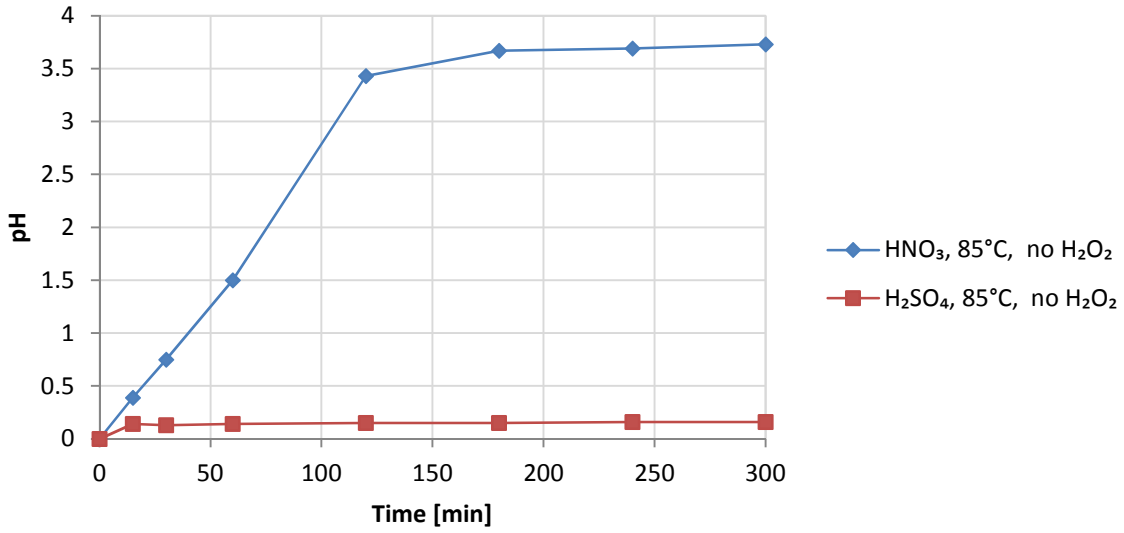

FIGURE 26: THE CHANGE IN pH OF THE REACTION SOLUTION DURING LEACHING WITH HNO_3 AND H_2SO_4 AT 85°C IN THE ABSENCE OF HYDROGEN PEROXIDE, S/L=1:10 W/V

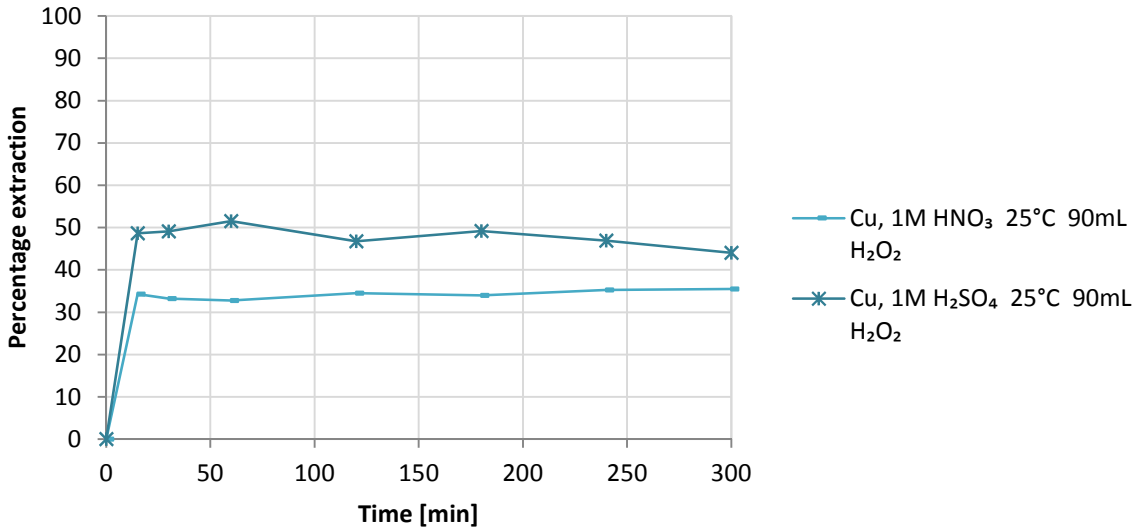

FIGURE 27: COMPARING THE USE OF 1 M HNO_3 AND 1 M H_2SO_4 FOR LEACHING CU AT 25°C WITH 90 ML OF 30 WT% HYDROGEN PEROXIDE (200% EXCESS), S/L RATIO=1:10 W/V

Figure 27 shows rapid initial dissolution of copper for both nitric acid and sulphuric acid. Copper dissolution stopped after 15 minutes for both acids. This was due to an apparently insufficient amount of H_2O_2 being consumed completely lowering the ORP in both cases, as shown in Figure 28. This reduced the thermodynamic favourability of copper dissolution. Figure 27 depicts the most extensive dissolution achieved with sulphuric acid during phase 1 experiments.

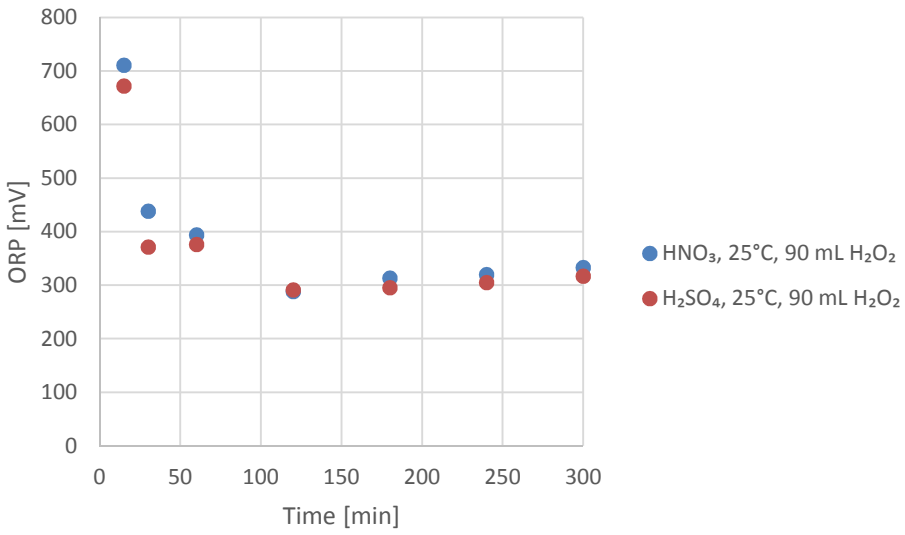

FIGURE 28: ORP MEASUREMENTS TAKEN (vs. Ag/AgCl) DURING LEACHING WITH 1 M HNO_3 AND 1 M H_2SO_4 AT 25°C AND A S/L RATIO OF 1/10.

4.1.2. THE EFFECT OF TEMPERATURE

Figure 29 compares the effect of different leaching temperatures on copper recovery in the presence of 200% excess hydrogen peroxide. It is interesting to note that a rise in temperature increases copper recovery in the nitric acid system while decreasing copper recovery in the sulphuric acid system.

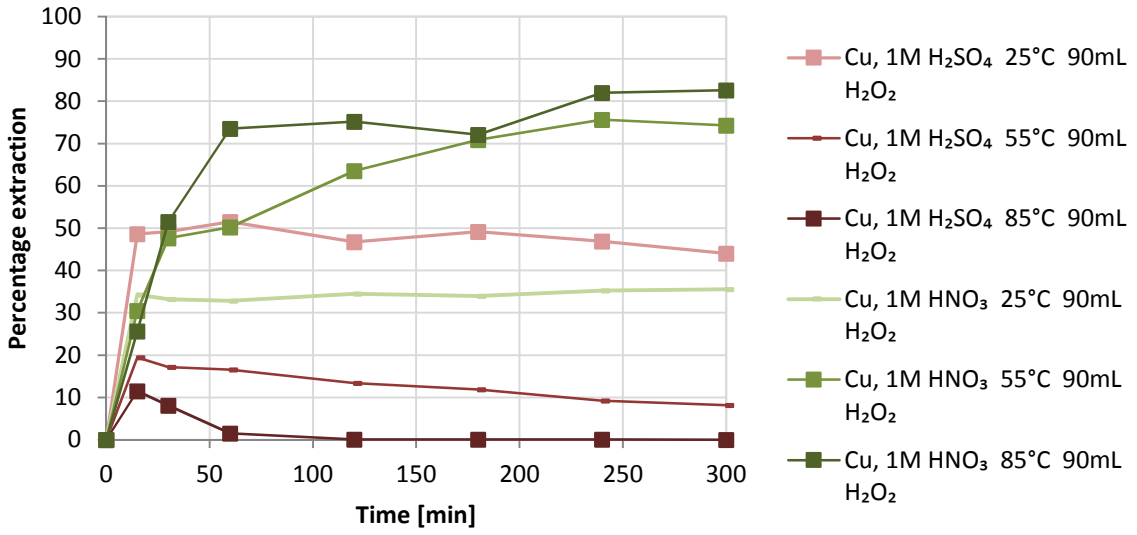

FIGURE 29: COMPARING DIFFERENT LEACHING TEMPERATURES FOR COPPER LEACHING USING 1M HNO_3 AND 1M H_2SO_4 WITH 200% EXCESS HYDROGEN PEROXIDE, S/L=1:10 W/V

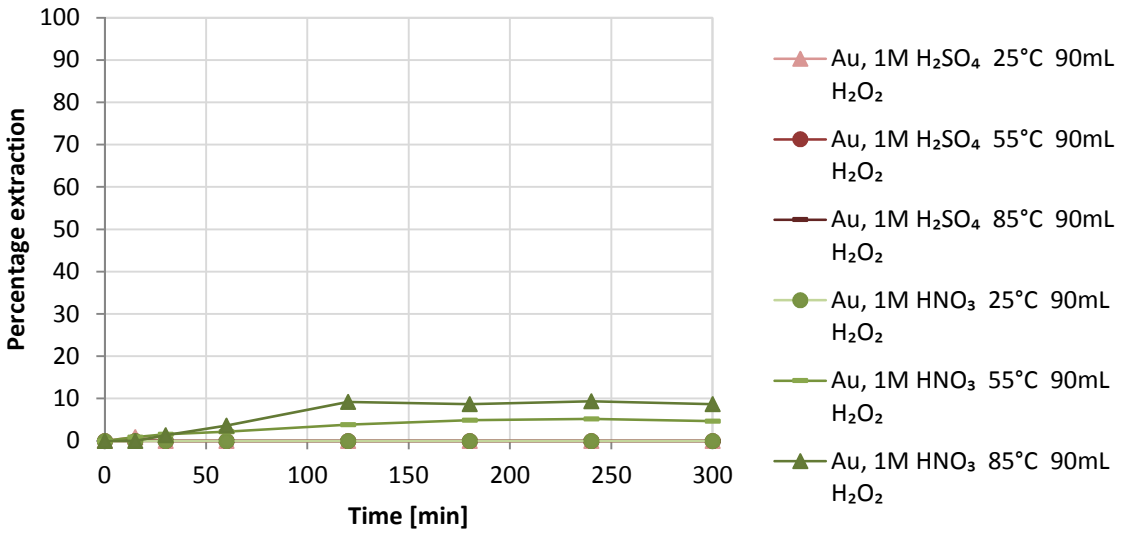

FIGURE 30: COMPARING DIFFERENT TEMPERATURES FOR GOLD LEACHING WITH NITRIC ACID AND SULPHURIC ACID WITH 200% EXCESS HYDROGEN PEROXIDE; S/L=1:10 W/V

The leaching of Au observed when using 1 M HNO_3 at 55°C and 85°C may be due to the presence of halogens in the leach solution. Halogens, specifically Cl and Br, are known to be active components of flame retardants used in electronics[74]. Heating of the flame retardant material provokes the release of Cl and/or Br[75,76]. Numerous flame retardants are known to be water soluble[77], which, once heated, could potentially add to the halogen content of the leach solution.

4.1.2.1. THE EFFECT OF TEMPERATURE ON SULPHURIC ACID SYSTEM

The most complete leaching of copper using sulphuric acid (i.e. 44% Cu dissolution) was achieved at 25°C.

The necessity of an oxidising agent for copper leaching with sulphuric acid implies a strong dependence on hydrogen peroxide availability. The higher temperatures accelerated the decomposition of hydrogen peroxide producing a less oxidising leaching environment. Without the presence of an oxidising agent, copper leaching was not thermodynamically favourable (see Table 13). In the absence of an oxidising agent, copper ions were reduced. Reduction of Cu^{2+} could have occurred by cementation reactions with Al, Fe or Zn. Consideration of a Pourbaix diagram for Cu behaviour at these conditions (see Figure B 5 in Appendix B) suggested that Cu^{2+} may have precipitated as $Cu_{(s)}$. This decreased the amount of copper in solution as seen in Figure 29 (see H_2SO_4 at 55°C & 85°C in Figure 29).

The results in Figure 30 show that no detectable amount of gold was leached using sulphuric acid at any of the tested temperatures. The Cu/Au selectivity of the sulphuric acid system could therefore not be quantified, but was superior to that of the nitric acid system which showed 9% co-extraction of Au at 85°C (see Figure 30).

4.1.2.2. THE EFFECT OF TEMPERATURE ON NITRIC ACID SYSTEM

Figure 29 shows nitric acid yielding a greater extent of copper recovery at the higher temperatures, 55°C and 85°C. Due to the oxidative nature of nitric acid, it does not require the presence of hydrogen peroxide to leach copper. The decomposition of hydrogen peroxide therefore did not influence the extent of copper leaching achieved at higher temperatures. After the decomposition of hydrogen peroxide at 15-30min, the leaching rate remained higher for the

85°C run than for the 55°C. The most complete leaching of copper during phase 1 was 85%, and was achieved by nitric acid at 85°C.

Although nitric acid at 85°C yields the most complete copper leach, Figure 30 shows that 8% of gold present was co-extracted at these conditions. A leaching selectivity of 10268 $\frac{g\ of\ Cu}{g\ of\ Au}$ was achieved. Reducing the temperature of nitric acid leach to 55°C increased leaching selectivity to 22223 $\frac{g\ of\ Cu}{g\ of\ Au}$. However, at 55°C, 7.9 percentage points less copper was recovered than at 85°C. It is worth noting that these recoveries and selectivities may change with variation in metals content of the crushed PCBs. The interaction between copper content and co-extraction of gold is not clear. Operating at a lower temperature to reduce co-extraction of gold may be a sensible trade-off despite the loss of copper as gold is 7800 times more valuable per weight than copper (goldprice.org, Feb 2015).

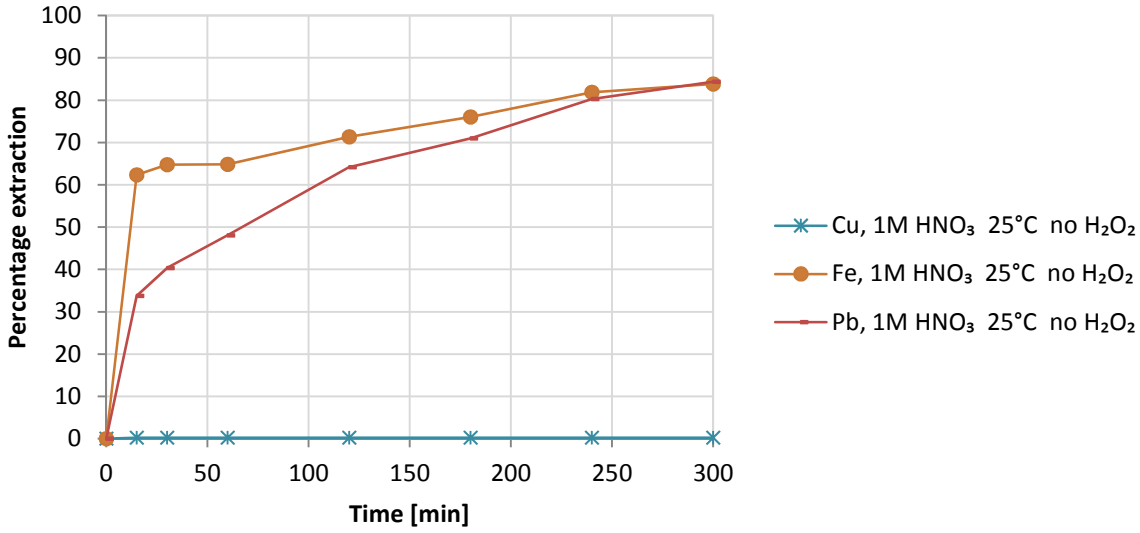

FIGURE 31: DISSOLUTION OF Cu, Fe AND Pb IN 1 M HNO_3 AT 25°C.

Although nitric acid leached no significant amount of copper at 25°C, Figure 31 shows 84% of Pb and 84% of Fe were leached at these conditions. This presents the possibility for selectively removing Fe and Pb prior to copper leaching in order to yield purer PLSs. The lack of observed Cu leaching at 25°C using 1 M HNO_3 agrees with results from Mecucci and Scott (2002) at 23°C.

4.1.3. THE EFFECT OF HYDROGEN PEROXIDE

Figure 32 shows how the presence of hydrogen peroxide affects the copper leaching. At 55°C, the presence of peroxide initially accelerated leaching, but leaching slowed quickly as peroxide decomposed. Note that the presence of peroxide ultimately did not influence the extent of copper leaching at 55°C and 85°C. At 25°C, the presence of peroxide increased copper leaching from 0.2% to 35%.

The change in free Gibbs energy for nitric acid leaching of copper in the absence peroxide is negative at 25°C. This indicates that copper leaching with HNO_3 at 25°C is in fact possible but does not occur to a significant extent probably due to slow reaction kinetics (see equation 4.1).

$$3Cu_{(s)} + 8HNO_{3(l)} \rightarrow 3Cu^{2+}_{(aq)} + 6NO^{-}_{3(aq)} + 4H_2O_{(l)} + 2NO_{(g)} \qquad \Delta G^o = -598\frac{kJ}{mol} \qquad (4.1)$$

$$Cu_{(s)} + H_2O_{2(l)} + 2H^+ \rightarrow Cu^{2+}_{(aq)} + 2H_2O \qquad \Delta G^o = -277.7\frac{kJ}{mol} \qquad (4.2)$$

The presence of hydrogen peroxide provides an alternative reaction for copper leaching (see equation 4.2) which does not require nitrate ion as an oxidising agent.

When leaching with nitric acid at 55°C and 85°C, the characteristic formation of orange $NO_{(g)}$ was observed. However, when leaching with nitric acid at 25°C with the aid of peroxide, the characteristic formation of orange $NO_{(g)}$ was not observed. This means that the 35% Cu extraction at 25°C seen in Figure 32 could not have occurred according to equation 4.1. The similarity in leaching trend in Figure 27 suggests that both nitric acid and sulphuric acid leaches copper according to equation 4.2 at 25°C.

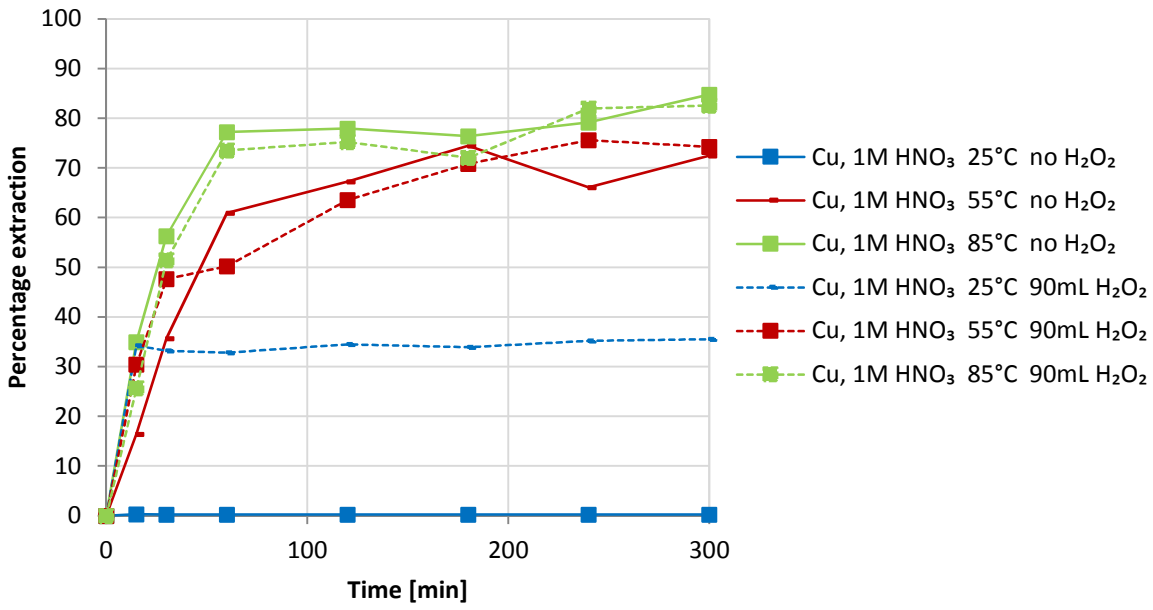

FIGURE 32: NITRIC ACID LEACHING OF COPPER WITH AND WITHOUT THE PRESENCE OF HYDROGEN PEROXIDE; S/L=1:10 W/V. THE BROKEN LINES REPRESENT Cu LEACHING WITH PEROXIDE AND THE SOLID LINES REPRESENT Cu LEACHING WITHOUT PEROXIDE

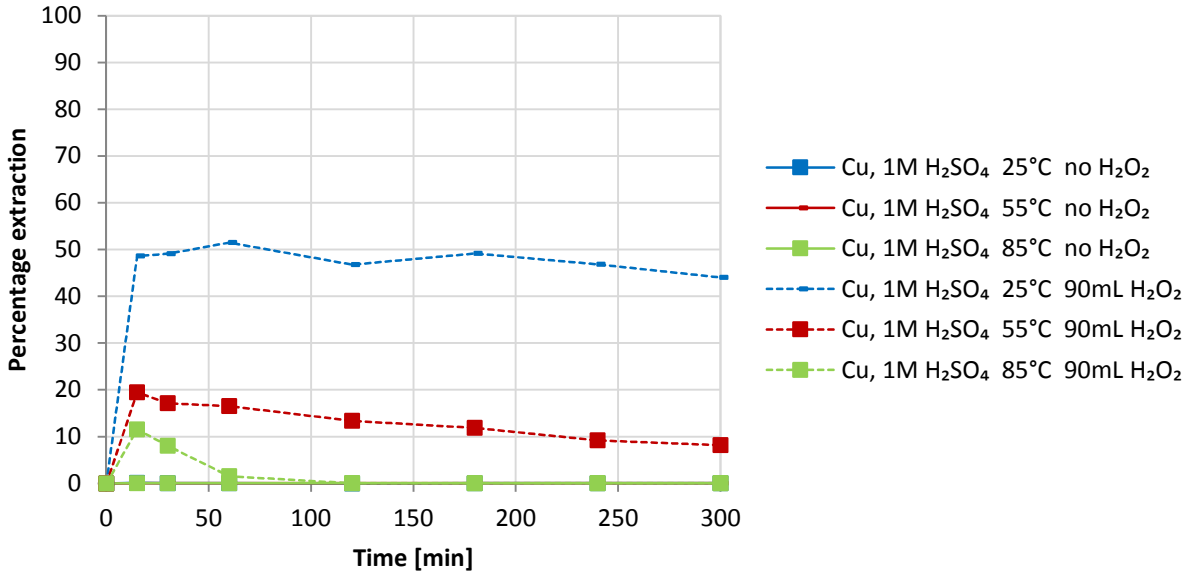

FIGURE 33: SULPHURIC ACID LEACHING OF COPPER WITH AND WITHOUT THE PRESENCE OF HYDROGEN PEROXIDE; S/L=1:10 W/V

Figure 33 shows the inability of sulphuric acid to leach copper in the absence of an oxidising agent. This is expected due to a positive Gibbs energy shown for the reaction (see equation 4.3). The presence of hydrogen peroxide allowed copper to be leached. Hydrogen peroxide decomposed quicker at the higher temperatures, leaving the system without an oxidising agent. The absence of hydrogen peroxide following its decomposition meant that the leaching reaction of copper could not be sustained. Copper leaching stopped at 15 minutes. At 55°C and 85°C copper was seen to leave solution once hydrogen peroxide was no longer present; possibly by a cementation reaction with undissolved Fe, Zn or Al.

$$Cu_{(s)} + 2H^{+} \rightarrow Cu^{2+}_{(aq)} + H_{2(g)} \qquad \Delta G^{o} = 65.5\ kJ/mol \qquad (4.3)$$

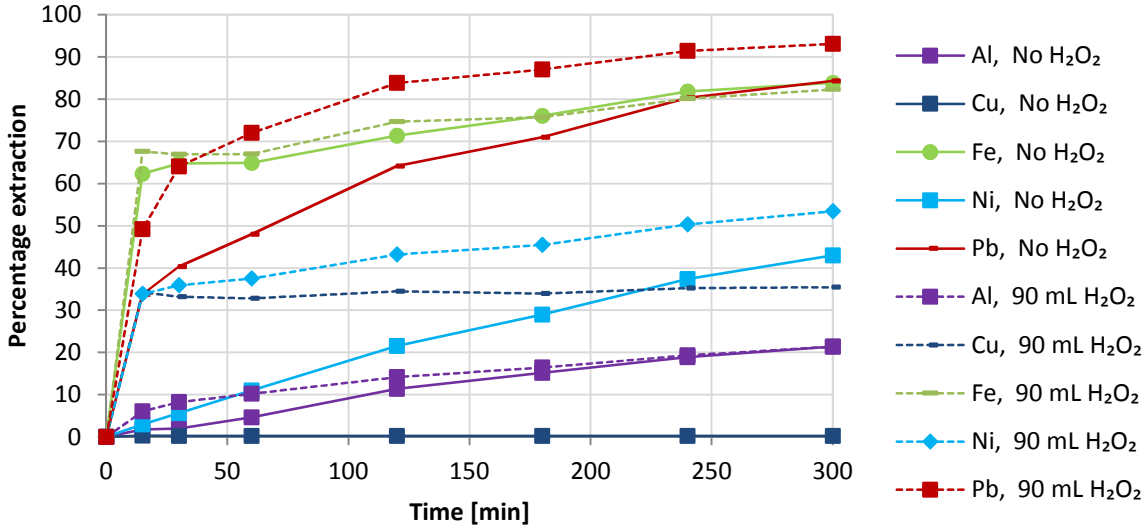

FIGURE 34: LEACHING WITH NITRIC ACID AT 25°C IN THE PRESENCE AND ABSENCE OF HYDROGEN PEROXIDE

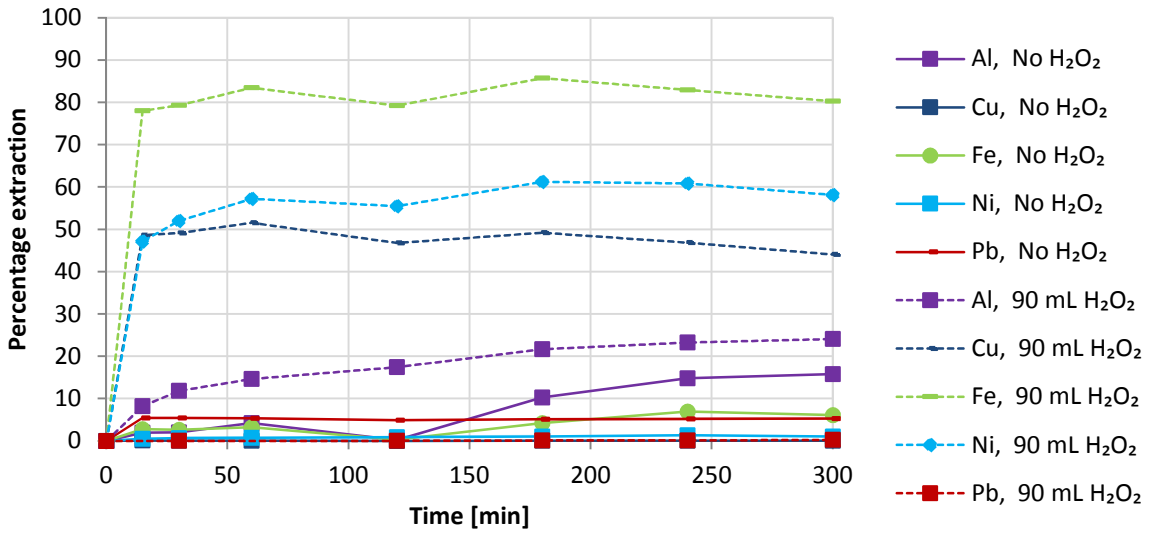

FIGURE 35: LEACHING WITH SULPHURIC ACID AT 25°C IN THE PRESENCE AND ABSENCE OF HYDROGEN PEROXIDE

Figure 34 and Figure 35 show the influence hydrogen peroxide addition had on base metal leaching using nitric acid and sulphuric acid respectively both at 25°C. Figure 34 shows that in the absence of hydrogen peroxide, lead, iron and nickel are leached 83.3%, 83.8% and 41.9% respectively using nitric acid. Sulphuric acid does not leach any of the former metals to a significant extent in the absence of hydrogen peroxide.

4.1.4. CONCLUSIONS FROM PHASE 1 EXPERIMENTS

Experiments confirmed the possibility of selective copper recovery from waste PCBs using either a nitric acid system or a sulphuric acid system. It was seen that the most complete extent of Cu recovery was 85% which could be achieved by nitric acid at a temperature of 85°C. The presence of hydrogen peroxide initially accelerated nitric acid leaching by providing an additional reaction path for copper dissolution. However, for the HNO_3 system the ultimate extent of copper dissolution at 55°C and 85°C after 5 hours remained unaffected by initial addition of hydrogen peroxide.

Although no appreciable amount of Cu was leached using 1 M HNO_3 at 25°C, the test did show 84% removal of Fe and Pb at these conditions. This suggests the possibility for selective removal of Fe and Pb prior to Cu leaching to yield purer PLSs.

It was decided that additional HNO_3 tests should be performed in the absence of peroxide at intermediate temperatures (55°C – 85°C) in order to better observe the relationship between temperature and co-extraction of Au.

Due to the rapid decomposition of hydrogen peroxide, the sulphuric acid leaching system could only achieve 43.8% Cu extraction. The sulphuric acid system showed superior Cu/Au selectivity and therefore warranted further investigation. It was decided to perform additional tests to determine whether alternative methods of hydrogen peroxide addition may limit peroxide decomposition and yield more effective extraction of base metals.

Following the additional investigations stated, final conclusions would be drawn with regards to the most suitable leaching agent, leaching temperature as well as peroxide addition.

4.1.5. ADDITIONAL TEMPERATURE INVESTIGATION FOR NITRIC ACID SYSTEM

Results from phase 1 showed 1 M HNO_3 achieving an 85% and 74% Cu extraction at 85°C and 55°C respectively. This greater extent of Cu extraction at 85°C of 85% was accompanied by poorer Cu/Au selectivity. The 55°C leaching temperature showed better Cu/Au selectivity but poorer extent of Cu dissolution.

A temperature range of 55°C to 85°C was investigated by performing experiments at 55°C, 65°C, 75°C and 85°C. Figure 36 shows the effect of temperature on Au extraction in the 1 M HNO_3 system. It is seen that the higher temperatures gave faster initial rates of Au extraction up to 60 minutes, where after Au behaviour followed no predictable trend.

Recall that no detectable amount of Au was leached when using H_2SO_4 as lixiviant. It was concluded that relative to H_2SO_4, the HNO_3 system showed inferior selectivity towards base metals through the co-extracting Au.

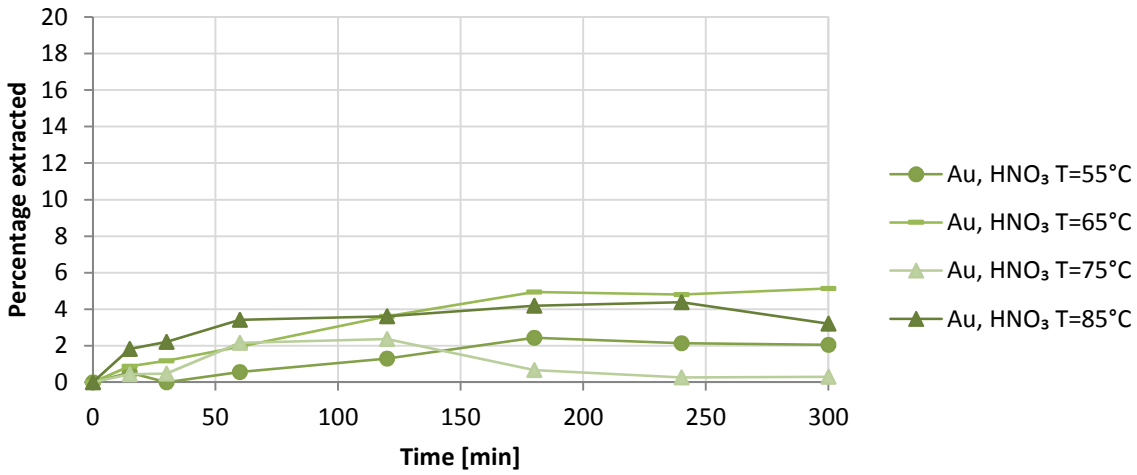

FIGURE 36: THE EFFECT OF TEMPERATURE ON PERCENTAGE Au EXTRACTION IN 1 M HNO_3 AT S/L RATIO OF 1/10.

4.1.6. METHOD OF PEROXIDE ADDITION

The single batch addition of peroxide at time zero during phase 1 appeared to be resulting in the decomposition of peroxide before it could be utilised in the leaching reactions. The amount and method of peroxide addition was therefore investigated while keeping all other parameters fixed at conditions stated in Table 20:

Firstly, increasing the batch size of peroxide added at time zero was considered. It was thought that adding more peroxide at time zero may prolong peroxide availability in the system and therefore sustain leaching reactions for longer. The oxidation potential would be a maximum by adding peroxide at time zero which would accelerate reaction kinetics [57]. This would allow for a greater extent of base metal extraction.

- Secondly, continuous addition of peroxide at various flow rates was considered. It was thought that lowering the concentration of peroxide may limit the rate of its decomposition. Continuous feeding would also guarantee the presence of peroxide in the system for at least the duration of the feeding period.

For optimisation of peroxide addition, focus was kept on Cu and Au extraction as they are the most abundant base metal and the most valuable precious metal respectively present in the PCBs.

TABLE 20: FIXED PARAMETERS DURING INVESTIGATION OF PEROXIDE ADDITION IN A SULPHURIC ACID LEACHING SYSTEM.

Parameter	Fixed set point	Comment
Temperature	25°C	The lower temperature limits peroxide decomposition. Peroxide was seen to be utilised more effectively at 25°C than at the higher temperatures (see Figure 33)
Lixiviant	1 M H_2SO_4	Compared to nitric acid, sulphuric acid showed a superior selectivity for Cu over Au.
S/L ratio	1:10	This parameter remains unchanged from previous experiments (see Table 15). 50 grams of crushed waste PCB is treated with 500 mL of 1 M H_2SO_4.
Agitation speed	500 rpm	Unchanged from previous experiments (see Table 15)

Figure 37 shows that increasing the batch volume of peroxide (30 wt% H_2O_2) added at time zero from 90 mL to 240 mL only increased copper recovery from 44% to 52%. This was due to both Cu leaching and H_2O_2 decompositions reactions (see equations 4.4 and 4.5 respectively) being exothermic. Both of these reactions therefore increased the system temperature, which accelerated the H_2O_2 decomposition reaction.

$$2H_2O_{2(l)} \rightarrow O_{2(g)} + 2H_2O_{(l)} \qquad \Delta H_r^o = -194\ kJ/mol \qquad (4.4.)$$

$$Cu_{(s)} + 2H^+_{(aq)} + H_2O_{2(l)} \rightarrow Cu^{2+}_{(aq)} + 2H_2O_{(l)} \qquad \Delta H_r^o = -318\ kJ/mol \qquad (4.5.)$$

After adding the 240mL peroxide batch at time zero the decomposition occurred rapidly and the cooling jacket was unable to maintain the system at the 25°C set point. Figure 38 shows the measured reactor temperature during the respective peroxide addition tests. The temperature of the system increased until all peroxide had decomposed, preventing any further Cu leaching. A maximum temperature of 75.9°C was reached.

Keeping the temperature below 30°C would have limited peroxide decomposition allowing for a greater extent of Cu extraction (see section 2.5.5.2). Due to insufficient cooling capability of the reactor, a low temperature could not be maintained. Several authors reported rapid decomposition of peroxide with increasing temperature [17,68,70].

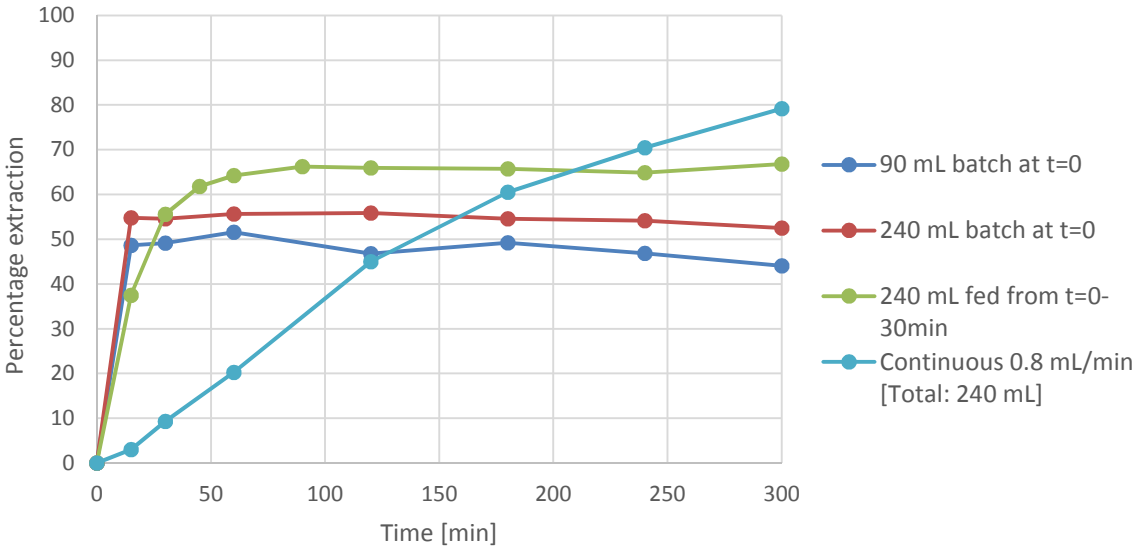

FIGURE 37: THE EFFECT OF ADDING DIFFERENT BATCH SIZES OF PEROXIDE AT TIME ZERO IN A 1 MOL/L SULPHURIC ACID LEACHING SYSTEM AT INITIAL TEMPERATURE OF 25°C

Continuous feeding of peroxide was considered next. Reducing the maximum amount of peroxide in the system by feeding continuously rather than batch wise limited the rate of the exothermic (leaching and H_2O_2 decomposition) reactions. This allowed the cooling jacket to be more effective at maintaining the system at the set point temperature, therefore limiting excessive peroxide decomposition.

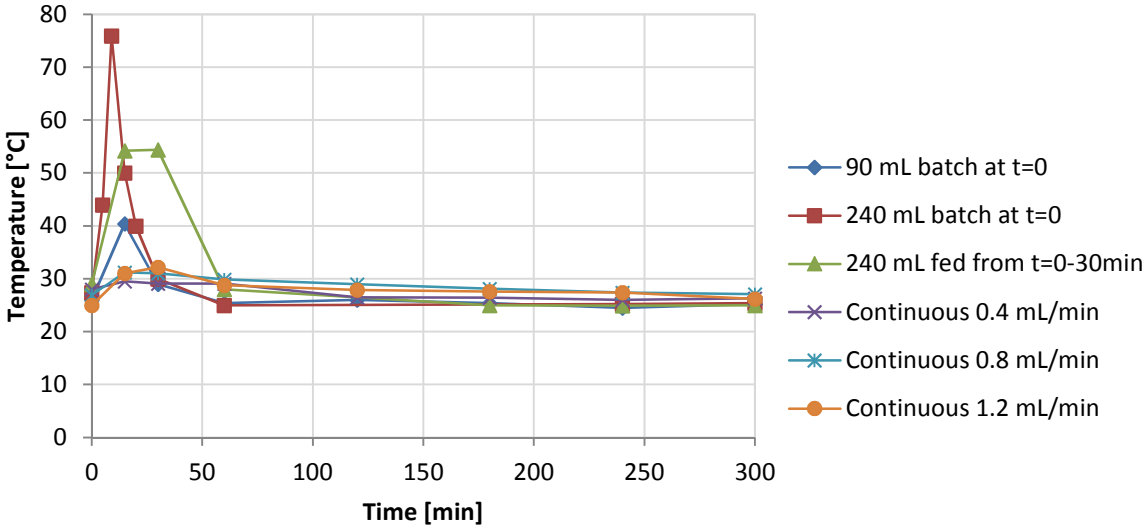

FIGURE 38: TEMPERATURE IN THE REACTOR DURING PEROXIDE ADDITION TESTS

Figure 37 shows that feeding 240 mL of peroxide continuously over the first 30 minutes rather than adding a batch volume at time zero increased Cu leaching from 52% to 66%. Once peroxide feeding stopped at 30 minutes, the rate of Cu leaching quickly decreased as remaining peroxide was used up or decomposed. Although the leaching temperature still exceeded the 25°C set point in this case, the greater extent of Cu leaching achieved indicated that peroxide could be utilised more effectively when introduced into the system slowly.

Subsequently, the rate of peroxide addition was slowed so that 240 mL of peroxide was fed over the entire 300 minutes of the experiment (see Figure 37). This correlates to a feed rate of 0.8 mL of peroxide per minute. Figure 37 shows that feeding 240 mL of peroxide over 300 minutes rather than 30 minutes increased the extent of Cu leaching from 66% to 79%. This was due a lower operating temperature that could be maintained reducing the decomposition of peroxide allowing for more effective utilisation.

Of all the methods tested to introduce peroxide into the leaching system, continuous addition during the entire course of the experiment was seen to be the most effective. The reason for this was attributed to the temperature controlling ability of the reactor being adequate only at low feed rates of peroxide. Two additional peroxide feed rates were tested. Figure 39 shows that increasing the peroxide feed rate from 0.8 mL/min to 1.2 mL/min increased copper leaching from 79% to 88% after 300 minutes.

The positive gradients observed between 240 minutes and 300 minutes for Cu leaching (see Figure 39) suggested that a greater extent of Cu leaching could be achieved given more leaching time. The duration of all subsequent leaching experiments were extended from 300 minutes to 480 minutes.

Continuous peroxide addition at a flow rate of 1.2 mL/min during the entire run was seen to yield the most complete extent of Cu leaching. No Au was leached at these conditions.

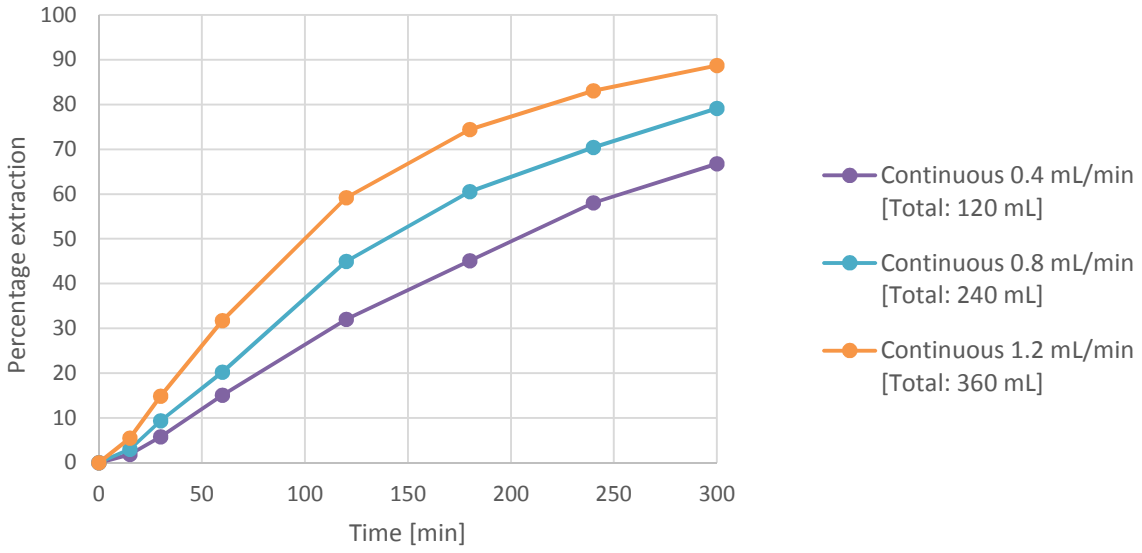

FIGURE 39: THE EFFECT OF DIFFERENT 30 WT% PEROXIDE FEED RATES ON Cu LEACHING IN 1 M H_2SO_4 AT 25°C AND S/L OF 1/10 W/V

4.1.7. PHASE 1 RECOMMENDATIONS

Results from HNO_3 tests, showed that in order to achieve a significant amount of base metal extraction, a temperature of 55°C or higher was required. It was seen that at these temperatures, co-extraction of 0.3 to 1.4 mg of Au occurred.

Initial leaching results showed the lower temperature of 25°C to be the most favourable for the H_2SO_4/H_2O_2 system. Variation of the method and amount of 30 wt% H_2O_2 addition to the H_2SO_4 leaching solution showed that continuous addition at a feed rate of 1.2 mL/min provided the

greatest extent (88%) of Cu extraction. No detectable co-extraction of Au occurred at these conditions.

Sulphuric acid at 25°C with a peroxide feed rate of 1.2 mL/min was selected for use in subsequent experiments for the following reasons:

- The H_2SO_4/H_2O_2 system had superior selectivity for base metals as it did not co-extract any detectable amount of Au. The HNO_3 system co-extracted between 0.3 to 1.4 mg of Au at 55°C and 85°C.
- The H_2SO_4/H_2O_2 system can be operated at a lower temperature of 25°C. The HNO_3 system required a temperature of that was ≥ 55°C in order to effectively extract base metals.
- The H_2SO_4/H_2O_2 system produced no toxic gasses as only $O_{2(g)}$ and $H_2O_{(vap)}$ formed during leaching. During HNO_3 leaching $NO_{x(g)}$ gasses are evolved which are hazardous.

4.2. PHASE 2: OPTIMISATION

Results from phase 1 experiments showed sulphuric acid co-extracting less Au than nitric acid. Investigation of peroxide addition in the sulphuric acid system showed a continuous peroxide flow rate of 1.2 mL/min yielding the most complete extent of base metal extraction.

Phase 2 investigated the effects of pre-treating feed by application of dense medium separation and a combination of dense medium separation and magnetic separation. The effects of acid concentration and solid to liquid ratio were also investigated.

4.2.1. FEED CHARACTERISATION

The three different feed types, namely, dense medium separation (DMS) treated feed, dense medium separation and magnetic separation (MS) treated feed (DMS and MS), and untreated feed (No Sep.) were characterised based on metals content.

DENSE MEDIUM SEPARATION

Application of dense medium separation was aimed at reducing feed volume by separation of metals from plastic based on difference in density. Tetra bromoethane (TBE) and acetone were mixed at a ratio of 1: 0.27 to yield a dense medium with an SG of 2.5. The resulting heavy and light fractions were then washed using acetone, dried and weighed. By weight, 37% of the material reported to the heavy fraction.

The fractions were characterised by sampling both light and heavy fractions using a rotary sampler (see Figure 21). The samples were digested using aqua regia and the aqueous phase analysed using ICP-OES. Variance in composition of the light and heavy fractions were used to construct 95% confidence intervals for the weight % of respective metals as show in Table 21.

Table 21 compares the composition of crushed PCBs with the heavy fraction and light fraction produced by applying DMS as described. The application of DMS enriched the total metals content from 48.7 Wt% to 75.3 Wt%. Applying DMS increased the grade of Cu from 27.7 Wt% to 46.5 Wt%. The grade of Au was decreased from 223 g/ton to 94 g/ton, implying that the majority of Au reported to the light fraction.

TABLE 21: AVERAGE WEIGHT% OF METALS IN CRUSHED PCB (NO SEP), AND FRACTIONS OF DENSE MEDIUM TREATED FEED (DMS). CONFIDENCE INTERVALS CALCULATED WITH α=0.05.

Metal	No Sep.	DMS (Light fraction)	DMS (Heavy fraction)
Ag	(0.07 ± 0.01) %	(0.01 ± 0) %	(0.06 ± 0.02) %
Al	(4.5 ± 0.2) %	(4.12 ± 0.72) %	(3.51 ± 0.26) %
Au	(0.02 ± 0) %	(0.02 ± 0) %	(0.01 ± 0) %
Co	(0.06 ± 0.07) %	(0 ± 0) %	(0.01 ± 0) %
Cu	(27.69 ± 0.88) %	(6.96 ± 0.42) %	(46.22 ± 2.77) %
Fe	(3.9 ± 0.16) %	(0.16 ± 0.04) %	(4.75 ± 0.37) %
Ni	(0.7 ± 0.05) %	(0.02 ± 0) %	(1.01 ± 0.06) %
Pb	(4.97 ± 0.79) %	(0.08 ± 0) %	(4.53 ± 1.3) %
Sn	(3.05 ± 0.36) %	(0.07 ± 0) %	(7.69 ± 0.72) %
Zn	(3.73 ± 0.22) %	(0.09 ± 0.02) %	(7.46 ± 0.31) %

Figure 40 shows the separation behaviour of the metals during DMS based on the digestion of samples taken from the light and heavy fractions. The fraction of the metal that reported to the light phase is shown in red while the fraction of the metal that reported to the heavy phase is shown in blue. Figure 40 shows that ~20% of Cu reported to the light phase along with ~70% of Au. This may be due to separation inefficiencies or could imply that the majority of Au was imbedded in resin or plastic layers, causing it to float in the dense medium. The Cu reporting to the light fraction may be attributed to incomplete liberation of printed circuits from plastics. The majority of Ag, Co, Cu, Fe, Ni, Pb, Sn and Zn reported to the heavy fraction as expected. The majority if Al reported to the light phase. This is due to the density of Al (2.7 g/cm^3) being close to that of the dense medium (2.5 g/cm^3). Veit et al. 2002 also reported a tendency of Al towards the light fraction during DMS using TBE and acetone at SG of 2.5.

Figure 41 shows a photo of the heavy and light fractions produced by DMS. As expected, the majority of the heavy fraction (shown on the left) consisted of liberated metal pieces. The light fraction (shown on the right) consisted mainly of plastic and resin.

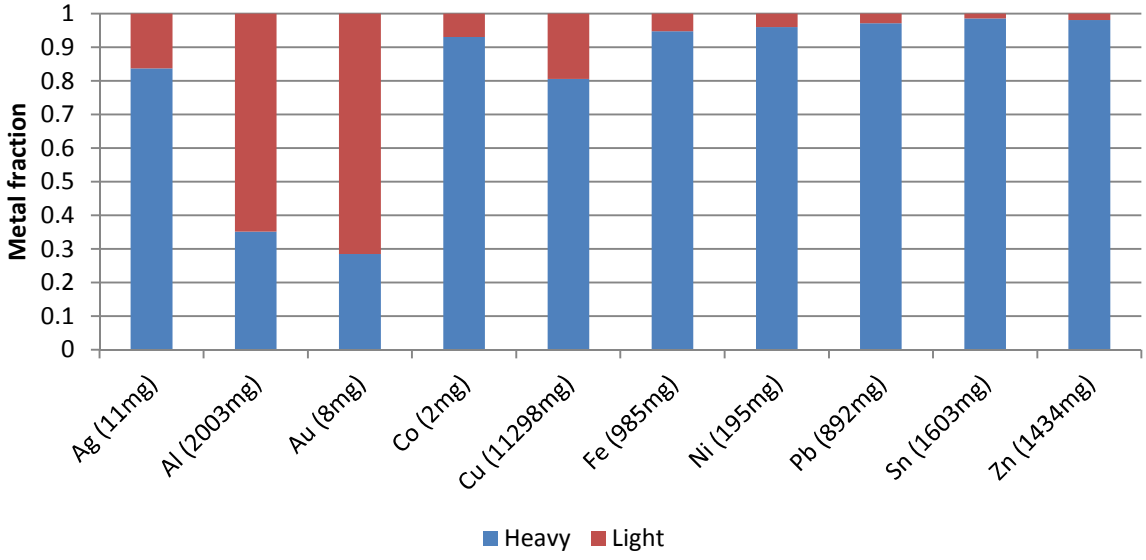

FIGURE 40: SEPARATION OF METALS DURING DENSE MEDIUM SEPRATION USING A MIXTURE OF TETRA BROMOETHANE (TBE) AND ACETONE AT SG: 2.5. THE MASS TOTALS OF METALS RECOVERED AFTER TREATMENT IN BOTH LIGHT AND HEAVY FRACTIONS OF A 50 GRAM SAMPLE OF CRUSHED PCB ARE SHOWN IN BRACKETS.

Figure 42 compares the fractions of metals that sank during application of DMS in the current work to fractions calculated from Veit et al. 2002. Note that Veit et al. 2002 used particle sizes of <1 mm while <2 mm was used for the current work. In the current work a greater fraction of Fe, Ni, Pb, Sn and Zn reported to the heavy fraction than in the literature case (see Figure 42). Contrary to the literature case, the majority of Ag in the current work reported to the heavy fraction. Variation in use of different metals between PCBs as well as method of comminution and final particle size may affect the extent of liberation achieved. The extent of liberation of metals from plastic will likely influence the separation achieved during DMS.

FIGURE 41: HEAVY AND LIGHT FRACTIONS PRODUCED BY DENSE MEDIUM SEPARATION USING A MIXTURE OF TETRA BROMOETHANE AND ACETONE AT AN SG OF 2.5. THE HEAVY FRACTION IS SHOWN ON THE LEFT AND THE LIGHT FRACTION IS SHOWN ON THE RIGHT.

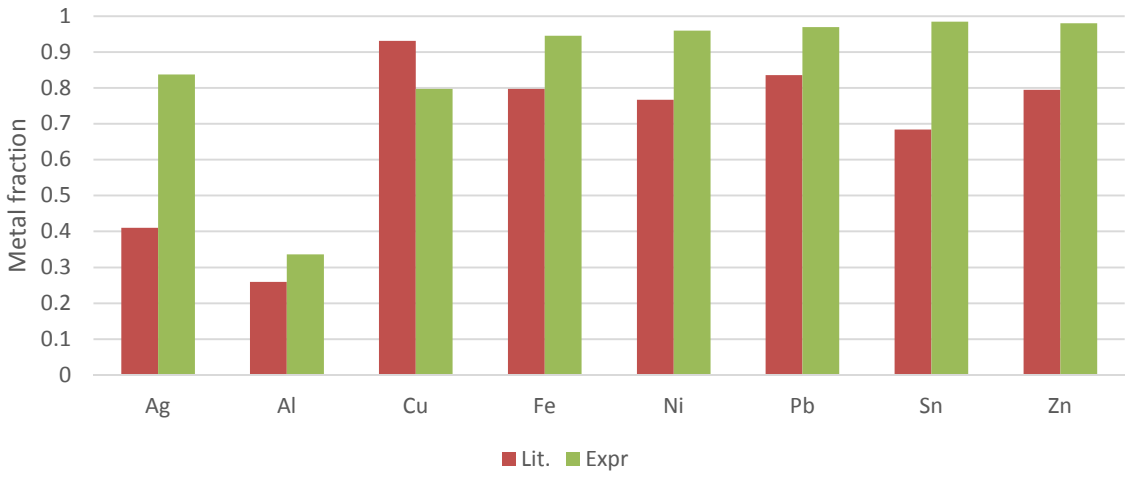

FIGURE 42: FRACTIONS OF METALS THAT SANK DURING DMS ARE SHOWN FOR BOTH LAB EXPERIMENTS AND CALUCLATED VALUES FROM LITERATURE BY VEIT ET AL. 2002. IN BOTH CASES A MIXTURE OF TBE WITH ACETONE AT SG: 2.5 WAS USED.

MAGNETIC SEPARATION

Magnetic separation was applied manually to the metals concentrate produced by DMS. The method used is shown in Figure 24. The magnet used was a Ba-Fe block magnet supplied by Allmag Industries with dimensions: 150x100x25mm.

TABLE 22: WEIGHT% OF RESPECTIVE METALS IN CRUSHED PCB (NO SEP), DENSE MEDIUM TREATED FEED (DMS) AND DENSE MEDIUM AND MAGNETIC SEPARATION TREATED FEED (DMS&MS)

Metal	No Sep.	DMS (Heavy fraction)	DMS&MS (Non-magnetic fraction)
Ag	(0.07 ± 0.01) %	(0.06 ± 0.02) %	(0.05 ± 0.02) %
Al	(4.5 ± 0.2) %	(3.51 ± 0.26) %	(3.93 ± 0.31) %
Au	(0.02 ± 0) %	(0.01 ± 0) %	(0.01 ± 0) %
Co	(0.06 ± 0.07) %	(0.01 ± 0) %	(0.02 ± 0.02) %
Cu	(27.69 ± 0.88) %	(46.22 ± 2.77) %	(47.84 ± 2.55) %
Fe	(3.9 ± 0.16) %	(4.75 ± 0.37) %	(1.83 ± 0.13) %
Ni	(0.7 ± 0.05) %	(1.01 ± 0.06) %	(0.43 ± 0.03) %
Pb	(4.97 ± 0.79) %	(4.53 ± 1.3) %	(4.35 ± 1.21) %
Sn	(3.05 ± 0.36) %	(7.69 ± 0.72) %	(7.53 ± 0.5) %
Zn	(3.73 ± 0.22) %	(7.46 ± 0.31) %	(7.31 ± 0.76) %

Table 22 shows the average weight percentages of the metals in the respective feed types with a confidence interval calculated using $\alpha = 0.05$. As expected, the application of MS was seen to have the most pronounced effect on ferromagnetic metals: Fe and Ni. Although Co is also a ferromagnetic metal, its intermittent presence in the samples prevented characterisation of its behaviour during MS.

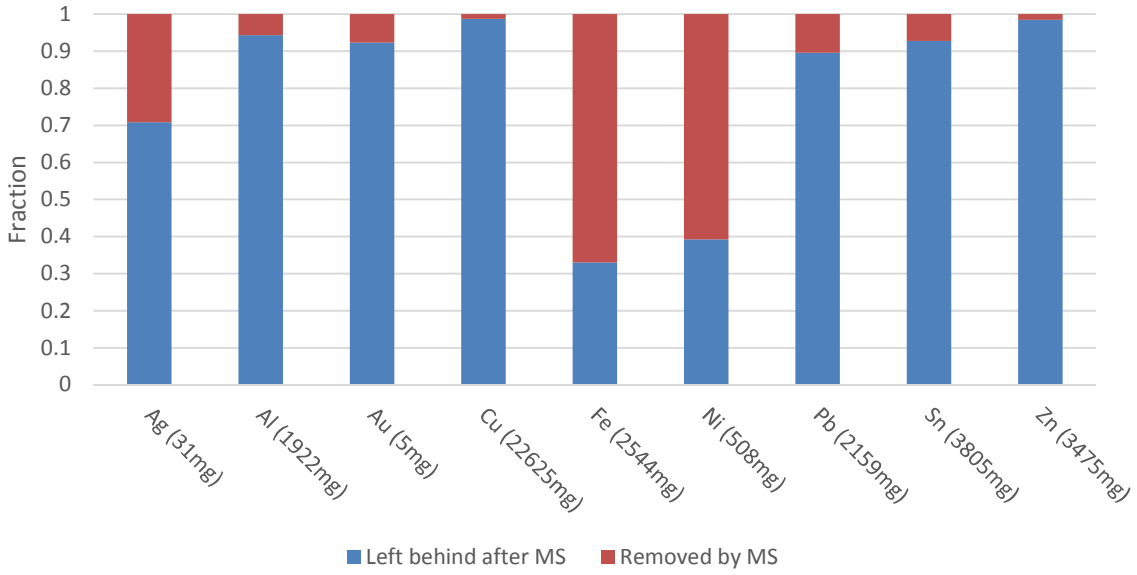

FIGURE 43: BEHAVIOUR OF METAL DURING APPLICATION OF MAGNETIC SEPARATION TO 50 GRAMS OF METALLIC CONCENTRATE PRODUCED BY DENSE MEDIUM SEPARATION. TOTAL MASS OF METAL IN SAMPLE IS SHOWN IN BRACKETS.

Figure 43 shows that application of magnetic separation removed 67% of Fe, 60% of Ni and 29% of Ag. The diamagnetic nature of Ag (please see Table 5) implies a small repulsive force towards magnetic fields. The partial removal of Ag by MS can therefore be attributed to Ag being physically connected to ferromagnetic metal. Due to weak magnetic susceptibilities and sufficient liberation from ferromagnetic material, Al, Au, Cu, Pb, Sn and Zn remained mostly unaffected by the application of MS.

The magnetic fraction produced in the current work was digested and its composition was compared to a calculated magnetic fraction composition from work by Veit et al. 2006. The comparison is shown in Figure 44. In both the literature case and the current work, the magnetic fraction consisted mostly of Fe, followed by approximately equal amounts Ni and Cu.

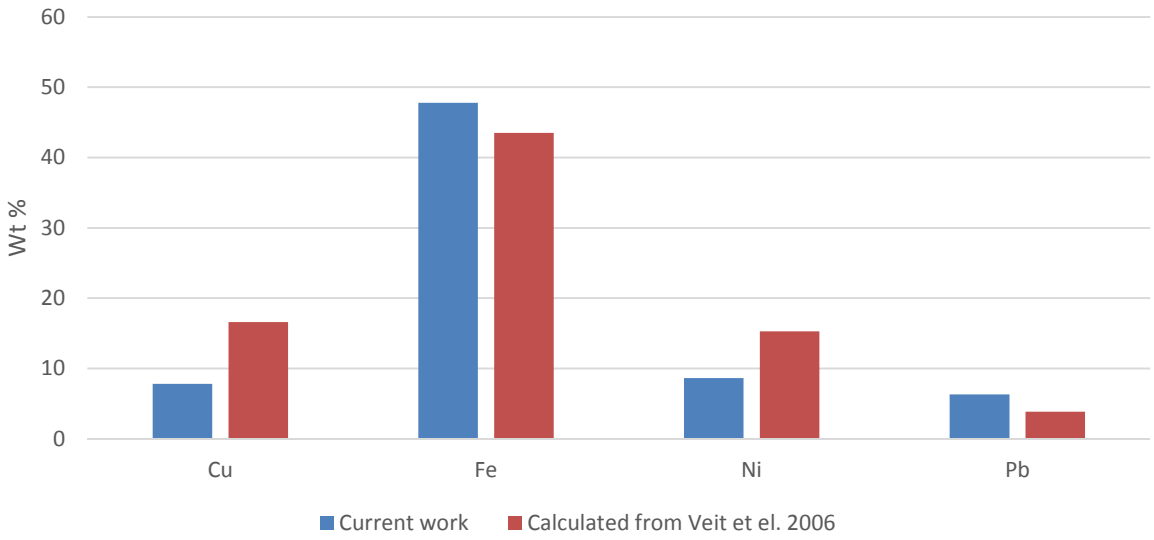

FIGURE 44: COMPARISON OF MAGNETIC FRACTION COMPOSITION IN CURRENT WORK TO A CALCULATED MAGNETIC FRACTION COMPOSITION FROM WORK BY VEIT ET EL. 2006

4.2.2. THE EFFECT OF MECHANICAL PRE-TREATMENT

4.2.2.1. BASE METAL EXTRACTION

Figure 45 compares the three different feed types by showing the mass of Cu extracted at a S/L ratio of 1/10 in 2.5 M H_2SO_4. It is seen that the concentrated feeds, i.e. DMS and DMS+MS, yielded more concentrated Cu solutions due to its higher Cu content. The extent of Cu extracted in Figure 45 is shown in Figure 46. Although the concentrated feeds contained around twice the amount of Cu as the untreated feed, Figure 46 shows that the time required to reach ~95% Cu extraction was the same. This implies that a greater S/L ratio for the untreated feed could potentially be used without significantly increasing the leaching time required for complete Cu extraction.

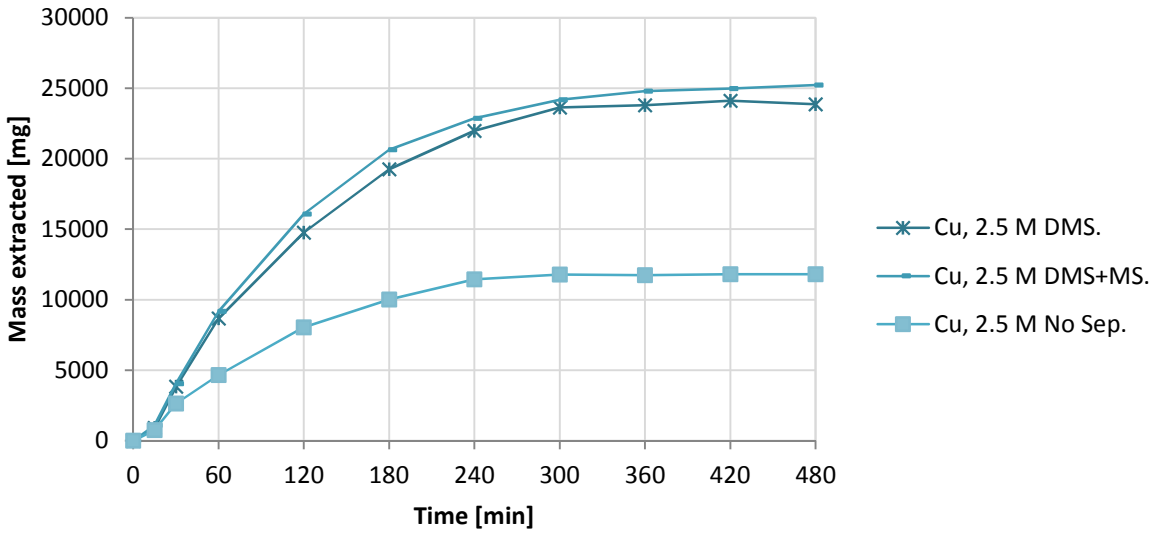

FIGURE 45: COMPARING DIFFERENT FEED TYPES BASED ON MASS Cu EXTRACTED IN 2.5 M H_2SO_4 AT S/L=1/10 WITH H_2O_2 30 WT% FEED RATE OF 1.2 ML/MIN.

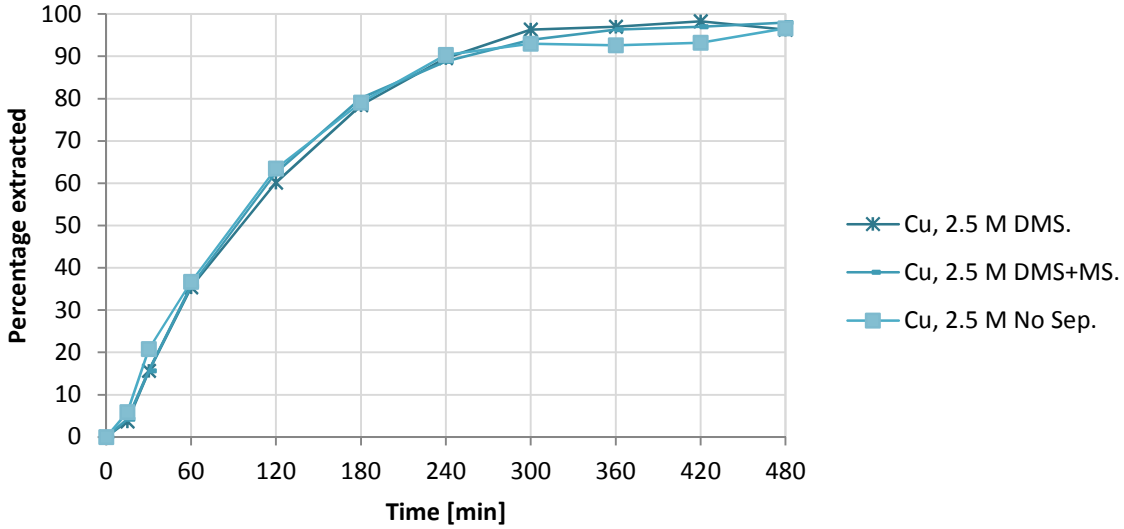

FIGURE 46: COMPARING DIFFERENT FEED TYPES BASED ON PERCENTAGE OF Cu EXTRACTED IN 2.5 M H_2SO_4 AT S/L=1/10 WITH H_2O_2 30 WT% FEED RATE OF 1.2 ML/MIN.

Figure 47 shows the mass of iron extracted from the different feed types. As expected the application of MS reduced the amount of Fe in DMS+MS feed. The lower amount of Fe in the DMS+MS feed made it reach complete (~95%) Fe extraction quicker at around 120 minutes than DMS feed at around 300 minutes. The untreated feed contained an intermediate amount of Fe and complete Fe extraction was achieved after 240 minutes. With the majority of Ni also being removed by MS, the leaching of Ni followed the same trend as that of Fe.

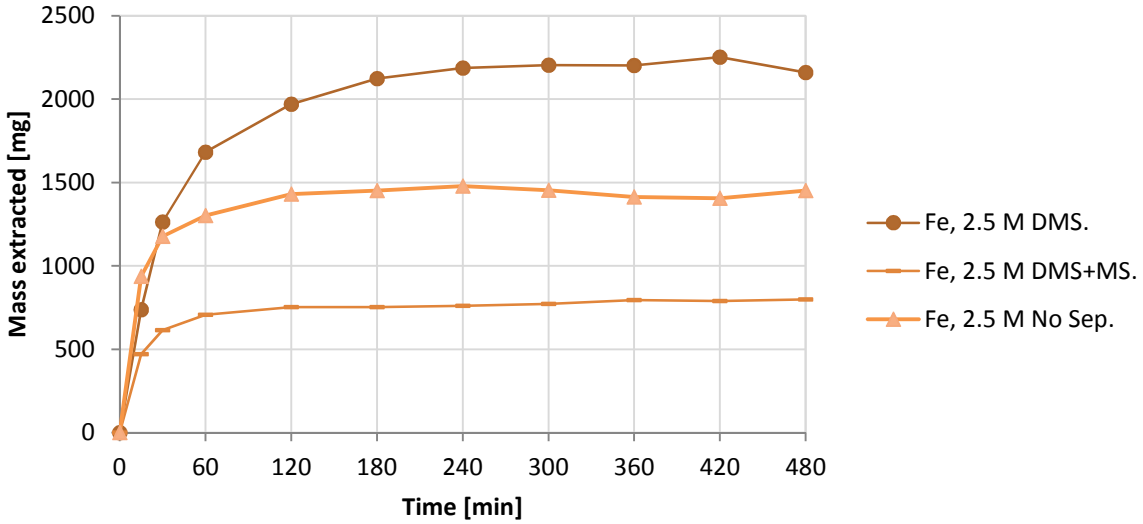

FIGURE 47: MASS OF Fe EXTRACTED FROM THE DIFFERENT FEED TYPES IN 2.5 M H_2SO_4 AT S/L=1/10 WITH H_2O_2 30 WT% FEED RATE OF 1.2 ML/MIN.

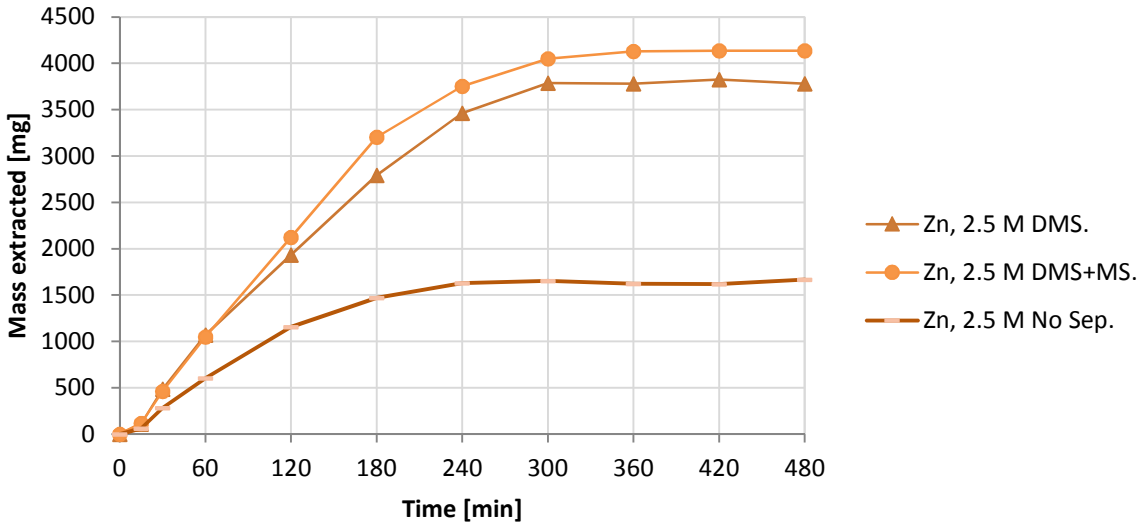

FIGURE 48: MASS OF Zn EXTRACTED FROM THE DIFFERENT FEED TYPES IN 2.5 M H_2SO_4 AT S/L=1/10 WITH H_2O_2 30 WT% FEED RATE OF 1.2 ML/MIN.

Figure 48 shows the leaching behaviour of Zn. It is seen that Zn extraction resembled that of Cu as shown in Figure 45. Compared to DMS feed, the greater mass of Zn extracted for DMS+MS feed can be attributed simply to a greater mass of Zn present in that feed sample.

Figure 49 compares the extraction of Al for the three different feed types. Al leached rapidly from time zero to 15 min, but then slowed down before accelerating again at time 180 min. Figure 50 shows a Pourbaix diagram for Al in the presence of expected combination of metals. According to Figure 50, complete dissolution of Al is expected in acidic and oxidising conditions. However, results from experiments seem to indicate possible passivation of Al at lower pH values. The same effect was not observed for the untreated feed for reasons unknown.

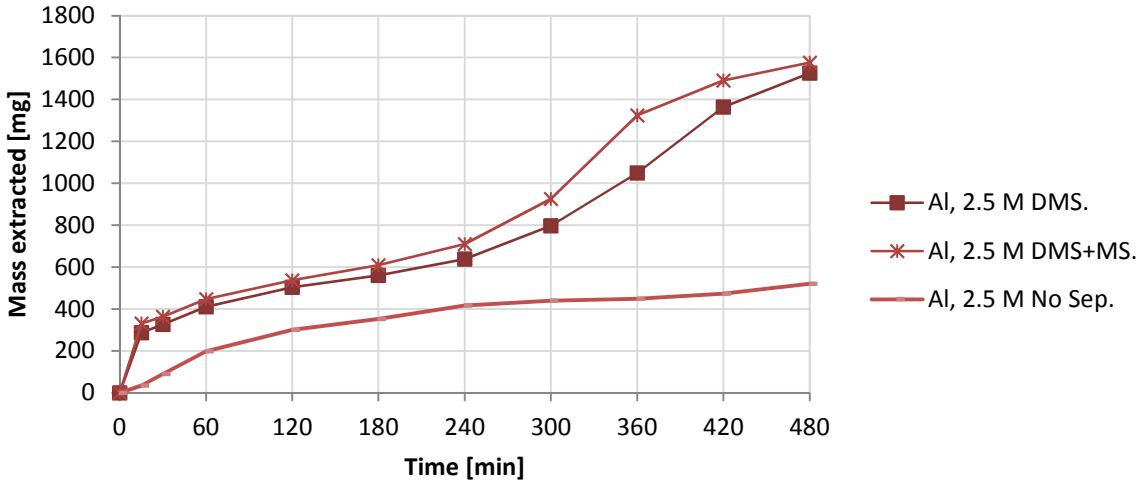

FIGURE 49: MASS OF Al EXTRACTED FROM THE DIFFERENT FEED TYPES IN 2.5 M H_2SO_4 AT S/L=1/10 WITH H_2O_2 30 WT% FEED RATE OF 1.2 ML/MIN.

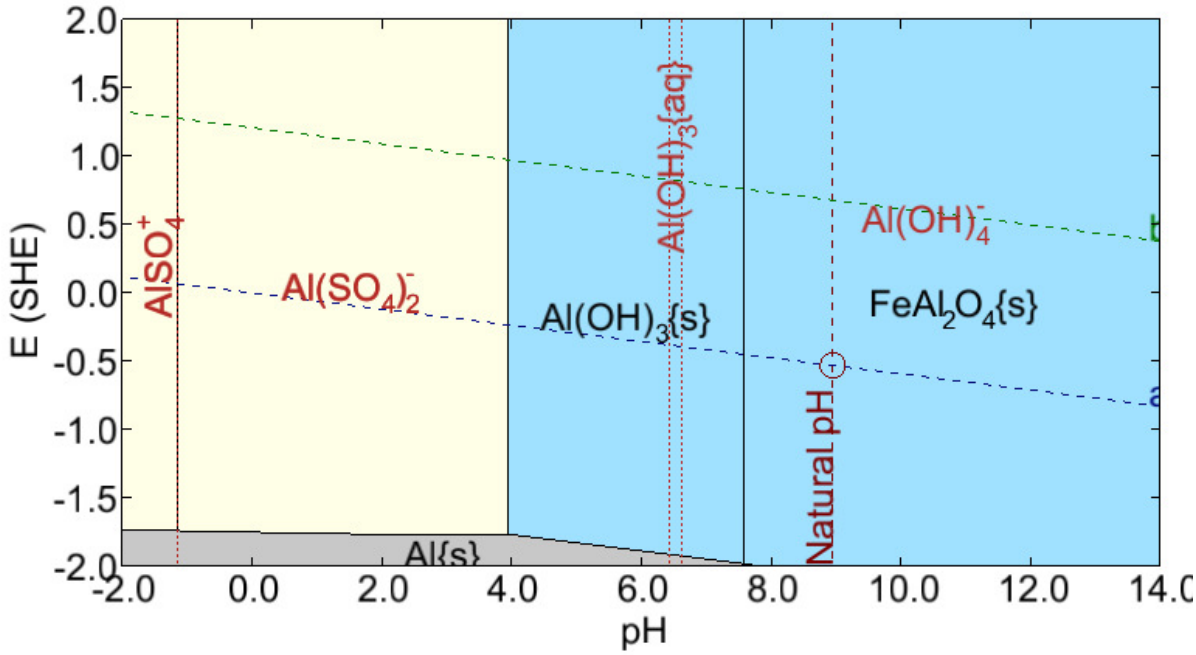

FIGURE 50: POURBAIX DIAGRAM PRODUCED BY OLI SYSTEMS FOR Al IN A SULPHURIC ACID SYSTEM AT 25°C IN THE PRESENCE OF EXPECTED COMBINATION OF METALS.

Figure 51 shows the mass of Sn extracted for the different feed types. For all three feeds, the dissolution of Sn was followed by subsequent precipitation. The relatively higher peaks for the concentrated feeds may be attributed simply to greater Sn content in the DMS and DMS+MS feeds.

Figure 52 shows the Pourbaix diagram for Sn in this specific system. The blue shaded area represents an area of stability for $SnO_{2(s)}$. Consideration of the Pourbaix diagram suggests that $Sn_{(s)}$ was oxidised to either $Sn(OH)_3^+$ or Sn^{2+}, possibly according to equations 4.6 and 4.7, respectively. This was followed by subsequent precipitation as $SnO_{2(s)}$, possibly according to equations 4.8 and 4.9:

$$Sn_{(s)} + 2H_2O_{2(l)} + H^+_{(aq)} \rightarrow Sn(OH)^+_{3(aq)} + H_2O_{(l)} \qquad \Delta G_r = -703\ kJ/mol \qquad (4.6.)$$

$$Sn_{(s)} + H_2O_{2(l)} + 2H^+_{(aq)} \rightarrow Sn^{2+}_{(aq)} + 2H_2O_{(l)} \qquad \Delta G_r = -146\ kJ/mol \qquad (4.7.)$$

$$Sn(OH)^+_{3(aq)} \rightarrow SnO_{2(s)} + H_2O_{(l)} + H^+_{(aq)} \qquad \Delta G_r = -51\ kJ/mol \qquad (4.8.)$$

$$Sn^{2+}_{(aq)} + H_2O_{2(l)} \rightarrow SnO_{2(s)} + 2H^+_{(aq)} \qquad \Delta G_r = -370\ kJ/mol \qquad (4.9.)$$

The peaks of dissolved Sn shown in Figure 51 may be due to the dissolution of Sn occurring faster than its precipitation. As the availability of native $Sn_{(s)}$ diminished in the system, the rate of dissolution became slower than the rate of precipitation. This reduced the nett amount of Sn in solution as shown in Figure 51. Miura et al. 2002 also reported the gradual oxidation of Sn^{2+} to form $SnO_{2(s)}$ in an oxidative sulphuric acid environment [67].

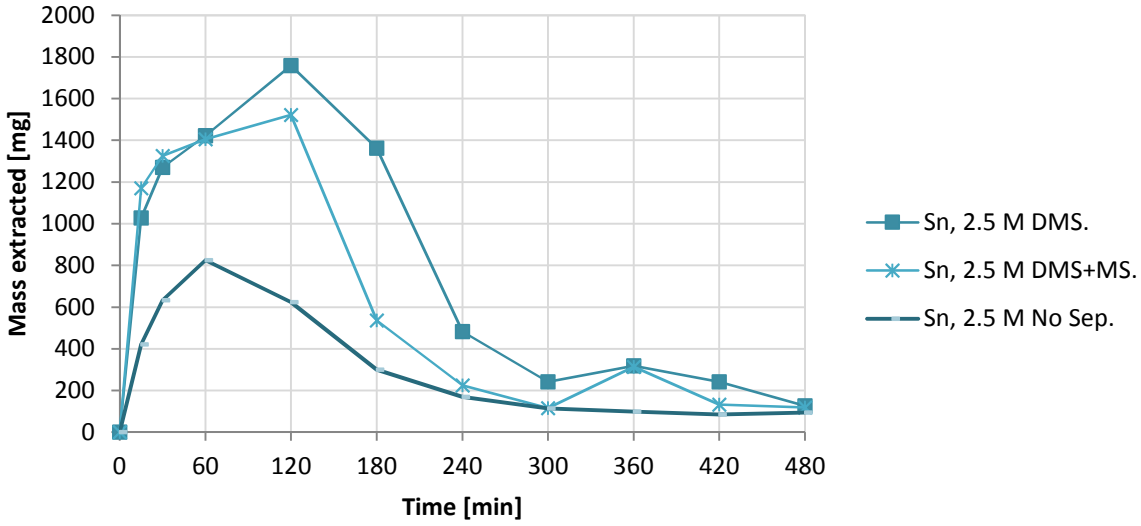

FIGURE 51: MASS OF SN EXTRACTED FROM THE DIFFERENT FEED TYPES IN 2.5 M H_2SO_4 AT S/L=1/10 WITH H_2O_2 30 WT% FEED RATE OF 1.2 ML/MIN.

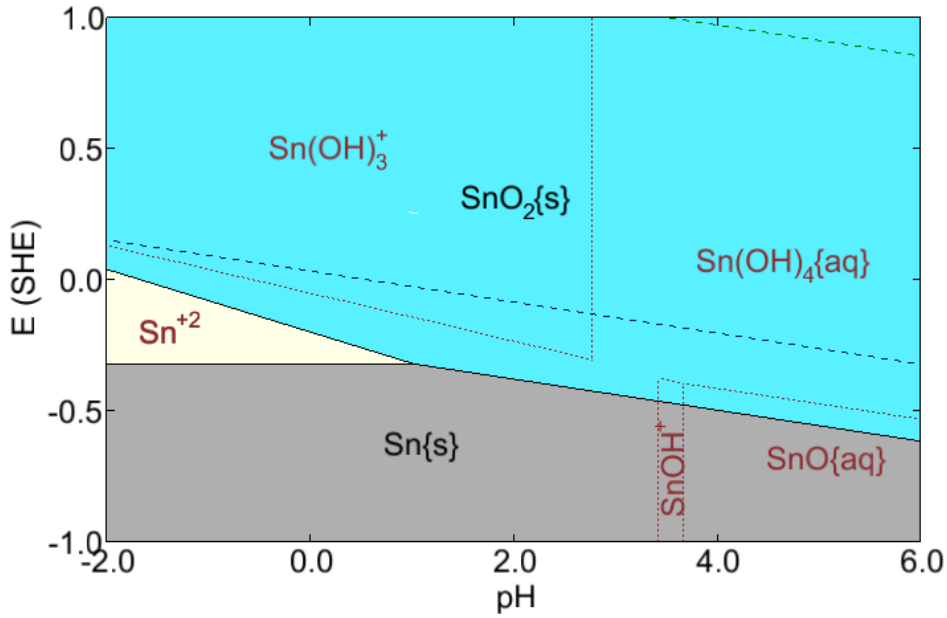

FIGURE 52: POURBAIX DIAGRAM PRODUCED BY OLI SYSTEMS FOR Sn IN A SULPHURIC ACID SYSTEM AT 25°C IN THE PRESENCE OF EXPECTED COMBINATION OF METALS.

No significant amount of Pb was extracted from any of the feed types. This is due to Pb being converted to $PbSO_{4(s)}$ in the presence of sulphuric acid.

4.2.2.2. PRECIOUS METAL EXTRACTION

Figure 53 shows that no significant amount of Au or Ag was extracted from any of the three different feed types. The application of mechanical pre-treatment did therefore not influence the selectivity of the leach for base metals.

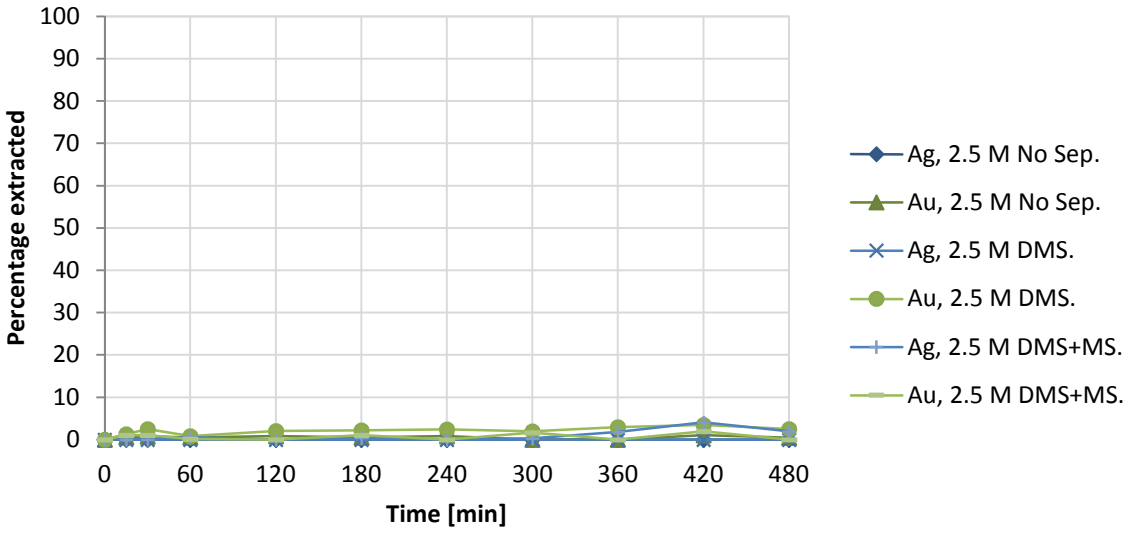

FIGURE 53: MASS OF Au AND Ag EXTRACTED FROM THE DIFFERENT FEED TYPES IN 2.5 M H_2SO_4 AT S/L=1/10 WITH H_2O_2 30 WT% FEED RATE OF 1.2 ML/MIN.

4.2.3. THE EFFECT OF ACID CONCENTRATION

4.2.3.1. BASE METALS

Figure 54 shows the effect of acid concentration on Cu and Fe extraction from DMS+MS feed at an S/L ratio of 0.6/10. Increasing H_2SO_4 concentration from 1 M to 2.5 M increased the rate of Cu extraction, decreasing the time required to reach equilibrium from 480 minutes to 240 minutes. Higher H_2SO_4 concentration also increased Fe extraction rate, but the effect is slightly less pronounced.

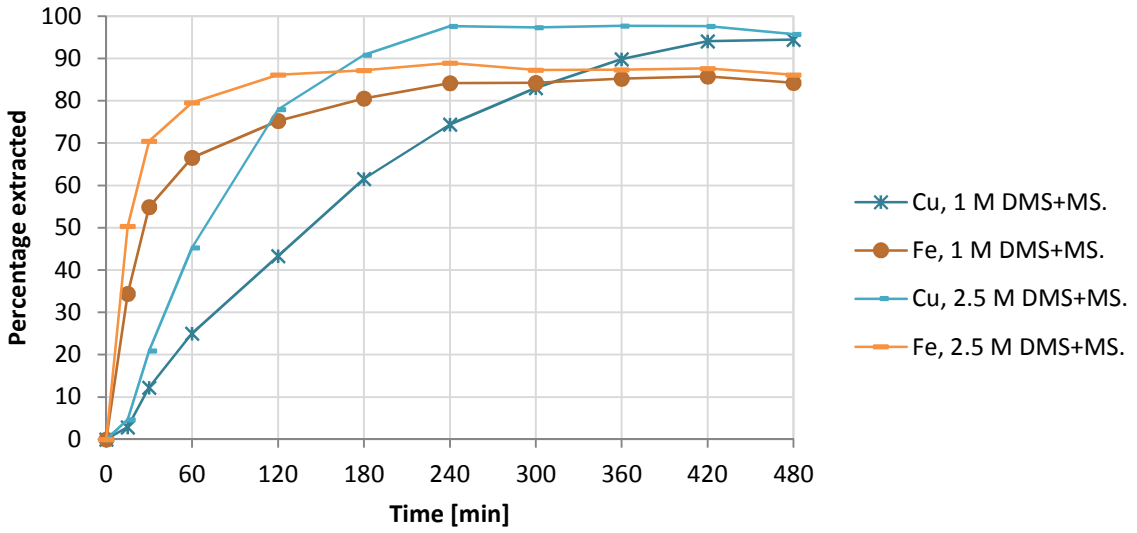

FIGURE 54: PERCENTAGE OF Cu AND Fe EXTRACTED FROM THE DMS+MS FEED AT S/L=0.6/10 AT DIFFERENT H_2SO_4 CONCENTRATIONS WITH H_2O_2 30 WT% FEED RATE OF 1.2 ML/MIN.

Similar Cu and Fe extraction trends to that observed for DMS+MS feed in Figure 54 was observed for DMS feed (see Figure 55) and untreated feed at an S/L ratio of 1/10 as shown in Figure 56. For the untreated feed, increasing the acid concentration from 1 M to 2.5 M was seen to have a less pronounced effect than for the DMS+MS feed.

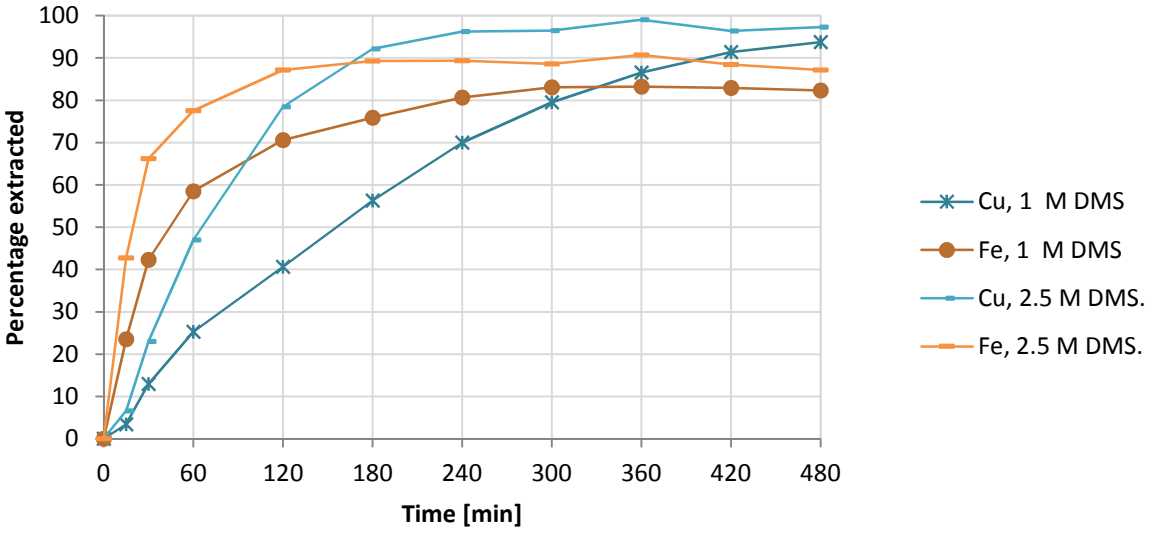

FIGURE 55: PERCENTAGE OF Cu AND Fe EXTRACTED FROM THE DMS FEED AT S/L=0.6/10 AT DIFFERENT H_2SO_4 CONCENTRATIONS WITH H_2O_2 30 WT% FEED RATE OF 1.2 ML/MIN.

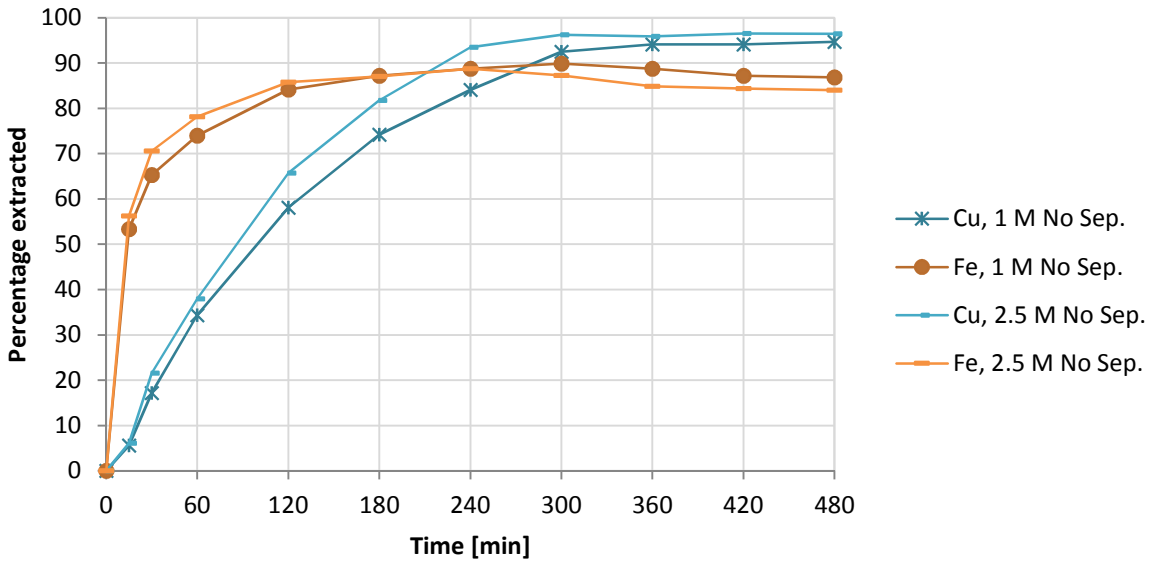

FIGURE 56: PERCENTAGE OF Cu AND Fe EXTRACTED FROM THE UNTREATED FEED AT S/L=1/10 AT H_2SO_4 CONCENTRATIONS OF 1 M AND 2.5 M WITH H_2O_2 30 WT% FEED RATE OF 1.2 ML/MIN.

Yang et al. 2011 reported that increasing H_2SO_4 concentration beyond 15 wt% (1.7 M) did not benefit Cu recovery from crushed PCBs at an S/L ratio of 1/10. Experiments at 4 M H_2SO_4 were performed on concentrated feeds (DMS and DMS+MS) at an S/L ratio of 1/10. Figure 57 shows that increasing H_2SO_4 concentration from 2.5 M to 4 M for DMS+MS feed only slightly increased the rate of Cu dissolution. The time required to reach equilibrium Cu extraction remained essentially the same at approximately 300 minutes. Increasing the acid concentration from 2.5 M to 4 M increased the rate of Fe extraction. Similar trends were observed for DMS feed.

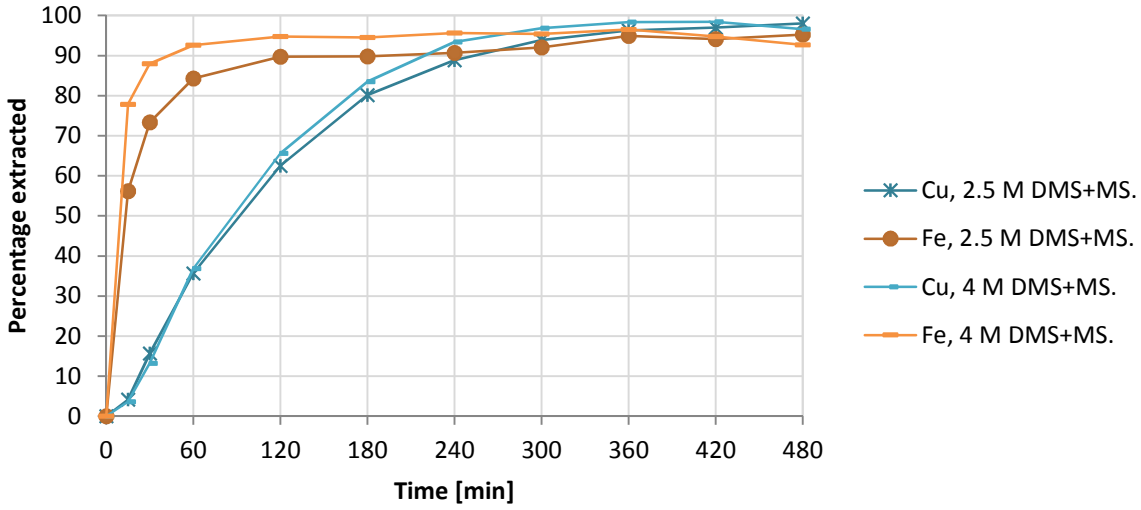

FIGURE 57: PERCENTAGE OF Cu AND Fe EXTRACTED FROM THE DMS+MS FEED AT S/L=1/10 AT H_2SO_4 CONCENTRATIONS OF 2.5 M AND 4 M WITH H_2O_2 30 WT% FEED RATE OF 1.2 ML/MIN.

Figure 58 shows how increasing the H_2SO_4 concentration from 1 M to 2.5 M affected Ni and Zn extraction for DMS+MS feed. Using 2.5 M H_2SO_4 decreased leaching time for Zn by 4 hours. Although complete extraction of Ni was not achieved at 2.5 M or 1 M H_2SO_4, the 2.5 M H_2SO_4 increased the extent of Ni extraction by approximately 15%. As with Cu and Fe in Figure 57, increasing the H_2SO_4 concentration from 2.5 M to 4 M was seen to be of limited benefit to the leaching rates of Ni and Zn from DMS+MS feed in Figure 59.

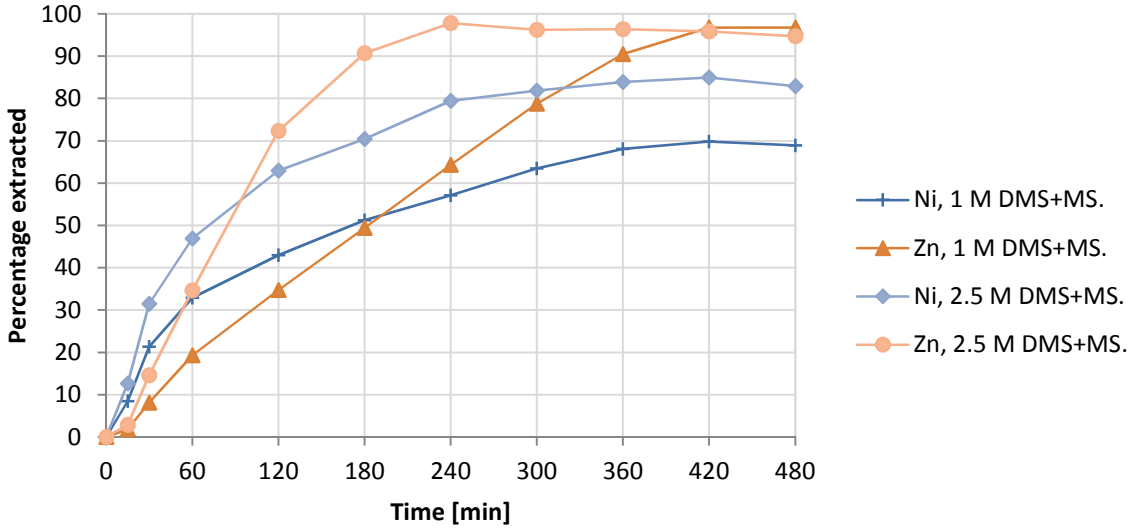

FIGURE 58: PERCENTAGE OF Ni AND Zn EXTRACTED FROM THE DMS+MS FEED AT S/L=0.6/10 AT H_2SO_4 CONCENTRATIONS OF 1 M AND 2.5 M WITH H_2O_2 30 WT% FEED RATE OF 1.2 ML/MIN.

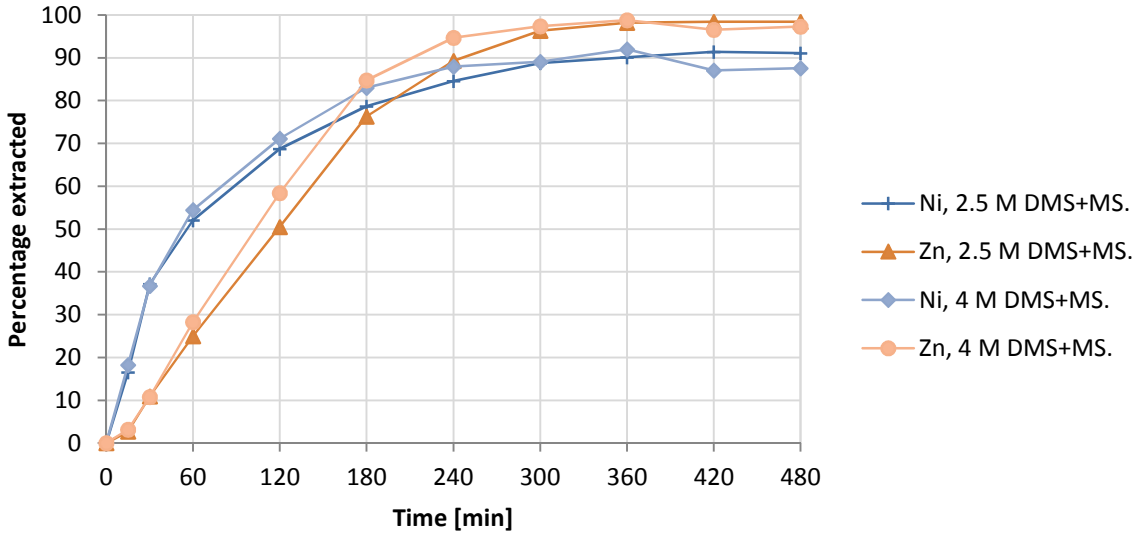

FIGURE 59: PERCENTAGE OF Ni AND Zn EXTRACTED FROM THE DMS+MS FEED AT S/L=1/10 AT H_2SO_4 CONCENTRATIONS OF 2.5 M AND 4 M WITH H_2O_2 30 WT% FEED RATE OF 1.2 ML/MIN.

The fact that a further increase in acid concentration (i.e. 2.5 M to 4 M) did not significantly increase the Cu, Fe, Zn or Ni leaching rates, suggests the existence of an alternative rate limiter. Equations 2.31 and 2.35 were used to determine the rate limiting factor for Cu dissolution at the respective acid concentrations. Figure 60 compares the fit of Cu extraction data at 1, 2.5 and 4 M H_2SO_4 to a) a chemical reaction limiting model and b) diffusion through a product layer. Figure 60 shows fit of chemical reaction limited model to worsen with increasing acid concentration. The fit of the diffusion controlled model improves with increasing acid concentration. Cu extraction was chemical reaction limited when leaching with 1 M H_2SO_4. There was little difference between the fit of the chemical reaction limited model and diffusion limited model when leaching with 2.5 M H_2SO_4. Leaching with 4 M H_2SO_4 appeared to be diffusion limited.

These results suggest that the leaching reaction rate was increased by increasing acid concentration until the rate of diffusion became the rate limiting step. This transition between a chemical reaction limited and a diffusion limited reaction occurred with 2.5 M H_2SO_4. With diffusion being the rate limiting factor, increasing the acid concentration from 2.5 M to 4 M H_2SO_4 would not be expected to significantly increase Cu recovery. Results in Figure 57 confirmed this to be the case.

Leaching Cu from DMS feed was also seen to become diffusion limited when increasing acid concentration from 1 M to 2.5 M H_2SO_4. Untreated feed was seen to be diffusion limited at both 1 M and 2.5 M H_2SO_4. The agitation as well as the presence of Cu and Fe in solution causes the decomposition of hydrogen peroxide which evolves oxygen. The plastics are hydrophobic causing oxygen bubbles to stick to its surface. These bubbles may then hinder particle-peroxide contact [17,68]. Mass transfer limitation agrees with the observed lack of effect when increasing acid concentration in Figure 56. The R-squared values obtained from fitting rate models to Cu extraction are shown in Table D 1, Table D 2 and Table D 3 for No Sep, DMS and DMS+MS feeds at respective acid concentrations and S/L ratios (see Appendix D).

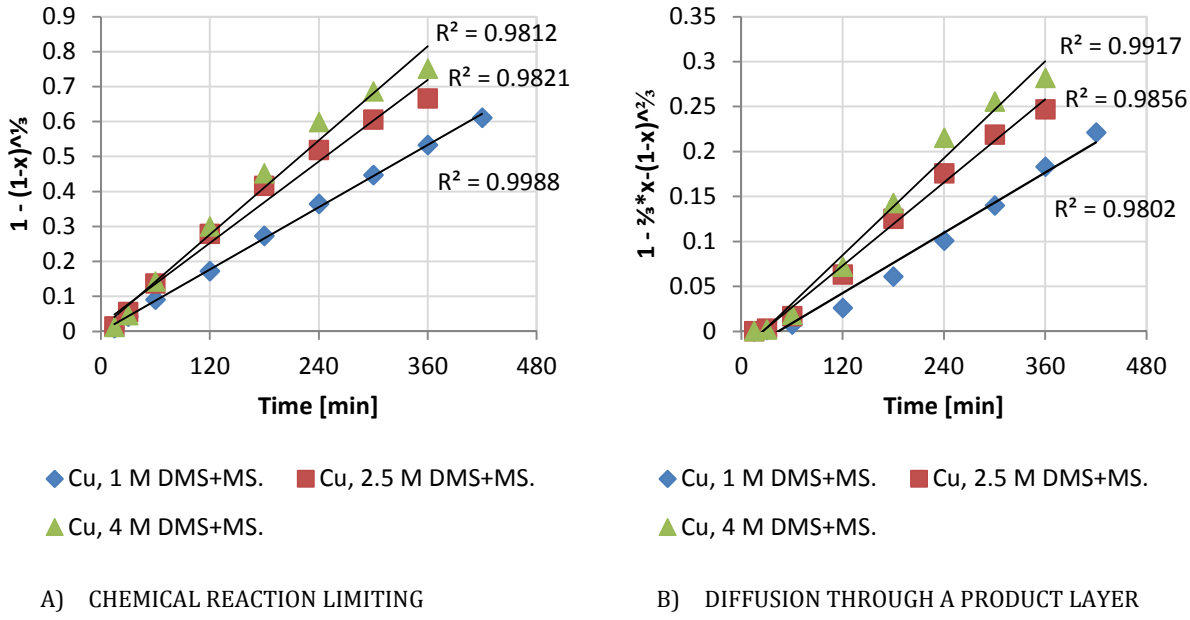

A) CHEMICAL REACTION LIMITING B) DIFFUSION THROUGH A PRODUCT LAYER

FIGURE 60: COMPARISON OF RATE LIMITING MODEL FITTING ON LEACHING OF Cu FROM DMS+MS FEED AT RESPECTIVE INITIAL H_2SO_4 CONCENTRATIONS.

Figure 61 shows the measured ORP during the three tested initial acid concentrations with DMS+MS feed. The concentration of hydrogen ions increased the redox potential of peroxide [68]. The higher potential measured at lower pH agrees with equation 2.40:

$$E = E^o + \frac{RT}{4F}\ln(a_{O_2}) - \frac{RT}{F}pH \qquad (2.40.)$$

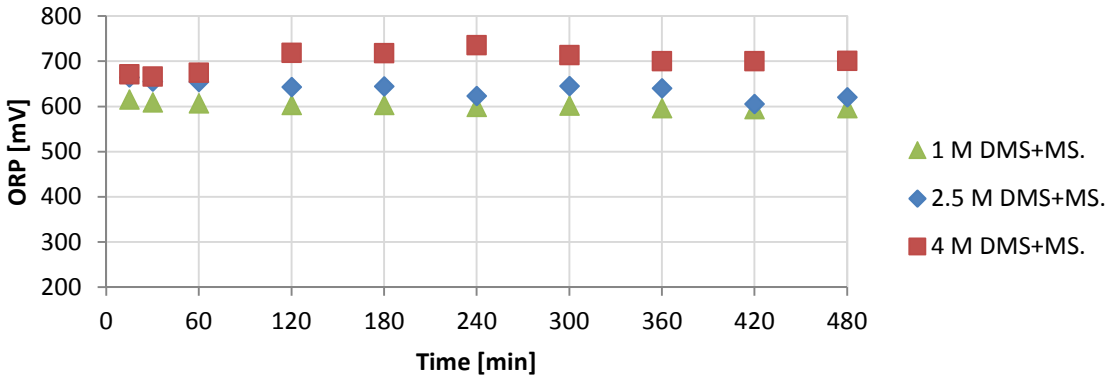

FIGURE 61: THE MEASURED ORP DURING LEACHING OF DMS+MS FEED USING 1 M, 2.5 M AND 4 M INITIAL H_2SO_4 CONCENTRATION WITH H_2O_2 30 WT% FEED RATE OF 1.2 ML/MIN.

Figure 62 shows the extraction of Al at different H_2SO_4 concentrations. In the first 15min, the extent of Al leaching for 1 M, 2.5 M and 4 M is the same at ±17%. For the 2.5 M and 4 M runs, the leaching then slows. The same trends were observed for DMS+MS feed. This was presumably due to the formation of a passivating layer on the Al surface at low pH values. The pH rose as leaching proceeded (see Figure 63). For the 2.5 M run, when the pH reached ± 0.2, the leaching of Al was seen to recommence.

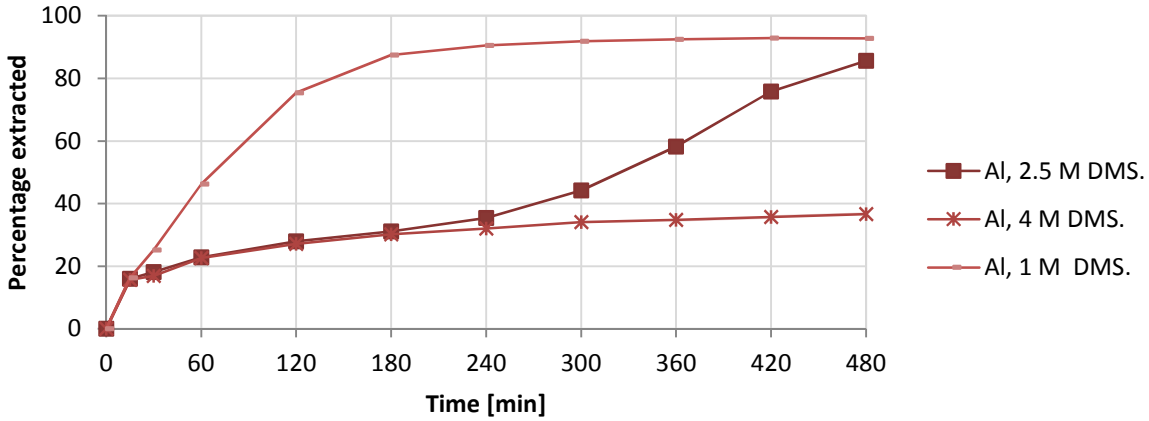

FIGURE 62: PERCENTAGE OF Al EXTRACTED FROM THE DMS FEED AT H_2SO_4 CONCENTRATIONS OF 1 M (WITH S/L=0.6/10), 2.5 M (WITH S/L=1/10) AND 4 M (WITH S/L=1/10) WITH H_2O_2 30 WT% FEED RATE OF 1.2 ML/MIN.

Figure 63 shows the calculated pH values during the leaching of DMS using 1, 2.5 and 4 M H_2SO_4 respectively. It was seen that the pH of the 4 M H_2SO_4 run, never reached the pH 0.2 where Al dissolution appeared to become favourable.

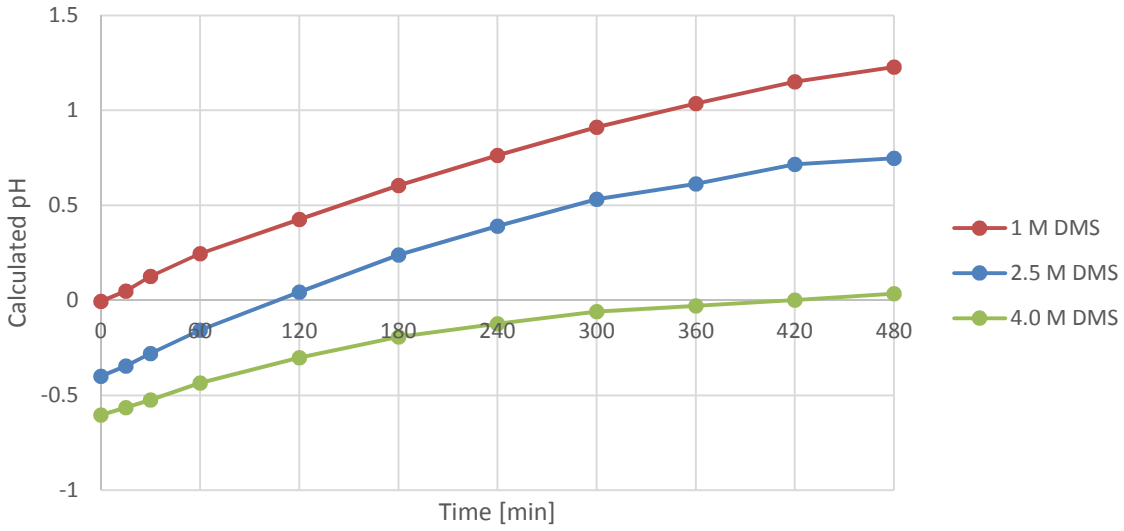

FIGURE 63: CALCULATED pH VALUES DURING DMS FEED LEACHING AT INITIAL H_2SO_4 CONCENTRATIONS OF 1 M (WITH S/L=0.6/10), 2.5 M (WITH S/L=1/10) AND 4 M (WITH S/L=1/10) WITH 30 WT% H_2O_2 FEED RATE OF 1.2 ML/MIN.

Figure 64 shows the extraction of Sn at different H_2SO_4 concentrations. Recall that the dissolution of Sn was followed by subsequent precipitation as SnO_2 in previously discussed results. It is seen that higher H_2SO_4 concentration of 4 M and 2.5 M gave higher peaks of dissolved Sn. This may be due to the dissolution reaction of Sn being favoured more by a lower pH than precipitation of dissolved Sn. This is expected as the precipitation of dissolved Sn as SnO_2 is accompanied by the release of H^+, which will be less favourable in a more acidic environment. The reluctance of dissolved Sn to precipitate completely at higher acid concentrations can be seen in Figure 64.

As expected, no significant amount of Pb was extracted at any of the tested H_2SO_4 concentrations.

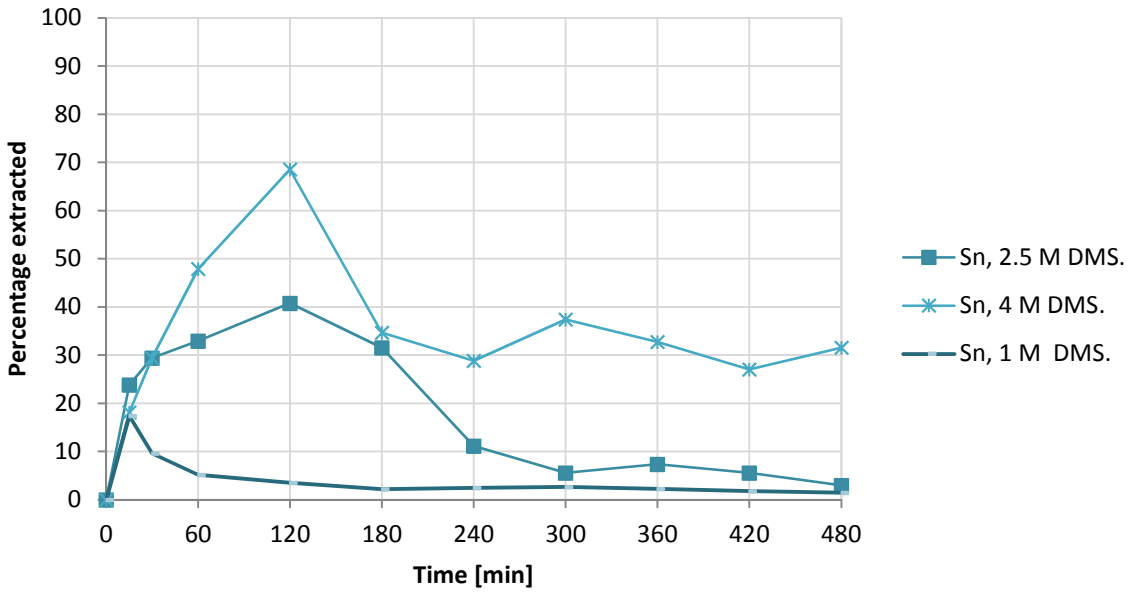

FIGURE 64: PERCENTAGE OF Sn EXTRACTED FROM THE DMS FEED AT H_2SO_4 CONCENTRATIONS OF 1 M (WITH S/L=0.6/10), 2.5 M (WITH S/L=1/10) AND 4 M (WITH S/L=1/10) WITH 30 WT% H_2O_2 FEED RATE OF 1.2 ML/MIN

4.2.3.2. PRECIOUS METALS

Figure 65 shows that hardly any detectable amount of Ag or Au was extracted at any of the tested H_2SO_4 concentrations for DMS feed. Similar results were seen for untreated feed and DMS+MS feed.

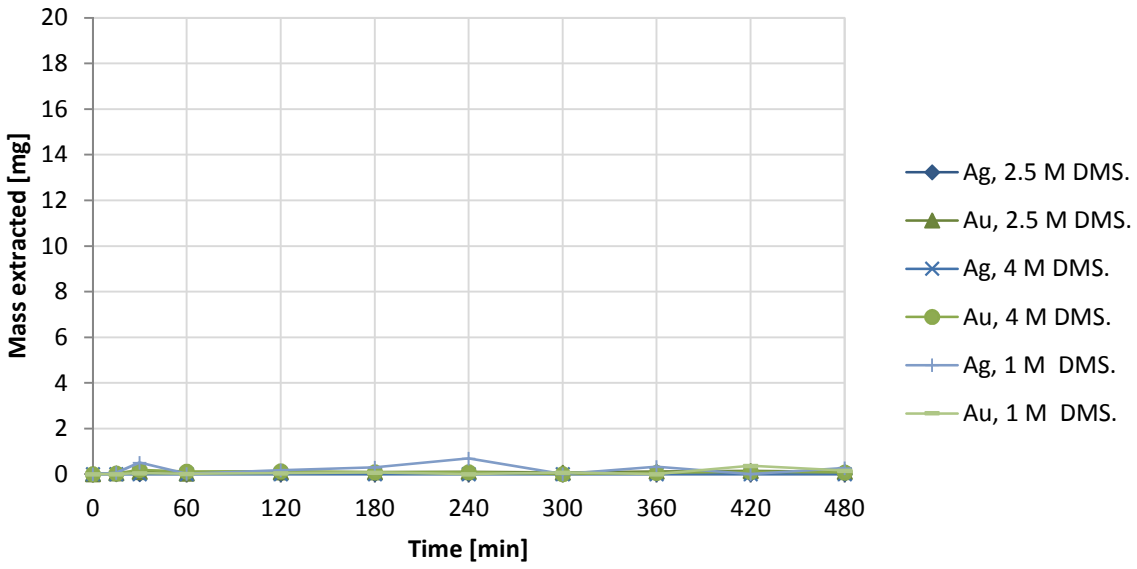

FIGURE 65: MASS OF Au AND Ag EXTRACTED AT 1 M, 2.5 M AND 4 M H_2SO_4 FROM DMS FEED WITH H_2O_2 30 WT% FEED RATE OF 1.2 ML/MIN

Figure 66 shows the Pourbaix diagram for Ag constructed using OLI systems software. The diagram was constructed taking the variety and mass of metals known to be present on PCBs into account. With the tested leaching systems typically operating between 0.5-0.6 V and between pH -0.4 to pH 1.3, it is seen that Ag was on the edge of a stability region for $Ag_{(s)}$. Figure 66 also shows that increasing the oxidation potential in the system may lead to complete Ag dissolution becoming thermodynamically favourable, forming $Ag^{+}_{(aq)}$.

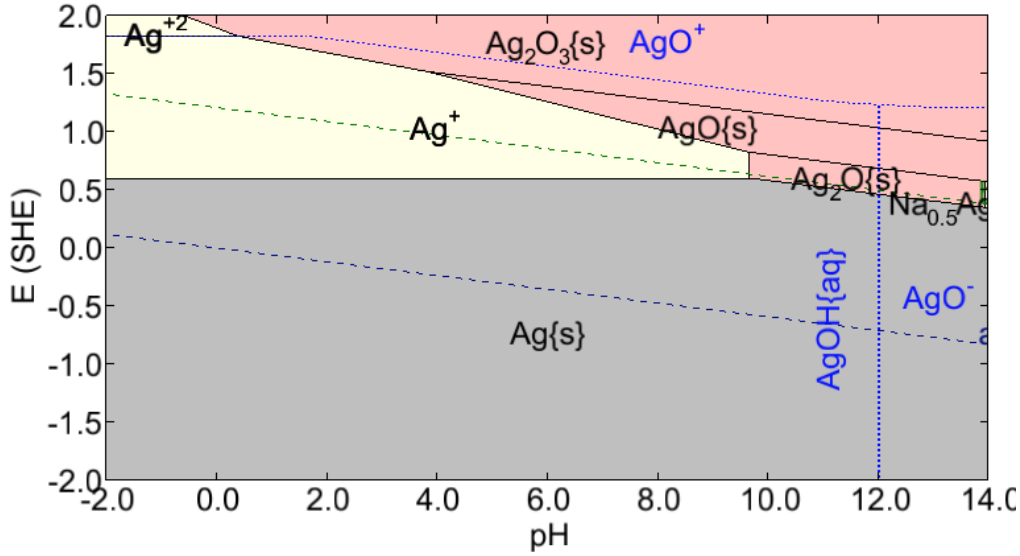

FIGURE 66: POURBAIX DIAGRAM PRODUCED BY OLI SYSTEMS FOR Ag IN A SULPHURIC ACID SYSTEM AT 25°C IN THE PRESENCE OF THE EXPECTED COMBINATION OF METALS.

Figure 67 shows the Pourbaix diagram for Au in a sulphuric acid system. It is seen that aqueous species of Au can exist in equilibrium with solid Au at all conditions. Results however showed these aqueous Au species to generally be below detectable limits at conditions tested using sulphuric acid.

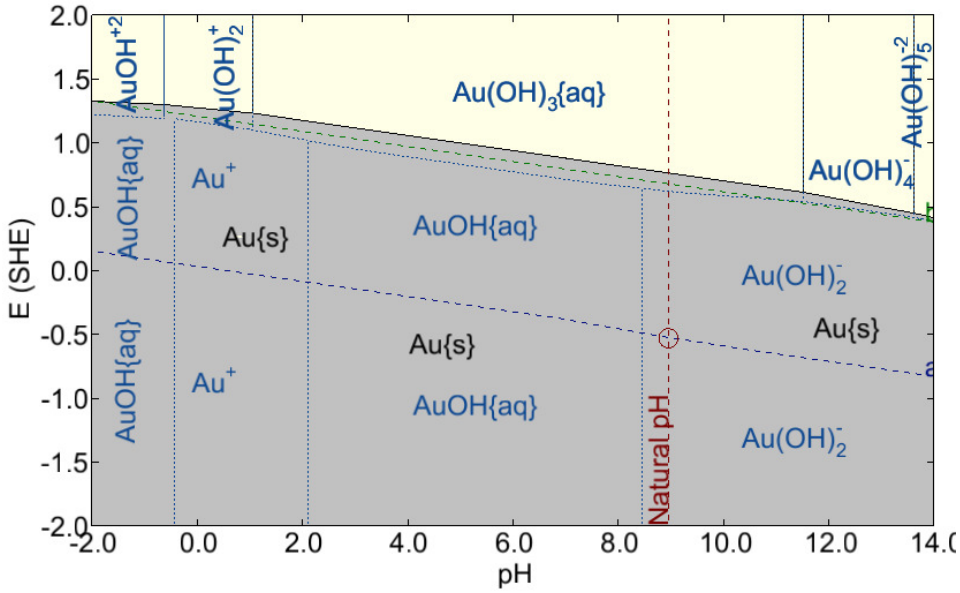

FIGURE 67: POURBAIX DIAGRAM PRODUCED BY OLI SYSTEMS FOR Au IN A SULPHURIC ACID SYSTEM AT 25°C IN THE PRESENCE OF THE EXPECTED COMBINATION OF METALS.

4.2.4. THE EFFECT OF SOLID TO LIQUID RATIO

Recall that variations in S/L ratio were conducted for the concentrated feeds (DMS and DMS+MS) only at an acid concentration of 2.5 M. The solid to liquid ratios investigated were 1/10 and 0.6/10. The former being a common S/L ratio used in literature and the latter being selected to be approximately the same metals to liquid ratio as that of untreated feed at an S/L ratio of 1/10.

Figure 68 shows how the amount of Cu and Fe extracted increased by introducing more solid feed into the system. The faster leaching rate observed for the higher solids loading may be attributed to greater surface area availability for reaction. Similar trends were observed for DMS+MS feed. Figure 69 shows that although the high S/L ratio contained nearly twice the amount of Cu as the lower S/L ratio, the time required to achieve complete (~95%) leaching was increased by only an hour. This implied that the leaching system would potentially be able to handle a larger S/L ratio for untreated feed as well without significantly extending the required leaching time.

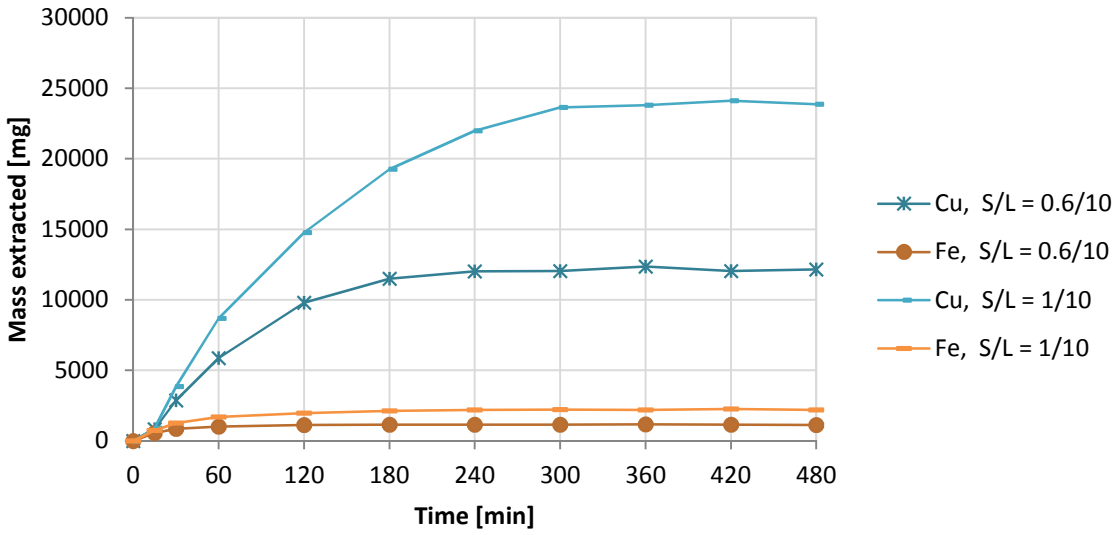

FIGURE 68: THE EFFECT S/L RATIO ON MASS OF Cu AND Fe EXTRACTED FROM DMS FEED USING 2.5 M H_2SO_4 WITH H_2O_2 30 WT% FEED RATE OF 1.2 ML/MIN AT 25°C.

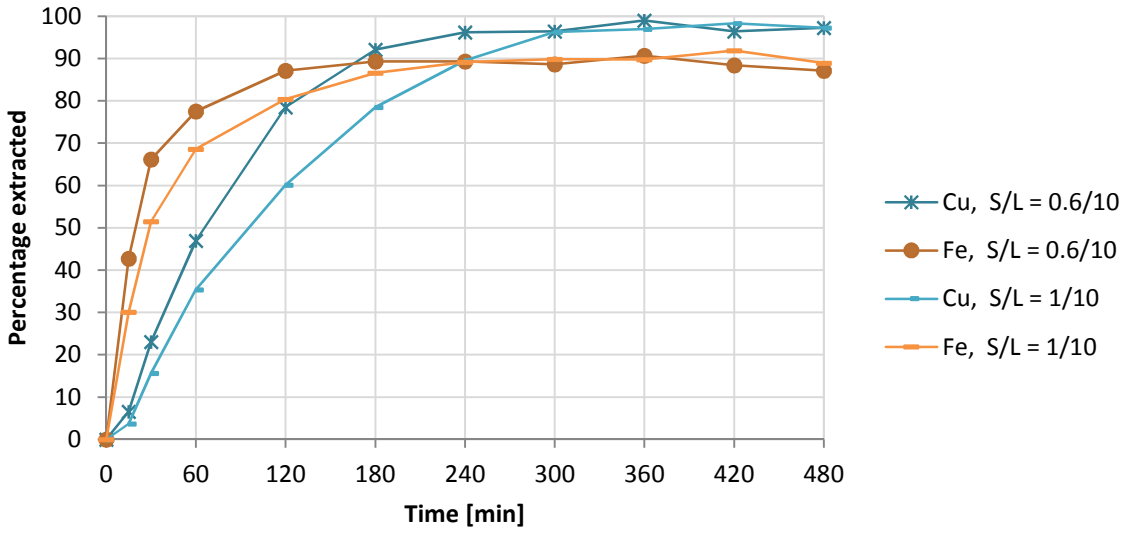

FIGURE 69: THE EFFECT S/L RATIO ON PERCENTAGE OF Cu AND Fe EXTRACTED FROM DMS FEED USING 2.5 M H_2SO_4 WITH H_2O_2 30 WT% FEED RATE OF 1.2 ML/MIN AT 25°C.

Similar trends were observed for the extraction of Ni and Zn.

Figure 70 shows Al leaching accelerated for the higher S/L at 240 min, while for the lower S/L ratio, the leaching rate remained slow. This was due to the higher feed loading causing to pH to rise to where Al dissolution was favourable. For the lower solids loading the pH remained low, preventing effective Al dissolution. The lower final pH for the S/L of 0.6/10 is also seen to prevent complete precipitation of dissolved Sn. The S/L of 1/10 allowed for relatively more complete precipitation.

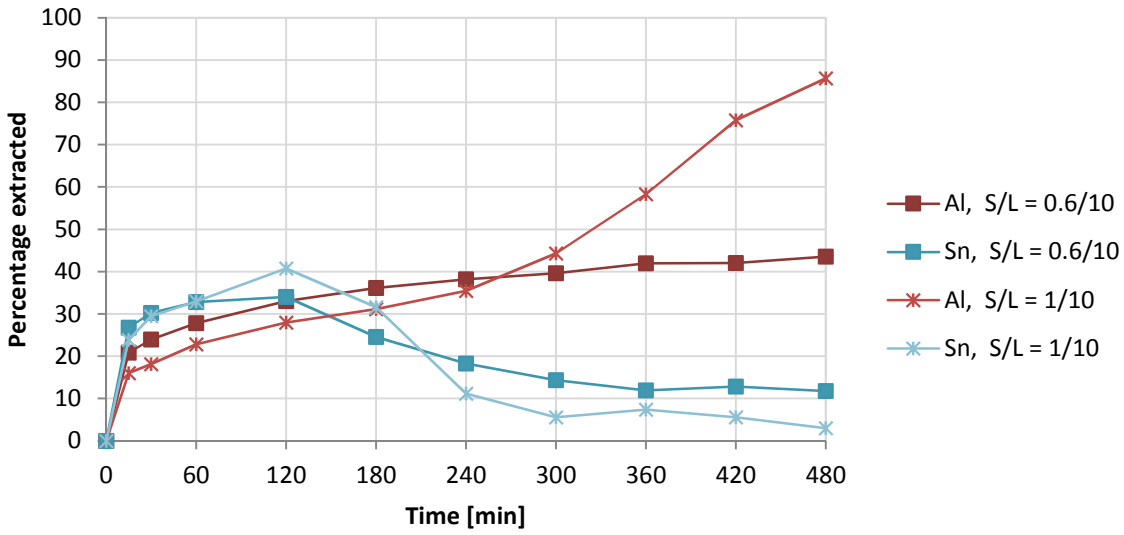

FIGURE 70: THE EFFECT S/L RATIO ON PERCENTAGE OF AL AND SN EXTRACTED FROM DMS FEED USING 2.5 M H_2SO_4 WITH H_2O_2 30 WT% FEED RATE OF 1.2 ML/MIN AT 25°C.

Variation in S/L ratio did not influence the extraction of Au or Ag.

4.2.5. CONCLUSIONS FROM PHASE 2 EXPERIMENTS

4.2.5.1. THE EFFECT OF MECHANICAL PRE-TREATMENT

Characterisation of the feed following application of DMS showed that 70% of Au and 20% of Cu report to the light fraction. The 70% Au amounts to around 50% of the metallic value of the PCB in this case. The high Cu content that accompanied the Au in the light fraction implies that Cu would likely still need to be leached from it before Au could be recovered. Seeing that Cu would also need to be leached from the heavy fraction prior to Au recovery, performing dense medium separation in the first place does not seem sensible.

Although the application of DMS succeeded in reducing feed weight by 63%, the concentrated feed did not show any significant benefit in leaching performance. The incurred metal losses by the application of DMS were not justifiable.

The application of magnetic separation reduced Fe and Ni content by 67% and 61%, respectively. Along with Fe and Ni, 29% of Ag was also removed. Reducing the Fe and Ni content prior to leaching allowed its complete extraction to occur faster due to a lower corresponding concentration in the leach solution. Although the application of MS did not significantly affect the leaching of non-ferromagnetic metals, the Fe and Ni content in the resulting PLS was reduced.

Leaching concentrated feed did show that a higher metals loading of 7.5 g metal instead of 4.6 g metal per 100 mL of leach solution could be leached without greatly extending the required leaching time. This suggests that untreated PCBs could also be leached at this metals loading which corresponds to an S/L ratio of 1.6/10.

4.2.5.2. THE EFFECT OF ACID CONCENTRATION

Results showed that the leaching rates of Cu, Fe, Ni and Zn were increased by increasing the initial H_2SO_4 concentration from 1 M to 2.5 M. The effect was seen to be less pronounced for untreated feed, presumably due to diffusion rate limitation. The diffusion limitation could be due to the adsorption of oxygen bubbles on the hydrophobic particle surface. Increasing the acid concentration further from 2.5 M to 4 M showed minimal benefit for Cu, Fe, Ni and Zn extraction with the required leaching time remaining mostly unaffected.

For the concentrated feeds it was seen that a pH of greater than 0.2 was required for Al to leach effectively. Higher acid concentrations therefore prevented effective dissolution. The same trend for Al was not observed for untreated feed for reasons unknown.

Dissolution of Sn was followed by some extent of precipitation at all acid concentrations. The higher acid concentrations showed more rapid initial dissolution and the low pH prevented complete precipitation.

Acid concentration did not influence the leaching of Pb, Ag or Au.

It is concluded that effective leaching of Cu, Fe, Ni and Zn could be obtained using 2.5 M H_2SO_4. Increasing acid concentration further did not show significant benefit.

4.2.5.3. THE EFFECT OF S/L RATIO

The S/L ratios of 1/10 and 0.6/10 for the concentrated feeds correspond to approximately 7.5 g and 4.6 g of metal per 100 mL of leach solution, respectively. It was seen that increasing the metals loading by ~60% only increased the required leaching time for Cu by an hour. The effect on extraction of Ni and Zn was seen to be similar. At the higher metals loading the greater amount of metal extracted caused the pH to rise to where Al dissolution became thermodynamically favourable. The subsequently higher pH also allowed Sn to precipitate to a relatively greater extent. The variation in S/L ratio did not influence Ag or Au extraction.

It is concluded that the benefit of a ~60% greater feed throughput would in general outweigh the expense of 1-2 hours additional leaching time. It therefore seems sensible to operate at the higher metals throughput of 7.5 g metal per 100 mL solution.

4.3. PHASE 3: PROCESS VALIDATION

Results were used to suggest suitable process flowsheets for the recovery of base metals. The flowsheet showing potential for greater extent of base metal recovery with minimal co-removal of precious metals was selected. The potential cost implications of process decisions were not considered in this study.

4.3.1. POTENTIAL FLOWSHEETS

Results showed that concentrating the feed by means of DMS did not benefit metal recovery. DMS was therefore omitted from the flowsheets.

Both MS and leaching with 1 M HNO_3 at 25°C showed potential for Fe removal prior to Cu leaching. Leaching with 1 M HNO_3 at 25°C to remove 84% of Fe showed the added benefit of removing 84% of Pb as well. Seeing that H_2SO_4 leaching does not remove Pb, this greatly reduces the amount of Pb expected to be in the solids residue. Pb could then be recovered from the nitric acid PLS by means of precipitation as $PbSO_4$ by the addition of sulphuric acid [29]

The application of MS removed 67% of Fe and 61% of Ni. The application of MS would be much simpler compared to an additional leaching stage. However, MS removed 17% less Fe than 1 M HNO_3 removed at 25°C and it does not address the removal of Pb. Although Pb has been reported to have a weak solubility at typical gold cyanidation conditions [78], due to Pb's contribution to the toxicity of e-waste [79-81], its removal prior to solids disposal is of environmental interest.

The H_2SO_4 concentration of 2.5 M was shown to be sufficient for near complete (~95%) Cu leaching. The effective leaching of concentrated feed suggested that non-concentrated feed could potentially be leached effectively up to an S/L ratio of at least 1.6/10 w/v.

With this in mind, two process routes were suggested for base metal recovery as shown in Figure 71:

- Route A: Crushed PCBs are subjected to MS to partially remove Fe and Ni. This would lead to a relatively purer PLS from for the H_2SO_4 leach. This will also reduce reagent consumption during the leaching step. The resulting solids are then leached in 2.5 M H_2SO_4 at 25°C with a 30 wt% H_2O_2 feed rate of 1.2 mL/min.
- Route B: Crushed PCBs are treated with 1 M HNO_3 at 25°C to remove Fe and Pb. After solid-liquid separation, the residue is leached in 2.5 M H_2SO_4 at 25°C with 30 wt% H_2O_2 feed rate of 1.2 mL/min. The pre-leaching with HNO_3 should lead to a purer H_2SO_4 PLS. The final solids would have a greater extent of Pb removal.

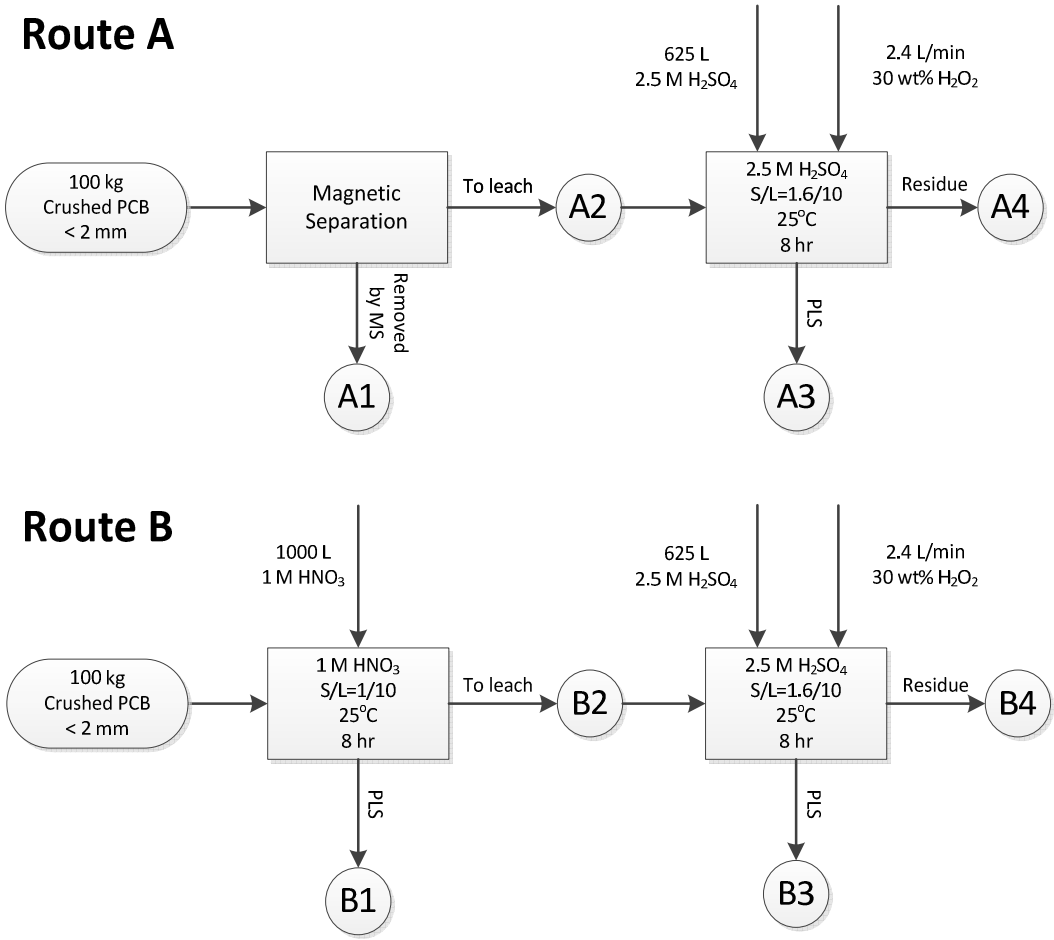

FIGURE 71: PROCESS ROUTES A AND B SUGGESTED FOR BASE METAL RECOVERY FROM CRUSHED WASTE PCBs

Based on the characterisation of feed following the application of MS, the expected separation behaviour during MS was estimated. As for the leaching, experimental results were used to estimate expected extents of extraction during each of the leaching stages.

For the flowsheets in Figure 71 a feed mass of 100 kg of crushed PCBs was assumed. The mass of metal present in each stream was estimated and is shown in stream tables in Table 23 and Table 24 for route A and B respectively. The mass of metal present is shown in the first column for every stream. The fraction of the metal that the mass represents is shown as a percentage in the second column for each stream.

Process route B showed potential for a greater final extent of Al, Fe and Pb removal than route A. Route B also showed to be more selective towards base metals as 27.1 percentage points more Ag and 7.6 percentage points more Au were estimated to be left in solids residue than for route A. The application of MS demonstrated the risk of potential removal of precious metals along with ferromagnetic material. This risk is mitigated by substituting MS in route A with a 1 M HNO_3 leach in route B. The 1 M HNO_3 leach showed minimal co-extraction of Ag and no detectable Au extraction. In doing so, a greater extent of Fe could potentially be removed along with 74 percentage points more Pb than route A. For these reasons, route B was selected for experimental validation.

TABLE 23: STREAM TABLE FOR PROCESS ROUTE A IN FIGURE 71

Stream →	**Feed stream**		**A1**		**A2**		**A3**		**A4**	
	Crushed PCBs < 2 mm		Removed by MS		To H_2SO_4 leach		Removed by H_2SO_4 leach		Un-leached in residue	
Metal	Mass [g]	Fraction of total	Mass [g]	Fraction of total	Mass [g]	Fraction of total	Mass [g]	Fraction of total	Mass [g]	Fraction of total
Ag	69	100%	20	29.2 %	49	70.8 %	0	0 %	49	70.8 %
Al	4500	100%	254	5.6 %	4246	94.4 %	1110	24.7 %	3136	69.7 %
Au	22	100%	2	7.7 %	21	92.3 %	0	0.4 %	21	91.9 %
Cu	27636	100%	341	1.2 %	27295	98.8 %	26329	95.3 %	966	3.5 %
Fe	3895	100%	2610	67 %	1285	33 %	1080	27.7 %	206	5.3 %
Ni	679	100%	413	60.8 %	266	39.2 %	192	28.3 %	74	10.9 %
Pb	4966	100%	520	10.5 %	4446	89.5 %	3	0.1 %	4444	89.5 %
Sn	3052	100%	221	7.3 %	2830	92.7 %	165	5.4 %	2666	87.3 %
Zn	3729	100%	57	1.5 %	3671	98.5 %	3385	90.8 %	286	7.7 %

TABLE 24: STREAM TABLE FOR PROCESS ROUTE B IN FIGURE 71

Stream →	**Feed stream**		**B1**		**B2**		**B3**		**B4**	
	Crushed PCBs < 2 mm		Removed by HNO_3		To H_2SO_4 leach		Removed by H_2SO_4 leach		Un-leached in residue	
Metal	Mass [g]	Fraction of total	Mass [g]	Fraction of total	Mass [g]	Fraction of total	Mass [g]	Fraction of total	Mass [g]	Fraction of total
Ag	69	100%	1	2.1 %	68	97.9 %	0	0 %	68	97.9 %
Al	4500	100%	961	21.4 %	3539	78.6 %	925	20.6 %	2613	58.1 %
Au	22	100%	0	0 %	22	100 %	0	0.5 %	22	99.5 %
Cu	27636	100%	58	0.2 %	27578	99.8 %	26602	96.3 %	976	3.5 %
Fe	3895	100%	3266	83.8 %	629	16.2 %	529	13.6 %	101	2.6 %
Ni	679	100%	292	43 %	387	57 %	279	41.2 %	108	15.9 %
Pb	4966	100%	4189	84.3 %	777	15.7 %	0	0 %	777	15.6 %
Sn	3052	100%	460	15.1 %	2592	84.9 %	151	4.9 %	2441	80 %
Zn	3729	100%	86	2.3 %	3643	97.7 %	3359	90.1 %	284	7.6 %

4.3.2. VALIDATION OF PROCESS ROUTE

The selected process route, route B, shown in Figure 71, shows a HNO_3 first stage leach at an S/L ratio of 1/10 followed by a H_2SO_4 second stage leach at an S/L ratio of 1.6/10. The first stage leach was therefore carried out using 80 grams of crushed PCBs with 800 mL of 1 M HNO_3 solution. With this higher solids loading 80 grams as opposed to a maximum of 50 grams used in previous experiments, it was necessary to increase the agitator speed from 500 rpm to 600 rpm to maintain particle suspension.

Residue from the 1 M HNO_3 leach was leached with 500 mL of 2.5 M H_2SO_4 with a 30 wt% H_2O_2 feed rate of 1.2 mL/min. The agitator speed of 600 rpm was maintained throughout the second stage leach as well.

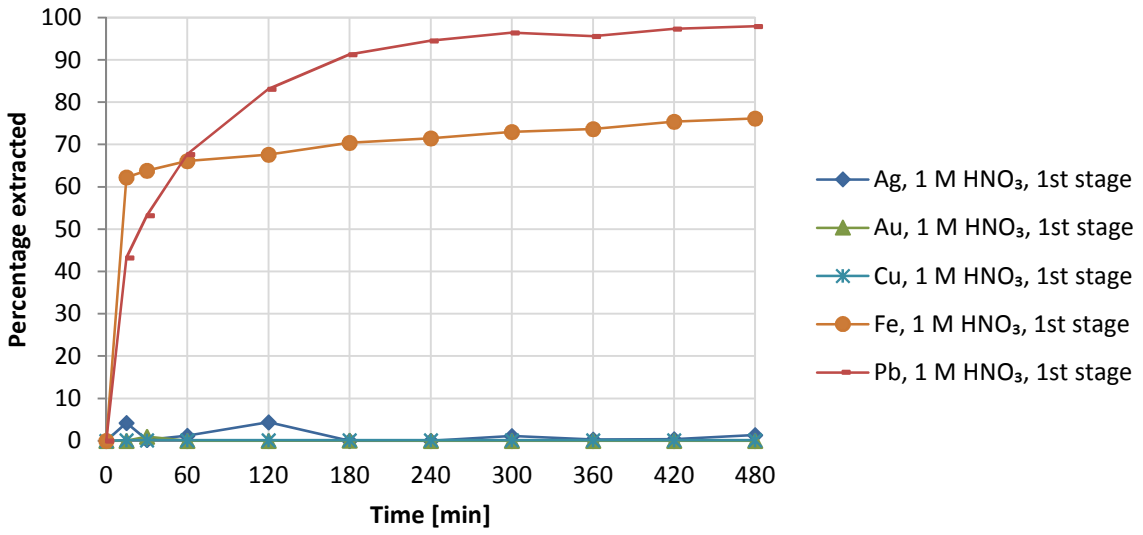

FIGURE 72: FIRST STAGE LEACHING BEHAVIOUR OF Ag, Au, Cu, Fe AND Pb IN 1 M HNO_3 WITH S/L RATIO OF 1/10 AT 25°C FOR 8 HOURS

Figure 72 shows the first stage HNO_3 leach removed 98% of Pb and 76% of Fe after 480 minutes. As expected, Cu and Au remained mostly undissolved. The sudden decrease in Fe leaching rate observed at 15 minutes may be due to Fe in certain alloys being more readily corroded by nitric acid than others at these conditions. Increasing HNO_3 concentration could potentially increase the rate and extent of Fe removal achieved, however this would likely result in greater co-extraction of Cu (see Figure 7) and the effect that this might have on Au leaching is uncertain. Small peaks of Ag dissolution was observed.

Figure 73 shows slow dissolution of Ni and Al that reached 34% and 15% extraction respectively. It was seen that approximately 1.5% of Zn dissolved. Consideration of the mass of dissolved Zn showed close resemblance to that of Cu. In the first 15 minutes, 23 mg Cu and 30 mg Zn was dissolved, 7 hours later, the amount of Cu in solution was the same and that of Zn had increased by only 9 mg. The dissolution of Sn was again seen to be followed by subsequent precipitation; presumably as $SnO_{2(s)}$ or meta-stannic acid.

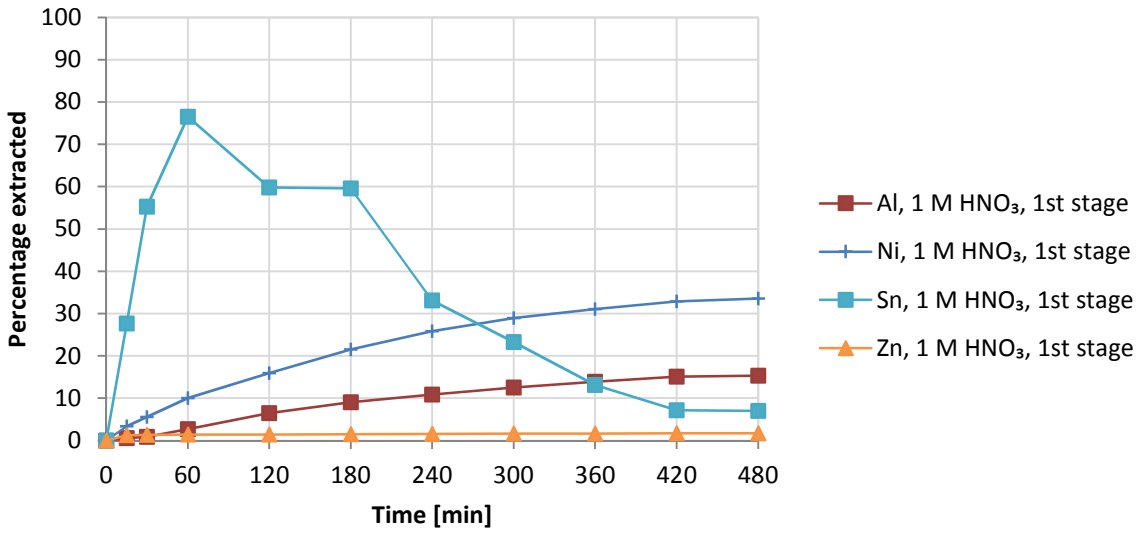

FIGURE 73: FIRST STAGE LEACHING BEHAVIOUR OF Al, Ni, Sn AND Zn IN 1 M HNO_3 WITH S/L RATIO OF 1/10 AT 25°C FOR 8 HOURS

Figure 74 and Figure 75 shows the second stage leaching behaviour. Figure 74 shows that 97% of Cu was removed after 480 minutes with no detectable removal of Au. The H_2SO_4 leach also removed 16% of Fe, bringing the total extent of Fe removal to 92%.

Ag was seen to dissolve at a steadily increasing rate, followed by steady precipitation from solution. Note that the observed behaviour of Ag in the Figure 74 was not observed during any of the previous experiment. This is presumably due to none of the other H_2SO_4 experiments being preceded by a HNO_3 leach. This implies that HNO_3 leaching altered the state of Ag in the sample.

Figure 75 shows 58% of Ni being removed bringing total Ni removal to 92%. The leached Sn seemed to remain in solution; this may be attributed to the low pH preventing complete precipitation. Near complete (~93%) dissolution of Zn was achieved at 300 minutes.

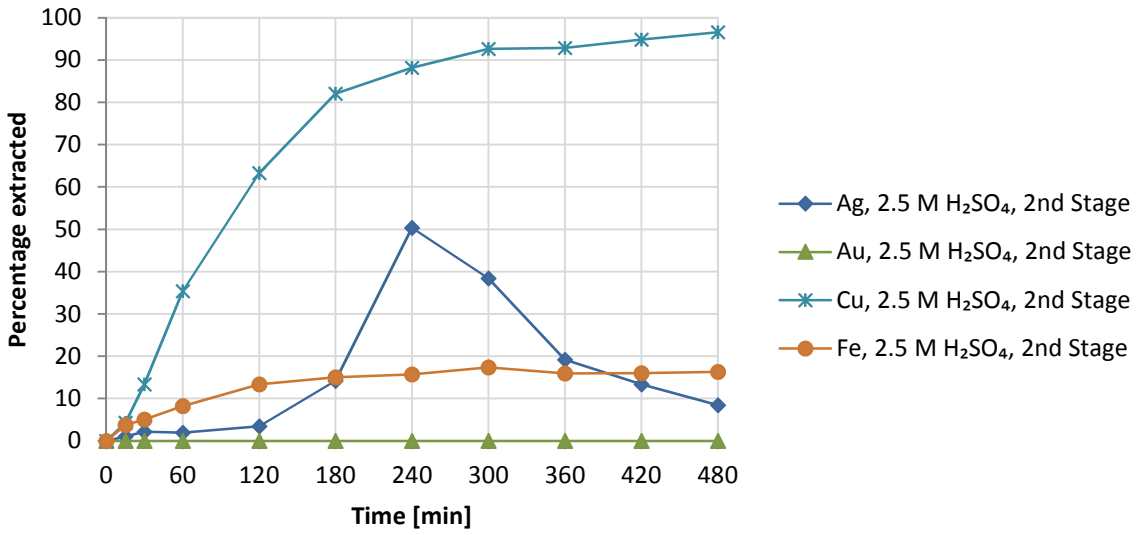

FIGURE 74: SECOND STAGE LEACHING BEHAVIOUR OF Ag, Au, Cu AND Fe IN 2.5 M H_2SO_4 WITH S/L RATIO OF 1.6/10 AT 25°C WITH A 30WT% H_2O_2 FEED RATE OF 1.2 ML/MIN FOR 8 HOURS

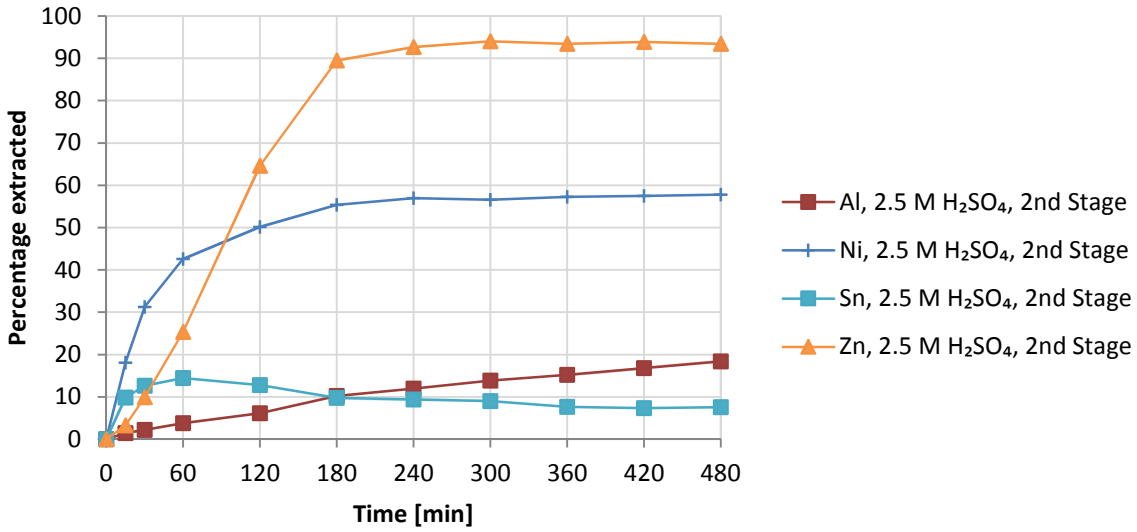

FIGURE 75: SECOND STAGE LEACHING BEHAVIOUR OF Al, Ni, Sn AND Zn IN 2.5 M H_2SO_4 WITH S/L RATIO OF 1.6/10 AT 25°C WITH A 30WT% H_2O_2 FEED RATE OF 1.2 ML/MIN FOR 8 HOURS

TABLE 25: EXTRACTION OF METALS DURING VALIDATION OF SUGGESTED PROCESS FLOWSHEET

Metal (mass in feed sample)	1st Stage Extraction in 1 M HNO_3 [%]	2nd Stage Extraction in 2.5 M H_2SO_4 [%]	Remaining in residue [%]	Predicted remainder [%]
Ag (16 mg)	1.3	8.5	90.2	97.9
Al (2742 mg)	15.3	18.4	66.3	58.1
Au (11 mg)	0.0	0.0	100.0	99.5
Cu (14167 mg)	0.2	96.5	3.3	3.5
Fe (1302 mg)	76.2	16.3	7.5	2.6
Ni (195 mg)	33.6	57.8	8.6	15.9
Pb (1228 mg)	97.9	0.0	2.1	15.6
Sn (946 mg)	7.0	7.5	85.5	80
Zn (2333 mg)	1.7	93.4	4.9	7.6

Table 25 shows the distribution of metals in the streams leaving the process. The column on the left shows the mass of the respective metals that were present in the feed sample. It was seen that Cu, Fe, Ni, Pb and Zn were removed to a relatively complete extent. All of the Au remained undissolved. About 10% of Ag was removed, mostly during solubilisation in the H_2SO_4 stage.

The majority of Sn and Al remained in the residue. This was expected based on results from previous experiments. If it were desired to completely remove Al and Sn from the residue, a high temperature hydrochloric acid leach could potentially be considered. In order to remove the remaining Sn, the residue could be treated with 5.5 M HCl at 90°C for 165 minutes [82]. The remaining Al could be removed by 3 M HCl at 104°C in the presence of 0.68 M fluorine ions [83]. The effects that these treatments may have on Au and Ag dissolution were not reported.

Comparison of metal extraction estimated in Table 24 to metal extraction achieved during validation in Table 25 shows good agreement. The estimated percentages of metals remaining in the residue from Table 24 are repeated in the final column of Table 25 for convenient comparison. Greater extents of Zn, Pb and Ni extraction was achieved of 2.7, 13.1 and 7.3 percentage points during validation. Somewhat poorer extents of Al, Fe and Sn extraction was observed of 8.2, 4.9 and 5.5 percentage points. Cu extraction behaved as predicted with 3.3% of Cu remaining in the residue. In conclusions, the process flow sheet confirmed the possibility of selective base metal leaching while leaving precious metals Au and Ag in the residue.

4.4. REPEATABILITY OF EXPERIMENTS

Although care was taken to ensure even distribution of metals throughout feed samples, the heterogeneous nature of PCBs and the intermittent presence of larger pieces of metal made this difficult. The largest source of variance in the experiments was identified as the composition of the feed. The variance in repeat measures was small compared to that in feed composition.

The aqua regia digestion of solid residue remaining after leaching allowed the total mass of the respective metals in each sample to be determined. The mean mass of each metal in the three feed types was calculated. Confidence intervals for these masses were calculated using an α value of 0.05 (i.e. 95% confidence). These confidence intervals are represented in Table 26 as a percentage of the mean mass of the respective metals in each feed type.

TABLE 26: CONFIDENCE INTERVAL EXPRESSED AS PERCENTAGE OF MEAN MASS WITH $\alpha = 0.05$ FOR THE RESPECTIVE METALS PRESENT IN THE FEED SAMPLES.

Feed Type→	No Sep.		DMS.		DMS+MS	
Metal ↓	Ave. mass in 50 g feed [mg]	95% Confidence	Ave. mass in 30 g feed [mg]	95% Confidence	Ave. mass in 30 g feed [mg]	95% Confidence
Ag	35	± 27.5 %	17	± 36.6 %	15	± 31.4 %
Al	2250	± 11.2 %	1056	± 7.5 %	1180	± 7.9 %
Au	11	± 9.9 %	3	± 12.1 %	3	± 19 %
Cu	13818	± 6.6 %	13865	± 6 %	14351	± 5.3 %
Fe	1948	± 9 %	1425	± 7.7 %	548	± 6.9 %
Ni	340	± 10.4 %	303	± 5.5 %	130	± 6.7 %
Pb	2483	± 11.9 %	1359	± 28.7 %	1306	± 27.8 %
Sn	1526	± 21 %	2307	± 9.3 %	2260	± 6.7 %
Zn	1864	± 14.6 %	2239	± 4.1 %	2193	± 10.4 %

Repeat runs were performed for No Sep, DMS and DMS+MS feed types. The solid to liquid ratio for the No Sep feed was 1/10 while 0.6/10 was used for the concentrated feeds DMS and DMS+MS. These S/L ratios corresponded to 50 g of feed for the No Sep runs and 30 g of feed for the DMS and DMS+MS runs as shown in Table 26. The H_2SO_4 concentration used in all three cases was 1 M and 30 Wt% H_2O_2 was fed at 1.2 mL/min.

Figure 76, Figure 77 and Figure 78 show repeat runs using No Sep, DMS and DMS+MS feeds respectively. The mass of metal leached is shown in red and blue for the respective runs. Dotted lines indicate a band which represents the percentage of feed variance shown in Table 26. Under the assumption that a greater feed mass of a metal would proportionally influence its extracted mass, intersections of dotted lines indicate that variation in extracted metal was within bounds of variation of metal content in feed. Extraction behaviour of Al, Au, Cu, Fe, Ni and Zn is considered for comparison, complete results are presented in Appendix C5.

Figure 76 shows differences in observed Al, Cu, Fe, Ni and Zn extraction were within range of what could be attributed to variation in metals content of feed.

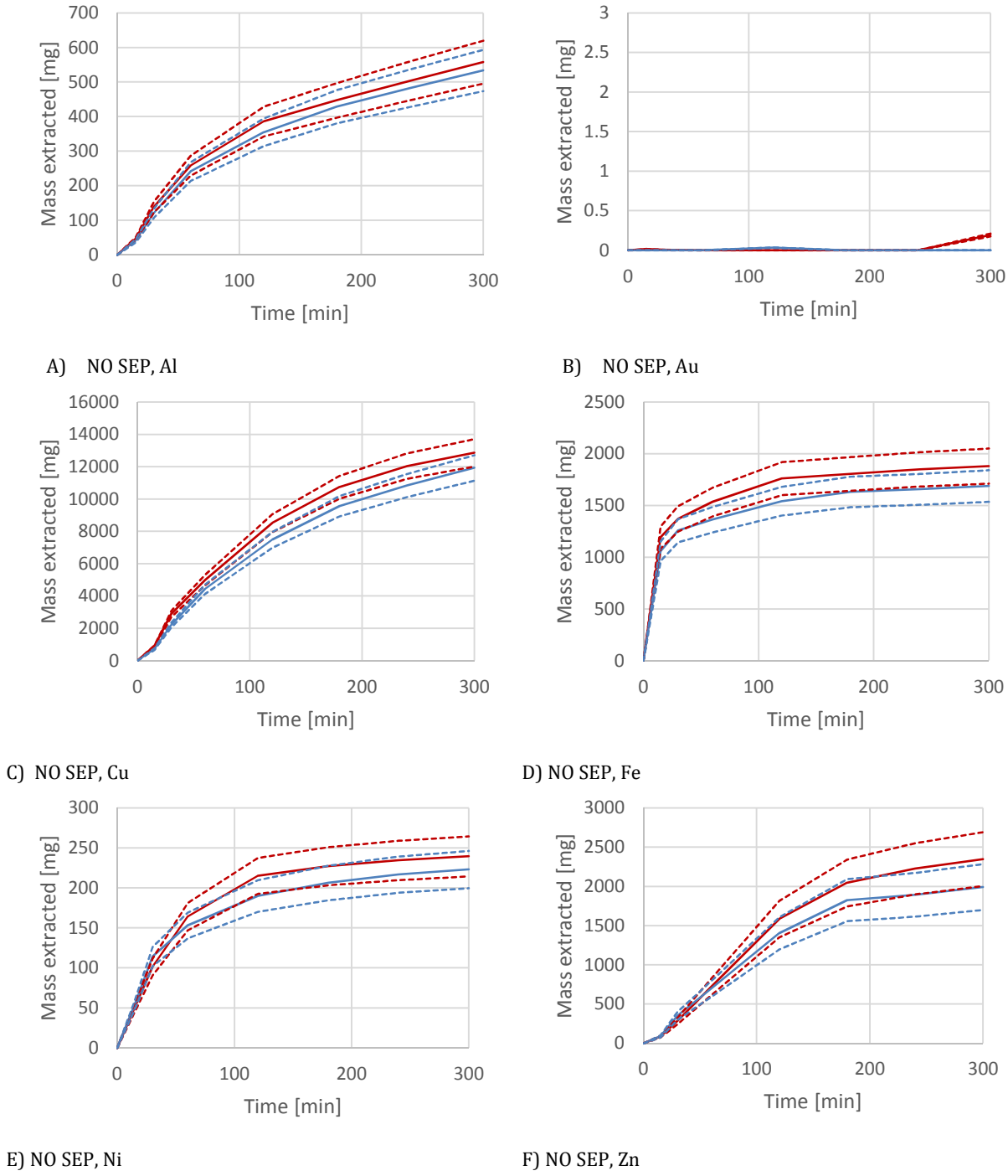

FIGURE 76: COMPARISON OF METALS LEACHED DURING REPEAT RUN USING NO SEP FEED OF A) Al, B) Au, C) Cu, D) Fe, E) Ni AND F) Zn

Figure 77 on the next page shows that for DMS feed the extraction of Al, Cu, Ni and Fe was within bounds of feed variation. The extraction of Zn, however, was not. Although the difference in observed Zn extraction was outside of what could be attributed to feed variation, the extraction curves could be seen to follow the same general trend.

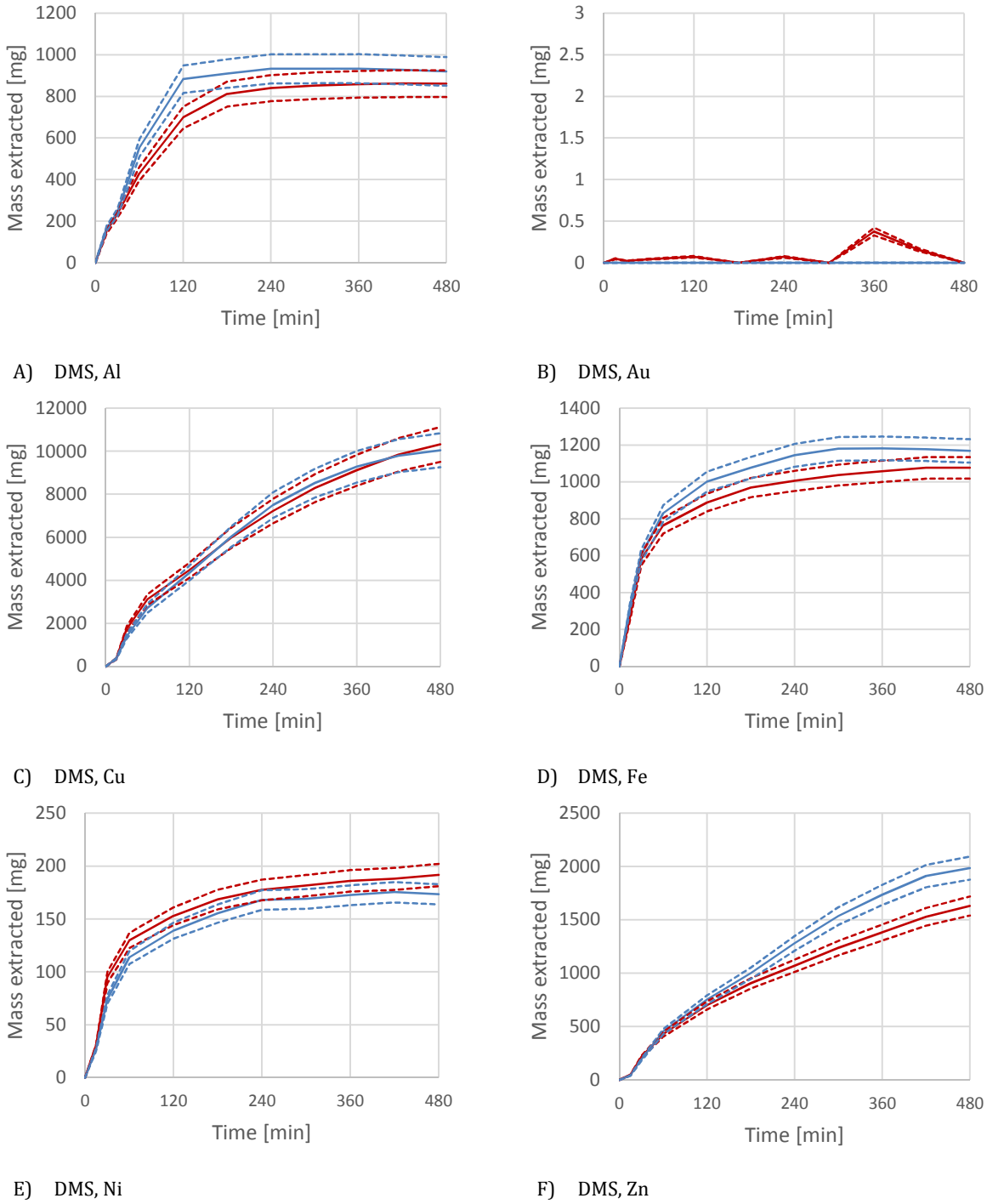

FIGURE 77: COMPARISON OF METALS LEACHED DURING REPEAT RUN USING DMS FEED OF A) Al, B) Au, C) Cu, D) Fe, E) Ni AND F) Zn

Figure 78 shows that for DMS+MS feed, differences in Cu, Fe and Ni extracted were within limits of what could be attributed to variations within feed content. As with DMS feed (see Figure 77 part D), extraction of Zn from DMS+MS feed (see Figure 78) fell outside of what could reasonably be attributed to variance in feed.

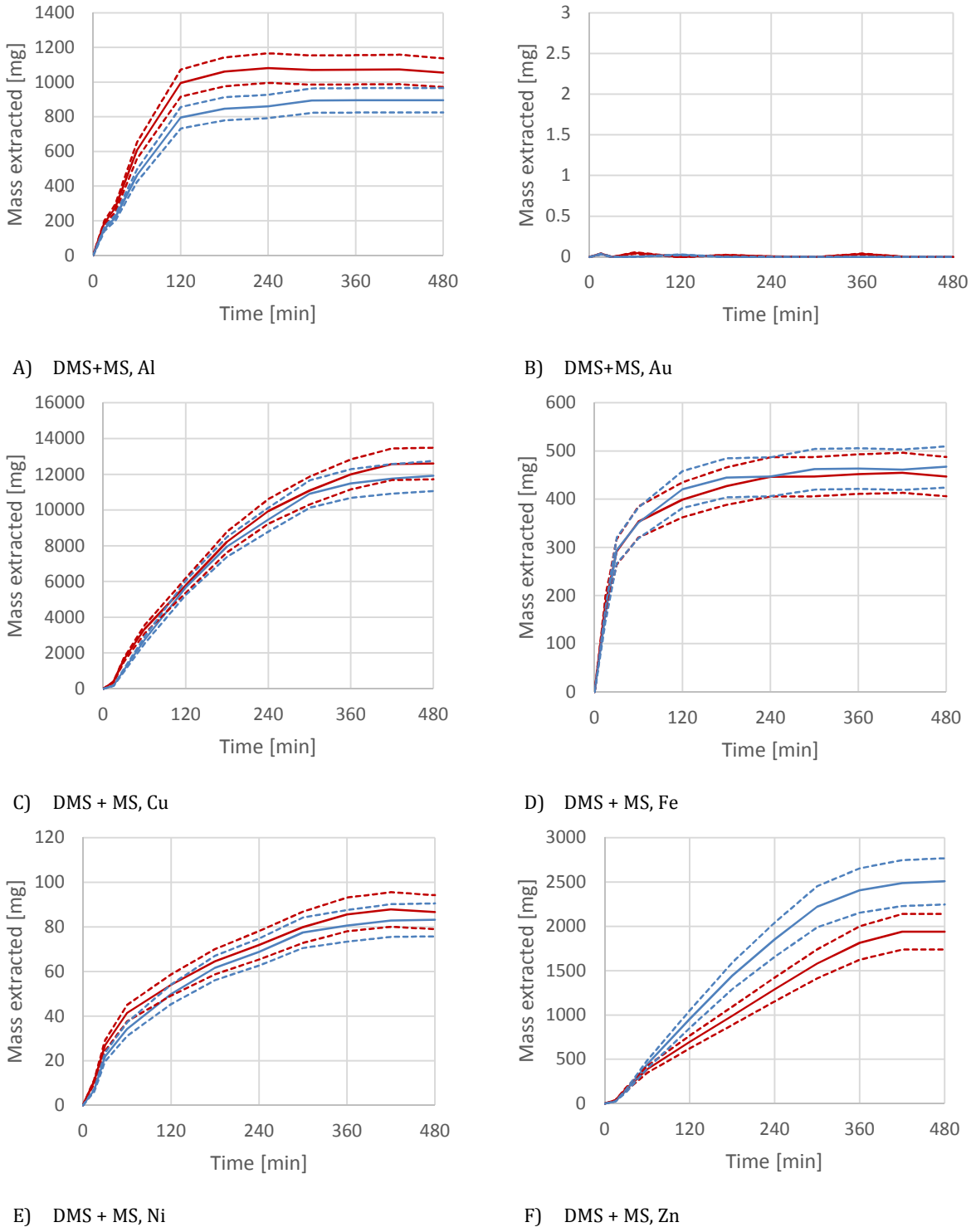

FIGURE 78: COMPARISON OF METALS LEACHED DURING REPEAT RUN USING DMS+MS FEED OF A) Al, B) Au, C) Cu, D) Fe, E) Ni AND F) Zn

With few exceptions, it was seen that metal extracted could be repeated to within a range of difference that could be attributed to variance in feed content.

5. CONCLUSIONS AND RECOMMENDATIONS

Conclusions are discussed according to the objectives stated in section 1.2.

5.1. LIXIVIANT AND TEMPERATURE INVESTIGATION

HNO_3 and H_2SO_4 leaching were investigated at different temperatures in the presence and absence of H_2O_2. It was seen that increasing temperature increased the rate and extent of Al, Cu, Ni and Zn extraction in the HNO_3 systems. For H_2SO_4 it was seen that the higher temperatures reduced the extent of Cu and Zn extracted from 49.2% Cu and 55.9% Zn at 25°C to 0% Cu and 12.4% Zn at 85°C. This was due to the rapid decomposition of H_2O_2 at the higher temperatures leading to a less oxidative environment where Cu and Zn dissolution was not favourable.

The HNO_3 system co-extracted up to 12% of Au, making it less selective than the H_2SO_4 / H_2O_2 system which showed no detectable Au extraction. Investigation of the amount and method of H_2O_2 addition to the H_2SO_4 system indicated that a peroxide feed rate of 1.2 mL/min of 30 Wt% H_2O_2 provided the most complete extent of Cu extraction. No Au was extracted at these conditions. Based on superior selectivity towards base metals, lower operating temperature and no toxic gas production, the H_2SO_4 / H_2O_2 system at 25°C was deemed most suitable.

5.2. REMOVAL OF NON-METALS

Non-metals were removed from crushed PCBs by dense medium separation using a TBE-acetone mixture at an SG of 2.5. Characterisation of the resulting heavy and light fractions showed 71% of Au reporting to the light phase along with 20% of Cu. Due to the large contribution of Au to the metallic value of PCBs, Au would most likely need to be recovered from both the light and the heavy fractions during industrial operation. Performing DMS to remove plastic would therefore fail to reduce feed volume as both heavy- and light fractions would require base metal removal prior to precious metal recovery.

The leaching of the concentrated feeds showed no clear benefit over non-concentrated feed. The concentrated feeds did however suggest that non-concentrated feed could be leached at higher S/L ratios to produce more concentrated PLSs.

5.3. REMOVAL OF FERROUS METALS

Magnetic separation was applied to a portion of the heavy fraction produced by DMS. Removal of 67% Fe and 61% Ni was achieved. The application of MS reduced the leaching time required for complete removal of Fe and Ni. This did not affect the leaching behaviour of other metals.

The partial removal of Fe and Ni prior to leaching reduced the reagent that would have been consumed during its leaching. The lower resulting Fe and Ni concentrations in the PLS implies that less reagent would be required during the refining stages for its removal.

5.4. SUGGESTION OF FLOWSHEET

Based on results from phase 1 and phase 2, two flowsheets for selective and complete base metal recovery were suggested. The selected flowsheet, repeated in Figure 79, showed superior potential for Pb and Fe removal.

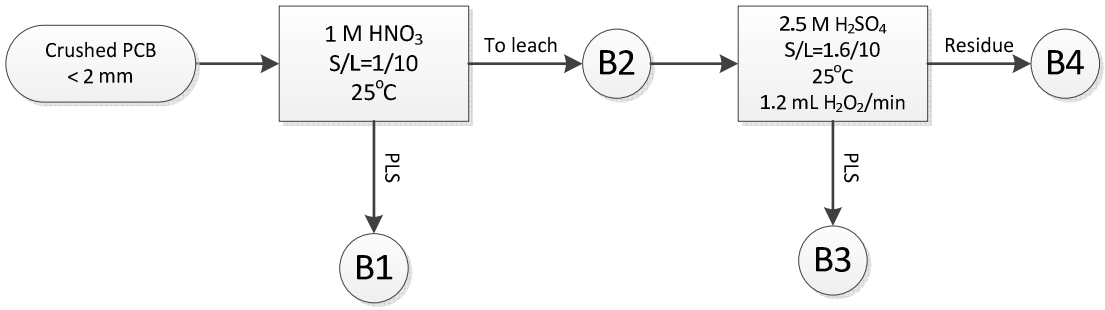

FIGURE 79: SELECTED PROCESS ROUTE FOR THE SELECTIVE RECOVERY OF BASE METALS FROM CRUSHED PCBS

The flowsheet consisted of a first stage leaching using $1M\ HNO_3$ at 25°C to primarily remove Fe and Pb. This would be performed at an S/L ratio of 1/10 for 8 hours. After solid-liquid separation, a second stage leach would be performed using 2.5 $M\ H_2SO_4$ at 25°C with an S/L ratio of 1.6/10 for 8 hours. This would remove 95% of Cu and Zn as well as the remaining Fe and Ni. The remaining residue would subsequently be free of the majority of Cu, Fe, Ni, Pb and Zn. The solid Ag and Au content would remain unaffected by the processes, but would be accompanied by 80% of the Sn and 58% of the Al originally present in the feed.

The process flowsheet was validated experimentally. A final extent of extraction of >95% Cu, Zn and Pb was achieved. Extraction of Ni and Fe was >90%. No detectable amount of Au was extracted. As expected, the majority of Al and Sn remained in the residue with only 33% and 14% removed respectively. A greater extent of Ag removal than expected was observed. This was attributed to the possible conversion of $Ag_2O_{3(s)}$ to $AgS_{(s)}$ or $Ag_{(s)}$ involving an aqueous intermediate.

The proposed flowsheet did not take potential cost implications into account. Therefore, although this flowsheet showed superior potential for base metal recovery compared to the proposed alternative, an economic analysis would be required to establish feasibility for large scale application.

5.5. RECOMMENDATIONS

Due to its presence in the solid residue, it is recommended that the effect of Al and Sn on recovery of Au be established. If residual Al and Sn proves detrimental to Au recovery, investigation into its selective removal may be justified; possibly by a hydrochloric acid leaching process. The next stage of research should investigate the recovery of Au from the residue. The treatment of the resulting leach solutions to recover high quality cathode should also be investigated.

The decomposition of hydrogen peroxide was seen to be accelerated at higher temperatures. The presence of Cu- and Fe salts in solution have also been shown to catalytically decompose hydrogen peroxide [70,84]. This implies that the rate of peroxide decomposition at a given temperature would likely increase as leaching proceeds due to the increasing amount Cu and Fe in solution. For optimal peroxide utilisation, the effect of peroxide concentration as well as the presence of various metal ions on peroxide decomposition would need to be established. This

would enable peroxide feeding to be conducted in such a way to ensure sufficient presence for leaching while limiting excess peroxide in the system.

Although feed samples with different extents of mechanical separation exposure were used in this study, the source material was the same, i.e. motherboards from Pentium 3 PCs and older. For a more thorough understanding of metals recovery from e-waste, leaching performance of different feed types (e.g. cell phones, DVD/VHS players, printers, TV-boards, etc.) would need to be compared. This would assist development of robust flowsheets for metal recovery from a variety of feed sources.

Selection of the proposed flowsheet for base metal recovery did not take into account the potential differences in operational and capital cost for large scale application. The extent and method of base metal removal would likely influence the required downstream processing units and reagent requirements. An overall techno-economic investigation of the entire metal recovery process (including crushing, leaching, PLS refining, waste disposal, etc.) would therefore be required to establish the most economical method of metal recovery.

CITED REFERENCES

1. Cui J, Forssberg E. Mechanical recycling of waste electric and electronic equipment: A review. *J Hazard Mater*. 2003;99(3):243-263.

2. Cui J, Zhang L. Metallurgical recovery of metals from electronic waste: A review. *J Hazard Mater*. 2008;158(2–3):228-256.

3. Bas A, Deveci H, Yazici E. Bioleaching of copper from low grade scrap TV circuit boards using mesophilic bacteria. *Hydrometallurgy*. 2013;138:65-70.

4. Hagelüken C. Improving metal returns and eco-efficiency in electronics recycling. *Proceedings of the 2006 IEEE Int Symposium on Electronics and the Environment IEEE*. 2006:218-223.

5. Yamane LH, de Moraes VT, Espinosa DCR, Tenório JAS. Recycling of WEEE: Characterization of spent printed circuit boards from mobile phones and computers. *Waste Manage*. 2011;31(12):2553-2558.

6. Yoo J, Jeong J, Yoo K, Lee J, Kim W. Enrichment of the metallic components from waste printed circuit boards by a mechanical separation process using a stamp mill. *Waste Manage*. 2009;29(3):1132-1137.

7. Spyrellis N, Masavetas I. Production of copper powder from printed circuit boards by electrodeposition. *Global NEST Journal*. 2009;11(2):241-247.

8. Kim E, Lee J, Kim B, Kim M, Jeong J. Leaching behavior of nickel from waste multi-layer ceramic capacitors. *Hydrometallurgy*. 2007;86(1):89-95.

9. Demir H, Özmetin C, Kocakerim MM, Yapıcı S, Çopur M. Determination of a semi empirical kinetic model for dissolution of metallic copper particles in HNO_3 solutions. *Chemical Engineering and Processing: Process Intensification*. 2004;43(8):1095-1100.

10. Long Le H, Jeong J, Lee J, Pandey BD, Yoo J, Huyunh TH. Hydrometallurgical process for copper recovery from waste printed circuit boards (PCBs). *Mineral Processing & Extractive Metallurgy Review*. 2011;32(2):90-104.

11. Kinoshita T, Akita S, Kobayashi N, Nii S, Kawaizumi F, Takahashi K. Metal recovery from non-mounted printed wiring boards via hydrometallurgical processing. *Hydrometallurgy*. 2003;69(1):73-79.

12. Maguyon MCC, Alfafara CG, Migo VP, Movillon JL, Rebancos CM. Recovery of copper from spent solid printed-circuit-board (PCB) wastes of a PCB manufacturing facility by two-step sequential acid extraction and electrochemical deposition. *Journal of Environmental Science and Management*. 2012;15(1):17-27.

13. Naseri Joda N, Rashchi F. Recovery of ultra fine grained silver and copper from PC board scraps. *Separation and Purification Technology*. 2012;92:36-42.

14. Söderström G, Marklund S. Combustion of brominated flame retardants. *BFR 2001*. 2001(Part 2):55.

15. Greim, Lutz WD Weber Helmut. The toxicity of brominated and mixed-halogenated dibenzo-p-dioxins and dibenzofurans: An overview. *Journal of Toxicology and Environmental Health Part A*. 1997;50(3):195-216.

16. Deveci H, Yazıcı E, Aydın U, Yazıcı R, Akcil A. Extraction of copper from scrap TV boards by sulphuric acid leaching under oxidising conditions. *Proceedings of Going Green-CARE INNOVATION 2010 Conference*. 2010:8-11.

17. Birloaga I, De Michelis I, Ferella F, Buzatu M, Vegliò F. Study on the influence of various factors in the hydrometallurgical processing of waste printed circuit boards for copper and gold recovery. *Waste Manage*. 2013;33(4):935-941.

18. Huang K, Guo J, Xu Z. Recycling of waste printed circuit boards: A review of current technologies and treatment status in china. *J Hazard Mater*. 2009;164(2–3):399-408.

19. Tuncuk A, Stazi V, Akcil A, Yazici E, Deveci H. Aqueous metal recovery techniques from e-scrap: Hydrometallurgy in recycling. *Minerals Eng*. 2012;25(1):28-37.

20. Quinet P, Proost J, Van Lierde A. Recovery of precious metals from electronic scrap by hydrometallurgical processing routes. *Minerals and Metallurgical Processing*. 2005;22(1):17-22.

21. Hageluken C. Recycling of electronic scrap at umicore precious metals refining. *Acta Metallurgica Slovaca*. 2006;12:111-120.

22. Bas AD, Deveci H, Yazici EY. Treatment of manufacturing scrap TV boards by nitric acid leaching. *Separation and Purification Technology*. 2014(130):151-159.

23. Das A, Vidyadhar A, Mehrotra SP. A novel flowsheet for the recovery of metal values from waste printed circuit boards. *Resour Conserv Recycling*. 2009;53(8):464-469.

24. Mecucci A, Scott K. Leaching and electrochemical recovery of copper, lead and tin from scrap printed circuit boards. *Journal of Chemical Technology and Biotechnology*. 2002;77(4):449-457.

25. Yazici E, Deveci H. Recovery of metals from E-wastes. *Madencilik*. 2009;48:3-18.

26. Dalrymple I, Wright N, Kellner R, et al. An integrated approach to electronic waste (WEEE) recycling. *Circuit World*. 2007;33(2):52-58.

27. Li J, Shrivastava P, Gao Z, Zhang H. Printed circuit board recycling: A state-of-the-art survey. *Electronics Packaging Manufacturing, IEEE Transactions on*. 2004;27(1):33-42.

28. Chatterjee S, Kumar K. Effective electronic waste management and recycling process involving formal and non-formal sectors. *International Journal of Physical Sciences*. 2009;4(13):893-905.

29. Yang H, Liu J, Yang J. Leaching copper from shredded particles of waste printed circuit boards. *J Hazard Mater*. 2011;187(1–3):393-400.

30. Zhou Y, Qiu K. A new technology for recycling materials from waste printed circuit boards. *J Hazard Mater*. 2010;175(1):823-828.

31. Li J, Lu H, Guo J, Xu Z, Zhou Y. Recycle technology for recovering resources and products from waste printed circuit boards. *Environ Sci Technol*. 2007;41(6):1995-2000.

32. He W, Li G, Ma X, et al. WEEE recovery strategies and the WEEE treatment status in china. *J Hazard Mater*. 2006;136(3):502-512.

33. Zhang S, Forssberg E. Mechanical separation-oriented characterization of electronic scrap. *Resour Conserv Recycling*. 1997;21(4):247-269.

34. Veasey A. *The physical separation and recovery of metals from waste, volume one.* Vol 1. CRC Press; 1993.

35. Fitzgibbon KE, Veasey TJ. Thermally assisted liberation - a review. *Minerals Eng*. 1990;3(1–2):181-185.

36. Eswaraiah C, Kavitha T, Vidyasagar S, Narayanan SS. Classification of metals and plastics from printed circuit boards (PCB) using air classifier. *Chemical Engineering and Processing: Process Intensification*. 2008;47(4):565-576.

37. Veit HM, Diehl TR, Salami AP, Rodrigues JS, Bernardes AM, Tenório JAS. Utilization of magnetic and electrostatic separation in the recycling of printed circuit boards scrap. *Waste Manage*. 2005;25(1):67-74.

38. Li J, Xu Z, Zhou Y. Application of corona discharge and electrostatic force to separate metals and nonmetals from crushed particles of waste printed circuit boards. *J Electrostatics*. 2007;65(4):233-238.

39. Zhang S, Forssberg E. Optimization of electrodynamic separation for metals recovery from electronic scrap. *Resour Conserv Recycling*. 1998;22(3):143-162.

40. Zhao Y, Wen X, Li B, Tao D. Recovery of copper from waste printed circuit boards. *Miner Metall Process*. 2004;21(2):99-102.

41. Veit HM, de Pereira CC, Bernardes AM. Using mechanical processing in recycling printed wiring boards. *JOM*. 2002;54(6):45-47.

42. Kamberovic ZJ. Hydrometallurgical process for extraction of metals from electronic waste-part I: Material characterization and process option selection. *Association of Metallurgical Engineers of Serbia*. 2009;15(4):231-243.

43. Huang J, Chen M, Chen H, Chen S, Sun Q. Leaching behavior of copper from waste printed circuit boards with brønsted acidic ionic liquid. *Waste Manage*. 2014;34(2):483-488.

44. Wu J, Li J, Xu Z. Electrostatic separation for recovering metals and nonmetals from waste printed circuit board: Problems and improvements. *Environ Sci Technol*. 2008;42(14):5272-5276.

45. Kang H, Schoenung JM. Electronic waste recycling: A review of US infrastructure and technology options. *Resour Conserv Recycling*. 2005;45(4):368-400.

46. Jupiter Magnetics. Permanent magnetic separators. Jupiter Magnetics Web site. http://www.jupitermagnetics.com/permanent_magnetic_seprator.htm. Updated May, 2014. Accessed 2014, 2/26, 2014.

47. Li J, Xu Z. Environmental friendly automatic line for recovering metal from waste printed circuit boards. *Environ Sci Technol*. 2010;44(4):1418-1423.

48. Castro L, Martins A. Recovery of tin and copper by recycling of printed circuit boards from obsolete computers. *Brazil J Chem Eng*. 2009;26(4):649-657.

49. Habashi F. *A textbook of hydrometallurgy.* Métallurgie Extractive Québec; 1999.

50. Shin D, Jeong J, Lee S, Pandey B, Lee J. Evaluation of bioleaching factors on gold recovery from ore by cyanide-producing bacteria. *Minerals Eng*. 2013;48:20-24.

51. Jha MK, Choubey PK, Kumari A, Kumar R, Kumar V, Lee J. Leaching of lead from solder material used in electrical and electronic equipment. *Proceedings of second symposium on Recycling of waste National Metallurgy Laboratory, Jamshedpur*. 2011;1(2):25-31.

52. Kumari A, Jha MK, Kumar V, Jeong J, Lee J. Recovery of lead from the solder of waste printed circuit boards. *Proceedings of the XI International Seminar on Mineral Processing Technology (MPT-2010)*. 2010;2(11):891-897.

53. Kamberović Ž, Korać M, Vračar S, Ranitović M. Preliminary process analysis and development of hydrometallurgical process for the recovery of copper from waste printed circuit boards. *8th International Symposium and Environmental Exhibition-Going Green CARE INNOVATION*. 2010:8-11.

54. Alibaba. Products page. www.alibaba.com/trade. Updated August, 2015. Accessed 2015, 8/27, 2015.

55. Havlik T, Orac D, Petranikova M, Miskufova A, Kukurugya F, Takacova Z. Leaching of copper and tin from used printed circuit boards after thermal treatment. *J Hazard Mater*. 2010;183(1):866-873.

56. Perry RH, Green DW, Maloney JO. *Perry's chemical engineers' handbook.* Vol 7. McGraw-Hill New York; 2008.

57. Birloaga I, Coman V, Kopacek B, Vegliò F. An advanced study on the hydrometallurgical processing of waste computer printed circuit boards to extract their valuable content of metals. *Waste Manage*. 2014;34(12):2581-2586.

58. Jackson E. *Hydrometallurgical extraction and reclamation.* Ellis Horwood Chichester; 1986.

59. Levenspiel O. Chemical reaction engineering. *Ind Eng Chem Res*. 1999;38(11):4140-4143.

60. Luo W, Feng Q, Ou L, Zhang G, Chen Y. Kinetics of saprolitic laterite leaching by sulphuric acid at atmospheric pressure. *Minerals Eng*. 2010;23(6):458-462.

61. Engel T, Reid P, McQuarrie DA. *Thermodynamics, statistical thermodynamics, & kinetics.* Vol 1000. ; 2006.

62. Gharabaghi M, Irannajad M, Azadmehr AR. Leaching behavior of cadmium from hazardous waste. *Separation and Purification Technology*. 2012;86(0):9-18.

63. Ping Z, ZeYun F, Jie L, Qiang L, GuangRen Q, Ming Z. Enhancement of leaching copper by electro-oxidation from metal powders of waste printed circuit board. *J Hazard Mater*. 2009;166(2):746-750.

64. Gubbins KE, Walker RD. The solubility and diffusivity of oxygen in electrolytic solutions. *J Electrochem Soc*. 1965;112(5):469-471.

65. Banza A, Gock E, Kongolo K. Base metals recovery from copper smelter slag by oxidising leaching and solvent extraction. *Hydrometallurgy*. 2002;67(1):63-69.

66. Kamberovic ZJ. Hydrometallurgical process for extraction of metals from electronic waste-part II: Development of the processes for the recovery of copper from printed circuit boards (PCB). *Association of Metallurgical Engineers of Serbia*. 2011;17(3):139-149.

67. Mori M, Miura K, Sasaki T, Ohtsuka T. Corrosion of tin alloys in sulfuric and nitric acids. *Corros Sci*. 2002;44(4):887-898.

68. Adebayo A, Ipinmoroti K, Ajayi O. Dissolution kinetics of chalcopyrite with hydrogen peroxide in sulphuric acid medium. *Chemical and biochemical engineering quarterly*. 2003;17(3):213-218.

69. Antonijević MM, Dimitrijević M, Janković Z. Leaching of pyrite with hydrogen peroxide in sulphuric acid. *Hydrometallurgy*. 1997;46(1–2):71-83.

70. Deveci H. Factors affecting decomposition of hydrogen peroxide. *Proceedings of the XIIth International Mineral Processing Symposium, Gülsoy ÖY, Ergün LŞ, Can NM and Çelik İB (Eds)*. 2010.

71. Huckaba CE, Keyes FG. The accuracy of estimation of hydrogen peroxide by potassium permanganate titration. *J Am Chem Soc*. 1948;70(4):1640-1644.

72. Sellers RM. Spectrophotometric determination of hydrogen peroxide using potassium titanium (IV) oxalate. *Analyst*. 1980;105(1255):950-954.

73. Harris DC. *Quantitative chemical analysis.* Macmillan; 2010.

74. Walter MD, Wajer MT. Overview of flame retardants including magnesium hydroxide. *Martin Marietta Magnesia Specialties LLC, Baltimore, Maryland*. 2006;31.

75. Bockhorn H, Hornung A, Hornung U, Jakobströer P, Kraus M. Dehydrochlorination of plastic mixtures. *J Anal Appl Pyrolysis*. 1999;49(1–2):97-106.

76. Freegard K, Tan G, Morton R. Develop a process to separate brominated flame retardants from WEEE polymers. *The Waste and Resources Action Programme (WRAP), UK*. 2006.

77. Biomonitoring California. Brominated and chlorinated organic chemical compounds used as flame retardants. *Meeting of the California Environmental Contaminant Biomonitoring Program (CECBP) Scientific Guidance Panel (SGP)*. 2008.

78. Kyle JH, Breuer PL, Bunney KG, Pleysier R. Review of trace toxic elements (Pb, Cd, Hg, As, Sb, Bi, se, Te) and their deportment in gold processing: Part II: Deportment in gold ore processing by cyanidation. *Hydrometallurgy*. 2012;111–112:10-21.

79. Spalvins E, Dubey B, Townsend T. Impact of electronic waste disposal on lead concentrations in landfill leachate. *Environ Sci Technol*. 2008;42(19):7452-7458.

80. Zheng L, Wu K, Li Y, et al. Blood lead and cadmium levels and relevant factors among children from an e-waste recycling town in china. *Environ Res*. 2008;108(1):15-20.

81. Jang Y, Townsend TG. Leaching of lead from computer printed wire boards and cathode ray tubes by municipal solid waste landfill leachates. *Environ Sci Technol*. 2003;37(20):4778-4784.

82. Jha MK, Choubey PK, Jha AK, et al. Leaching studies for tin recovery from waste e-scrap. *Waste Manage*. 2012;32(10):1919-1925.

83. Bailey NT, Chapman RJ. The use of coal spoils as feed materials for alumina recovery by acid leaching routes V. the effect of fluoride additions on the extraction of aluminium with hydrochloric acid. *Hydrometallurgy*. 1987;18(3):337-350.

84. Haber F, Weiss J. The catalytic decomposition of hydrogen peroxide by iron salts. *Proceedings of the Royal Society of London A: Mathematical, Physical and Engineering Sciences*. The Royal Society, 1934;147(861):332-351.

APPENDIX A: SUPPLEMENTARY TABLES AND FIGURES

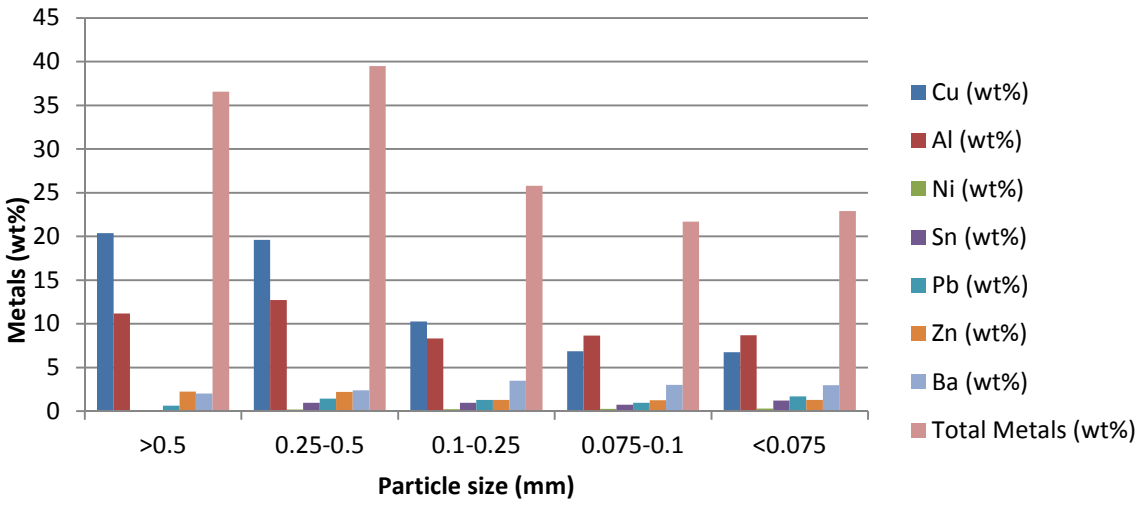

Figure A 1: Distribution of metals in different size classes of comminuted WPCBs, redrawn from results of Huang et al [43].

TABLE A 1: CALCULATING THE AMOUNT OF STOCK NITRIC ACID REQUIRED TO MAKE UP DESIRED CONCENTRATION OF LEACHING SOLUTION

Density of stock sol.	1.339	g/mL
Formula weight	63.01	g/mol
Weight percentage	55	% w/w
Desired final volume	500	mL
Desired concentration	1	M
Volume stock required	42.8	mL

TABLE A 2: CALCULATING THE AMOUNT OF STOCK NITRIC ACID REQUIRED TO MAKE UP DESIRED CONCENTRATION OF LEACHING SOLUTION

Density of stock	1.84	g/mL
Formula weight	98.08	g/mol
Weight percentage	98	% w/w
Desired final volume	500	mL
Desired concentration	1	M
Volume stock required	27.2	mL

APPENDIX B: THERMODYNAMIC SIMULATION USING OLI SOFTWARE

B1: NITRIC ACID LEACHING

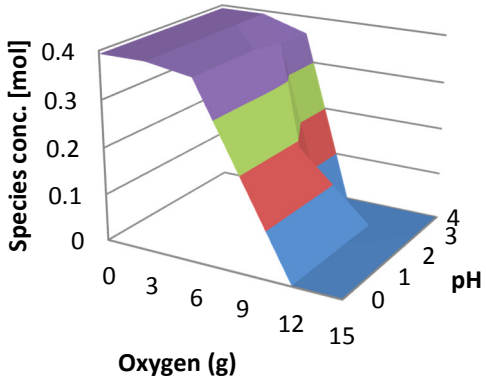

A) $Cu_{(s)}$

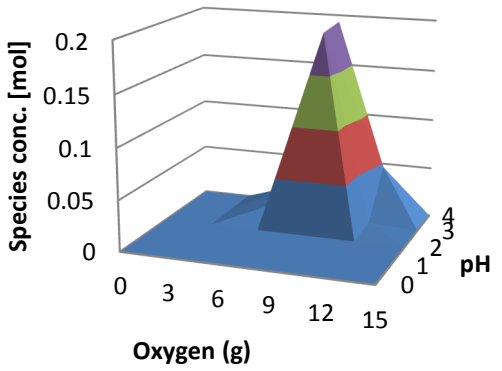

B) $Cu_2O_{(s)}$

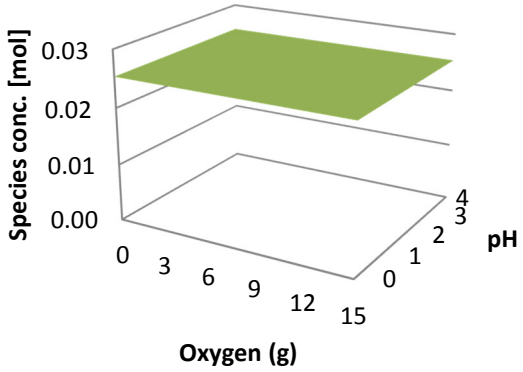

C) $Au_{(s)}$

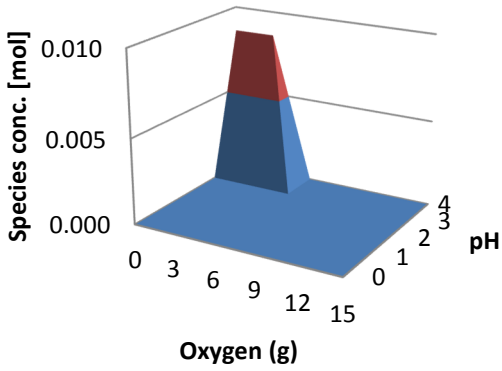

D) $Pb_{(s)}$

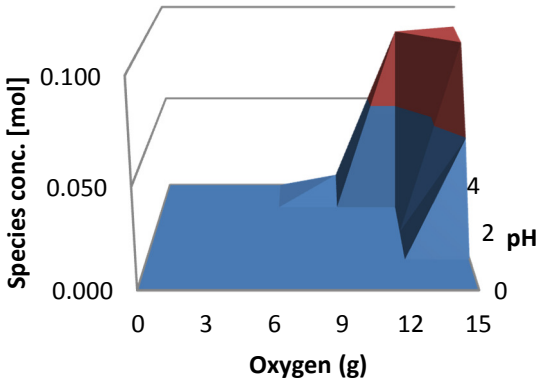

E) $Fe(OH)_{3(s)}$

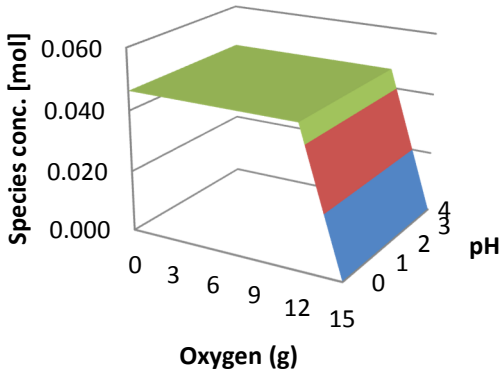

F) $Ag_{(s)}$

FIGURE B 1: OLI SYSTEMS NITRIC ACID SIMULATION RESULTS SHOWING SOLID SPECIES PRESENT AT pH 0 TO pH 4 AND WITH OXYGEN ADDITION OF ZERO TO 12 GRAMS

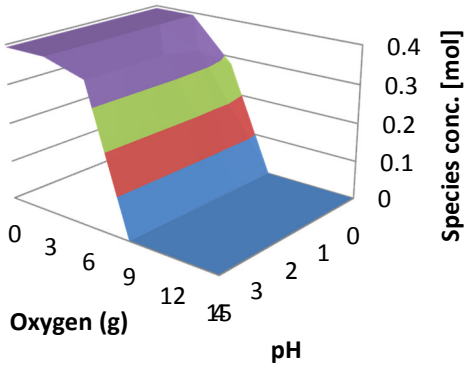

A) $Cu_{(s)}$

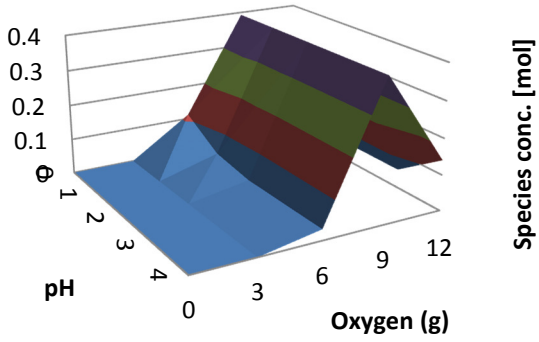

B) $CuCl_{(s)}$

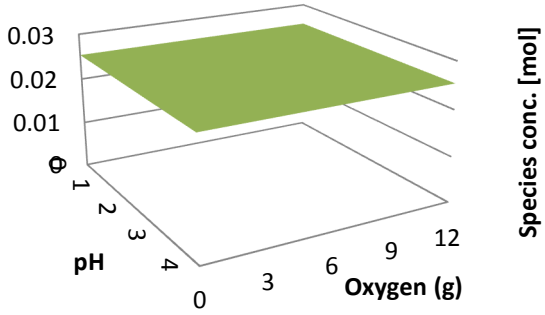

C) $Au_{(s)}$

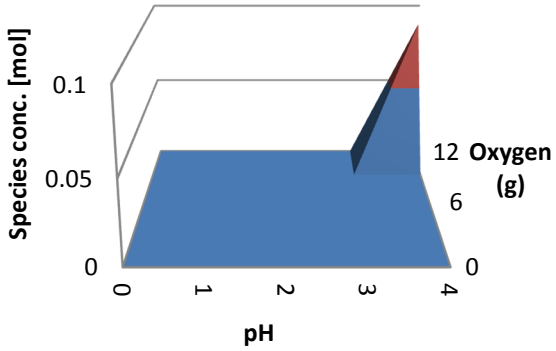

D) $Fe(OH)_{3(s)}$

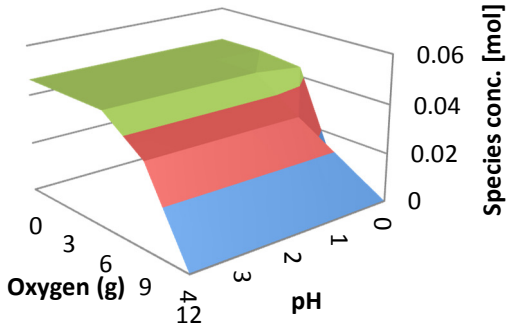

E) $Ag_{(s)}$

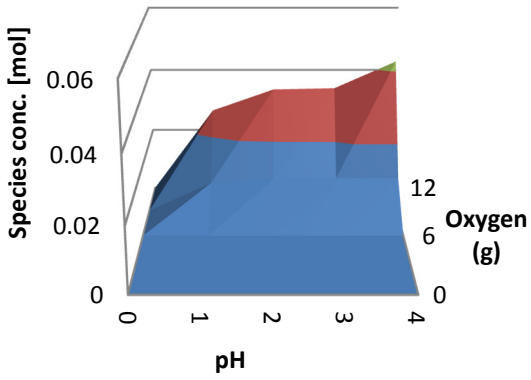

F) $AgCl_{(s)}$

FIGURE B 2: OLI SYSTEMS HYDROCHLORIC ACID SIMULATION RESULTS SHOWING SOLID SPECIES PRESENT AT pH 0 TO pH 4 AND WITH OXYGEN ADDITION OF ZERO TO 12 GRAMS

B3: SULPHURIC ACID LEACHING

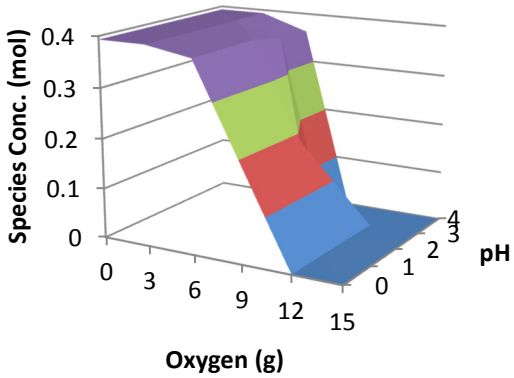

A) $Cu_{(s)}$

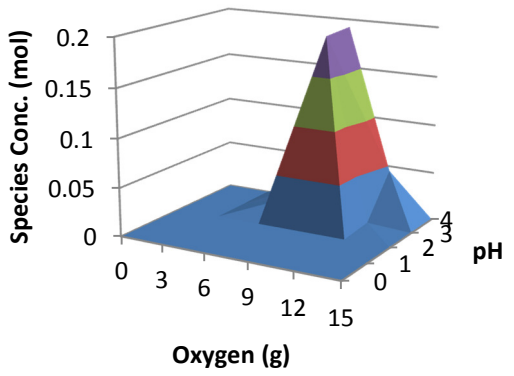

B) $CuO_{(s)}$

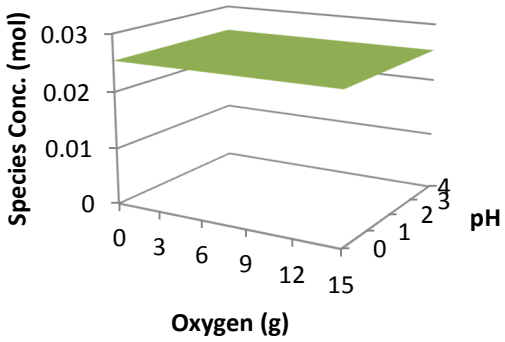

C) $Au_{(s)}$

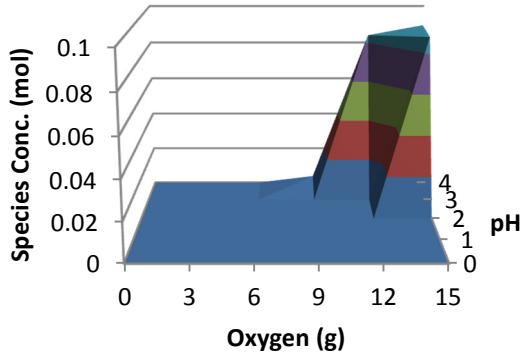

D) $Fe(OH)_{3(s)}$

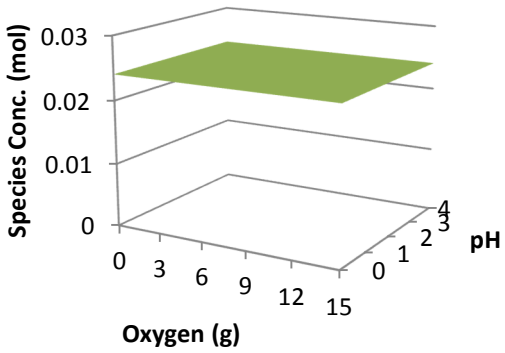

E) $PbSO_{4(s)}$

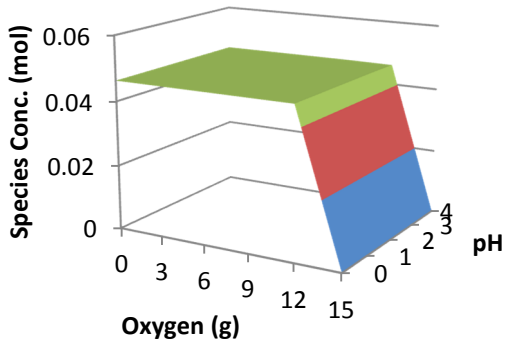

F) $Ag_{(s)}$

FIGURE B 3: OLI SYSTEMS SULPHURIC ACID SIMULATION RESULTS SHOWING SOLID SPECIES PRESENT AT pH 0 TO pH 4 AND WITH OXYGEN ADDITION OF ZERO TO 12 GRAMS

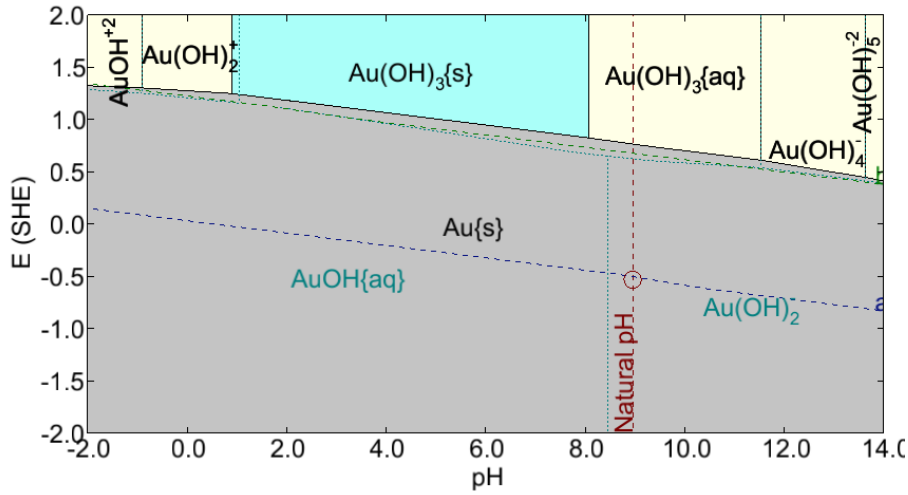

FIGURE B 4: POURBAIX DIAGRAM FOR Au IN A NITRIC ACID SYSTEM AT 25°C

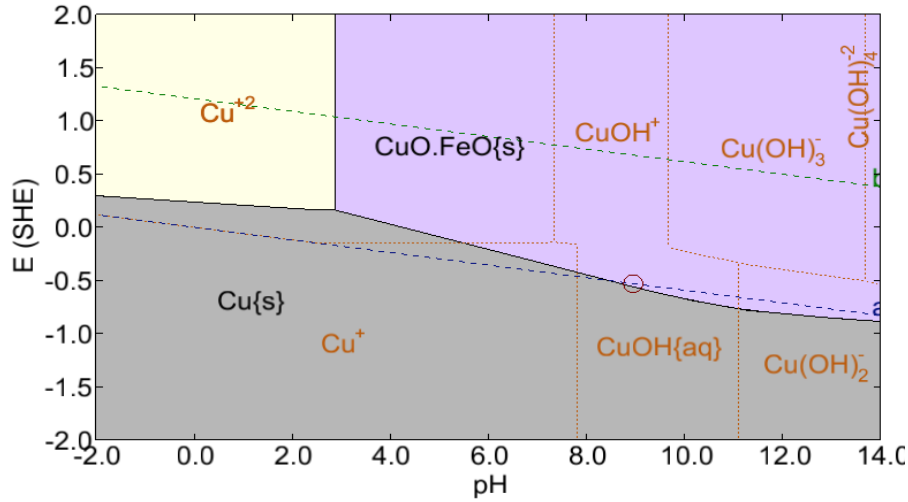

FIGURE B 5: POURBAIX DIAGRAM FOR Cu IN A SULPHURIC ACID SYSTEM AT 25°C

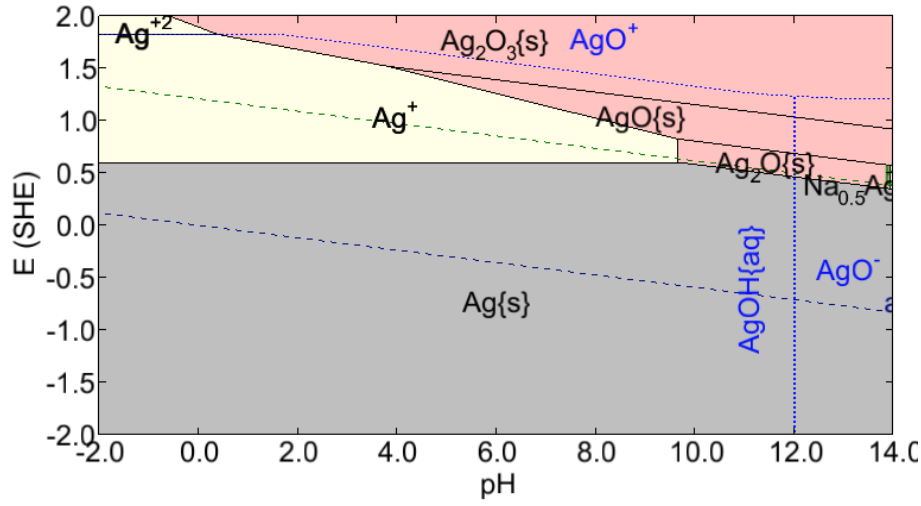

FIGURE B 6: POURBAIX DIAGRAM FOR Ag IN A SULPHURIC ACID SYSTEM AT 25°C

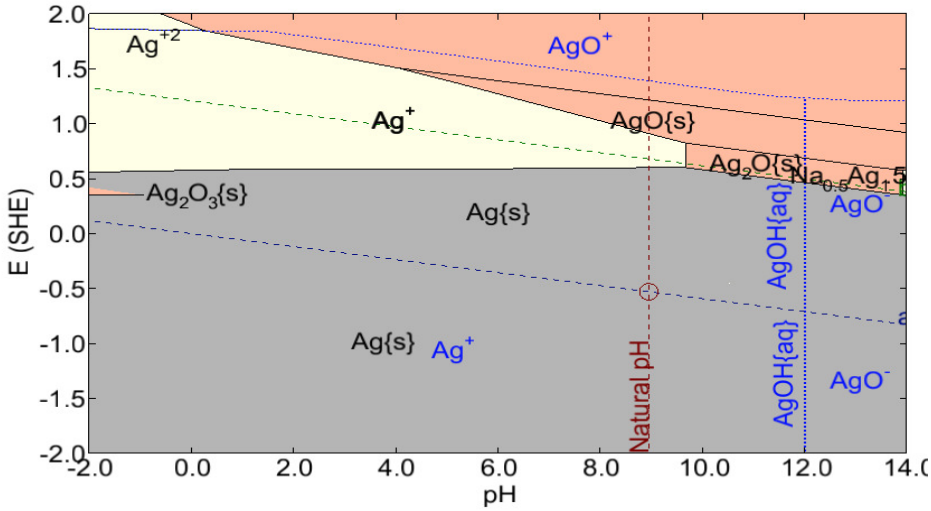

FIGURE B 7: POURBAIX DIAGRAM FOR Ag IN A NITRIC ACID SYSTEM AT 25°C

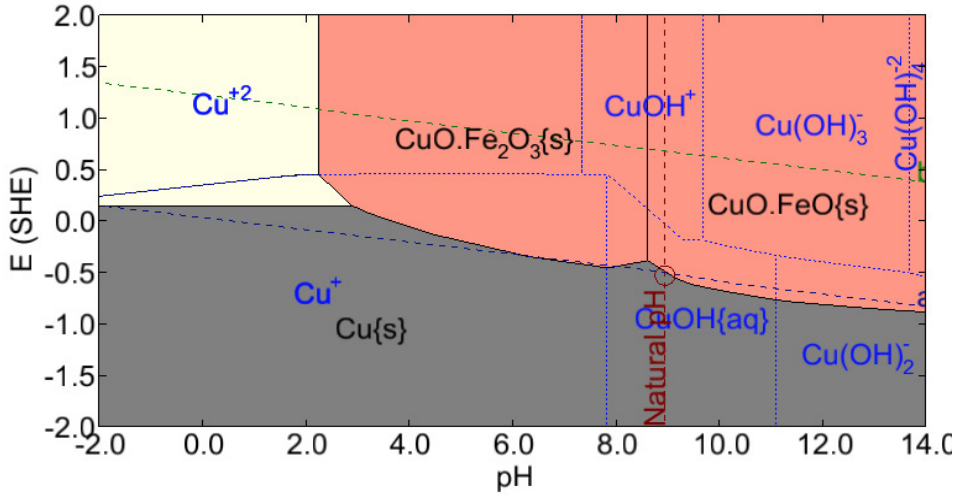

FIGURE B 8: POURBAIX DIAGRAM FOR Cu IN A NITRIC ACID SYSTEM AT 25°C

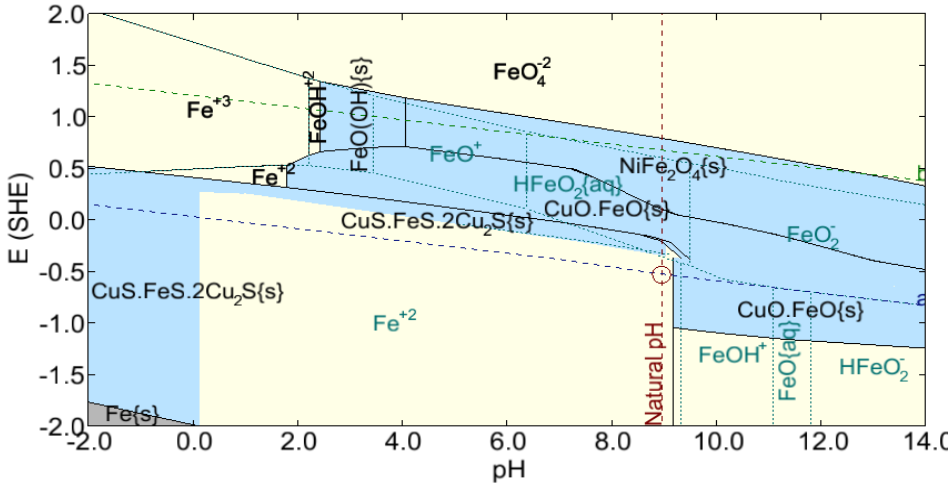

FIGURE B 9: POURBAIX DIAGRAM FOR Fe IN A SULPHURIC ACID SYSTEM AT 25°C

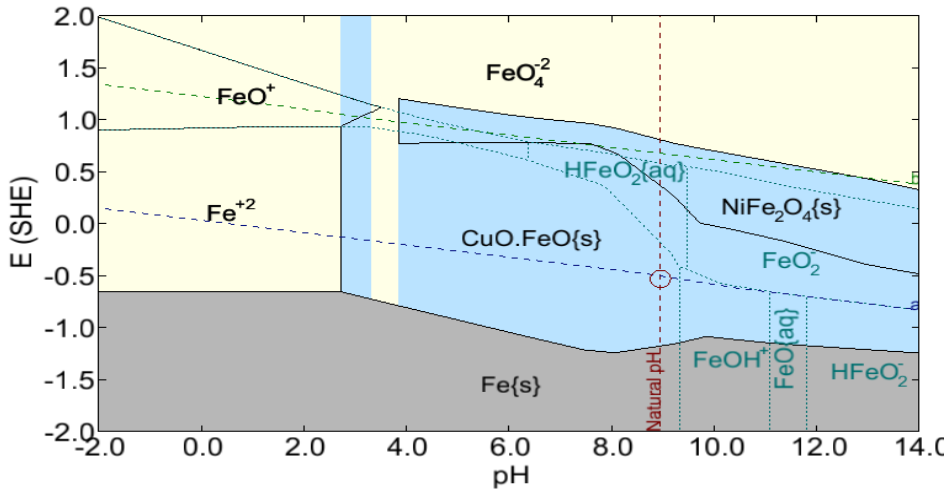

FIGURE B 10: POURBAIX DIAGRAM FOR Fe IN A NITRIC ACID SYSTEM AT 25°C

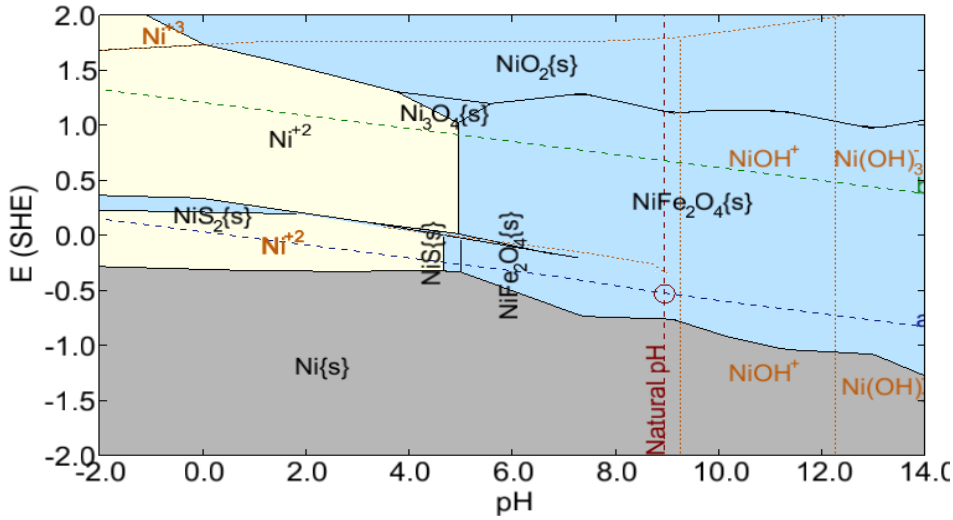

FIGURE B 11: POURBAIX DIAGRAM FOR Ni IN A SULPHURIC ACID SYSTEM AT 25°C

APPENDIX C: EXPERIMENTAL RESULTS

C1. PHASE 1: SCREENING

C1.1. MASS EXTRACTED

The values in the tables show the extent of leaching of that metal (mg).

TABLE C 1: MASS OF METAL EXTRACTED [mg] AFTER 60 MINUTES DURING PHASE 1 EXPERIMENTS

Acid type	Temperature	H_2O_2 Addition	Ag	Al	Au	Cu	Fe	Ni	Pb	Sn	Zn
1M HNO_3	25°C	no H_2O_2	1.5 ± 0.1	89.3 ± 5.1	0 ± 0	24.7 ± 1.4	1238.6 ± 69.4	31.2 ± 1.9	1828.9 ± 51.2	110.6 ± 7.9	27.6 ± 1.8
1M HNO_3	85°C	no H_2O_2	1.2 ± 0	1087.2 ± 14.1	0.7 ± 0	10172 ± 162.8	74 ± 1.7	247.6 ± 4	3276.2 ± 26.2	10.1 ± 0.2	1264 ± 11.4
1M H_2SO_4	25°C	no H_2O_2	0.1 ± 0	93.8 ± 2.3	0 ± 0	4.7 ± 0.1	58.9 ± 1.5	2.7 ± 0.1	166 ± 2.8	91 ± 1.7	24.8 ± 0.4
1M H_2SO_4	85°C	no H_2O_2	2.3 ± 0.5	881.1 ± 125.1	0 ± 0	4.4 ± 0.6	439.2 ± 59.3	17 ± 2.3	163.7 ± 21.8	77.9 ± 11.1	57.7 ± 8.2
1M HNO_3	55°C	no H_2O_2	0.1 ± 0	598.6 ± 16.8	0.1 ± 0	8484.9 ± 254.5	1155.1 ± 28.9	158.6 ± 4.1	3380.8 ± 131.9	196.8 ± 5.7	1127.6 ± 31.6
1M H_2SO_4	55°C	no H_2O_2	0.4 ± 0.1	471.7 ± 22.2	0 ± 0	2.8 ± 0.2	83.7 ± 2.3	4 ± 0.2	5.3 ± 0.1	60.6 ± 2.2	19.2 ± 0.9
1M H_2SO_4	85°C	90mL H_2O_2	0.7 ± 0.1	1390 ± 9.7	0 ± 0	227 ± 2.5	1769.5 ± 21.2	157.2 ± 1.6	15.1 ± 0.2	41 ± 0.5	264.5 ± 2.9
1M HNO_3	25°C	90mL H_2O_2	0.7 ± 0	198.8 ± 6.8	0 ± 0	4693.2 ± 159.6	1237.5 ± 63.1	119.7 ± 4.3	2772.5 ± 135.9	366.8 ± 11.4	508.6 ± 17.3
1M H_2SO_4	25°C	90mL H_2O_2	0 ± 0	312.9 ± 10	0 ± 0	7526.3 ± 263.4	1625.7 ± 55.3	160.7 ± 5.5	0 ± 0	34.9 ± 1.4	918.9 ± 27.6
1M HNO_3	85°C	90mL H_2O_2	0.2 ± 0	930 ± 56.7	0.4 ± 0	10264.4 ± 554.3	852.1 ± 46	239.2 ± 13.9	3439.4 ± 41.3	14.5 ± 1	1304.8 ± 63.9
1M HNO_3	55°C	90mL H_2O_2	0.3 ± 0	634.4 ± 24.1	0.2 ± 0	8178.2 ± 318.9	1182.5 ± 36.7	200.5 ± 7.4	3135.6 ± 103.5	63.6 ± 2	1036.5 ± 34.2
1M H_2SO_4	55°C	90mL H_2O_2	0.1 ± 0	952.5 ± 29.5	0 ± 0	2403.2 ± 57.7	1561.4 ± 51.5	156.7 ± 4.9	15.1 ± 0.5	61 ± 2	363.4 ± 12.4

TABLE C 2: MASS OF METAL EXTRACTED [mg] AFTER 180 MINUTES DURING PHASE 1 EXPERIMENTS

Acid type	Temperature	H_2O_2 Addition	Ag	Al	Au	Cu	Fe	Ni	Pb	Sn	Zn
1M HNO_3	25°C	no H_2O_2	0.9 ± 0	292.9 ± 16.7	0 ± 0	30.5 ± 1.8	1451.7 ± 81.3	82.5 ± 5	2704.2 ± 75.7	180.4 ± 12.8	32.5 ± 2.1
1M HNO_3	85°C	no H_2O_2	1.5 ± 0	1039.2 ± 13.5	1.4 ± 0	10057.9 ± 160.9	3.3 ± 0.1	221 ± 3.5	2824.6 ± 22.6	17.5 ± 0.3	1397.8 ± 12.6
1M H_2SO_4	25°C	no H_2O_2	0.8 ± 0.1	229.8 ± 5.7	0 ± 0	5.2 ± 0.1	76.9 ± 2	3.5 ± 0.1	159.1 ± 2.7	18.6 ± 0.4	27.8 ± 0.5
1M H_2SO_4	85°C	no H_2O_2	2.2 ± 0.5	1312.5 ± 186.4	0 ± 0	2.7 ± 0.4	758 ± 102.3	22 ± 3	163.6 ± 21.8	59.1 ± 8.5	76.6 ± 11
1M HNO_3	55°C	no H_2O_2	0.1 ± 0	788.9 ± 22.1	0.3 ± 0	10372.7 ± 311.2	27.1 ± 0.7	175.3 ± 4.6	3299.6 ± 128.7	5.5 ± 0.2	1570.6 ± 44
1M H_2SO_4	55°C	no H_2O_2	0.1 ± 0	770.3 ± 36.2	0 ± 0	2.9 ± 0.2	178 ± 4.8	6.8 ± 0.4	3.8 ± 0.1	134.9 ± 5	28.4 ± 1.3
1M H_2SO_4	85°C	90mL H_2O_2	0 ± 0	1736.1 ± 12.2	0 ± 0	6.2 ± 0.1	1713 ± 20.6	161.5 ± 1.6	12.6 ± 0.1	99.1 ± 1.3	217.5 ± 2.4
1M HNO_3	25°C	90mL H_2O_2	0 ± 0	319.9 ± 10.9	0 ± 0	4856.2 ± 165.1	1398.8 ± 71.3	145.2 ± 5.2	3348.6 ± 164.1	219.1 ± 6.8	552 ± 18.8
1M H_2SO_4	25°C	90mL H_2O_2	0 ± 0	462.5 ± 14.8	0 ± 0	7182.3 ± 251.4	1670.4 ± 56.8	171.9 ± 5.8	3.5 ± 0.1	176.8 ± 7.1	934.8 ± 28
1M HNO_3	85°C	90mL H_2O_2	0.1 ± 0	1010.5 ± 61.6	1 ± 0.1	10060.8 ± 543.3	2.2 ± 0.1	212 ± 12.3	2739 ± 32.9	0 ± 0	1407.5 ± 69
1M HNO_3	55°C	90mL H_2O_2	0.4 ± 0	925.6 ± 35.2	0.5 ± 0	11537.2 ± 449.9	275.4 ± 8.5	250.5 ± 9.3	3712.4 ± 122.5	5.4 ± 0.2	1635.7 ± 54
1M H_2SO_4	55°C	90mL H_2O_2	0.4 ± 0	1321.3 ± 41	0 ± 0	1725.1 ± 41.4	1725.2 ± 56.9	193.8 ± 6	13.5 ± 0.5	83.3 ± 2.8	393 ± 13.4

TABLE C 3: MASS OF METAL EXTRACTED [mg] AFTER 300 MINUTES DURING PHASE 1 EXPERIMENTS

Acid type	Temperature	H_2O_2 Addition	Ag	Al	Au	Cu	Fe	Ni	Pb	Sn	Zn
1M HNO_3	25°C	no H_2O_2	1 ± 0	412.4 ± 23.5	0 ± 0	25.3 ± 1.5	1600.8 ± 89.6	122.3 ± 7.5	3212.5 ± 89.9	140.9 ± 10	35.9 ± 2.3
1M HNO_3	85°C	no H_2O_2	1.9 ± 0	1113 ± 14.5	1.3 ± 0	11163.7 ± 178.6	4.2 ± 0.1	234.8 ± 3.8	2966.6 ± 23.7	14.8 ± 0.3	1528.3 ± 13.8
1M H_2SO_4	25°C	no H_2O_2	0.1 ± 0	353 ± 8.8	0 ± 0	6.1 ± 0.1	111.3 ± 2.9	3.5 ± 0.1	165.7 ± 2.8	30 ± 0.6	31.1 ± 0.5
1M H_2SO_4	85°C	no H_2O_2	2 ± 0.4	1598.2 ± 226.9	0 ± 0	2.6 ± 0.4	1003.8 ± 135.5	28.9 ± 4	206.6 ± 27.5	122.2 ± 17.5	86.4 ± 12.4
1M HNO_3	55°C	no H_2O_2	0.2 ± 0	825.3 ± 23.1	0.2 ± 0	10098 ± 302.9	7.7 ± 0.2	168.8 ± 4.4	3010.1 ± 117.4	3.3 ± 0.1	1561.6 ± 43.7
1M H_2SO_4	55°C	no H_2O_2	0.5 ± 0.1	990.8 ± 46.6	0 ± 0	4 ± 0.2	283.1 ± 7.6	8.8 ± 0.5	5.1 ± 0.1	213.5 ± 7.9	36.4 ± 1.6
1M H_2SO_4	85°C	90mL H_2O_2	0 ± 0	1855.3 ± 13	0 ± 0	4.6 ± 0.1	1675 ± 20.1	163.7 ± 1.6	12.7 ± 0.1	126 ± 1.6	232.5 ± 2.6
1M HNO_3	25°C	90mL H_2O_2	0.3 ± 0	415.6 ± 14.1	0 ± 0	5081.8 ± 172.8	1520.8 ± 77.6	170.6 ± 6.1	3583.3 ± 175.6	107 ± 3.3	584.2 ± 19.9
1M H_2SO_4	25°C	90mL H_2O_2	0.2 ± 0	514 ± 16.4	0 ± 0	6434.4 ± 225.2	1564.2 ± 53.2	163.2 ± 5.5	7 ± 0.2	151.4 ± 6.1	858.2 ± 25.7
1M HNO_3	85°C	90mL H_2O_2	0.3 ± 0	1184.3 ± 72.2	1.1 ± 0.1	11522 ± 622.2	1.5 ± 0.1	240.3 ± 13.9	3083.8 ± 37	5.8 ± 0.4	1615.1 ± 79.1
1M HNO_3	55°C	90mL H_2O_2	0.8 ± 0	1006.7 ± 38.3	0.5 ± 0	12087.3 ± 471.4	4.2 ± 0.1	247.2 ± 9.1	3471.1 ± 114.5	2.9 ± 0.1	1716.8 ± 56.7
1M H_2SO_4	55°C	90mL H_2O_2	0.1 ± 0	1414.9 ± 43.9	0 ± 0	1188.8 ± 28.5	1624.8 ± 53.6	190.2 ± 5.9	13.8 ± 0.5	91.4 ± 3	365.4 ± 12.4

C1.2. PERCENTAGE EXTRACTED

TABLE C 4: PERCENTAGE OF METAL EXTRACTED AFTER 60 MINUTES DURING PHASE 1 EXPERIMENTS

Acid type	Temperature	H_2O_2 Addition	Ag	Al	Au	Cu	Fe	Ni	Pb	Sn	Zn
1M HNO_3	25°C	no H_2O_2	3.3 ± 0.1	4.6 ± 0.3	0 ± 0	0.2 ± 0	64.9 ± 3.6	11 ± 0.7	48 ± 1.3	11.8 ± 0.8	1.8 ± 0.1
1M HNO_3	85°C	no H_2O_2	2.8 ± 0	55.2 ± 0.7	6.2 ± 0	77.2 ± 1.2	4.1 ± 0.1	72.1 ± 1.2	91.2 ± 0.7	1.8 ± 0	72.8 ± 0.7
1M H_2SO_4	25°C	no H_2O_2	0.2 ± 0	4.2 ± 0.1	0 ± 0	0 ± 0	3.2 ± 0.1	0.8 ± 0	5.3 ± 0.1	5.7 ± 0.1	1.3 ± 0
1M H_2SO_4	85°C	no H_2O_2	5.7 ± 1.2	36.8 ± 5.2	0 ± 0	0 ± 0	22 ± 3	5.4 ± 0.7	5.4 ± 0.7	3.9 ± 0.6	3.5 ± 0.5
1M HNO_3	55°C	no H_2O_2	0.3 ± 0	30.9 ± 0.9	0.8 ± 0	60.9 ± 1.8	72.3 ± 1.8	54.8 ± 1.4	94.9 ± 3.7	17.6 ± 0.5	58.1 ± 1.6
1M H_2SO_4	55°C	no H_2O_2	1 ± 0.1	20.3 ± 1	0.1 ± 0	0 ± 0	4.5 ± 0.1	1.1 ± 0.1	0.2 ± 0	2.6 ± 0.1	1 ± 0
1M H_2SO_4	85°C	90mL H_2O_2	1.9 ± 0.2	53.7 ± 0.4	0 ± 0	1.5 ± 0	86.3 ± 1	54 ± 0.5	0.5 ± 0	2.3 ± 0	15.1 ± 0.2
1M HNO_3	25°C	90mL H_2O_2	1.7 ± 0.1	10.2 ± 0.3	0 ± 0	32.8 ± 1.1	67 ± 3.4	37.5 ± 1.4	72 ± 3.5	22.9 ± 0.7	27.3 ± 0.9
1M H_2SO_4	25°C	90mL H_2O_2	0 ± 0	14.7 ± 0.5	0 ± 0	51.5 ± 1.8	83.5 ± 2.8	57.2 ± 1.9	0 ± 0	2.8 ± 0.1	55 ± 1.6
1M HNO_3	85°C	90mL H_2O_2	0.4 ± 0	36.7 ± 2.2	3.6 ± 0.2	73.6 ± 4	39.8 ± 2.2	52.3 ± 3	95.6 ± 1.1	1.8 ± 0.1	70.3 ± 3.4
1M HNO_3	55°C	90mL H_2O_2	1 ± 0.1	25.1 ± 1	2.2 ± 0	50.2 ± 2	57.9 ± 1.8	54.5 ± 2	74.6 ± 2.5	3.3 ± 0.1	47.6 ± 1.6
1M H_2SO_4	55°C	90mL H_2O_2	0.2 ± 0	39.1 ± 1.2	0 ± 0	16.5 ± 0.4	78.2 ± 2.6	49.3 ± 1.5	0.5 ± 0	3.8 ± 0.1	22.4 ± 0.8

TABLE C 5: PERCENTAGE OF METAL EXTRACTED AFTER 180 MINUTES DURING PHASE 1 EXPERIMENTS

Acid type	Temperature	H_2O_2 Addition	Ag	Al	Au	Cu	Fe	Ni	Pb	Sn	Zn
1M HNO_3	25°C	no H_2O_2	2 ± 0.1	15.2 ± 0.9	0 ± 0	0.3 ± 0	76 ± 4.3	29 ± 1.8	71 ± 2	19.3 ± 1.4	2.1 ± 0.1
1M HNO_3	85°C	no H_2O_2	3.4 ± 0	52.7 ± 0.7	13.2 ± 0.1	76.4 ± 1.2	0.2 ± 0	64.3 ± 1	78.6 ± 0.6	3.1 ± 0.1	80.5 ± 0.7
1M H_2SO_4	25°C	no H_2O_2	1.5 ± 0.1	10.3 ± 0.3	0 ± 0	0 ± 0	4.2 ± 0.1	1 ± 0	5.1 ± 0.1	1.2 ± 0	1.5 ± 0
1M H_2SO_4	85°C	no H_2O_2	5.2 ± 1.1	54.8 ± 7.8	0 ± 0	0 ± 0	38 ± 5.1	7 ± 1	5.4 ± 0.7	3 ± 0.4	4.6 ± 0.7
1M HNO_3	55°C	no H_2O_2	0.2 ± 0	40.7 ± 1.1	2.7 ± 0.1	74.4 ± 2.2	1.7 ± 0	60.6 ± 1.6	92.6 ± 3.6	0.5 ± 0	81 ± 2.3
1M H_2SO_4	55°C	no H_2O_2	0.3 ± 0	33.1 ± 1.6	0 ± 0	0 ± 0	9.7 ± 0.3	1.8 ± 0.1	0.1 ± 0	5.8 ± 0.2	1.5 ± 0.1
1M H_2SO_4	85°C	90mL H_2O_2	0.1 ± 0	67 ± 0.5	0 ± 0	0 ± 0	83.5 ± 1	55.4 ± 0.6	0.4 ± 0	5.5 ± 0.1	12.4 ± 0.1
1M HNO_3	25°C	90mL H_2O_2	0 ± 0	16.5 ± 0.6	0 ± 0	33.9 ± 1.2	75.8 ± 3.9	45.5 ± 1.6	87 ± 4.3	13.7 ± 0.4	29.7 ± 1
1M H_2SO_4	25°C	90mL H_2O_2	0 ± 0	21.7 ± 0.7	0 ± 0	49.2 ± 1.7	85.8 ± 2.9	61.2 ± 2.1	0.1 ± 0	14.1 ± 0.6	55.9 ± 1.7
1M HNO_3	85°C	90mL H_2O_2	0.2 ± 0	39.8 ± 2.4	8.6 ± 0.5	72.1 ± 3.9	0.1 ± 0	46.4 ± 2.7	76.1 ± 0.9	0 ± 0	75.9 ± 3.7
1M HNO_3	55°C	90mL H_2O_2	1.4 ± 0.1	36.6 ± 1.4	4.9 ± 0.1	70.9 ± 2.8	13.5 ± 0.4	68.1 ± 2.5	88.3 ± 2.9	0.3 ± 0	75.2 ± 2.5
1M H_2SO_4	55°C	90mL H_2O_2	1 ± 0.1	54.2 ± 1.7	0 ± 0	11.9 ± 0.3	86.4 ± 2.9	61 ± 1.9	0.4 ± 0	5.2 ± 0.2	24.2 ± 0.8

TABLE C 6: PERCENTAGE OF METAL EXTRACTED AFTER 300 MINUTES DURING PHASE 1 EXPERIMENTS

Acid type	Temperature	H_2O_2 Addition	Ag	Al	Au	Cu	Fe	Ni	Pb	Sn	Zn
1M HNO_3	25°C	no H_2O_2	2 ± 0.1	15.2 ± 0.9	0 ± 0	0.3 ± 0	76 ± 4.3	29 ± 1.8	71 ± 2	19.3 ± 1.4	2.1 ± 0.1
1M HNO_3	85°C	no H_2O_2	3.4 ± 0	52.7 ± 0.7	13.2 ± 0.1	76.4 ± 1.2	0.2 ± 0	64.3 ± 1	78.6 ± 0.6	3.1 ± 0.1	80.5 ± 0.7
1M H_2SO_4	25°C	no H_2O_2	1.5 ± 0.1	10.3 ± 0.3	0 ± 0	0 ± 0	4.2 ± 0.1	1 ± 0	5.1 ± 0.1	1.2 ± 0	1.5 ± 0
1M H_2SO_4	85°C	no H_2O_2	5.2 ± 1.1	54.8 ± 7.8	0 ± 0	0 ± 0	38 ± 5.1	7 ± 1	5.4 ± 0.7	3 ± 0.4	4.6 ± 0.7
1M HNO_3	55°C	no H_2O_2	0.2 ± 0	40.7 ± 1.1	2.7 ± 0.1	74.4 ± 2.2	1.7 ± 0	60.6 ± 1.6	92.6 ± 3.6	0.5 ± 0	81 ± 2.3
1M H_2SO_4	55°C	no H_2O_2	0.3 ± 0	33.1 ± 1.6	0 ± 0	0 ± 0	9.7 ± 0.3	1.8 ± 0.1	0.1 ± 0	5.8 ± 0.2	1.5 ± 0.1
1M H_2SO_4	85°C	90mL H_2O_2	0.1 ± 0	67 ± 0.5	0 ± 0	0 ± 0	83.5 ± 1	55.4 ± 0.6	0.4 ± 0	5.5 ± 0.1	12.4 ± 0.1
1M HNO_3	25°C	90mL H_2O_2	0 ± 0	16.5 ± 0.6	0 ± 0	33.9 ± 1.2	75.8 ± 3.9	45.5 ± 1.6	87 ± 4.3	13.7 ± 0.4	29.7 ± 1
1M H_2SO_4	25°C	90mL H_2O_2	0 ± 0	21.7 ± 0.7	0 ± 0	49.2 ± 1.7	85.8 ± 2.9	61.2 ± 2.1	0.1 ± 0	14.1 ± 0.6	55.9 ± 1.7
1M HNO_3	85°C	90mL H_2O_2	0.2 ± 0	39.8 ± 2.4	8.6 ± 0.5	72.1 ± 3.9	0.1 ± 0	46.4 ± 2.7	76.1 ± 0.9	0 ± 0	75.9 ± 3.7
1M HNO_3	55°C	90mL H_2O_2	1.4 ± 0.1	36.6 ± 1.4	4.9 ± 0.1	70.9 ± 2.8	13.5 ± 0.4	68.1 ± 2.5	88.3 ± 2.9	0.3 ± 0	75.2 ± 2.5
1M H_2SO_4	55°C	90mL H_2O_2	1 ± 0.1	54.2 ± 1.7	0 ± 0	11.9 ± 0.3	86.4 ± 2.9	61 ± 1.9	0.4 ± 0	5.2 ± 0.2	24.2 ± 0.8

TABLE C 7: CONFIDENCE INTERVAL CALCULATED WITH α=0.05 FOR REPEAT MEASUREMENTS AND EXPRESSED AS A PERCENTAGE OF THE MEASURED VALUE

Acid type	Temperature	H_2O_2 Addition	Ag	Al	Au	Cu	Fe	Ni	Pb	Sn	Zn
1M HNO_3	25°C	no H_2O_2	3.7	5.7	6.5	5.8	5.6	6.1	2.8	7.1	6.5
1M HNO_3	85°C	no H_2O_2	1.4	1.3	0.6	1.6	2.3	1.6	0.8	1.8	0.9
1M H_2SO_4	25°C	no H_2O_2	7.1	2.5	0.7	2.4	2.6	2.9	1.7	1.9	1.7
1M H_2SO_4	85°C	no H_2O_2	21.9	14.2	14.3	14.2	13.5	13.7	13.3	14.3	14.3
1M HNO_3	55°C	no H_2O_2	1.8	2.8	3.3	3	2.5	2.6	3.9	2.9	2.8
1M H_2SO_4	55°C	no H_2O_2	12	4.7	5.7	5.5	2.7	5.3	2.3	3.7	4.5
1M H_2SO_4	85°C	90mL H_2O_2	8.1	0.7	3.2	1.1	1.2	1	1.1	1.3	1.1
1M HNO_3	25°C	90mL H_2O_2	3.2	3.4	2.3	3.4	5.1	3.6	4.9	3.1	3.4
1M H_2SO_4	25°C	90mL H_2O_2	3.9	3.2	3.9	3.5	3.4	3.4	2.8	4	3
1M HNO_3	85°C	90mL H_2O_2	5.1	6.1	5.9	5.4	5.4	5.8	1.2	6.7	4.9
1M HNO_3	55°C	90mL H_2O_2	4.8	3.8	1.6	3.9	3.1	3.7	3.3	3.2	3.3
1M H_2SO_4	55°C	90mL H_2O_2	7	3.1	3.5	2.4	3.3	3.1	3.4	3.3	3.4

C2. ADDITIONAL TEMPERATURE VARIATION FOR 1 M HNO_3

C2.1. MASS EXTRACTED

TABLE C 8: MASS OF METAL EXTRACTED [mg] AFTER 60 MINUTES DURING ADDITIONAL TEMPERATURE VARIATION EXPERIMENTS FOR 1 M HNO_3

Temperature	Ag	Al	Au	Cu	Fe	Ni	Pb	Sn	Zn
HNO_3 T=55°C	0.2 ± 0	599.4 ± 4.7	0.1 ± 0	4951.3 ± 39.5	1227.7 ± 10.4	151.7 ± 2.5	1356.3 ± 5.4	110.2 ± 0.5	405.4 ± 2.2
HNO_3 T=65°C	0.3 ± 0	633.6 ± 4.8	0.2 ± 0	7963.9 ± 60.8	1209.7 ± 17.8	235.7 ± 3	1402.6 ± 5.7	6 ± 0	805.2 ± 4
HNO_3 T=75°C	0.4 ± 0	930.4 ± 5.2	0.4 ± 0	8074.6 ± 55.3	421.9 ± 2.9	222.3 ± 0.7	1648.4 ± 36	1.6 ± 0	886.7 ± 6
HNO_3 T=85°C	0.1 ± 0	824.4 ± 5.6	0.3 ± 0	7945.4 ± 47.6	525 ± 1.2	195.1 ± 0.7	1619.1 ± 14.9	1 ± 0	916.4 ± 6

TABLE C 9: MASS OF METAL EXTRACTED [mg] AFTER 180 MINUTES DURING ADDITIONAL TEMPERATURE VARIATION EXPERIMENTS FOR 1 M HNO_3

Temperature	Ag	Al	Au	Cu	Fe	Ni	Pb	Sn	Zn
HNO_3 T=55°C	0.2 ± 0	844.4 ± 6.6	0.3 ± 0	9299.4 ± 74.2	465.5 ± 3.9	185.4 ± 3	1580.1 ± 6.3	1.8 ± 0	1061.5 ± 5.7
HNO_3 T=65°C	0.6 ± 0	812.8 ± 6.2	0.6 ± 0	9204.6 ± 70.3	3.9 ± 0.1	238 ± 3	1274.8 ± 5.2	0.6 ± 0	1061.8 ± 5.3
HNO_3 T=75°C	0.5 ± 0	1037.3 ± 5.7	0.5 ± 0	9662.7 ± 66.2	2.5 ± 0	238.7 ± 0.8	1615.7 ± 35.3	1 ± 0	1190.8 ± 8.1
HNO_3 T=85°C	0.5 ± 0	911.7 ± 6.2	0.1 ± 0	8640 ± 51.8	3.9 ± 0	202.1 ± 0.7	1488.7 ± 13.7	0.5 ± 0	1097.5 ± 7.2

TABLE C 10: MASS OF METAL EXTRACTED [mg] AFTER 300 MINUTES DURING ADDITIONAL TEMPERATURE VARIATION EXPERIMENTS FOR 1 M HNO_3

Temperature	Ag	Al	Au	Cu	Fe	Ni	Pb	Sn	Zn
HNO_3 T=55°C	0.5 ± 0	893.9 ± 7	0.2 ± 0	9076.6 ± 72.4	4.7 ± 0	173.6 ± 2.8	1355 ± 5.4	0.7 ± 0	1110.3 ± 6
HNO_3 T=65°C	0.6 ± 0	890 ± 6.8	0.6 ± 0	9524.9 ± 72.8	3.3 ± 0	245.1 ± 3.1	1237.4 ± 5.1	0.5 ± 0	1104.5 ± 5.5
HNO_3 T=75°C	0.5 ± 0	1026.6 ± 5.7	0.4 ± 0	9810.5 ± 67.2	2.9 ± 0	234.3 ± 0.7	1575.8 ± 34.5	1.8 ± 0	1236.1 ± 8.4
HNO_3 T=85°C	0.5 ± 0	936.7 ± 6.4	0 ± 0	8616.6 ± 51.6	15.4 ± 0	201.6 ± 0.7	1483.5 ± 13.7	0.4 ± 0	1127.7 ± 7.4

C2.2. PERCENTAGE EXTRACTED

TABLE C 11: PERCENTAGE OF METAL EXTRACTED AFTER 60 MINUTES DURING ADDITIONAL TEMPERATURE VARIATION EXPERIMENTS FOR 1 M HNO_3

Temperature	Ag	Al	Au	Cu	Fe	Ni	Pb	Sn	Zn
HNO_3 T=55°C	0.5 ± 0	27.8 ± 0.2	0.6 ± 0	36.4 ± 0.3	67.6 ± 0.6	48.7 ± 0.8	75 ± 0.3	6.5 ± 0	23.3 ± 0.1
HNO_3 T=65°C	0.9 ± 0	30.2 ± 0.2	2 ± 0	62.7 ± 0.5	64.1 ± 0.9	66.8 ± 0.8	85.4 ± 0.3	0.4 ± 0	56.6 ± 0.3
HNO_3 T=75°C	1.2 ± 0.1	43.8 ± 0.2	3.4 ± 0	58.5 ± 0.4	19.7 ± 0.1	65.9 ± 0.2	86.5 ± 1.9	0.1 ± 0	49.8 ± 0.3
HNO_3 T=85°C	0.4 ± 0	37.6 ± 0.3	2.1 ± 0	57.2 ± 0.3	26.4 ± 0.1	55.2 ± 0.2	87 ± 0.8	0.1 ± 0	51.6 ± 0.3

TABLE C 12: PERCENTAGE OF METAL EXTRACTED AFTER 180 MINUTES DURING ADDITIONAL TEMPERATURE VARIATION EXPERIMENTS FOR 1 M HNO_3

Temperature	Ag	Al	Au	Cu	Fe	Ni	Pb	Sn	Zn
HNO_3 T=55°C	0.8 ± 0	39.1 ± 0.3	2.4 ± 0	68.3 ± 0.5	25.7 ± 0.2	59.5 ± 1	87.3 ± 0.3	0.1 ± 0	61 ± 0.3
HNO_3 T=65°C	1.6 ± 0	38.7 ± 0.3	4.9 ± 0	72.4 ± 0.6	0.2 ± 0	67.5 ± 0.9	77.7 ± 0.3	0 ± 0	74.6 ± 0.4
HNO_3 T=75°C	1.6 ± 0.1	48.8 ± 0.3	4.2 ± 0	70 ± 0.5	0.1 ± 0	70.7 ± 0.2	84.8 ± 1.9	0.1 ± 0	66.9 ± 0.5
HNO_3 T=85°C	1.3 ± 0.1	41.6 ± 0.3	0.7 ± 0	62.2 ± 0.4	0.2 ± 0	57.2 ± 0.2	80 ± 0.7	0 ± 0	61.8 ± 0.4

TABLE C 13: PERCENTAGE OF METAL EXTRACTED AFTER 300 MINUTES DURING ADDITIONAL TEMPERATURE VARIATION EXPERIMENTS FOR 1 M HNO_3

Temperature	Ag	Al	Au	Cu	Fe	Ni	Pb	Sn	Zn
HNO_3 T=55°C	0.8 ± 0	39.1 ± 0.3	2.4 ± 0	68.3 ± 0.5	25.7 ± 0.2	59.5 ± 1	87.3 ± 0.3	0.1 ± 0	61 ± 0.3
HNO_3 T=65°C	1.6 ± 0	38.7 ± 0.3	4.9 ± 0	72.4 ± 0.6	0.2 ± 0	67.5 ± 0.9	77.7 ± 0.3	0 ± 0	74.6 ± 0.4
HNO_3 T=75°C	1.6 ± 0.1	48.8 ± 0.3	4.2 ± 0	70 ± 0.5	0.1 ± 0	70.7 ± 0.2	84.8 ± 1.9	0.1 ± 0	66.9 ± 0.5
HNO_3 T=85°C	1.3 ± 0.1	41.6 ± 0.3	0.7 ± 0	62.2 ± 0.4	0.2 ± 0	57.2 ± 0.2	80 ± 0.7	0 ± 0	61.8 ± 0.4

TABLE C 14: CONFIDENCE INTERVAL CALCULATED WITH α=0.05 FOR REPEAT MEASUREMENTS AND EXPRESSED AS A PERCENTAGE OF THE MEASURED VALUE

Temperature	Ag	Al	Au	Co	Cu	Fe	Ni	Pb	Pd	Pt	Sn	Zn
HNO_3 T=55°C	2.8	0.8	0.6	2.2	0.8	0.8	1.6	0.4	78.4	66.7	0.5	0.5
HNO_3 T=65°C	0.7	0.8	0.5	0.9	0.8	1.5	1.3	0.4	38.9	102.9	0.7	0.5
HNO_3 T=75°C	6.8	0.6	0.2	2.9	0.7	0.7	0.3	2.2	14.7	120.9	0.7	0.7
HNO_3 T=85°C	6.4	0.7	2.3	0.3	0.6	0.2	0.3	0.9	84.3	83.1	1.2	0.7

C3. PEROXIDE ADDITION FOR 1 M H_2SO_4

C3.1. MASS EXTRACTED

TABLE C 15: MASS OF METAL EXTRACTED [mg] AFTER 60 MINUTES DURING PEROXIDE ADDITION EXPERIMENTS FOR 1 M H_2SO_4 AT 25°C

Method of H_2O_2 addition	Ag	Al	Au	Cu	Fe	Ni	Pb	Sn	Zn
H_2O_2 fed 30min	0 ± 0	404.9 ± 5	0 ± 0	9034.3 ± 47.9	1438.8 ± 5.9	187 ± 1.2	0 ± 0	14.3 ± 0.1	1286.7 ± 3.2
H_2O_2 240mL at t = 0	1.6 ± 0.1	411.4 ± 0.9	0 ± 0	8011.2 ± 8.8	1466.1 ± 5.1	126.4 ± 0.5	5 ± 0	8.7 ± 0.1	1152.3 ± 0.9
H_2O_2 fed 0.4 mL/min	0.4 ± 0	276.6 ± 3.2	0 ± 0	1959.8 ± 11	1237.5 ± 9.7	74.9 ± 1.1	8.1 ± 0.2	147.2 ± 3.1	199.5 ± 1.1
H_2O_2 fed 0.8 mL/min	1.7 ± 0.1	231.7 ± 3.2	0 ± 0	2889.7 ± 8.4	1148.8 ± 7.1	98.4 ± 0.6	4.2 ± 0.1	33.3 ± 1	350.3 ± 1
H_2O_2 fed 1.2 mL/min	0.6 ± 0	258.3 ± 2.4	0 ± 0	5044.9 ± 4.5	1535.9 ± 12.4	164.1 ± 0.3	7.1 ± 0	26.5 ± 0.1	719.6 ± 2.8
H_2O_2 fed 1.2 mL/min	0.9 ± 0	241.3 ± 6.4	0 ± 0	4994.5 ± 12.5	1364.1 ± 9.3	153.1 ± 2.7	3.9 ± 0.1	20.2 ± 0.6	695 ± 2.1

TABLE C 16: MASS OF METAL EXTRACTED [mg] AFTER 180 MINUTES DURING PEROXIDE ADDITION EXPERIMENTS FOR 1 M H_2SO_4 AT 25°C

Method of H_2O_2 addition	Ag	Al	Au	Cu	Fe	Ni	Pb	Sn	Zn
H_2O_2 fed 30min	0.7 ± 0.1	477.6 ± 5.9	0 ± 0	9006.2 ± 47.7	1423.8 ± 5.8	197.8 ± 1.3	0 ± 0	9.7 ± 0.1	1298 ± 3.2
H_2O_2 240mL at t = 0	0.4 ± 0	483.3 ± 1.1	0 ± 0	7616.2 ± 8.4	1464.5 ± 5.1	139.7 ± 0.6	3.4 ± 0	65.9 ± 0.4	1147.2 ± 0.9
H_2O_2 fed 0.4 mL/min	0.5 ± 0	450.4 ± 5.3	0 ± 0	5872.4 ± 32.9	1469.7 ± 11.5	140.6 ± 2.1	6.7 ± 0.1	87.1 ± 1.8	885.8 ± 5
H_2O_2 fed 0.8 mL/min	0.6 ± 0	439.3 ± 6.1	0 ± 0	8652.4 ± 25.1	1464 ± 9.1	158.3 ± 0.9	2.3 ± 0.1	8.4 ± 0.3	1281.7 ± 3.6
H_2O_2 fed 1.2 mL/min	1 ± 0	447.3 ± 4.2	0 ± 0	11833.7 ± 10.7	1806.7 ± 14.6	227.3 ± 0.4	0.1 ± 0	7 ± 0	2045.5 ± 8
H_2O_2 fed 1.2 mL/min	1.1 ± 0.1	428.7 ± 11.4	0 ± 0	10739.7 ± 26.8	1631.8 ± 11.1	206.3 ± 3.7	0.4 ± 0	8.4 ± 0.3	1825.5 ± 5.5

TABLE C 17: MASS OF METAL EXTRACTED [mg] AFTER 300 MINUTES DURING PEROXIDE ADDITION EXPERIMENTS FOR 1 M H_2SO_4 AT 25°C

Method of H_2O_2 addition	Ag	Al	Au	Cu	Fe	Ni	Pb	Sn	Zn
H_2O_2 fed 30min	1.2 ± 0.1	540.9 ± 6.7	0 ± 0	9173.3 ± 48.6	1464.7 ± 6	210.2 ± 1.3	0.3 ± 0	14.7 ± 0.1	1329.2 ± 3.3
H_2O_2 240mL at t = 0	0.7 ± 0.1	546.5 ± 1.2	0 ± 0	7532.4 ± 8.3	1499 ± 5.2	146.5 ± 0.6	5.5 ± 0	50.9 ± 0.3	1148.8 ± 0.9
H_2O_2 fed 0.4 mL/min	0.5 ± 0	562.2 ± 6.6	0 ± 0	8702.5 ± 48.7	1528.1 ± 11.9	167.4 ± 2.5	3.9 ± 0.1	32.9 ± 0.7	1353.4 ± 7.7
H_2O_2 fed 0.8 mL/min	0.8 ± 0	533.2 ± 7.4	0 ± 0	11313.8 ± 32.8	1527.9 ± 9.5	172.8 ± 1	0 ± 0	29.2 ± 0.9	1629.5 ± 4.6
H_2O_2 fed 1.2 mL/min	1.1 ± 0	557.7 ± 5.2	0.2 ± 0	14106.1 ± 12.7	1881.5 ± 15.2	239.6 ± 0.5	0 ± 0	19.5 ± 0.1	2348.8 ± 9.2
H_2O_2 fed 1.2 mL/min	1.7 ± 0.1	533.6 ± 14.2	0 ± 0	12874.5 ± 32.2	1688.9 ± 11.5	223.2 ± 4	0 ± 0	17 ± 0.5	1993.1 ± 6

C3.2. PERCENTAGE EXTRACTED

TABLE C 18: PERCENTAGE OF METAL EXTRACTED AFTER 60 MINUTES DURING PEROXIDE ADDITION EXPERIMENTS FOR 1 M H_2SO_4 AT 25°C

Method of H_2O_2 addition	Ag	Al	Au	Cu	Fe	Ni	Pb	Sn	Zn
H_2O_2 fed 30min	0 ± 0	18.4 ± 0.2	0 ± 0	63.1 ± 0.3	79 ± 0.3	51.7 ± 0.3	0 ± 0	1.3 ± 0	74 ± 0.1
H_2O_2 240mL at t = 0	3.3 ± 0.3	16.3 ± 0	0 ± 0	54.4 ± 0.1	79.9 ± 0.3	40.5 ± 0.2	0.3 ± 0	0.8 ± 0	62.8 ± 0.1
H_2O_2 fed 0.4 mL/min	1.3 ± 0	12.7 ± 0.2	0.1 ± 0	15 ± 0.1	50.2 ± 0.4	15.2 ± 0.2	0.6 ± 0	13.4 ± 0.3	10.9 ± 0.1
H_2O_2 fed 0.8 mL/min	6 ± 0.3	8.6 ± 0.1	0.1 ± 0	20.2 ± 0.1	53.4 ± 0.3	32.1 ± 0.2	0.2 ± 0	1.7 ± 0.1	14.7 ± 0
H_2O_2 fed 1.2 mL/min	2.3 ± 0.1	10 ± 0.1	0 ± 0	31.7 ± 0	68.4 ± 0.5	42.5 ± 0.1	0.4 ± 0	1.2 ± 0	27.2 ± 0.1
H_2O_2 fed 1.2 mL/min	3.7 ± 0.2	9.6 ± 0.3	0 ± 0	33.8 ± 0.1	65.5 ± 0.5	39.8 ± 0.7	0.2 ± 0	0.9 ± 0	29.7 ± 0.1

TABLE C 19: PERCENTAGE OF METAL EXTRACTED AFTER 180 MINUTES DURING PEROXIDE ADDITION EXPERIMENTS FOR 1 M H_2SO_4 AT 25°C

Method of H_2O_2 addition	Ag	Al	Au	Cu	Fe	Ni	Pb	Sn	Zn
H_2O_2 fed 30min	1.8 ± 0.2	21.7 ± 0.3	0.3 ± 0	62.9 ± 0.3	78.2 ± 0.3	54.7 ± 0.3	0 ± 0	0.9 ± 0	74.6 ± 0.1
H_2O_2 240mL at t = 0	0.9 ± 0.1	19.1 ± 0	0 ± 0	51.7 ± 0.1	79.8 ± 0.3	44.8 ± 0.2	0.2 ± 0	5.8 ± 0	62.5 ± 0.1
H_2O_2 fed 0.4 mL/min	1.6 ± 0	20.7 ± 0.2	0 ± 0	45.1 ± 0.3	59.6 ± 0.5	28.5 ± 0.4	0.5 ± 0	7.9 ± 0.2	48.4 ± 0.3
H_2O_2 fed 0.8 mL/min	2 ± 0.1	16.3 ± 0.2	0 ± 0	60.5 ± 0.2	68.1 ± 0.4	51.6 ± 0.3	0.1 ± 0	0.4 ± 0	53.7 ± 0.2
H_2O_2 fed 1.2 mL/min	3.5 ± 0.1	17.4 ± 0.2	0 ± 0	74.5 ± 0.1	80.5 ± 0.6	58.9 ± 0.1	0 ± 0	0.3 ± 0	77.2 ± 0.3
H_2O_2 fed 1.2 mL/min	4.6 ± 0.2	17.1 ± 0.5	0 ± 0	72.6 ± 0.1	78.4 ± 0.5	53.6 ± 1	0 ± 0	0.4 ± 0	78 ± 0.2

TABLE C 20: PERCENTAGE OF METAL EXTRACTED AFTER 300 MINUTES DURING PEROXIDE ADDITION EXPERIMENTS FOR 1 M H_2SO_4 AT 25°C

Method of H_2O_2 addition	Ag	Al	Au	Cu	Fe	Ni	Pb	Sn	Zn
H_2O_2 fed 30min	3.2 ± 0.4	24.6 ± 0.3	0.3 ± 0	64.1 ± 0.3	80.4 ± 0.3	58.2 ± 0.3	0 ± 0	1.3 ± 0	76.4 ± 0.2
H_2O_2 240mL at t = 0	1.5 ± 0.1	21.6 ± 0	0 ± 0	51.1 ± 0.1	81.7 ± 0.3	47 ± 0.2	0.3 ± 0	4.5 ± 0	62.6 ± 0.1
H_2O_2 fed 0.4 mL/min	1.5 ± 0	25.8 ± 0.3	0.1 ± 0	66.8 ± 0.4	62 ± 0.5	33.9 ± 0.5	0.3 ± 0	3 ± 0.1	73.9 ± 0.4
H_2O_2 fed 0.8 mL/min	2.7 ± 0.1	19.8 ± 0.3	0 ± 0	79.2 ± 0.2	71 ± 0.4	56.4 ± 0.3	0 ± 0	1.5 ± 0	68.2 ± 0.2
H_2O_2 fed 1.2 mL/min	4.2 ± 0.1	21.6 ± 0.2	1.5 ± 0	88.7 ± 0.1	83.8 ± 0.7	62.1 ± 0.1	0 ± 0	0.9 ± 0	88.7 ± 0.4
H_2O_2 fed 1.2 mL/min	7 ± 0.3	21.3 ± 0.6	0 ± 0	87.1 ± 0.2	81.1 ± 0.6	58 ± 1	0 ± 0	0.8 ± 0	85.1 ± 0.3

TABLE C 21: CONFIDENCE INTERVAL CALCULATED WITH α=0.05 FOR REPEAT MEASUREMENTS AND EXPRESSED AS A PERCENTAGE OF THE MEASURED VALUE

Method of H_2O_2 addition	Ag	Al	Au	Cu	Fe	Ni	Pb	Sn	Zn
H_2O_2 fed 30min	12.2	1.2	1.1	0.5	0.4	0.6	0.7	0.8	0.2
H_2O_2 240mL at t = 0	7.8	0.2	2.3	0.1	0.4	0.4	0.4	0.6	0.1
H_2O_2 fed 0.4 mL/min	3.1	1.2	2.6	0.6	0.8	1.5	1.9	2.1	0.6
H_2O_2 fed 0.8 mL/min	4.7	1.4	5.5	0.3	0.6	0.6	2.3	3	0.3
H_2O_2 fed 1.2 mL/min	2.3	0.9	1.6	0.1	0.8	0.2	0.4	0.6	0.4
H_2O_2 fed 1.2 mL/min	4.7	2.7	3.8	0.2	0.7	1.8	2.8	3.2	0.3

C4. PHASE 2: OPTIMISATION

C4.1. MASS EXTRACTED

TABLE C 22: MASS OF METAL EXTRACTED [mg] AFTER 60 MINUTES DURING PHASE 2 EXPERIMENTS WITH H_2SO_4 AT 25°C WITH 30 WT% H_2O_2 FED AT 1.2 ML/MIN

Acid Conc.	Feed	S/L	Ag	Al	Au	Cu	Fe	Ni	Pb	Sn	Zn
1 M	No Sep.	S/L = 1/10	0 ± 0	145.5 ± 2.6	0.1 ± 0	4430.8 ± 66.5	1224.4 ± 6.1	122.1 ± 2	2.2 ± 0	37.5 ± 0.4	538.8 ± 5.4
2.5 M	No Sep.	S/L = 1/10	0 ± 0	198.9 ± 2.6	0.1 ± 0	4646 ± 46.5	1301.7 ± 46.9	152.1 ± 2.1	2 ± 0	825.4 ± 20.6	602.3 ± 11.4
2.5 M	DMS.	S/L = 1/10	0 ± 0	410.8 ± 2.5	0 ± 0	8683.2 ± 8.7	1681.2 ± 33.6	293.7 ± 0.9	1.7 ± 0	1422.4 ± 31.3	1069.5 ± 6.4
4 M	DMS.	S/L = 1/10	0 ± 0	437.5 ± 3.9	0.1 ± 0	9026 ± 72.2	1766 ± 28.3	303.7 ± 4.3	0 ± 0	1781.2 ± 37.4	1180.7 ± 9.4
2.5 M	DMS+MS.	S/L = 1/10	0.1 ± 0	447.5 ± 10.3	0 ± 0	9181.5 ± 202	706.7 ± 19.1	114.2 ± 4.5	4.1 ± 0.1	1405.2 ± 37.9	1049.3 ± 39.9
4 M	DMS+MS.	S/L = 1/10	0 ± 0	562.5 ± 12.9	0 ± 0	8576.3 ± 171.5	850.6 ± 29.8	108 ± 3.3	0.6 ± 0	1666.1 ± 13.3	945.5 ± 5.7
2.5 M	DMS.	S/L = 0.6/10	0 ± 0	269.6 ± 7.6	0.1 ± 0	5867.9 ± 164.3	999.3 ± 31	192.3 ± 6.2	4.3 ± 0.1	734.9 ± 25.7	752.1 ± 20.3
2.5 M	DMS+MS.	S/L = 0.6/10	0 ± 0	274 ± 0.8	0.1 ± 0	6369.9 ± 12.7	464.8 ± 13	64.4 ± 2.3	3.2 ± 0	725.9 ± 7.3	745.3 ± 1.5
1 M	DMS.	S/L = 0.6/10	0 ± 0	429.2 ± 12	0 ± 0	3116.7 ± 43.6	763.5 ± 11.5	129.8 ± 2.9	6.7 ± 0	102.5 ± 0.4	427.7 ± 2.6
1 M	DMS+MS.	S/L = 0.6/10	0 ± 0	605.3 ± 9.7	0 ± 0	3339.2 ± 46.7	353.1 ± 10.6	41.4 ± 1	6.5 ± 0.1	106 ± 1.4	387 ± 4.6

TABLE C 23: MASS OF METAL EXTRACTED [mg] AFTER 180 MINUTES DURING PHASE 2 EXPERIMENTS WITH H_2SO_4 AT 25°C WITH 30 WT% H_2O_2 FED AT 1.2 ML/MIN

Acid Conc.	Feed	S/L	Ag	Al	Au	Cu	Fe	Ni	Pb	Sn	Zn
1 M	No Sep.	S/L = 1/10	0 ± 0	296.7 ± 5.3	0.1 ± 0	9570.3 ± 143.6	1442.6 ± 7.2	176.3 ± 2.8	0 ± 0	23.2 ± 0.3	1453.1 ± 14.5
2.5 M	No Sep.	S/L = 1/10	0 ± 0	353.2 ± 4.6	0 ± 0	10015.9 ± 100.2	1451 ± 52.2	197.4 ± 2.8	0.6 ± 0	300.4 ± 7.5	1470.8 ± 27.9
2.5 M	DMS.	S/L = 1/10	0 ± 0	560.9 ± 3.4	0.1 ± 0	19255.1 ± 19.3	2122.8 ± 42.5	386.2 ± 1.2	0 ± 0	1362.4 ± 30	2792.3 ± 16.8
4 M	DMS.	S/L = 1/10	0 ± 0	582.5 ± 5.2	0.1 ± 0	20346 ± 162.8	2219.1 ± 35.5	406.6 ± 5.7	0 ± 0	1288.5 ± 27.1	3271.5 ± 26.2
2.5 M	DMS+MS.	S/L = 1/10	0.1 ± 0	609.1 ± 14	0 ± 0	20627.5 ± 453.8	753 ± 20.3	172.7 ± 6.7	5.5 ± 0.1	535.6 ± 14.5	3205 ± 121.8
4 M	DMS+MS.	S/L = 1/10	0 ± 0	675 ± 15.5	0 ± 0	19428.6 ± 388.6	868 ± 30.4	164.6 ± 5.1	3.2 ± 0.1	2565.1 ± 20.5	2834.8 ± 17
2.5 M	DMS.	S/L = 0.6/10	0.3 ± 0	350.9 ± 9.8	0.1 ± 0	11504.8 ± 322.1	1151 ± 35.7	223.2 ± 7.1	4 ± 0.1	550.6 ± 19.3	1845.3 ± 49.8
2.5 M	DMS+MS.	S/L = 0.6/10	0.4 ± 0	365.1 ± 1.1	0 ± 0	12786.2 ± 25.6	509.4 ± 14.3	96.8 ± 3.4	3.9 ± 0	570 ± 5.7	1951.1 ± 3.9
1 M	DMS.	S/L = 0.6/10	0.3 ± 0	811.1 ± 22.7	0.1 ± 0	5984.7 ± 83.8	970 ± 14.6	168.5 ± 3.7	7.9 ± 0	43.6 ± 0.2	905.6 ± 5.4
1 M	DMS+MS.	S/L = 0.6/10	0.3 ± 0	1060.2 ± 17	0 ± 0	8221 ± 115.1	427.2 ± 12.8	64.5 ± 1.6	6.3 ± 0.1	63.2 ± 0.8	990.3 ± 11.9

TABLE C 24: MASS OF METAL EXTRACTED [mg] AFTER 300 MINUTES DURING PHASE 2 EXPERIMENTS WITH H_2SO_4 AT 25°C WITH 30 WT% H_2O_2 FED AT 1.2 ML/MIN

Acid Conc.	Feed	S/L	Ag	Al	Au	Cu	Fe	Ni	Pb	Sn	Zn
1 M	No Sep.	S/L = 1/10	0 ± 0	366.6 ± 6.6	0 ± 0	11931.7 ± 179	1486.9 ± 7.4	193 ± 3.1	0 ± 0	31.5 ± 0.3	1759.1 ± 17.6
2.5 M	No Sep.	S/L = 1/10	0 ± 0	439.7 ± 5.7	0 ± 0	11789.4 ± 117.9	1454.2 ± 52.4	232 ± 3.2	0.4 ± 0	113.6 ± 2.8	1651.6 ± 31.4
2.5 M	DMS.	S/L = 1/10	0 ± 0	796.8 ± 4.8	0.1 ± 0	23627.6 ± 23.6	2203.1 ± 44.1	414.2 ± 1.2	0 ± 0	241 ± 5.3	3786.2 ± 22.7
4 M	DMS.	S/L = 1/10	0 ± 0	658.6 ± 5.9	0 ± 0	23448.8 ± 187.6	2340.7 ± 37.5	445 ± 6.2	0 ± 0	1389.1 ± 29.2	3710.8 ± 29.7
2.5 M	DMS+MS.	S/L = 1/10	0.1 ± 0	925.4 ± 21.3	0.1 ± 0	24166.8 ± 531.7	771.9 ± 20.8	194.7 ± 7.6	6.9 ± 0.2	116 ± 3.1	4049.4 ± 153.9
4 M	DMS+MS.	S/L = 1/10	0.2 ± 0	732.9 ± 16.9	0.2 ± 0	22537.8 ± 450.8	876.4 ± 30.7	176.7 ± 5.5	5.1 ± 0.1	2583.4 ± 20.7	3257.5 ± 19.5
2.5 M	DMS.	S/L = 0.6/10	0.9 ± 0	384.5 ± 10.8	0.1 ± 0	12045.8 ± 337.3	1142.1 ± 35.4	218 ± 7	3.2 ± 0.1	321.4 ± 11.2	1964.3 ± 53
2.5 M	DMS+MS.	S/L = 0.6/10	0.7 ± 0	406.2 ± 1.2	0 ± 0	13695.6 ± 27.4	509.9 ± 14.3	112.5 ± 3.9	5.7 ± 0	339.4 ± 3.4	2070 ± 4.1
1 M	DMS.	S/L = 0.6/10	0 ± 0	851.7 ± 23.8	0.1 ± 0	8288 ± 116	1037.9 ± 15.6	181.6 ± 4	7 ± 0	52.9 ± 0.2	1236.3 ± 7.4
1 M	DMS+MS.	S/L = 0.6/10	0 ± 0	1069.7 ± 17.1	0 ± 0	11092.8 ± 155.3	447.1 ± 13.4	79.8 ± 2	3.7 ± 0	33.3 ± 0.4	1579.4 ± 19

TABLE C 25: MASS OF METAL EXTRACTED [mg] AFTER 480 MINUTES DURING PHASE 2 EXPERIMENTS WITH H_2SO_4 AT 25°C WITH 30 WT% H_2O_2 FED AT 1.2 ML/MIN

Acid Conc.	Feed	S/L	Ag	Al	Au	Cu	Fe	Ni	Pb	Sn	Zn
1 M	No Sep.	S/L = 1/10	0 ± 0	437.6 ± 7.9	0.2 ± 0	12209.7 ± 183.1	1436.7 ± 7.2	190.5 ± 3	2.3 ± 0	19.3 ± 0.2	1764.8 ± 17.6
2.5 M	No Sep.	S/L = 1/10	0 ± 0	502.1 ± 6.5	0 ± 0	11814.9 ± 118.1	1400 ± 50.4	209.9 ± 2.9	0.5 ± 0	91.4 ± 2.3	1608.4 ± 30.6
2.5 M	DMS.	S/L = 1/10	0 ± 0	1541.5 ± 9.2	0.1 ± 0	23860.5 ± 23.9	2181.7 ± 43.6	409.5 ± 1.2	0 ± 0	128.2 ± 2.8	3818.8 ± 22.9
4 M	DMS.	S/L = 1/10	0 ± 0	708.1 ± 6.4	0.1 ± 0	23770 ± 190.2	2303 ± 36.8	439.7 ± 6.2	0 ± 0	1173.7 ± 24.6	3687.2 ± 29.5
2.5 M	DMS+MS.	S/L = 1/10	0.5 ± 0	1576.2 ± 36.3	0 ± 0	25230 ± 555.1	798.5 ± 21.6	199.8 ± 7.8	5 ± 0.1	119.1 ± 3.2	4137 ± 157.2
4 M	DMS+MS.	S/L = 1/10	0 ± 0	787.1 ± 18.1	0 ± 0	22488 ± 449.8	851.1 ± 29.8	173.6 ± 5.4	5.3 ± 0.1	488.7 ± 3.9	3254.7 ± 19.5
2.5 M	DMS.	S/L = 0.6/10	0.2 ± 0	422.6 ± 11.8	0 ± 0	12148.8 ± 340.2	1123.4 ± 34.8	218.9 ± 7	5 ± 0.2	264.2 ± 9.2	1833.3 ± 49.5
2.5 M	DMS+MS.	S/L = 0.6/10	0.7 ± 0	431.8 ± 1.3	0 ± 0	13473.9 ± 26.9	503.2 ± 14.1	113.9 ± 4	5.8 ± 0	294.4 ± 2.9	2036.9 ± 4.1
1 M	DMS.	S/L = 0.6/10	0.3 ± 0	860.8 ± 24.1	0.2 ± 0	10319.5 ± 144.5	1077 ± 16.2	191.6 ± 4.2	6.4 ± 0	29.3 ± 0.1	1630.9 ± 9.8
1 M	DMS+MS.	S/L = 0.6/10	0.5 ± 0	1055.3 ± 16.9	0 ± 0	12608.5 ± 176.5	447.1 ± 13.4	86.6 ± 2.2	10.5 ± 0.1	12.1 ± 0.2	1939.4 ± 23.3

C4.2. PERCENTAGE EXTRACTED

TABLE C 26: PERCENTAGE OF METAL EXTRACTED AFTER 60 MINUTES DURING PHASE 2 EXPERIMENTS WITH H_2SO_4 AT 25°C WITH 30 WT% H_2O_2 FED AT 1.2 ML/MIN

Acid Conc	Feed	S/L	Ag	Al	Au	Cu	Fe	Ni	Pb	Sn	Zn
1 M	No Sep.	S/L = 1/10	0 ± 0	7.9 ± 0.1	0.6 ± 0	34.3 ± 0.5	74 ± 0.4	46.1 ± 0.7	0.2 ± 0	2.4 ± 0	28.6 ± 0.3
2.5 M	No Sep.	S/L = 1/10	0 ± 0	10.4 ± 0.1	0.5 ± 0	37.9 ± 0.4	78.1 ± 2.8	52.3 ± 0.7	0.3 ± 0	52.6 ± 1.3	34.5 ± 0.7
2.5 M	DMS.	S/L = 1/10	0 ± 0	22.8 ± 0.1	0.8 ± 0	35.4 ± 0	68.6 ± 1.4	58.2 ± 0.2	0.1 ± 0	33 ± 0.7	27.4 ± 0.2
4 M	DMS.	S/L = 1/10	0 ± 0	22.7 ± 0.2	2.4 ± 0.1	37.4 ± 0.3	67.8 ± 1.1	59 ± 0.8	0 ± 0	47.9 ± 1	30.8 ± 0.2
2.5 M	DMS+MS.	S/L = 1/10	0.6 ± 0	23.4 ± 0.5	0.2 ± 0	35.7 ± 0.8	84.3 ± 2.3	52 ± 2	0.2 ± 0	34.5 ± 0.9	25 ± 0.9
4 M	DMS+MS.	S/L = 1/10	0 ± 0	29.3 ± 0.7	0.8 ± 0	36.8 ± 0.7	92.6 ± 3.2	54.4 ± 1.7	0 ± 0	44.7 ± 0.4	27.8 ± 0.2
2.5 M	DMS.	S/L = 0.6/10	0 ± 0	27.8 ± 0.8	2.8 ± 0.1	47 ± 1.3	77.5 ± 2.4	71.9 ± 2.3	0.3 ± 0	32.8 ± 1.1	36.8 ± 1
2.5 M	DMS+MS.	S/L = 0.6/10	0 ± 0	25.4 ± 0.1	1.9 ± 0	45.3 ± 0.1	79.6 ± 2.2	46.9 ± 1.6	0.2 ± 0	32.3 ± 0.3	34.7 ± 0.1
1 M	DMS.	S/L = 0.6/10	0.1 ± 0	46.3 ± 1.3	0.8 ± 0	24.8 ± 0.3	60.7 ± 0.9	42.4 ± 0.9	0.4 ± 0	5.2 ± 0	20.5 ± 0.1
1 M	DMS+MS.	S/L = 0.6/10	0 ± 0	46.9 ± 0.8	1.4 ± 0	25 ± 0.4	66.6 ± 2	32.9 ± 0.8	0.4 ± 0	5.2 ± 0.1	19.3 ± 0.2

TABLE C 27: PERCENTAGE OF METAL EXTRACTED AFTER 180 MINUTES DURING PHASE 2 EXPERIMENTS WITH H_2SO_4 AT 25°C WITH 30 WT% H_2O_2 FED AT 1.2 ML/MIN

Acid Conc	Feed	S/L	Ag	Al	Au	Cu	Fe	Ni	Pb	Sn	Zn
1 M	No Sep.	S/L = 1/10	0 ± 0	16.1 ± 0.3	1.3 ± 0	74.2 ± 1.1	87.2 ± 0.4	66.5 ± 1.1	0 ± 0	1.5 ± 0	77.3 ± 0.8
2.5 M	No Sep.	S/L = 1/10	0 ± 0	18.4 ± 0.2	0.5 ± 0	81.8 ± 0.8	87.1 ± 3.1	67.9 ± 1	0.1 ± 0	19.1 ± 0.5	84.3 ± 1.6
2.5 M	DMS.	S/L = 1/10	0 ± 0	31.2 ± 0.2	2.2 ± 0.1	78.5 ± 0.1	86.6 ± 1.7	76.5 ± 0.2	0 ± 0	31.6 ± 0.7	71.5 ± 0.4
4 M	DMS.	S/L = 1/10	0 ± 0	30.2 ± 0.3	1.9 ± 0.1	84.2 ± 0.7	85.1 ± 1.4	79 ± 1.1	0 ± 0	34.7 ± 0.7	85.4 ± 0.7
2.5 M	DMS+MS.	S/L = 1/10	0.4 ± 0	31.8 ± 0.7	1 ± 0	80.1 ± 1.8	89.8 ± 2.4	78.7 ± 3.1	0.2 ± 0	13.2 ± 0.4	76.3 ± 2.9
4 M	DMS+MS.	S/L = 1/10	0.2 ± 0	35.2 ± 0.8	0.2 ± 0	83.5 ± 1.7	94.5 ± 3.3	83 ± 2.6	0.2 ± 0	68.8 ± 0.6	83.4 ± 0.5
2.5 M	DMS.	S/L = 0.6/10	1.8 ± 0.1	36.2 ± 1	2.2 ± 0.1	92.1 ± 2.6	89.3 ± 2.8	83.5 ± 2.7	0.3 ± 0	24.5 ± 0.9	90.3 ± 2.4
2.5 M	DMS+MS.	S/L = 0.6/10	2.2 ± 0	33.8 ± 0.1	0 ± 0	90.9 ± 0.2	87.2 ± 2.4	70.4 ± 2.5	0.3 ± 0	25.4 ± 0.3	90.7 ± 0.2
1 M	DMS.	S/L = 0.6/10	1.3 ± 0.1	87.4 ± 2.4	2.3 ± 0	47.5 ± 0.7	77.1 ± 1.2	55 ± 1.2	0.5 ± 0	2.2 ± 0	43.5 ± 0.3
1 M	DMS+MS.	S/L = 0.6/10	1.8 ± 0.1	82.2 ± 1.3	0.6 ± 0	61.6 ± 0.9	80.5 ± 2.4	51.2 ± 1.3	0.4 ± 0	3.1 ± 0	49.4 ± 0.6

TABLE C 28: PERCENTAGE OF METAL EXTRACTED AFTER 300 MINUTES DURING PHASE 2 EXPERIMENTS WITH H_2SO_4 AT 25°C WITH 30 WT% H_2O_2 FED AT 1.2 ML/MIN

Acid Conc	Feed	S/L	Ag	Al	Au	Cu	Fe	Ni	Pb	Sn	Zn
1 M	No Sep.	S/L = 1/10	0 ± 0	19.9 ± 0.4	0.3 ± 0	92.5 ± 1.4	89.8 ± 0.4	72.8 ± 1.2	0 ± 0	2 ± 0	93.5 ± 0.9
2.5 M	No Sep.	S/L = 1/10	0 ± 0	22.9 ± 0.3	0 ± 0	96.3 ± 1	87.3 ± 3.1	79.7 ± 1.1	0 ± 0	7.2 ± 0.2	94.7 ± 1.8
2.5 M	DMS.	S/L = 1/10	0 ± 0	44.3 ± 0.3	1.9 ± 0.1	96.3 ± 0.1	89.9 ± 1.8	82 ± 0.2	0 ± 0	5.6 ± 0.1	96.9 ± 0.6
4 M	DMS.	S/L = 1/10	0 ± 0	34.1 ± 0.3	0.2 ± 0	97.1 ± 0.8	89.8 ± 1.4	86.4 ± 1.2	0 ± 0	37.4 ± 0.8	96.9 ± 0.8
2.5 M	DMS+MS.	S/L = 1/10	0.3 ± 0	48.3 ± 1.1	1.7 ± 0.1	93.9 ± 2.1	92.1 ± 2.5	88.8 ± 3.5	0.3 ± 0	2.8 ± 0.1	96.4 ± 3.7
4 M	DMS+MS.	S/L = 1/10	1.5 ± 0.1	38.2 ± 0.9	4 ± 0.1	96.8 ± 1.9	95.4 ± 3.3	89.1 ± 2.8	0.4 ± 0	69.3 ± 0.6	95.9 ± 0.6
2.5 M	DMS.	S/L = 0.6/10	4.7 ± 0.2	39.6 ± 1.1	4.1 ± 0.2	96.5 ± 2.7	88.6 ± 2.7	81.6 ± 2.6	0.2 ± 0	14.3 ± 0.5	96.2 ± 2.6
2.5 M	DMS+MS.	S/L = 0.6/10	3.8 ± 0.1	37.6 ± 0.1	1.4 ± 0	97.3 ± 0.2	87.3 ± 2.4	81.9 ± 2.9	0.4 ± 0	15.1 ± 0.2	96.2 ± 0.2
1 M	DMS.	S/L = 0.6/10	0 ± 0	91.8 ± 2.6	2.3 ± 0	65.8 ± 0.9	82.5 ± 1.2	59.3 ± 1.3	0.4 ± 0	2.7 ± 0	59.4 ± 0.4
1 M	DMS+MS.	S/L = 0.6/10	0 ± 0	83 ± 1.3	0 ± 0	83.1 ± 1.2	84.3 ± 2.5	63.5 ± 1.6	0.2 ± 0	1.6 ± 0	78.8 ± 0.9

TABLE C 29: PERCENTAGE OF METAL EXTRACTED AFTER 480 MINUTES DURING PHASE 2 EXPERIMENTS WITH H_2SO_4 AT 25°C WITH 30 WT% H_2O_2 FED AT 1.2 ML/MIN

Acid Conc	Feed	S/L	Ag	Al	Au	Cu	Fe	Ni	Pb	Sn	Zn
1 M	No Sep.	S/L = 1/10	0 ± 0	23.8 ± 0.4	1.5 ± 0	94.6 ± 1.4	86.8 ± 0.4	71.9 ± 1.2	0.2 ± 0	1.2 ± 0	93.8 ± 0.9
2.5 M	No Sep.	S/L = 1/10	0 ± 0	26.1 ± 0.3	0.5 ± 0	96.5 ± 1	84 ± 3	72.2 ± 1	0.1 ± 0	5.8 ± 0.1	92.2 ± 1.8
2.5 M	DMS.	S/L = 1/10	0 ± 0	85.6 ± 0.5	2.5 ± 0.1	97.3 ± 0.1	89 ± 1.8	81.1 ± 0.2	0 ± 0	3 ± 0.1	97.8 ± 0.6
4 M	DMS.	S/L = 1/10	0 ± 0	36.7 ± 0.3	1.7 ± 0	98.4 ± 0.8	88.4 ± 1.4	85.4 ± 1.2	0 ± 0	31.6 ± 0.7	96.3 ± 0.8
2.5 M	DMS+MS.	S/L = 1/10	1.9 ± 0	82.3 ± 1.9	0 ± 0	98 ± 2.2	95.2 ± 2.6	91.1 ± 3.6	0.2 ± 0	2.9 ± 0.1	98.4 ± 3.7
4 M	DMS+MS.	S/L = 1/10	0 ± 0	41.1 ± 0.9	0 ± 0	96.6 ± 1.9	92.7 ± 3.2	87.6 ± 2.7	0.4 ± 0	13.1 ± 0.1	95.8 ± 0.6
2.5 M	DMS.	S/L = 0.6/10	1.1 ± 0.1	43.5 ± 1.2	1.4 ± 0.1	97.3 ± 2.7	87.2 ± 2.7	81.9 ± 2.6	0.4 ± 0	11.8 ± 0.4	89.8 ± 2.4
2.5 M	DMS+MS.	S/L = 0.6/10	4.1 ± 0.1	40 ± 0.1	0 ± 0	95.8 ± 0.2	86.1 ± 2.4	82.9 ± 2.9	0.4 ± 0	13.1 ± 0.1	94.7 ± 0.2
1 M	DMS.	S/L = 0.6/10	1.2 ± 0.1	92.8 ± 2.6	4.9 ± 0.1	82 ± 1.1	85.6 ± 1.3	62.6 ± 1.4	0.4 ± 0	1.5 ± 0	78.3 ± 0.5
1 M	DMS+MS.	S/L = 0.6/10	2.7 ± 0.2	81.8 ± 1.3	0 ± 0	94.4 ± 1.3	84.3 ± 2.5	68.9 ± 1.7	0.7 ± 0	0.6 ± 0	96.7 ± 1.2

TABLE C 30: CONFIDENCE INTERVAL CALCULATED WITH α=0.05 FOR REPEAT MEASUREMENTS AND EXPRESSED AS A PERCENTAGE OF THE MEASURED VALUE

Acid Conc	Feed	S/L	Ag	Al	Au	Cu	Fe	Ni	Pb	Sn	Zn
1 M	No Sep.	S/L = 1/10	2.4	1.8	1.4	1.5	0.5	1.6	1.1	1.1	1
2.5 M	No Sep.	S/L = 1/10	1.2	1.3	4.5	1	3.6	1.4	2	2.5	1.9
2.5 M	DMS.	S/L = 1/10	9.9	0.6	3.4	0.1	2	0.3	2.1	2.2	0.6
4 M	DMS.	S/L = 1/10	4.1	0.9	2.8	0.8	1.6	1.4	1.5	2.1	0.8
2.5 M	DMS+MS.	S/L = 1/10	1.1	2.3	3.5	2.2	2.7	3.9	2.4	2.7	3.8
4 M	DMS+MS.	S/L = 1/10	6	2.3	2.4	2	3.5	3.1	2	0.8	0.6
2.5 M	DMS.	S/L = 0.6/10	4.6	2.8	4.8	2.8	3.1	3.2	3.2	3.5	2.7
2.5 M	DMS+MS.	S/L = 0.6/10	1.9	0.3	1.3	0.2	2.8	3.5	0.7	1	0.2
1 M	DMS.	S/L = 0.6/10	8	2.8	1.7	1.4	1.5	2.2	0.3	0.4	0.6
1 M	DMS+MS.	S/L = 0.6/10	8	1.6	1	1.4	3	2.5	1.3	1.3	1.2

C5. REPEAT RUNS

C5.1. MASS EXTRACTED

TABLE C 31: COMPARISON OF MASS OF Ag, Al, Au, Cu AND Fe LEACHED [mg] DURING REPEAT RUNS USING NO SEP FEED IN 1 M H_2SO_4 AT 25°C WITH 30 WT% H_2O_2 FED AT 1.2 ML/MIN

Time [min]	Ag, run A	Ag, run B	Al, run A	Al, run B	Au, run A	Au, run B	Cu, run A	Cu, run B	Fe, run A	Fe, run B
15	1.4 ± 0	2.1 ± 0.1	46 ± 0.4	40.7 ± 1.1	0 ± 0	0 ± 0	871.5 ± 0.8	898.2 ± 2.2	1193.1 ± 9.6	1060.2 ± 7.2
30	1.3 ± 0	1.1 ± 0.1	139 ± 1.3	120.9 ± 3.2	0 ± 0	0 ± 0	2364.8 ± 2.2	2901.6 ± 7.2	1371.4 ± 11.1	1257.8 ± 8.5
60	0.6 ± 0	0.9 ± 0	258.3 ± 2.4	241.3 ± 6.4	0 ± 0	0 ± 0	5044.9 ± 4.6	4994.5 ± 12.4	1535.9 ± 12.4	1364.1 ± 9.3
120	0.2 ± 0	0.5 ± 0	385.9 ± 3.6	354.8 ± 9.4	0 ± 0	0 ± 0	9402.1 ± 8.6	8515.7 ± 21.1	1761.1 ± 14.2	1542.4 ± 10.5
180	1 ± 0	1.1 ± 0.1	447.3 ± 4.2	428.7 ± 11.4	0 ± 0	0 ± 0	11833.7 ± 10.8	10739.7 ± 26.6	1806.7 ± 14.6	1631.8 ± 11.1
240	1.4 ± 0	1.4 ± 0.1	503.7 ± 4.7	482.4 ± 12.8	0 ± 0	0 ± 0	13206.1 ± 12.1	12045.7 ± 29.8	1849.8 ± 15	1657.9 ± 11.2
300	1.1 ± 0	1.7 ± 0.1	557.7 ± 5.3	533.6 ± 14.2	0.2 ± 0	0 ± 0	14106.1 ± 12.9	12874.5 ± 31.9	1881.5 ± 15.2	1688.9 ± 11.5

TABLE C 32: COMPARISON OF MASS OF Ni, Pb, Sn AND Zn LEACHED [mg] DURING REPEAT RUNS USING NO SEP FEED IN 1 M H_2SO_4 AT 25°C WITH 30 WT% H_2O_2 FED AT 1.2 ML/MIN

Time [min]	Ni, run A	Ni, run B	Pb, run A	Pb, run B	Sn, run A	Sn, run B	Zn, run A	Zn, run B
15	51.1 ± 0.1	54.2 ± 1	5.5 ± 0	7.1 ± 0.2	48.2 ± 0.3	49.2 ± 1.6	85.3 ± 0.3	88.4 ± 0.3
30	101.4 ± 0.2	114.2 ± 2	7.1 ± 0	5.6 ± 0.2	40.9 ± 0.2	37.9 ± 1.2	284.7 ± 1.1	350.8 ± 1.1
60	164.1 ± 0.3	153.1 ± 2.7	7.1 ± 0	3.9 ± 0.1	26.5 ± 0.1	20.2 ± 0.6	719.6 ± 2.8	695 ± 2.1
120	215 ± 0.4	189.9 ± 3.4	2.2 ± 0	3.1 ± 0.1	13.5 ± 0.1	10.7 ± 0.3	1584.9 ± 6.2	1402.7 ± 4.3
180	227.3 ± 0.4	206.3 ± 3.7	0.1 ± 0	0.4 ± 0	7 ± 0	8.4 ± 0.3	2045.5 ± 8.1	1825.5 ± 5.6
240	234.5 ± 0.4	216.8 ± 3.8	0 ± 0	0.4 ± 0	10.4 ± 0.1	12.9 ± 0.4	2226.6 ± 8.8	1894.3 ± 5.8
300	239.6 ± 0.4	223.2 ± 3.9	0 ± 0	0 ± 0	19.5 ± 0.1	17 ± 0.5	2348.8 ± 9.3	1993.1 ± 6.1

TABLE C 33: COMPARISON OF MASS OF Ag, Al, Au, Cu AND Fe LEACHED [mg] DURING REPEAT RUNS USING DMS FEED IN 1 M H_2SO_4 AT 25°C WITH 30 WT% H_2O_2 FED AT 1.2 ML/MIN

Time [min]	Ag, run A	Ag, run B	Al, run A	Al, run B	Au, run A	Au, run B	Cu, run A	Cu, run B	Fe, run A	Fe, run B
15	0.1 ± 0	0.4 ± 0	150.9 ± 4.3	165.2 ± 0.6	0 ± 0	0 ± 0	355.5 ± 5	363.1 ± 1	275.9 ± 4.2	334.7 ± 2.8
30	0.5 ± 0	0.4 ± 0	234.2 ± 6.7	242.7 ± 0.8	0 ± 0	0 ± 0	1727.8 ± 24.1	1391.1 ± 3.8	580.7 ± 8.9	601.3 ± 5
60	0 ± 0	0.4 ± 0	429.2 ± 12.2	553.4 ± 1.9	0 ± 0	0 ± 0	3116.7 ± 43.4	2713.6 ± 7.4	763.5 ± 11.7	830.3 ± 6.9
120	0.2 ± 0	0.4 ± 0	698.9 ± 19.9	882.5 ± 3	0 ± 0	0 ± 0	4476.9 ± 62.4	4353.2 ± 11.9	888.8 ± 13.6	1002.6 ± 8.3
180	0.3 ± 0	0 ± 0	811.1 ± 23.1	909.8 ± 3.1	0.1 ± 0	0 ± 0	5984.7 ± 83.4	6034.1 ± 16.5	970 ± 14.8	1077.7 ± 9
240	0.7 ± 0.1	0 ± 0	840.1 ± 23.9	932.4 ± 3.2	0 ± 0	0 ± 0	7224.5 ± 100.7	7501.6 ± 20.5	1006.4 ± 15.4	1145.5 ± 9.5
300	0 ± 0	0 ± 0	851.7 ± 24.2	932.7 ± 3.2	0.1 ± 0	0 ± 0	8288 ± 115.5	8521.2 ± 23.3	1037.9 ± 15.9	1179.9 ± 9.8
360	0.3 ± 0	0 ± 0	857.8 ± 24.4	933.2 ± 3.2	0 ± 0	0 ± 0	9117.6 ± 127	9282.7 ± 25.4	1057.9 ± 16.2	1182.3 ± 9.8
420	0 ± 0	0.4 ± 0	861.6 ± 24.5	927.5 ± 3.2	0.4 ± 0	0 ± 0	9840.4 ± 137.1	9796.1 ± 26.8	1076.7 ± 16.4	1177.7 ± 9.8
480	0.3 ± 0	0 ± 0	860.8 ± 24.5	920.2 ± 3.2	0.2 ± 0	0 ± 0	10319.5 ± 143.8	10048.5 ± 27.5	1077 ± 16.5	1168.9 ± 9.7

TABLE C 34: COMPARISON OF MASS OF Ni, Pb, Sn AND Zn LEACHED [mg] DURING REPEAT RUNS USING DMS FEED IN 1 M H_2SO_4 AT 25°C WITH 30 WT% H_2O_2 FED AT 1.2 ML/MIN

Time [min]	Ni, run A	Ni, run B	Pb, run A	Pb, run B	Sn, run A	Sn, run B	Zn, run A	Zn, run B
15	30.5 ± 0.7	27.3 ± 0.4	4.2 ± 0	3.3 ± 0.1	343.4 ± 1.2	393.6 ± 17.5	45.2 ± 0.3	41.5 ± 0.1
30	94.9 ± 2.1	74.1 ± 1.1	5 ± 0	6 ± 0.3	189.3 ± 0.7	193.1 ± 8.6	211.6 ± 1.3	188.8 ± 0.5
60	129.8 ± 2.8	113.7 ± 1.7	6.7 ± 0	4.6 ± 0.2	102.5 ± 0.4	110.2 ± 4.9	427.7 ± 2.7	452.7 ± 1.3
120	152.7 ± 3.3	139 ± 2	7.4 ± 0	2.1 ± 0.1	69.5 ± 0.3	66.8 ± 3	699.2 ± 4.4	752.8 ± 2.2
180	168.5 ± 3.7	155.3 ± 2.3	7.9 ± 0	2.1 ± 0.1	43.6 ± 0.2	55.6 ± 2.5	905.6 ± 5.7	1000 ± 2.9
240	177.5 ± 3.9	168 ± 2.5	7.3 ± 0	1.6 ± 0.1	48.3 ± 0.2	45.5 ± 2	1070.1 ± 6.7	1281 ± 3.7
300	181.6 ± 4	169 ± 2.5	7 ± 0	0 ± 0	52.9 ± 0.2	26.5 ± 1.2	1236.3 ± 7.7	1536.8 ± 4.5
360	186.1 ± 4.1	172.5 ± 2.5	7.1 ± 0	0 ± 0	44.8 ± 0.2	11 ± 0.5	1381.8 ± 8.6	1734.1 ± 5
420	187.9 ± 4.1	175.4 ± 2.6	6.8 ± 0	0 ± 0	35.1 ± 0.1	4.2 ± 0.2	1529.2 ± 9.6	1911.7 ± 5.6
480	191.6 ± 4.2	173.4 ± 2.5	6.4 ± 0	0.5 ± 0	29.3 ± 0.1	0.7 ± 0	1630.9 ± 10.2	1986 ± 5.8

TABLE C 35: COMPARISON OF MASS OF Ag, Al, Au, Cu AND Fe LEACHED [mg] DURING REPEAT RUNS USING DMS+MS FEED IN 1 M H_2SO_4 AT 25°C WITH 30 WT% H_2O_2 FED AT 1.2 ML/MIN

Time [min]	Ag, run A	Ag, run B	Al, run A	Al, run B	Au, run A	Au, run B	Cu, run A	Cu, run B	Fe, run A	Fe, run B
15	0.4 ± 0	0.3 ± 0	186.4 ± 3	152.3 ± 0.3	0 ± 0	0 ± 0	383.4 ± 5.4	181.6 ± 0.1	182.7 ± 5.5	161.8 ± 8
30	0.7 ± 0.1	0.1 ± 0	273.5 ± 4.3	216.2 ± 0.5	0 ± 0	0 ± 0	1631.5 ± 23	1044.3 ± 0.9	291.1 ± 8.8	293.7 ± 14.6
60	0 ± 0	0.1 ± 0	605.3 ± 9.6	461.1 ± 1	0 ± 0	0 ± 0	3339.2 ± 47	2732.4 ± 2.2	353.1 ± 10.6	351.2 ± 17.4
120	0.1 ± 0	0.1 ± 0	995 ± 15.8	795.1 ± 1.7	0 ± 0	0 ± 0	5785.4 ± 81.4	5664.5 ± 4.6	399.2 ± 12	420.3 ± 20.8
180	0.3 ± 0	0 ± 0	1060.2 ± 16.8	847 ± 1.8	0 ± 0	0 ± 0	8221 ± 115.7	7948.2 ± 6.5	427.2 ± 12.9	444.5 ± 22
240	0.4 ± 0	0.4 ± 0	1081.4 ± 17.1	859.9 ± 1.9	0 ± 0	0 ± 0	9937.4 ± 139.9	9465.8 ± 7.7	446.5 ± 13.4	446.7 ± 22.1
300	0 ± 0	0.5 ± 0	1069.7 ± 17	894.4 ± 1.9	0 ± 0	0 ± 0	11092.8 ± 156.1	10901.8 ± 8.9	447.1 ± 13.5	462.3 ± 22.9
360	0.6 ± 0.1	0.9 ± 0	1072.2 ± 17	895.5 ± 1.9	0 ± 0	0 ± 0	11995.2 ± 168.8	11489.7 ± 9.4	452.1 ± 13.6	463.7 ± 23
420	0.4 ± 0	0.5 ± 0	1073.8 ± 17	894.8 ± 1.9	0 ± 0	0 ± 0	12567.2 ± 176.9	11752.9 ± 9.6	454.9 ± 13.7	461.4 ± 22.9
480	0.5 ± 0	0.7 ± 0	1055.3 ± 16.7	895.3 ± 1.9	0 ± 0	0 ± 0	12608.5 ± 177.5	11912.9 ± 9.7	447.1 ± 13.4	467.2 ± 23.2

TABLE C 36: COMPARISON OF MASS OF Ni, Pb, Sn AND Zn LEACHED [mg] DURING REPEAT RUNS USING DMS+MS FEED IN 1 M H_2SO_4 AT 25°C WITH 30 WT% H_2O_2 FED AT 1.2 ML/MIN

Time [min]	Ni, run A	Ni, run B	Pb, run A	Pb, run B	Sn, run A	Sn, run B	Zn, run A	Zn, run B
15	10.7 ± 0.3	6.7 ± 0.1	4.4 ± 0.1	4 ± 0	269.4 ± 3.4	238.2 ± 2.9	37.1 ± 0.4	25.9 ± 0
30	26.9 ± 0.7	21.7 ± 0.3	3.8 ± 0	3 ± 0	146 ± 1.8	190.8 ± 2.3	162 ± 1.9	143 ± 0.1
60	41.4 ± 1	34.2 ± 0.5	6.5 ± 0.1	4.2 ± 0	106 ± 1.3	82.1 ± 1	387 ± 4.6	442.5 ± 0.2
120	54 ± 1.4	49.9 ± 0.7	7.1 ± 0.1	2.7 ± 0	63.3 ± 0.8	35.1 ± 0.4	696.6 ± 8.3	953.1 ± 0.5
180	64.5 ± 1.6	61.7 ± 0.9	6.3 ± 0.1	0 ± 0	63.2 ± 0.8	27 ± 0.3	990.3 ± 11.9	1441.6 ± 0.7
240	71.9 ± 1.8	68.8 ± 1	4.7 ± 0.1	0.2 ± 0	50.2 ± 0.6	24.3 ± 0.3	1289.9 ± 15.5	1852 ± 0.9
300	79.8 ± 2	77.5 ± 1.2	3.7 ± 0	0 ± 0	33.3 ± 0.4	11.6 ± 0.1	1579.4 ± 18.9	2223.2 ± 1.1
360	85.6 ± 2.2	80.6 ± 1.2	6.1 ± 0.1	0 ± 0	22.7 ± 0.3	0.9 ± 0	1813.5 ± 21.7	2406.2 ± 1.2
420	87.8 ± 2.2	82.9 ± 1.2	4.4 ± 0.1	0 ± 0	15.6 ± 0.2	3.6 ± 0	1940 ± 23.2	2489.8 ± 1.2
480	86.6 ± 2.2	83.2 ± 1.2	10.5 ± 0.1	0 ± 0	12.1 ± 0.2	3.2 ± 0	1939.4 ± 23.2	2508.4 ± 1.2

C5.2. PERCENTAGE EXTRACTED

TABLE C 37: COMPARISON OF PERCENTAGE OF Ag, Al, Au, Cu AND Fe LEACHED DURING REPEAT RUNS USING NO SEP FEED IN 1 M H_2SO_4 AT 25°C WITH 30 WT% H_2O_2 FED AT 1.2 ML/MIN

Time [min]	Ag, run A	Ag, run B	Al, run A	Al, run B	Au, run A	Au, run B	Cu, run A	Cu, run B	Fe, run A	Fe, run B
15	5.1 ± 0.1	8.8 ± 0.4	1.8 ± 0	1.6 ± 0	0.1 ± 0	0 ± 0	5.5 ± 0	6.1 ± 0	53.1 ± 0.4	50.9 ± 0.3
30	4.6 ± 0.1	4.6 ± 0.2	5.4 ± 0.1	4.8 ± 0.1	0 ± 0	0 ± 0	14.9 ± 0	19.6 ± 0	61.1 ± 0.5	60.4 ± 0.4
60	2.3 ± 0.1	3.7 ± 0.2	10 ± 0.1	9.6 ± 0.3	0 ± 0	0 ± 0	31.7 ± 0	33.8 ± 0.1	68.4 ± 0.6	65.5 ± 0.4
120	0.9 ± 0	2 ± 0.1	15 ± 0.1	14.2 ± 0.4	0 ± 0	0.3 ± 0	59.2 ± 0.1	57.6 ± 0.1	78.4 ± 0.6	74.1 ± 0.5
180	3.5 ± 0.1	4.6 ± 0.2	17.4 ± 0.2	17.1 ± 0.5	0 ± 0	0 ± 0	74.5 ± 0.1	72.6 ± 0.2	80.5 ± 0.7	78.4 ± 0.5
240	5 ± 0.1	5.8 ± 0.3	19.5 ± 0.2	19.2 ± 0.5	0 ± 0	0 ± 0	83.1 ± 0.1	81.5 ± 0.2	82.4 ± 0.7	79.7 ± 0.5
300	4.2 ± 0.1	7 ± 0.3	21.6 ± 0.2	21.3 ± 0.6	1.5 ± 0	0 ± 0	88.7 ± 0.1	87.1 ± 0.2	83.8 ± 0.7	81.1 ± 0.6

TABLE C 38: COMPARISON OF PERCENTAGE OF Ni, Pb, Sn AND Zn LEACHED DURING REPEAT RUNS USING NO SEP FEED IN 1 M H_2SO_4 AT 25°C WITH 30 WT% H_2O_2 FED AT 1.2 ML/MIN

Time [min]	Ni, run A	Ni, run B	Pb, run A	Pb, run B	Sn, run A	Sn, run B	Zn, run A	Zn, run B
15	13.2 ± 0	14.1 ± 0.2	0.3 ± 0	0.4 ± 0	2.2 ± 0	2.3 ± 0.1	3.2 ± 0	3.8 ± 0
30	26.3 ± 0	29.7 ± 0.5	0.4 ± 0	0.3 ± 0	1.9 ± 0	1.8 ± 0.1	10.8 ± 0	15 ± 0
60	42.5 ± 0.1	39.8 ± 0.7	0.4 ± 0	0.2 ± 0	1.2 ± 0	0.9 ± 0	27.2 ± 0.1	29.7 ± 0.1
120	55.7 ± 0.1	49.3 ± 0.9	0.1 ± 0	0.2 ± 0	0.6 ± 0	0.5 ± 0	59.8 ± 0.2	59.9 ± 0.2
180	58.9 ± 0.1	53.6 ± 0.9	0 ± 0	0 ± 0	0.3 ± 0	0.4 ± 0	77.2 ± 0.3	78 ± 0.2
240	60.8 ± 0.1	56.3 ± 1	0 ± 0	0 ± 0	0.5 ± 0	0.6 ± 0	84.1 ± 0.3	80.9 ± 0.2
300	62.1 ± 0.1	58 ± 1	0 ± 0	0 ± 0	0.9 ± 0	0.8 ± 0	88.7 ± 0.3	85.1 ± 0.3

TABLE C 39: COMPARISON OF PERCENTAGE OF Ag, Al, Au, Cu AND Fe LEACHED DURING REPEAT RUNS USING DMS FEED IN 1 M H_2SO_4 AT 25°C WITH 30 WT% H_2O_2 FED AT 1.2 ML/MIN

Time [min]	Ag, run A	Ag, run B	Al, run A	Al, run B	Au, run A	Au, run B	Cu, run A	Cu, run B	Fe, run A	Fe, run B
15	0.3 ± 0	1.7 ± 0.1	16.3 ± 0.5	16.2 ± 0.1	0 ± 0	0 ± 0	2.8 ± 0	3.4 ± 0	21.9 ± 0.3	23.6 ± 0.2
30	2.2 ± 0.2	1.6 ± 0.1	25.2 ± 0.7	23.8 ± 0.1	1.5 ± 0	0 ± 0	13.7 ± 0.2	13 ± 0	46.2 ± 0.7	42.3 ± 0.4
60	0.1 ± 0	1.8 ± 0.1	46.3 ± 1.3	54.2 ± 0.2	0.8 ± 0	0 ± 0	24.8 ± 0.3	25.3 ± 0.1	60.7 ± 0.9	58.5 ± 0.5
120	0.8 ± 0.1	1.8 ± 0.1	75.3 ± 2.1	86.4 ± 0.3	1.4 ± 0	0 ± 0	35.6 ± 0.5	40.6 ± 0.1	70.6 ± 1.1	70.6 ± 0.6
180	1.3 ± 0.1	0.1 ± 0	87.4 ± 2.5	89.1 ± 0.3	2.3 ± 0	0 ± 0	47.5 ± 0.7	56.3 ± 0.2	77.1 ± 1.2	75.9 ± 0.6
240	3 ± 0.2	0.1 ± 0	90.6 ± 2.6	91.3 ± 0.3	0 ± 0	0 ± 0	57.4 ± 0.8	70 ± 0.2	80 ± 1.2	80.6 ± 0.7
300	0 ± 0	0.1 ± 0	91.8 ± 2.6	91.4 ± 0.3	2.3 ± 0	0 ± 0	65.8 ± 0.9	79.5 ± 0.2	82.5 ± 1.3	83.1 ± 0.7
360	1.4 ± 0.1	0 ± 0	92.5 ± 2.6	91.4 ± 0.3	0 ± 0	0 ± 0	72.4 ± 1	86.6 ± 0.2	84.1 ± 1.3	83.2 ± 0.7
420	0 ± 0	1.6 ± 0.1	92.9 ± 2.6	90.9 ± 0.3	11.9 ± 0.2	0 ± 0	78.2 ± 1.1	91.4 ± 0.3	85.6 ± 1.3	82.9 ± 0.7
480	1.2 ± 0.1	0 ± 0	92.8 ± 2.6	90.1 ± 0.3	4.9 ± 0.1	0 ± 0	82 ± 1.1	93.7 ± 0.3	85.6 ± 1.3	82.3 ± 0.7

TABLE C 40: COMPARISON OF PERCENTAGE OF Ni, Pb, Sn AND Zn LEACHED DURING REPEAT RUNS USING DMS FEED IN 1 M H_2SO_4 AT 25°C WITH 30 WT% H_2O_2 FED AT 1.2 ML/MIN

Time [min]	Ni, run A	Ni, run B	Pb, run A	Pb, run B	Sn, run A	Sn, run B	Zn, run A	Zn, run B
15	10 ± 0.2	11 ± 0.2	0.2 ± 0	0.2 ± 0	17.4 ± 0.1	19.2 ± 0.9	2.2 ± 0	1.9 ± 0
30	31 ± 0.7	29.8 ± 0.4	0.3 ± 0	0.4 ± 0	9.6 ± 0	9.4 ± 0.4	10.2 ± 0.1	8.9 ± 0
60	42.4 ± 0.9	45.7 ± 0.7	0.4 ± 0	0.3 ± 0	5.2 ± 0	5.4 ± 0.2	20.5 ± 0.1	21.2 ± 0.1
120	49.9 ± 1.1	55.9 ± 0.8	0.4 ± 0	0.1 ± 0	3.5 ± 0	3.3 ± 0.1	33.6 ± 0.2	35.3 ± 0.1
180	55 ± 1.2	62.5 ± 0.9	0.5 ± 0	0.1 ± 0	2.2 ± 0	2.7 ± 0.1	43.5 ± 0.3	46.9 ± 0.1
240	58 ± 1.3	67.6 ± 1	0.4 ± 0	0.1 ± 0	2.5 ± 0	2.2 ± 0.1	51.4 ± 0.3	60.1 ± 0.2
300	59.3 ± 1.3	68 ± 1	0.4 ± 0	0 ± 0	2.7 ± 0	1.3 ± 0.1	59.4 ± 0.4	72.1 ± 0.2
360	60.8 ± 1.3	69.4 ± 1	0.4 ± 0	0 ± 0	2.3 ± 0	0.5 ± 0	66.4 ± 0.4	81.4 ± 0.2
420	61.4 ± 1.3	70.6 ± 1	0.4 ± 0	0 ± 0	1.8 ± 0	0.2 ± 0	73.5 ± 0.5	89.7 ± 0.3
480	62.6 ± 1.4	69.7 ± 1	0.4 ± 0	0 ± 0	1.5 ± 0	0 ± 0	78.3 ± 0.5	93.2 ± 0.3

TABLE C 41: COMPARISON OF PERCENTAGE OF Ag, Al, Au, Cu AND Fe LEACHED DURING REPEAT RUNS USING DMS+MS FEED IN 1 M H_2SO_4 AT 25°C WITH 30 WT% H_2O_2 FED AT 1.2 ML/MIN

Time [min]	Ag, run A	Ag, run B	Al, run A	Al, run B	Au, run A	Au, run B	Cu, run A	Cu, run B	Fe, run A	Fe, run B
15	2.3 ± 0.2	1.2 ± 0	14.5 ± 0.2	14 ± 0	1.1 ± 0	0.8 ± 0	2.9 ± 0	1.4 ± 0	34.4 ± 1	27.7 ± 1.4
30	3.7 ± 0.3	0.6 ± 0	21.2 ± 0.3	19.9 ± 0	0 ± 0	0 ± 0	12.2 ± 0.2	7.9 ± 0	54.9 ± 1.7	50.3 ± 2.5
60	0 ± 0	0.4 ± 0	46.9 ± 0.7	42.5 ± 0.1	1.4 ± 0	0 ± 0	25 ± 0.4	20.7 ± 0	66.6 ± 2	60.1 ± 3
120	0.4 ± 0	0.3 ± 0	77.2 ± 1.2	73.3 ± 0.2	0 ± 0	0.6 ± 0	43.3 ± 0.6	42.9 ± 0	75.2 ± 2.3	71.9 ± 3.6
180	1.8 ± 0.1	0 ± 0	82.2 ± 1.3	78 ± 0.2	0.6 ± 0	0 ± 0	61.6 ± 0.9	60.2 ± 0	80.5 ± 2.4	76.1 ± 3.8
240	2.4 ± 0.2	1.8 ± 0	83.9 ± 1.3	79.2 ± 0.2	0.1 ± 0	0 ± 0	74.4 ± 1	71.7 ± 0.1	84.2 ± 2.5	76.4 ± 3.8
300	0 ± 0	2.3 ± 0.1	83 ± 1.3	82.4 ± 0.2	0 ± 0	0 ± 0	83.1 ± 1.2	82.6 ± 0.1	84.3 ± 2.5	79.1 ± 3.9
360	3.4 ± 0.3	4.5 ± 0.1	83.2 ± 1.3	82.5 ± 0.2	1 ± 0	0 ± 0	89.8 ± 1.3	87 ± 0.1	85.2 ± 2.6	79.4 ± 3.9
420	2 ± 0.2	2.4 ± 0.1	83.3 ± 1.3	82.4 ± 0.2	0 ± 0	0 ± 0	94.1 ± 1.3	89 ± 0.1	85.7 ± 2.6	79 ± 3.9
480	2.7 ± 0.2	3.3 ± 0.1	81.8 ± 1.3	82.5 ± 0.2	0 ± 0	0 ± 0	94.4 ± 1.3	90.2 ± 0.1	84.3 ± 2.5	80 ± 4

TABLE C 42: COMPARISON OF PERCENTAGE OF Ni, Pb, Sn AND Zn LEACHED DURING REPEAT RUNS USING DMS+MS FEED IN 1 M H_2SO_4 AT 25°C WITH 30 WT% H_2O_2 FED AT 1.2 ML/MIN

Time [min]	Ni, run A	Ni, run B	Pb, run A	Pb, run B	Sn, run A	Sn, run B	Zn, run A	Zn, run B
15	8.5 ± 0.2	4.6 ± 0.1	0.3 ± 0	0.1 ± 0	13.3 ± 0.2	5.7 ± 0.1	1.8 ± 0	1 ± 0
30	21.4 ± 0.5	14.9 ± 0.2	0.2 ± 0	0.1 ± 0	7.2 ± 0.1	4.6 ± 0.1	8.1 ± 0.1	5.4 ± 0
60	32.9 ± 0.8	23.5 ± 0.4	0.4 ± 0	0.1 ± 0	5.2 ± 0.1	2 ± 0	19.3 ± 0.2	16.7 ± 0
120	42.9 ± 1.1	34.3 ± 0.5	0.4 ± 0	0.1 ± 0	3.1 ± 0	0.8 ± 0	34.7 ± 0.4	35.9 ± 0
180	51.2 ± 1.3	42.5 ± 0.6	0.4 ± 0	0 ± 0	3.1 ± 0	0.6 ± 0	49.4 ± 0.6	54.3 ± 0
240	57.1 ± 1.4	47.4 ± 0.7	0.3 ± 0	0 ± 0	2.5 ± 0	0.6 ± 0	64.3 ± 0.8	69.7 ± 0
300	63.5 ± 1.6	53.4 ± 0.8	0.2 ± 0	0 ± 0	1.6 ± 0	0.3 ± 0	78.8 ± 0.9	83.7 ± 0
360	68.1 ± 1.7	55.5 ± 0.8	0.4 ± 0	0 ± 0	1.1 ± 0	0 ± 0	90.4 ± 1.1	90.6 ± 0
420	69.8 ± 1.8	57.1 ± 0.9	0.3 ± 0	0 ± 0	0.8 ± 0	0.1 ± 0	96.7 ± 1.2	93.7 ± 0
480	68.9 ± 1.7	57.3 ± 0.9	0.7 ± 0	0 ± 0	0.6 ± 0	0.1 ± 0	96.7 ± 1.2	94.4 ± 0

C6. PHASE 3: PROCESS ROUTE VALIDATION

C6.1. MASS EXTRACTED

TABLE C 43: MASS OF METAL LEACHED [mg] FROM 80 GRAMS OF NO SEP FEED DURING FIRST STAGE LEACH USING 1 M HNO_3 AT 25°C AT S/L RATIO OF 1/10

Time [min]	Ag	Al	Au	Co	Cu	Fe	Ni	Pb	Pd	Pt	Sn	Zn
15	0.7 ± 0.1	16.6 ± 0.4	0 ± 0	0 ± 0	22.8 ± 0	810.4 ± 0.4	6.5 ± 0	531.7 ± 0.6	0 ± 0	0.2 ± 0	261.8 ± 0.9	29.7 ± 0
30	0 ± 0	24 ± 0.6	0.1 ± 0	0 ± 0	22.5 ± 0	830.6 ± 0.4	10.9 ± 0	653.8 ± 0.8	0 ± 0	0.2 ± 0	522.3 ± 1.7	30.9 ± 0
60	0.2 ± 0	73.8 ± 1.7	0 ± 0	0.2 ± 0	19.6 ± 0	860.8 ± 0.4	19.5 ± 0	831.5 ± 1	0 ± 0	0.2 ± 0	723.6 ± 2.4	32.3 ± 0
120	0.7 ± 0.1	177.5 ± 4.2	0 ± 0	0.2 ± 0	16.3 ± 0	879.9 ± 0.4	31 ± 0.1	1021.3 ± 1.2	0 ± 0	0.2 ± 0	565.2 ± 1.9	33.4 ± 0.1
180	0 ± 0	246.8 ± 5.8	0 ± 0	0.4 ± 0	16.9 ± 0	917.2 ± 0.5	41.9 ± 0.1	1121 ± 1.3	0 ± 0	0.2 ± 0	563.4 ± 1.9	35 ± 0.1
240	0 ± 0	297 ± 7	0 ± 0	0.5 ± 0	18.3 ± 0	930.4 ± 0.5	50.4 ± 0.1	1160.7 ± 1.3	0 ± 0	0.1 ± 0	312.9 ± 1	36 ± 0.1
300	0.2 ± 0	343.8 ± 8.1	0 ± 0	0.6 ± 0	20.3 ± 0	950 ± 0.5	56.4 ± 0.1	1184.5 ± 1.4	0 ± 0	0.1 ± 0	219.7 ± 0.7	37.2 ± 0.1
360	0 ± 0	380.4 ± 9	0 ± 0	0.8 ± 0	21.4 ± 0	958.7 ± 0.5	60.5 ± 0.1	1173.7 ± 1.4	0 ± 0	0.2 ± 0	123.9 ± 0.4	37.8 ± 0.1
420	0.1 ± 0	414.6 ± 9.8	0 ± 0	0.9 ± 0	21.6 ± 0	981.5 ± 0.5	64 ± 0.1	1195.6 ± 1.4	0 ± 0	0.4 ± 0	67.6 ± 0.2	39 ± 0.1
480	0.2 ± 0	419.8 ± 9.9	0 ± 0	1 ± 0	22.1 ± 0	992.1 ± 0.5	65.4 ± 0.1	1202.6 ± 1.4	0 ± 0	0.2 ± 0	66.1 ± 0.2	39.5 ± 0.1

TABLE C 44: MASS OF METAL LEACHED [mg] DURING SECOND STAGE LEACH USING 2.5 M H_2SO_4 AT 25°C AT S/L RATIO OF 1.6/10 WITH 30 WT% H_2O_2 FEED RATE OF 1.2 ML/MIN

Time [min]	Ag	Al	Au	Co	Cu	Fe	Ni	Pb	Pd	Pt	Sn	Zn
15	0.2 ± 0	38.6 ± 0.9	0 ± 0	0.2 ± 0	610.4 ± 0.8	48.6 ± 0	35.2 ± 0.1	1.6 ± 0	0.5 ± 0.1	0.2 ± 0	93.3 ± 0.3	75.4 ± 0.1
30	0.3 ± 0	60.4 ± 1.4	0 ± 0	0.5 ± 0	1887.8 ± 2.3	65.4 ± 0	60.8 ± 0.1	0 ± 0	0.9 ± 0.1	0.4 ± 0	119.7 ± 0.4	231.1 ± 0.3
60	0.3 ± 0	103.1 ± 2.4	0 ± 0	0.9 ± 0	5009.7 ± 6.2	107.3 ± 0.1	83 ± 0.2	0 ± 0	1.4 ± 0.2	0.4 ± 0	136.4 ± 0.5	591.4 ± 0.9
120	0.5 ± 0	168.3 ± 4	0 ± 0	1.1 ± 0	8962.8 ± 11.1	173.8 ± 0.1	97.7 ± 0.2	0 ± 0	2.3 ± 0.3	0.2 ± 0	120.8 ± 0.4	1507.2 ± 2.3
180	2.2 ± 0.2	280.8 ± 6.6	0 ± 0	1 ± 0	11624.3 ± 14.4	195.2 ± 0.1	107.9 ± 0.2	0 ± 0	3.1 ± 0.4	0.2 ± 0	92.2 ± 0.3	2087.1 ± 3.1
240	7.8 ± 0.6	327.5 ± 7.8	0 ± 0	1.2 ± 0	12491.6 ± 15.4	204.2 ± 0.1	111 ± 0.2	0 ± 0	3.2 ± 0.4	0.4 ± 0	88.6 ± 0.3	2162.1 ± 3.3
300	6 ± 0.5	379.4 ± 9	0 ± 0	1.1 ± 0	13125.9 ± 16.2	225.7 ± 0.1	110.2 ± 0.2	0 ± 0	2.8 ± 0.3	0.5 ± 0	85 ± 0.3	2193.7 ± 3.3
360	3 ± 0.2	417.1 ± 9.9	0 ± 0	1.1 ± 0	13154.5 ± 16.3	207.8 ± 0.1	111.5 ± 0.2	0 ± 0	3.5 ± 0.4	0.6 ± 0	72.5 ± 0.2	2179.6 ± 3.3
420	2.1 ± 0.2	461.3 ± 10.9	0 ± 0	1.1 ± 0	13433.9 ± 16.6	208.7 ± 0.1	111.9 ± 0.2	0 ± 0	4 ± 0.5	0.3 ± 0	69.6 ± 0.2	2189.9 ± 3.3
480	1.3 ± 0.1	504.5 ± 11.9	0 ± 0	1.1 ± 0	13674.9 ± 16.9	212 ± 0.1	112.5 ± 0.2	0 ± 0	4 ± 0.5	0.4 ± 0	71.2 ± 0.2	2179 ± 3.3

C6.2. PERCENTAGE EXTRACTED

TABLE C 45: PERCENTAGE OF METAL LEACHED FROM 80 GRAMS OF NO SEP FEED DURING FIRST STAGE LEACH USING 1 M HNO_3 AT 25°C AT S/L RATIO OF 1/10

Time [min]	Ag	Al	Au	Co	Cu	Fe	Ni	Pb	Pd	Pt	Sn	Zn
15	4.2 ± 0.3	0.6 ± 0	0 ± 0	2 ± 0	0.2 ± 0	62.2 ± 0	3.4 ± 0	43.3 ± 0.1	0 ± 0	14.5 ± 0.8	27.7 ± 0.1	1.3 ± 0
30	0.2 ± 0	0.9 ± 0	1 ± 0	1.7 ± 0	0.2 ± 0	63.8 ± 0	5.6 ± 0	53.2 ± 0.1	0 ± 0	14 ± 0.7	55.2 ± 0.2	1.3 ± 0
60	1.2 ± 0.1	2.7 ± 0.1	0 ± 0	7.6 ± 0.1	0.1 ± 0	66.1 ± 0	10 ± 0	67.7 ± 0.1	0 ± 0	17.3 ± 0.9	76.5 ± 0.3	1.4 ± 0
120	4.4 ± 0.4	6.5 ± 0.2	0 ± 0	10 ± 0.2	0.1 ± 0	67.6 ± 0	15.9 ± 0	83.2 ± 0.1	0 ± 0	13.9 ± 0.7	59.8 ± 0.2	1.4 ± 0
180	0 ± 0	9 ± 0.2	0.1 ± 0	16.7 ± 0.3	0.1 ± 0	70.4 ± 0	21.5 ± 0	91.3 ± 0.1	0 ± 0	14.6 ± 0.8	59.6 ± 0.2	1.5 ± 0
240	0 ± 0	10.8 ± 0.3	0 ± 0	21.3 ± 0.4	0.1 ± 0	71.5 ± 0	25.9 ± 0.1	94.5 ± 0.1	0 ± 0	4 ± 0.2	33.1 ± 0.1	1.5 ± 0
300	1.1 ± 0.1	12.5 ± 0.3	0 ± 0	27 ± 0.5	0.1 ± 0	73 ± 0	29 ± 0.1	96.4 ± 0.1	0 ± 0	9.2 ± 0.5	23.2 ± 0.1	1.6 ± 0
360	0.3 ± 0	13.9 ± 0.3	0 ± 0	33.7 ± 0.6	0.2 ± 0	73.6 ± 0	31.1 ± 0.1	95.6 ± 0.1	0 ± 0	18.2 ± 0.9	13.1 ± 0	1.6 ± 0
420	0.4 ± 0	15.1 ± 0.4	0 ± 0	39.8 ± 0.7	0.2 ± 0	75.4 ± 0	32.9 ± 0.1	97.3 ± 0.1	0 ± 0	26.6 ± 1.4	7.2 ± 0	1.7 ± 0
480	1.3 ± 0.1	15.3 ± 0.4	0 ± 0	40.8 ± 0.7	0.2 ± 0	76.2 ± 0	33.6 ± 0.1	97.9 ± 0.1	0 ± 0	16.6 ± 0.9	7 ± 0	1.7 ± 0

TABLE C 46: PERCENTAGE OF METAL LEACHED DURING SECOND STAGE LEACH USING 2.5 M H_2SO_4 AT 25°C AT S/L RATIO OF 1.6/10 WITH 30 WT% H_2O_2 FEED RATE OF 1.2 ML/MIN

Time [min]	Ag	Al	Au	Co	Cu	Fe	Ni	Pb	Pd	Pt	Sn	Zn
15	1 ± 0.1	1.4 ± 0	0 ± 0	9 ± 0.2	4.3 ± 0	3.7 ± 0	18.1 ± 0	0.1 ± 0	8.7 ± 1.1	15.1 ± 0.8	9.9 ± 0	3.2 ± 0
30	2.2 ± 0.2	2.2 ± 0.1	0 ± 0	20.8 ± 0.4	13.3 ± 0	5 ± 0	31.2 ± 0.1	0 ± 0	16.1 ± 2	30.7 ± 1.6	12.7 ± 0	9.9 ± 0
60	1.9 ± 0.2	3.8 ± 0.1	0 ± 0	39.2 ± 0.7	35.4 ± 0	8.2 ± 0	42.6 ± 0.1	0 ± 0	26.2 ± 3.3	27.4 ± 1.4	14.4 ± 0	25.3 ± 0
120	3.4 ± 0.3	6.1 ± 0.1	0 ± 0	46.2 ± 0.8	63.3 ± 0.1	13.3 ± 0	50.2 ± 0.1	0 ± 0	43.5 ± 5.4	13.3 ± 0.7	12.8 ± 0	64.6 ± 0.1
180	14.2 ± 1.1	10.2 ± 0.2	0 ± 0	41.7 ± 0.7	82.1 ± 0.1	15 ± 0	55.4 ± 0.1	0 ± 0	59.5 ± 7.4	15.2 ± 0.8	9.8 ± 0	89.5 ± 0.1
240	50.3 ± 4	11.9 ± 0.3	0 ± 0	49.8 ± 0.9	88.2 ± 0.1	15.7 ± 0	57 ± 0.1	0 ± 0	59.8 ± 7.4	32.2 ± 1.7	9.4 ± 0	92.7 ± 0.1
300	38.4 ± 3.1	13.8 ± 0.3	0 ± 0	45 ± 0.8	92.7 ± 0.1	17.3 ± 0	56.6 ± 0.1	0 ± 0	52.2 ± 6.5	35 ± 1.8	9 ± 0	94 ± 0.1
360	19.2 ± 1.5	15.2 ± 0.4	0 ± 0	46.7 ± 0.8	92.9 ± 0.1	16 ± 0	57.2 ± 0.1	0 ± 0	66.8 ± 8.3	45.7 ± 2.4	7.7 ± 0	93.4 ± 0.1
420	13.3 ± 1.1	16.8 ± 0.4	0 ± 0	48.6 ± 0.8	94.8 ± 0.1	16 ± 0	57.5 ± 0.1	0 ± 0	75.3 ± 9.3	24.7 ± 1.3	7.4 ± 0	93.9 ± 0.1
480	8.5 ± 0.7	18.4 ± 0.4	0 ± 0	47.7 ± 0.8	96.5 ± 0.1	16.3 ± 0	57.8 ± 0.1	0 ± 0	75.2 ± 9.3	27.4 ± 1.4	7.5 ± 0	93.4 ± 0.1

TABLE C 47: THE SELECTIVITY OF COPPER LEACHING IN GRAMS COPPER LEACHED PER GRAM GOLD WITH PEROXIDE ADDITION

Peroxide			Selectivity [g Cu/g Au]	
Experiment	Temp	Lixiviant	no H_2O_2	200% excess H_2O_2
E1 E8	25°C	HNO_3	N/A	N/A
E3 E9	25°C	H_2SO_4	N/A	N/A
E5 E11	55°C	HNO_3	39430	22223
E6 E12	55°C	H_2SO_4	N/A	N/A
E2 E10	85°C	HNO_3	8868	10268
E4 E7	85°C	H_2SO_4	N/A	N/A

TABLE C 48: THE SELECTIVITY OF COPPER LEACHING IN GRAMS COPPER LEACHED PER GRAM GOLD WITH CHANGE IN TEMPERATURE

Temperature			Selectivity [g Cu/g Au]		
Experiment	Lixiviant	Peroxide	25°C	55°C	85°C
E1 E5 E2	HNO_3	none	N/A	39429	8867
E3 E6 E4	H_2SO_4	none	N/A	N/A	N/A
E8 E11 E10	HNO_3	200% excess	N/A	22222	10267
E9 E12 E7	H_2SO_4	200% excess	N/A	N/A	N/A

APPENDIX D: FITTING RATE MODELS

Leaching No Sep, DMS and DMS+MS using 1 M H_2SO_4

Comparison of rate model fitting to the respective feeds show the concentrated feeds fitting better with chemical reaction control at 1 M H_2SO_4. There was little difference in the fit of chemical reaction control and diffusion control for the untreated feed indicating that both factors could potentially be limiting. For untreated feed, a slightly better fit was achieved with the diffusion model. The fit of film diffusion model is shown here graphically because it was not seen to provide a best fit to any of the feeds types.

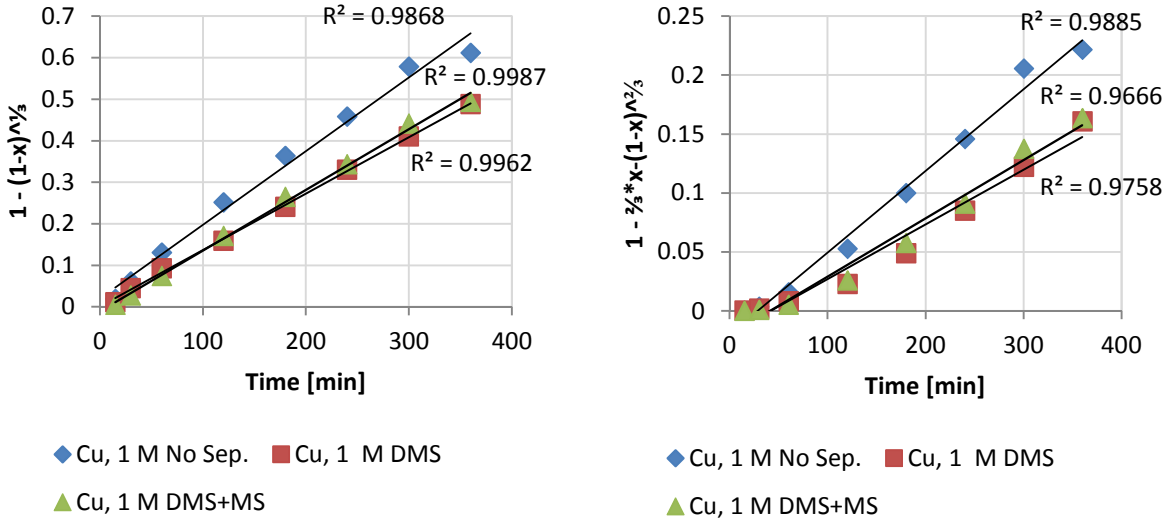

A) CHEMICAL REACTION CONTROL

B) DIFFUSION THROUGH PRODUCT LAYER

FIGURE D 1: FITTING REACTION MODELS TO 1M H_2SO_4 LEACHING OF CU FROM NO SEP FEED AT S/L RATIO OF 1/10 AND CONCENTRATED FEEDS DMS AND DMS+MS BOTH WITH S/L OF 0.6/10

Model fits at respective conditions

Comparisons of models fits are shown for the phase 2 experiments. The model providing the best fit (i.e. having the highest relative R-squared value) is stated in the final column.

TABLE D 1: R-SQUARED VALUES FOR FITTING DIFFERENT RATE MODELS ON LEACHING OF Cu FROM UNTREATED FEED USING H_2SO_4.

Acid concentration	S/L ratio	Chemical reaction control	Product layer diffusion	Film diffusion	Control
1 M	1/10	0.9868	0.9885	0.9551	Diffusion
2.5 M	1/10	0.9591	0.9649	0.9192	Diffusion

TABLE D 2: R-SQUARED VALUES FOR FITTING DIFFERENT RATE MODELS ON LEACHING OF Cu FROM DMS FEED USING H_2SO_4.

Acid concentration	S/L ratio	Chemical reaction	Product layer diffusion	Film diffusion	Control
1 M	0.6/10	0.9987	0.9666	0.9964	Chemical reaction
2.5 M	0.6/10	0.9362	0.9507	0.8991	Diffusion
2.5 M	1.0/10	0.9812	0.9917	0.961	Diffusion
4 M	1.0/10	0.9656	0.9722	0.9448	Diffusion

TABLE D 3: R-SQUARED VALUES FOR FITTING DIFFERENT RATE MODELS ON LEACHING OF Cu FROM DMS+MS FEED USING H_2SO_4.

Acid concentration	S/L ratio	Chemical reaction control	Product layer diffusion	Film diffusion	Control
1 M	0.6/10	0.9962	0.9758	0.9905	Chemical reaction
2.5 M	0.6/10	0.9061	0.9222	0.8796	Diffusion
2.5 M	1.0/10	0.9815	0.9854	0.961	Diffusion
4 M	1.0/10	0.9812	0.9917	0.9581	Diffusion